BERICHTE
aus dem Fachbereich Geowissenschaften
der Universität Bremen

No. 224

Kolonic, S.

.

MECHANISMS AND BIOGEOCHEMICAL IMPLICATIONS OF CENOMANIAN/TURONIAN BLACK SHALE FORMATION IN NORTH AFRICA: AN INTEGRATED GEOCHEMICAL, MILLENNIAL-SCALE STUDY FROM THE TARFAYA-LAAYOUNE BASIN IN SW MOROCCO

Berichte, Fachbereich Geowissenschaften, Universität Bremen, No. 224,
174 pages, Bremen 2004

ISSN 0931-0800

The "Berichte aus dem Fachbereich Geowissenschaften" are produced at irregular intervals by the Department of Geosciences, Bremen University.

They serve for the publication of experimental works, Ph.D.-theses and scientific contributions made by members of the department.

Reports can be ordered from:

Monika Bachur

Forschungszentrum Ozeanränder, RCOM

Universität Bremen

Postfach 330 440

D 28334 BREMEN

Phone: (49) 421 218-8960

Fax: (49) 421 218-3116

e-mail: MBachur@uni-bremen.de

Citation:
Kolonic, S.
Mechanisms and biogeochemical implications of Cenomanian/Turonian black shale formation in North Africa: An integrated geochemical, millennial-scale study from the Tarfaya-LaAyoune Basin in SW Morocco. Berichte, Fachbereich Geowissenschaften, Universität Bremen, No. 224, 174 pages, Bremen, 2004.

ISSN 0931-0800

…You have been told also life is darkness,
and in your weariness you echo what was said by the weary.
And I say that life is indeed darkness save when there is urge,
and all urge is blind save when there is knowledge,
and all knowledge is vain save when there is work,
and all work is empty save when there is love;
And when you work with love you bind yourself to yourself,
and to one another,
and to God.

Khalil Gibran "*The Prophet*"

…za Iman, za Umet, za Vatan Bosnu

Mechanisms and biogeochemical implications of Cenomanian/Turonian black shale formation in North Africa:

An integrated geochemical, millennial-scale study from the Tarfaya-LaAyoune Basin in SW Morocco

Dissertation
zur Erlangung des Doktorgrades der Naturwissenschaften
(Dr. rer. nat.)
am Fachbereich Geowissenschaften
der Universität Bremen, Deutschland

Dissertation
Submitted for a degree of Doctor in Natural Sciences
(Dr. rer. nat.)
at the Faculty of Geosciences
at Bremen University, Germany

Vorgelegt von
Sadat Kolonic, Dipl. Geol.
aus
Ljubija / Prijedor, Bosnien-Herzegowina

Presented by
Sadat Kolonic, M.Sc.
from
Ljubija / Prijedor, Bosnia-Hercegovina

Bremen, August 2003

Tag des Kolloquiums:

21.11.2003

Thema des Kolloquimvortrages:

Bildungsmechanismen und Biogeochemie kretazischer Schwarzschiefer

Gutachter:

PD. Dr. T. Wagner
Prof. Dr. J. Peckmann

Prüfer:

Prof. Dr. J. H. Kuss
Prof. Dr. R. Rendle-Bühring

Preface

This thesis summarizes 3.5 years of doctoral research, carried out between 2000-2003 at the University of Bremen, Germany. The thematic context and the scope and framework of the thesis is outlined in the Chapter 1. Chapters 2-7 comprise six scientific papers of which I am a co-author; the papers deal with mid-Cretaceous black shales in North Africa, and have been published or are submitted for publication in international Geo-science journals. My own contribution to the individual papers (Chapters) is as follows;

Chapter 2. An integrated depositional model for the Cenomanian/Turonian organic-rich strata in North Africa

Authors: *Lüning, S., S. Kolonic, E.M. Belhadj, Z. Belhadj, L. Cota, G. Baric, and T. Wagner*

Status: in press **Journal:** Earth-Science Reviews

Contributions: compilation of regional maps for individual black shale systems; integration of published and accessible unpublished data obtained from the oil industry (research visits to RWE-DEA Hamburg, Preussag-Energie Lingen and INA, Zagreb, Croatia) geologic interpretation; graphical presentation and authorship.

Chapter 3. Morocco basin`s sedimentary record may provide correlations for Cretaceous paleoceanographic events worldwide

Authors: *Kuhnt, W., E.H. Chellai, A. Holbourn, F. Luderer, J. Thurow, T. Wagner, A. El Albani, B. Beckmann, J.-P. Herbin, H. Kawamura, S. Kolonic, S. Nederbragt, and C. Street*

Status: published **Journal:** Eos Transactions AGU 82, 361-364, 2001

Contributions: field work; data processing; interpretation of geochemical data; geologic interpretation and authorship.

Chapter 4. Geochemical characterization of Cenomanian/Turonian black shales from the Tarfaya Basin (SW Morocco): relationships between paleoenvironmental conditions and early sulphurization of sedimentary organic matter

Authors: *Kolonic, S., J.S. Sinninghe Damsté, M.E. Böttcher, M.M.M. Kuypers, W. Kuhnt, B. Beckmann, G. Scheeder, and T. Wagner*

Status: published **Journal:** Journal of Petroleum Geology 25, 325-350, 2002

Contributions: field work; analytical work (selective and bulk organic and inorganic geochemical procedures and subsequent analysis); data processing; geologic interpretation; graphical presentation and authorship.

Chapter 5. **Uranium spectral gamma-ray response as a proxy for organic richness in black shales: applicability and limitations**

Authors: *Lüning, S. and S. Kolonic*

Status: published **Journal:** Journal of Petroleum Geology, 26, 153-174, 2003.

Contributions: field work; analytical work (selective and bulk organic and inorganic geochemical procedures and subsequent analysis); data processing; geologic interpretation; graphical presentation and authorship.

Chapter 6. **Carbon-isotope stratigraphy recorded by the Cenomanian/Turonian Oceanic Anoxic Event: correlation and implications based on three key-localities**

Authors*: Tsikos, H., H.C. Jenkyns, B. Walsworth-Bell, M.R. Petrizzo, E. Erba, I. Premoli Silva, A. Forster, S. Kolonic, M. Baas, T. Wagner and J.S. Sinninghe Damsté*

Status: submitted **Journal:** Journal of the Geological Society, London

Contributions: analytical work (selective and bulk organic and inorganic geochemical procedures and subsequent analysis); data processing; geologic interpretation and authorship.

Chapter 7. **Mechanisms of black shale deposition at the NW African Shelf during the Cenomanian/Turonian Oceanic Anoxic Event: implications for climate coupling and global organic carbon burial**

Authors: *Kolonic, S., T. Wagner, A. Forster, J.S. Sinninghe Damsté, B. Walsworth-Bell, S. Turgeon, H.-J. Brumsack, W. Kuhnt, H. Tsikos and M.M.M. Kuypers*

Status: submitted **Journal:** *Paleoceanography*

Contributions: field work; analytical work (selective and bulk organic and inorganic geochemical procedures and subsequent analysis); data processing; geologic interpretation; graphical presentation and authorship.

Acknowledgements

In the first place, I would like to thank PD. Dr. T. Wagner for setting up the project, for continuous, motivating support and invaluable scientific input, and for the numerous discussions we had during the course of the study. He reviewed the whole thesis critically and improved its quality significantly. During our joint fieldwork in the Tarfaya-LaAyoune Basin we experienced several remarkable and unforgettable adventures which we tackled with combined strength to overcome.

I am extremely grateful for the effective and smooth collaboration with Prof. Dr. El Hassane Chellai (University of Marrakech, Morocco), who enormously expanded the dimensions of the project.

Special thanks go to my chap Sebastian Lüning (Univ. of Bremen) and my Dutch mate Marcel Kuypers (MPI-Bremen) for their continuous support, enthusiasm and encouragement; their discussions and help were most valuable. Much of my research was field-based and in this regard I would especially like to thank Sebastian who made these challenging trips so successful.

The co-operation with Jaap S. Sinninghe-Damsté was highly successful and I am grateful to him for his assistance, numerous discussions and hospitality during my stay on Texel.

I am very grateful to Christopher Tiratsoo who significantly improved the grammar of the thesis but also my cover letters for various employment applications.

For fruitful and enjoyable scientific cooperation I am grateful to my co-authors H Tsikos and H.C. Jenkyns (Univ. of Oxford), J.S. Sinninghe-Damsté, A. Forster and M. Baas (NIOZ-Texel), M.E. Böttcher and Marcel Kuypers (MPI-Bremen), B. Walsworth-Bell, M.R. Petrizzo, E. Erba and. I. Premoli Silva (Univ. of Milano), G. Scheeder (BGR-Hannover), W. Kuhnt, A. Holbourn, F. Luderer and H. Kawamura (Univ. of Kiel), S. Nederbragt, C. Street, K. Ravilious and J. Thurow (Univ. College London), A. El Albani (Univ. of Poitiers), B. Beckmann and Sebastian Lüning (Univ. of Bremen), J.-P. Herbin (IFP-Rueil Malmaison), S. Turgeon and H.-J. Brumsack (ICBM Oldenburg), E.M. Belhadj and Z. Belhadj (Sonatrach, Algeria), L. Cota and G. Baric (INA, Croatia) and El Hassane Chellai (Univ. of Marrakech). I am also indebted to the management of Moroccan ONAREP and SHELL International (Dr. Kees Kommeren) for providing well material.

The discussion and exchange of ideas provided by work colleagues and friends from the C/T-Net has been very much helpful. I am grateful to them for providing me with valuable suggestions, hints and support through the course of the study.

My colleagues in Bremen are thanked for providing a very enjoyable working atmosphere. I acknowledge valuable technical support provided by the Renate Henning, Helga Heilmanm, Ralf Bätzel (Univ. Bremen) and Marianne Baas (NIOZ).

This project was financially supported (2.5 years) by the Deutsche Forschungsgemeinschaft (DFG grants Wa 1036/6 and Ku 649/9) while further funding (6 months) came from the University of Bremen (FNK grant Sadat Kolonic). I also acknowledge the financial support provided through the European Union's Improving Human Potential Programme under contract HPRN-CT-1999-00055, C/T-Net.

Finally, I thank all my friends and my family (my aunts, uncles, cousins) my sister Farah, her husband Damir, and their sons Din and Benjamin for their moral support. Above all, however, I am indebted to my parents, Faruk and Tesmija, for their encouragement, enthusiasm but also financial support. Without their constant backing none of this would have been possible!

Last but not least, a large bouquet of Bakara Roses goes to my wife Zeynep. She generously tolerated (especially during her pregnancy with our son Kerim) my various geological expeditions deep into the Sahara and my frequent absences for lab-work in Holland and England. I am grateful to her unselfish technical assistance in various ways, her continuous moral support and patience during the busy episodes of the project.

Finally I would like to commemorate all my friends and other Bosnian teenagers killed during the aggression *(1992-1995)* against our country. I am sure that if they were alive today, they would make better parents, students, engineers or scientists than I am or ever will be! *Shehidi Inshanallah….*

Sadat Kolonic

Abstract

Cenomanian/Turonian (C/T; ~94 Ma ago) black shale successions from various N African basins, in particular from the Tarfaya-LaAyoune Basin (SW Morocco), have been studied in great detail using data from the field (including gamma-ray resistivity logging), sedimentology and advanced geochemical trace metal, biomarker and stable isotope methods. Deposition of these black shale units in most of the region was restricted to a short time envelope termed "the C/T oceanic anoxic event" (OAE2). During this short period, a favourable combination of factors existed which led to the development of exceptionally strong oxygen-deficiency in the N African Tethys and in particular in the southern proto-North Atlantic oceans. The C/T black shales in N Africa are laterally discontinuous and their distribution and thickness were controlled by the palaeorelief. The thickest and regionally most extensive C/T organic-rich shales in N Africa occur in Morocco namely in the Atlantic Tarfaya-LaAyoune Basin. The laminated biogenic sediments from this NW African shallow marine basin were deposited with very high sedimentation rates (av. 5-10 cm/ka) enabling the investigation of mid-Cretaceous paleoceanographic events at high temporal resolution with respect to rapid climate change and associated hydrocarbon source-rock formation. The low level of thermal maturity and the high degree of sulphurisation of the organic matter (kerogen) makes these black shale successions suitable for advanced inorganic and organic geochemical investigations.

In cooperation with various other national and international Institutions/Universities, high-resolution geophysical, organic/inorganic and isotope geochemical investigations were performed on C/T sections from four sites along a NW-SE (paleo-) transect through the northern part of the Tarfaya-LaAyoune Basin. This alignment of the investigated sites is of about 120 km in length and runs from the deepest part of the basin (Sites S13) via transitional locations (Site S57 and S75), to a proximal location close to the paleocoastline (Mohammed Plage, Mpl). The investigated black shales are characterized by high hydrogen indices between 400 and 800 (mgHC/gTOC), indicating a dominant marine origin of sedimentary organic matter (type I-IIS kerogen). Organic petrological studies show that the OM is almost entirely composed of a brightly fluorescing groundmass with high abundances of lamalginite and bituminite, while detrital vitrinite and inertinite are only present in trace amounts. The persistence of low Tmax values (404-425°C) supports an immature to very early mature level of thermal maturation in terms of hydrocarbon generation. Abundant presence of isorenieratane derivatives indicates temporary development of photic zone euxinia. Inorganic geochemical investigations reveal an average ten-fold enrichment of redox sensitive trace metals (e.g. V, Mp, Ni and Zn) compared to the average shale composition.

Through the calibration of $\delta^{13}C$ isotope profiles (chemostratigraphy) from the investigated sites against those from Eastbourne, Pueblo and Gubio allow a revised cyclostratigraphic model for the C/T transition to be proposed, thus allowing a revised assessment of the timing and duration of the global OAE2 to be made. Following the new time model, the black shale cycles in the Tarfaya-LaAyoune Basin most probably represent short eccentricity (100 ka). In this case the duration of the OAE2 is estimated to be ~500 ka. The multidisciplinary high-resolution geochemical records obtained favour a coupled atmosphere-ocean mechanism that allowed repetitive and short-term fluctuations in upwelling-induced inflow of oxygen-depleted nutrient-rich intermediate waters coupled to enhanced marine productivity. Hence, it is suggested that photic zone and bottom water euxinia alternated with periods of better oxygenation of the water column in response to climate forcing. This is indicated by the high-amplitude fluctuations in accumulation rates of organic carbon, redox-sensitive and sulphide-forming trace metals, and biomarkers indicative of photic zone euxinia. These fluctuations are in general coeval and thus imply a strong relationship of OC burial and water column redox conditions. The estimated organic carbon preservation factor and export primary productivity range between 5-15% and 100-200 $gC/m^2 \cdot a$, respectively. The resulting efficient carbon burial in the Tarfaya-LaAyoune Basin and elsewhere on the NW African shelf contributed significantly to global carbon burial associated with the OAE2. Between 2 and 5 % of the overall global excess organic carbon burial during the OAE2 was deposited in the relatively small coastal Tarfaya-LaAyoune Basin. Assuming an equal distribution of organic carbon burial in the C/T oceans an enrichment factor of at least 50 is estimated for the Tarfaya-LaAyoune Basin.

The results of these investigations form a suitable platform to assess and distinguish the feedback mechanisms that controlled marine productivity and the development of deep and surface water anoxia/euxinia along the NW African continental margin during C/T.

Table of Contents

Part I:

Chapter 1

Introduction and outline of the thesis

Chapter 1.

1.1. Background

Several times during the Phanerozoic period, black shales were deposited over large areas of the ocean floor. Black shales are organic carbon (OC) rich, fine-grained sedimentary rocks with paleoecological, sedimentological and geochemical characteristics associated with deposition under oxygen-deficient or oxygen-free bottom waters. They generally exhibit the following characteristics; (i) they are commonly laminate; (ii) they contain relatively high amounts of pyrite; (iii) they include mainly marine organic matter with high abundances of sulphur-bound compounds (TOCs range from 1-10% up to 40%, and hydrogen indices range between 350-850 mg Hydrocarbons/gTOC; see Chapter 2 for a review); and (iv) they are highly enriched in trace-metals. These peculiar sedimentary rocks have attracted interest from geologist for many reasons, not least of which is their great economic importance as the source of more than 90% of global recoverable oil and gas reserves. In the geological record, they are more or less restricted to six stratigraphic intervals, in ascending order: (1) the Silurian, ~430 Ma ago (this interval generated 9% of the world's reserves); (2) the Upper Devonian, ~370 Ma ago (8% of reserves); (3) the Carboniferous/Permian transition, ~295 Ma ago (8% of reserves); (4) the Upper Jurassic, ~145 Ma ago (25% of reserves); (5) the mid-Cretaceous, ~95 Ma ago (29% of reserves); and (6) the Oligocene/Miocene transition, ~23 Ma ago (12.5% of reserves) [e.g. *Tiratsoo,* 1986; *Hunt,* 1996; *Ulmishek and Klemme*, 1990] (Fig. 1a).

Despite intense research during the last two decades on the mechanisms of black shale deposition, there is little consensus concerning any of the requirements for their formation. They have an uneven temporal and spatial distribution, and their geochemical character differs from one interval to another. Consequently, more than one factor has been put forward to control the genesis of black shales. Primary factors include (1) the plate tectonic configuration of continents and the opening/closure of marine seaways; (2) sea level rise and the flooding of shelves; (3) the structure of the basins in which deposition occurred; and (4) the evolution of marine and terrestrial biota and thus climate change. Furthermore, it has became clear that only favourable combinations of a number of factors (tectonic, climatic, oceanographic, and biologic) could have resulted in widespread black shale deposition during these six intervals. Nevertheless, black shales are still amongst the least understood of all sedimentary rock types. Decoding the mechanisms which resulted in black shale deposition has become increasingly important, both within the oil industry and in academia. From a petroleum geochemical perspective, detailed source rock studies could lead to saveings in time and money during exploration/production programmes. On the other hand, the academic community has realized that black shales provide valuable information about past climates, including periods of rapid climate change.

For several reasons, the mid-Cretaceous is a promising time envelope to study modes and mechanisms of black shale formation. These reasons include (1) the existence of accurate global ocean/continent paleogeographic reconstructions; (2) the relatively accurate information on mid-Cretaceous ocean chemistry and faunal (planktonic) diversity; and (3) the presence of complete records of sediments deposited in epicontinental seas with a distinctive lithological character, such as alternations of pelagic limestones with marls and/or black shales, providing good time control on sedimentation. In the early 1970´s Deep Sea Drilling Project (DSDP) discovered large quantities of mid-Cretaceous black shales in the deep Atlantic as well as Pacific Ocean basins. These discoveries initiated a flurry of investigations on the origin of the black shales, and developed an awareness among geologists both within the oil industry and the academic community that this time-interval was an extraordinary period in earth history. Hence, black shales deposited within the short time interval between the Barremian and Turonian (~124-90 Ma) are today considered as type examples for other black shale systems (Fig 1b). Research on mid-Cretaceous black shales has therefore proceeded with considerable impetus and has particularly been facilitated by new approaches in organic and inorganic geochemistry. Nonetheless, the extremely diverse data set obtained since then have resulted in a wide range of mutually contradictory models and theories concerning black shale deposition. It seems clear that many of the ideas and theories put forward in the black shale "literature" do not cover all aspects and therefore requires further investigations on this topic.

North Africa is particularly suitable for the genetic analysis of oxygen-depleted sedimentary sytems during the mid-Cretaceous, because individual black shale packages can be traced along outcrop belts for several thousands of kilometres (see Chapter 2). In contrast to terrane-dominated continents such as Europe or North America, N Africa remained tectonically undeformed throughout the Phanerozoic, so that present-day locations outside the Atlas Belt are mostly in their Palaeozoic and younger positions. A better understanding of small- and large-scale processes gained from these N African black shale systems will help with improved tectono-sedimentary reconstructions of similar depositional systems in more poorly-exposed and tectonically dissected regions.

1.2. The mid-Cretaceous

The mid-Cretaceous was an extraordinary period in Earth history. It was a "greenhouse world" characterised by high atmospheric pCO_2 concentrations in the range between 500 and 7500 ppm (estimated to be 3-12 times pre-industrial pCO_2 [*Berner*, 1992, 1994; *Bice and Norris,* 2002]); a general absence of polar ice caps; reduced temperature gradients from the Equator to the poles; high sea levels and oceans much warmer than today (Fig. 1b). There is a general consensus [e.g. *Larson & Olson,* 1991; *Erbacher et al*., 1996; *Gröcke*, 1997; *Glatzmaler et al.,* 1999; *Gale*, 2000; *Kent & Olson,* 2000; *Wallmann,* 2001; *Wilson & Norris,* 2001; *Wignall,* 2001] that mid-Cretaceous "greenhouse" conditions coincided with changes in mantle circulation as manifested by a long period of unchanging geomagnetic polarity, the emplacement of enormous oceanic plateau basalts, and the concomitant release of large volumes of mantle CO_2. During the same period, elevated marine productivity accompanied by high fluxes of organic matter to the sea floor and/or low seawater oxygenation associated with sluggish deep-water circulation, repeatedly favoured in many parts of the world ocean, both in shallow and deep environments, large-scale deposition of sedimentary rocks anomalously rich in OC [see *Leckie et al.*, 2002 for review] (Fig. 1b). Three distinct stratigraphic intervals of particulary high OC sedimentation are distinguished in the marine Cretaceous record, occurring in the Aptian/Albian, Cenomanian/Turonian (C/T), and in the Coniacian/Santonian (Fig. 1b). These periods of enhanced global OC sequestration, commonly termed „oceanic anoxic events" (OAEs) [*Schlanger and Jenkyns*, 1976; *Jenkyns*, 1980], favoured the formation of one-third of our present-day petroleum reserves. The term OAE was originally introduced to describe the episodic expansion and intensification of the oxygen minimum zone (OMZ), which was proposed to explain the seemingly global distribution of laminated black shales in pelagic successions of mid-Cretaceous age [*Schlanger and Jenkyns,* 1976].

Although new insights into the functioning of the mid-Cretaceous ocean-atmosphere system have been gained in recent years [e.g., *Hay et al.,* 1999; *Larson and Erba,* 1999; *Jones and Jenkyns,* 2001; *Leckie et al.,* 2002, *Wallmann,* 2001; *Bice and Norris,* 2002; *Kuypers et al.,* 1999, 2002; *Hofmann et al.,* 2003; *Beckmann et al.,* in press], the environmental factors that triggered and sustained these OAEs remain enigmatic and controversial. In general, during the Cretaceous several tectonic and climatic factors favoured the development of anoxic conditions in the Ocean. *Schlanger and Jenkyns* [1976] observed a coincidence between OAE's and major transgressions. High global sea level during the mid-Cretaceous is related to high rates of sea-floor spreading and concomitant increase in the volume of mid-ocean ridges (e.g. *Hays and Pitman*, 1973), as well as thermal uplift of the sea floor associated with massive submarine volcanism [*Schlanger et al.,* 1981; *Larson,* 1991] and the emplacement of large igneous provenances (LIPs). Maximum sea level during the mid-Cretaceous was probably 255 m higher [*Haq et al.,* 1987] and shelf areas were twice as large, as those of today [e.g. *Arthur et al.,* 1987; *Tyson,* 1995]. In addition, high levels of pCO_2 in the atmosphere resulted in comparatively temperate polar regions and extremely warm sea-surface temperatures [*Wilson and Norris, 2001*]. Proposed peak temperature of ~32-33±3°C [*Wilson and Norris, 2001*] for the mid-Cretaceous tropics might be underestimates. Recent experimental work by *Zeebe* [2001] has shown that changes in seawater pH may have had a marked effect on the oxygen isotope composition of foraminifera, thus implying that mid-Cretaceous sea surface temperatures were possibly higher (by ~2-3.5°C). Consequently, formation of cool oxygenated bottom-waters is unlikely to have occurred during the mid-Cretaceous, and was probably replaced by salinity-driven deep-water formation. This may have resulted in pronounced density stratification of the mid-Cretaceous oceans and basin-wide oxygen deficiency (most pronounced in the deepest areas). The complete lack of dissolved oxygen in

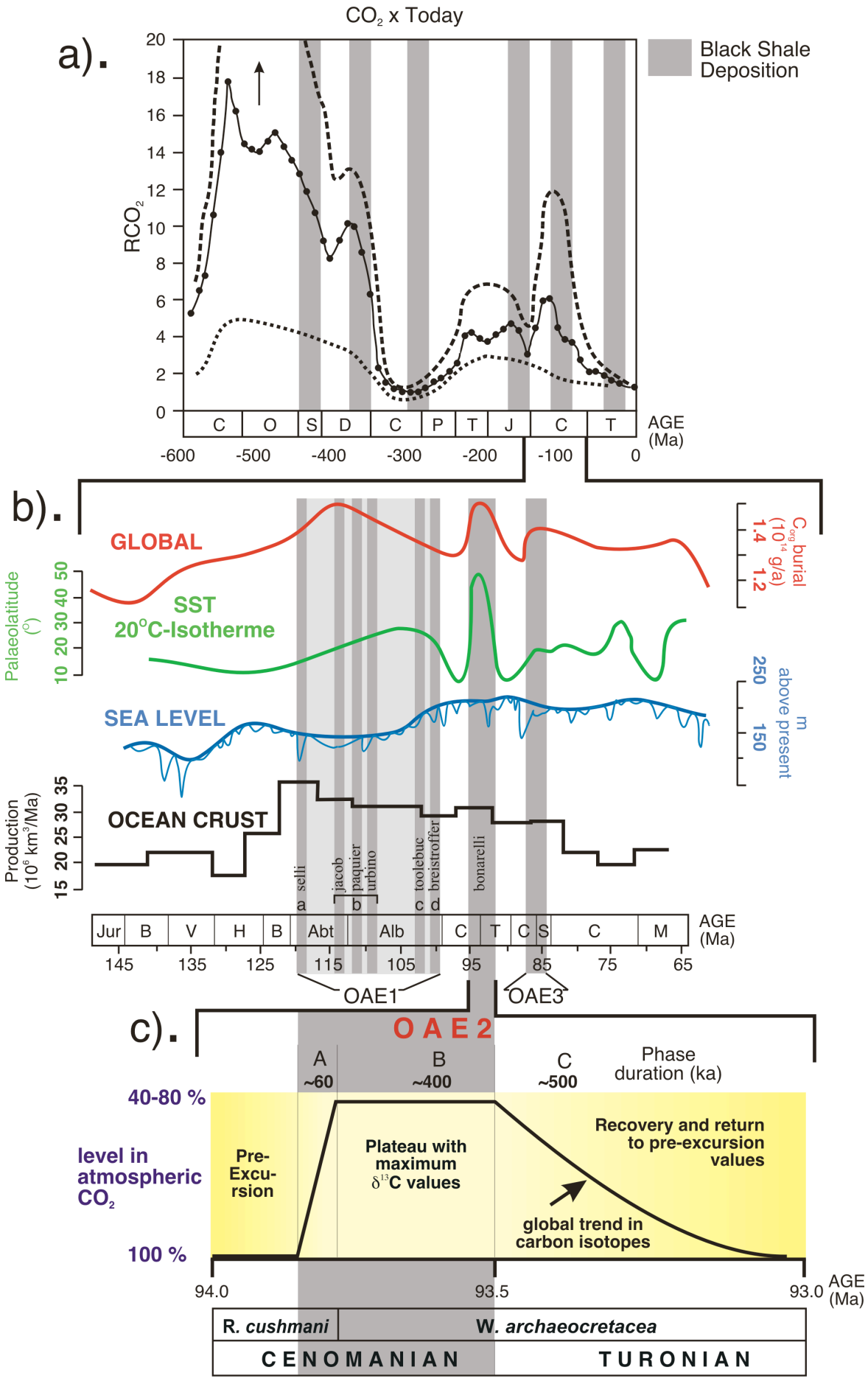
a).
CO2 x Today
Black Shale Deposition
RCO2
20
18
16
14
12
10
8
6
4
2
0
C O S D C P T J C T
AGE (Ma)
-600 -500 -400 -300 -200 -100 0
b).
GLOBAL
SST
20°C-Isotherme
SEA LEVEL
OCEAN CRUST
Palaeolatitude (°)
10 20 30 40 50
Corg burial (10^14 g/a)
1.4 1.2
m above present
250 150
Production (10^6 km^3/Ma)
15 20 25 30 35
selli
jacob
paquier
urbino
toolebuc
breistroffer
bonarelli
a
b
c d
Jur B V H B Abt Alb C T C S C M
AGE (Ma)
145 135 125 115 105 95 85 75 65
OAE1
OAE3
c).
O A E 2
A ~60
B ~400
C ~500
Phase duration (ka)
40-80 %
level in atmospheric CO2
100 %
Pre-Excu-rsion
Plateau with maximum δ13C values
Recovery and return to pre-excursion values
global trend in carbon isotopes
94.0
93.5
93.0
AGE (Ma)
R. cushmani
W. archaeocretacea
CENOMANIAN
TURONIAN

Figure 2. a) The six principal intervals in which black shale deposition occurred in relation to the best RCO_2 estimates (i.e. the CO_2 concentration at a given time normalized to the present day value) versus time. The arrow denotes that early Paleozoic RCO_2 values may be higher. The dashed lines represent a rough estimate of errors based on sensitivity studies (modified after *Berner* [1991]). b) The mid-Cretaceous record of major black shales and OAEs in the context of ocean crust production, changing global sea level, mean global sea surface temperature (SST) and global OC burial (modified after *Larson* [1991ab]). OAE1a early Aptian (''Selli event''), OAE1b spans the Aptian/Albian boundary (including the ''Jacob,'' ''Paquier,'' and ''Urbino'' events) and the less pronounced "Toolebuc" and "Breistroffer" events in the uppermost Albian, the OAE2 at the C/T boundary (''Bonarelli event''), and the OAE3 at the Coniac/Santonian boundary. c) Idealised representation of the C/T stable carbon isotope excursion showing the bio-/chronostratigraphic position of the three main phases (modified after Gale et al. [1993]).

such a Black Sea-type environment is suggested in many C/T sections by thinly-laminated OM-rich sediments devoid of benthic fauna (other than bacteria). Consistent with this, sedimentological and geochemical data from abyssal DSDP Sites 367 and 368 suggest that anoxic conditions persisted in the deeper part of the southern and SE proto-southern N Atlantic during most of the Albian to Turonian [*de Graciansky et al.,* 1984; *Sinninghe Damsté and Köster,* 1998; *Kuypers et al.,* 2002].

Increased submarine igneous activity associated with the formation of the Caribbean Oceanic Plateau, resulting in enhanced hydrothermal supply of bio-limiting metals and more efficient nutrient cycling due to a breakdown in thermal stratification, has been put forward as one possible trigger mechanism for the OAEs [*Larson and Erba,* 1999] (Fig. 1b). Indeed, recent seawater strontium-isotope data has indicated an increase in sea-floor spreading, submarine volcanism and hydrothermal activity across the C/T transition [*Ingram et al.,* 1994; *Jones et al.,* 1994]; and a recent high-resolution record suggests a correlation with the C/T carbon-isotope excursion [*Vonhof et al.,* 1999]. Alternatively, these submarine igneous activities also substantially increased the flux of sulphide, formed by thermogenic reduction through contact with hot basalts [*von Damm et al.,* 1985], from the mid-Atlantic ridge to the ocean [*Walker,* 1986] and formed a source of sulphide, independent of primary production. The latter proposes an upward expansion of sulphidic conditions (euxinia) from ridge-crests and other hydrothermal centres. Such a scenario is supported by the sequential extinction of first benthic and subsequently intermediate-water foraminifera during the C/T event, which appears to record the gradual upward expansion of toxic, sulphidic waters [e.g. *Jarvis et al.,* 1988; *Sinninghe Damsté and Köster,* 1998; Chapter 7]. Also, $\delta^{34}S$ data from both pyrite and organic sulphur from C/T black shales [Kolonic, unpublished data] indicate significant enrichment, relative to other sediments from euxinic basins [*Passier et al.,* 1999], suggesting that reduced sulphur may indeed have been formed by thermochemical sulphate reduction (a process with a much reduced fractionation effect relative to biological sulphate reduction). However these factors alone do not provide a satisfactory explanation as to why OC burial dramatically increased within the OAEs.

The geological processes which brought about these enormous differences from today's World are poorly understood. However, their investigation is essential since present-day anthropogenic emissions of CO_2 could lead to a rapid increase in atmospheric CO_2 levels with concomitant global warming. It is predicted that continuation of this trend may lead to a change from the present "ice-house" climate to a "greenhouse" climate [e.g., *Berner*, 1992, 1994]. Therefore, the greenhouse episode of global climate change in the mid-Cretaceous represents a naturally occurring excursion which may provide key information on the functioning of global biogeochemical cycles, and on possible feedback mechanisms such as the widespread genesis of oil-prone source rocks.

1.3. The Cenomanian/Turonian Ocean Anoxic Event (OAE2)

The most pronounced and certainly most global OAE occurred ~94 Ma ago, during the C/T transition (hereafter referred to as "OAE2"), and is regarded as the type example of Mesozoic OAEs [e.g., *Schlanger and Jenkyns*, 1976; *Jenkyns*, 1980; *Arthur et al.*, 1988; *Wignall,* 1994]. Interestingly, OAE2 is characterized by a distinct positive excursion in the stable carbon-isotopic composition ($\delta^{13}C$) of carbonate and organic matter (OM) (see also Chapters 2, 6 and 7 for review) (Fig. 1c). These positive $\delta^{13}C$ shifts are conventionally related to the widespread removal of isotopically-light OC into black shales, leading to enrichment in ^{13}C of the atmospheric and oceanic reservoirs of CO_2 [*Arthur et al.,* 1987, 1988; *Scholle and Arthur,* 1980]. The extent of the carbon isotope excursion for carbonate is

typically 2.5-3.0‰, whereas that for OC varies from 2.5-6.0‰. These excursions begin sharply in the uppermost *Rotalipora cushmanii* planktonic foraminiferal zone and are essentially completed at the end of the *Whiteinella archeocretacea* zone (for detailed descriptions of biostratigraphy of the C/T boundary, see Chapters 2, 6 and 7) (Fig. 1c). Although the OAE2 $\delta^{13}C$ excursions are characterized by several spikes and nudges in the various key sections reported from the Atlantic and Tethyan realms, it has been suggested that the excursion is most easily divided into three major phases [*Kuypers et al.*, 2002]: Phase A, a rapid increase in $\delta^{13}C$ values in the uppermost *R. cushmani* zone; Phase B, a plateau of maximum $\delta^{13}C$ values in the lower *W. archaeocretacea* zone; and Phase C, a gradual return to pre-excursion values, which ends in the *Helvetoglobotruncana helvetica* zone (Fig. 1c). Phases A and B represent the isotopic expression, and thus the stratigraphic extent, of the OAE2 (Fig. 1c). Estimates of the duration of the OAE2 vary between 0.25 Ma [*Arthur and Premoli Silva,* 1982*; Lamolda et al.,* 1994*; Paul et al.,* 1994] and 0.7 Ma [*Arthur and Premoli Silva*, 1982], partly due to application of varying OAE2 definitions. These inconsistencies become increasingly important as high-resolution marine records from different paleoceanographic settings and latitudes become available, many of them which have the potential to reconstruct mid-Cretaceous climate and environmental variability at orbital and even shorter time scales (see Chapter 7).

Widespread OC burial in black shales across the OAE2 also affected the mid-Cretaceous climate. *Arthur et al*. [1999] demonstrated that this may have caused a significant drop in the atmospheric pCO_2 concentration (Fig. 1a,c; see also Chapter 7 for detailed discussion), which resulted in apparent global climatic cooling. Consistent with this, the positive $\delta^{13}C$ shift of up to 16‰ for individual leaf wax components extracted from sediments from an abyssal site in the southern-North Atlantic indicates a sudden change in plant communities of the N African continent [*Kuypers et al.,* 1999]. Specifically, this suggests that plants using the C3-type photosynthetic pathway were succeeded by plants using the C4-type pathway. Because C4 plants can outcompete C3 plants only at pCO_2 levels below 500 ppmv, the observed change indicates an even larger reduction in C/T pCO_2 levels (40-80%). The 6‰ excursion found in marine phytoplankton in the same sediments is in agreement with this dramatic reduction in pCO_2 [*Kuypers et al.,* 1999]. This decline is also documented indirectly by oxygen isotope data, which suggest an 8-13°C cooling at high latitudes during the early Turonian (at the end of the $\delta^{13}C$ isotope excursions) [*Arthur et al.,* 1988; *Jenkyns et al.,* 1994]. Furthermore, additional indication of global cooling is provided by micropaleontological data, showing an excursion of boreal fauna into low latitude seas [*Kuhnt et al.,* 1986].

By contrast, *Kuhnt et al.* [in press] postulate that the observed climate change across the C/T transition probably occurred independent of CO_2 levels and may have been controlled by other greenhouse gases such as water vapour and/or methane. Accordingly, if for example atmospheric methane concentrations were higher during the mid-Cretaceous, then less CO_2 would be required to produce reasonable matches to minimum and maximum temperature estimates [see for review *Bice and Norris*. 2002]. However, in their study on C/T samples from Site S75 (Shell exploration well, Tarfaya-LaAyoune Basin, SW Morocco), *Kuhnt et al.* [in press] observed a significant mismatch between changes in paleotemperature, pCO_2 levels [*Kuypers et al.,* 1999], OC accumulation rates, ^{13}C isotope values and extinction events. According to these authors, the time lags between the individual events are significant. Thus, the maximum OC accumulation in the Tarfaya Basin occurred at least 10 ka after the planktonic foraminiferal extinction; more than 30 ka after the first main peak in the ^{13}C isotope curve; almost 60 ka later than the onset of the reduction of the atmospheric CO_2 content [*Kuypers et al.,* 1999]; and approx. 90 ka after the onset of the ^{13}C isotope excursion. From the latter succession of events, *Kuhnt et al.* [in press] concluded that there may have been alternative mechanisms to increase temperature at constant and/or lowering pCO_2 levels, for example due to increased methane and water vapour in the atmosphere.

Despite the challenging implications of *Kuhnt et al.* [in press], there is currently no proxy indicator for atmospheric methane and it is also unclear how much more methane would have been required on larger or shorter timescales during the mid-Cretaceous to maintain the inferred climate change. In addition, significant mid-Cretaceous fluxes of lightning due to greater elevations of convective clouds [*Thubrun and Craig* 1997] may have produced nitrous oxide and ozone [e.g. *Pickering et al.,* 1998; *Hauglustaine et al.,* 2001; *Tie et al.,* 2001], both of which are just as efficient greenhouse gasses as methane. Subsequently, the release of nitrous oxide and ozone by intensified lightning in strong convective storms would have transformed methane into CO_2. The latter considerations illustrates the complexity of climatic dynamics associated with climate changes during the C/T transition.

Although the large number of environmental factors that triggered and sustained the OAE2 still remain controversial, the ultimate cause for the short-term decrease in pCO_2 values and apparent climate cooling was most probably the rapid increase in OC accumulation rates. Excess burial of OC during the OAE2 probably withdrew much of the CO_2 from the ocean-atmosphere system to result in an inverse greenhouse effect. Coupled with the effects of elevated OC burial, the atmospheric oxygen concentration could have significantly increased during this event, thus causing climatic deterioration in turn leading to more oxygenated ocean waters and the end black shale deposition [*Arthur et al.,* 1988]. For example, *Ohkouchi et al.,* [1999] calculated the excess oxygen flux to the atmosphere during the OAE2 as 200%-600% of the average during the Phanerozoic. It is anticipated that, with decreased rates of OC burial but still relative high rates of volcanic outgassing, pCO_2 values increased rapidly again, producing atmospheric conditions comparable to those of the present day. Unfortunately, there is even less information with respect to this time interval of the C/T event.

However, although black shale deposition occurred on a global scale, recent evidence indicates that estimated OC accumulation rates varied by a factor of 100 within different depositional areas across the OAE2 [*Kuhnt et al.,* 1990; *Kuypers et al.,* 1999]. From mapping of OAE2 black shale distribution, it is known that, especially the southern proto-North Atlantic Ocean, both the shelf and the abyssal plain were major sites of OC burial. Furthermore, perhaps as much as 50-90% of the OC burial required to account for the $\delta^{13}C$ isotope excursion may have occurred in the southern proto-North Atlantic Ocean ([*Kuypers et al.,* 1999], see also Chapter 7). These OC mass accumulation rate estimates could be determined by the recognition of Milankovich cycles in proxy records in many C/T sections, establishing an accurate age model (see also Chapter 3 and 7). Accordingly, the highest OC mass accumulation rates across the OAE2 are observed in low latitude areas, culminating between the Equator and 15°N (off-shore Senegal and the Tarfaya-LaAyoun Basin); they then rapidly decrease towards the north and the south (see Chapter 3). For example, in the western Tethyan Realm (e.g. Vergon in the French Alps, NW Germany, and the N African margin i.e. the Bahloul Formation in Tunisia and Algeria; see Chapter 3) estimated OC mass accumulation rates are lower by a factor of ten. The reasons for these variations in OC mass accumulation rates in different depositional environments, however, are yet far from understood. However, it has been suggested that the high OC mass accumulation rates co-occurred with most severe anoxic conditions [*Sinninghe Damsté and Köster*, 1998]

1.4. Principal mechanisms of black shale formation across the OAE2

Two different models have been invoked to explain enhanced OC burial rates during the OAE2, namely increased marine productivity [*Pedersen and Calvert,* 1990] and/or increased thermal or haline stratification fostering preservation [*Demaison and Moore,* 1980]. The latter mechanism proposes reduced organic matter (OM) remineralization as a result of decreased bottom water oxygen levels, independent of marine productivity. Deposition of C/T black shales has often been associated with intensification and expansion of an oxygen minimum zone (OMZ) along the Atlantic and Tethyan continental margins (see Chapter 2). *Thurow and Kuhnt* [1986], for example, proposed that anoxic water masses impinging along the mid-Cretaceous NW African continental margin locally extended down to at least 3 km water depth. In the present-day oceans, enhanced oxygen consumption due to OM decomposition and slow downward mixing and diffusion of dissolved oxygen from the surface waters can lead to very oxygen-deficient intermediate waters (i.e. the establishment of an oxygen minimum zone "OMZ" across the shelf and upper slope of continental margins). However, anoxic or even euxinic conditions are generally restricted to basins tectonically isolated from oxygenated deep-sea circulation. In the mid-Cretaceous, anoxic conditions may have developed more readily, as minimal equator-to-pole thermal gradients may have resulted in decreased formation of oxygenated bottom-waters [*Barron,* 1983]. In addition, a halothermal mode of circulation has been proposed for the mid-Cretaceous [*Brass et al.,* 1982; *Hay,* 1988]. This envisages the formation of oxygen-poor, warm deep-waters in subtropical, net evaporative regions. It contrasts with the thermohaline circulation characteristic of the present-day, in which deep ocean circulation is driven by the convective sinking of cold, dense, well-oxygenated water in polar-regions. This could have resulted in basin-wide oxygen deficiency, with the most intense anoxia occurring in the deepest parts of tectonically isolated basins such as the Cretaceous North and South Atlantic [*Zimmerman et al.,* 1987; *De Graciansky et al.,* 1984]. Such extreme paleoceanographic conditions are supported by the

presence of specific biomarkers (e.g. isorenietratene and chlorobactane) [*Sinninghe Damsté and Köster*, 1998; *Kuypers et al.*, 2002] which suggest temporary widespread euxinic zone in the southern proto-N Atlantic. However, it is difficult to consider the Atlantic Ocean during the mid-Cretaceous as a stagnant basin comparable to the Black Sea, in which euxinic conditions have been established through density stratification even with a low biological productivity.

By contrast, the productivity model proposes a more dynamic interaction between biological and chemical processes as the causal mechanism for enhanced OM storage during the OAE2. Extremely high sea levels during the OAE2 fostered increased surface-water productivity on a global scale via increased sea-surface area availability for marine phytoplankton colonization, enhanced upwelling of nutrient-rich intermediate water masses along continental margins and large-scale nutrient leaching of flooded lowlands may have induced anoxic, and perhaps even euxinic conditions in the water column. By contrast, some authors have estimated organic-matter productivity to have been low to moderate in the C/T southern proto-N Atlantic Ocean [*Bralower and Thierstein*, 1984; *Sinninghe Damsté and Köster,* 1998]. It was apparently much lower than present-day upwelling systems where, despite the high productivity, the water column is not sulphidic.

Kuypers et al. [2002] demonstrated that deep-water black shale formation during the C/T in the low-latitude North Atlantic probably resulted from a combination of enhanced preservation, due to increased anoxia, and increased productivity. Based on inorganic and organic geochemical records, *Kuypers et al.* [2002] concluded that a prominent influx of saline, old, oxygen-deficient waters from the South Atlantic into the proto-North Atlantic may have displaced nutrient-rich deep and intermediate waters towards the ocean surface, thereby stimulating widespread ocean productivity. The opening of the Cretaceous Equatorial Gateway was probably sufficiently far advanced by that time to allow a vigorous deep-water exchange between the South and North Atlantic basins [*Wagner and Pletsch*, 1999, *Pletsch et al.*, 2001]. Kuypers' model implies that the proto-North Atlantic may have acted as a major nutrient trap, comparable to the Holocene Black Sea and Cariaco Trench which contain high levels of dissolved nutrients such as ammonium and phosphorus [e.g., *Jia-Zhong and Millero,* 1993; *Werne et al*., 2000]. Furthermore, these processes could have supported a progressive shoaling of the chemocline into the lower photic zone, as supported by an increase in the concentration of isorenieratane.

Despite these interesting insights into the functioning of the mid-Cretaceous ocean-atmosphere system, Kuypers' study mainly focussed on processes operating in the deep ocean, which in general integrate over longer time scales due to low average sedimentation rates in the mid-Cretaceous deep ocean and large, i.e. basin-wide, distances. In general, the time resolution of most deep-sea records is often not sufficient to resolve higher frequency fluctuations, which may document the intimate interactions between marine black shale formation and continental climate variability. These interactions are an important feature of Cretaceous black shale records in general, that resemble cyclic bedding rhythms displaying periodicities in the Milankovitch frequency band [e.g., *Dean et al.,* 1984; *Kuhnt et al.,* 1997, 2001, *Hofmann et al.,* 2003, *Beckmann et al.,* in press]. It appears therefore that atmospheric and oceanic circulation in the mid-Cretaceous was intimately linked to orbital-driven environmental changes, although the mechanisms and temporal phase relationships that have linked the atmospheric component of the climate system to its oceanic counterpart are poorly constrained. Nevertheless, our understanding continues to improve as *Beckmann et al*. [in press] demonstrated that atmospheric circulation was the driving force that triggered Coniacian/Santonian tropical Atlantic black shale sedimentation in response to orbital forced shifts in continental climate belts. These authors suggest that atmospheric response to insolation rather then oceanic feedback was the primary force driving the ocean-atmosphere system, thus implying that continental runoff was the key mechanism for black shale sedimentation off equatorial West Africa. Accordingly changes in Milankovitch frequencies, mainly in Obliquity and Precession, may have had an significant atmospheric influence on the tropics via monsoonal wind circulation systems. Changes in continental heating may be also have been important in areas north of the tropical convergence zone (TCZ) during C/T time, such as the NW African Continental Margin. It is well known that this region was very prone for black shale sedimentation for more than 11 Ma (upper Albian to lower Campanian). In particular, the Tarfaya-LaAyoun Basin of SW Morocco (Fig. 2) that inherits more than 600m of mid-Cretaceous laminated biogenic sediments and is known for its high sedimentation rates and OC accumulation, offers a particularly high representation of the C/T succession. The Tarfaya-LaAyoun Basin at approximately 15°N paleolatitude, may already have been within the TCZ during the C/T and

provides an excellent opportunity to study the postulated interactions of climate-forced processes on land, as well their links to processes that controlled ocean fertility and associated black formation before, during and after the C/T OAE (see Chapter 7 for detailed discussion).

1.5. Targets and aims of this thesis

This project was divided into two complementary work stages. In the first stage, an attempt was made to characterise the different depositional settings of OC-rich sedimentation during the C/T transition in N Africa. Within this stage, it is thought to provide a comprehensive discussion of the lateral distribution of organic-rich and organic-poor C/T strata in N Africa within a paleogeographic, tectonic and sequence stratigraphic context (see Chapters 2 and 3 for further discussion). Based on the findings from stage one, it was decided in the second stage to investigate the **Tarfaya-LaAyoune** black shale deposits in greater detail (Fig. 2). In the Tarfaya-LaAyoune Basin (SW Morocco) Mesozoic sediments accumulated to a thickness locally exceeding 12 km. An exceptionally thick (>600 m) OM-rich shallow-marine sedimentary succession spanning the mid-Cretaceous comprises perhaps the most stratigraphically complete C/T interval known (see Chapters 2, 3, 6 and 7). These laminated biogenic sediments were deposited with sedimentation rates exceeding 10 cm/ka during transgressive phases (Late Albian/early Cenomanian, Late Cenomanian, Early Turonian, Late Santonian/Early Campanian). They permit the investigation of mid-Cretaceous paleoceanographic and climate fluctuations at a high temporal resolution with respect to rapid climate change and associated source rock deposition. The low thermal maturity degree and the high sulphurisation of the Tarfaya kerogen qualifies these black shales for advanced inorganic and organic geochemical approaches (see Chapter 4). Therefore, specific assemblages of organic and inorganic geochemical proxy records were distinguished with the following specific objectives:

- to obtain high-resolution stable carbon isotope data for carbonate and bulk OC through the main phases of the C/T event. This will allow detailed stratigraphic correlation of the different sections studied and will determine, on a global scale, whether black-shale deposition in the N Atlantic and western Tethyan realm occurred synchronously.
- to test the feasibility of field gamma-ray resistivity logging methods, their applicability and limitation as a supplementary tool in a source rock investigation.
- to provide a detailed bulk characterisation of the OM by TOC and Rock Eval determinations.
- to characterise the OM optically to estimate the contribution of terrestrial and marine OM.
- to assess the abundance of free and bound biomarkers, in order to trace changes in the phytoplanktonic community, in water-column anoxia and in the terrestrial contribution.
- to determine concentrations of major elements, in order to characterise the bulk sediment and to identify variations in terrigenous detrital sources.
- to obtain high-resolution records of redox-sensitive and/or sulphide-forming elements, in order to reconstruct oxygenation levels of the water column.
- to link these observed variations to Milankovich and Sub-Milankovitch cyclicity, enabling a high-resolution time scale for determination of changes in OC, biomarker and trace element mass accumulation rates.
- finally, to evaluate the importance of the Tarfaya-LaAyoune Basin with respect to global carbon burial.

During the course of the study, the research objectives listed above became of scientific interest to the European Union's funded C/T-Net research group. This resulted in efficient collaboration with other geoscientists and biogeochemists from England, Italy, the Netherlands and Germany also studying C/T shale successions from the North Atlantic and western Tethys with respect to rapid climate change and associated source rock formation. Under the title "RAPID GLOBAL CHANGE DURING THE CENOMANIAN/TURONIAN OCEANIC ANOXIC EVENT: EXAMINATION OF A NATURAL CLIMATIC EXPERIMENT IN EARTH HISTORY" and co-ordinated by Jaap Sinninghe Damsté (NIOZ, Texel), the C/T-Net research group intends to integrate multidisciplinary proxy records to develop a global model for the OAE2.

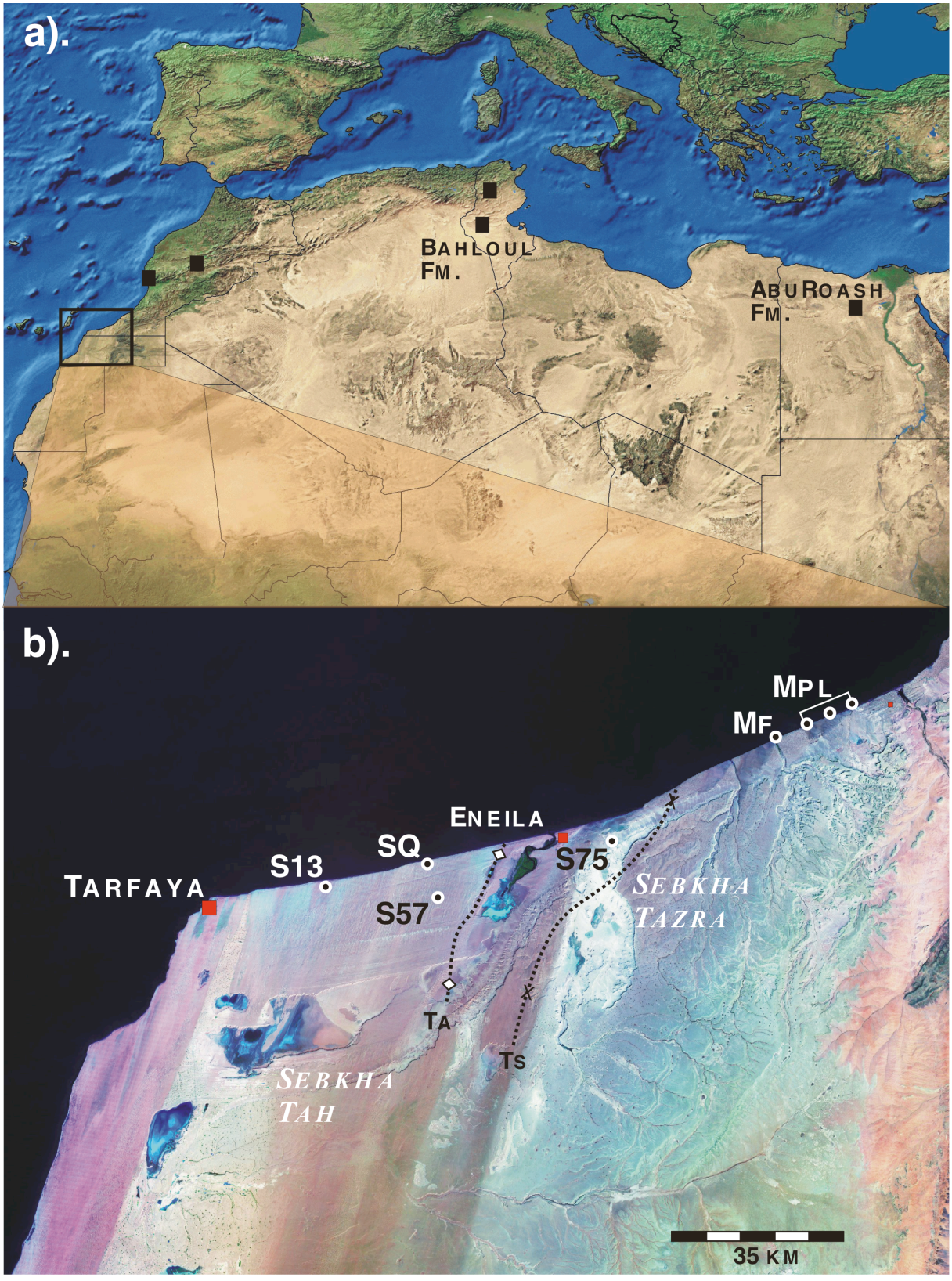

Figure 2. a). Topographic map of N Africa showing the locations studied in the field. b). Locations investigated in the Tarfaya Basin. Abbreviations; MF, Oued MaFatma; MPL, Mohammed-Plage; SQ, Shell quarry; TA, Tazra anticline; TS, Tazra syncline.

1.6. Materials and analytical approach

As the Tarfaya-LaAyoune Basin was selected as the key section for this study a total of three field seasons between 2000 and 2003 were undertaken for mapping, sampling and geophysical (gamma-ray) logging. Aadditional, complementary field work in other parts of Morocco and also in Tunisia and Egypt was performed to study selected C/T shale successions in greater detail (Fig. 2a). It was decided to focus on samples obtained from four sites along a 120 km long, NW-SE (paleo-) transect through the Tarfaya Basin (Fig. 2b). The transect connects the deepest part of the basin (Site S13), via transitional locations (Sites S57 and S75), to a proximal location close to the palaeocoastline (Mohammed Plage, Mpl) (Fig 2b). Site S13 and S57 were drilled near the village of Tarfaya, and well S75 near the small settlement of Enaila near to Sabkha Tazra (Fig 2b). S13 is the most distal site, being approximately 20 km SW of well S57 (Fig 2b). Site S75 is located another 35 km NE from well S57 at the northern part of the flank of the Tazra anticline. The Mpl coastal outcrop is located about 65 km NE of well S75 at the northern rim of the Tarfaya Basin (Fig 2b).

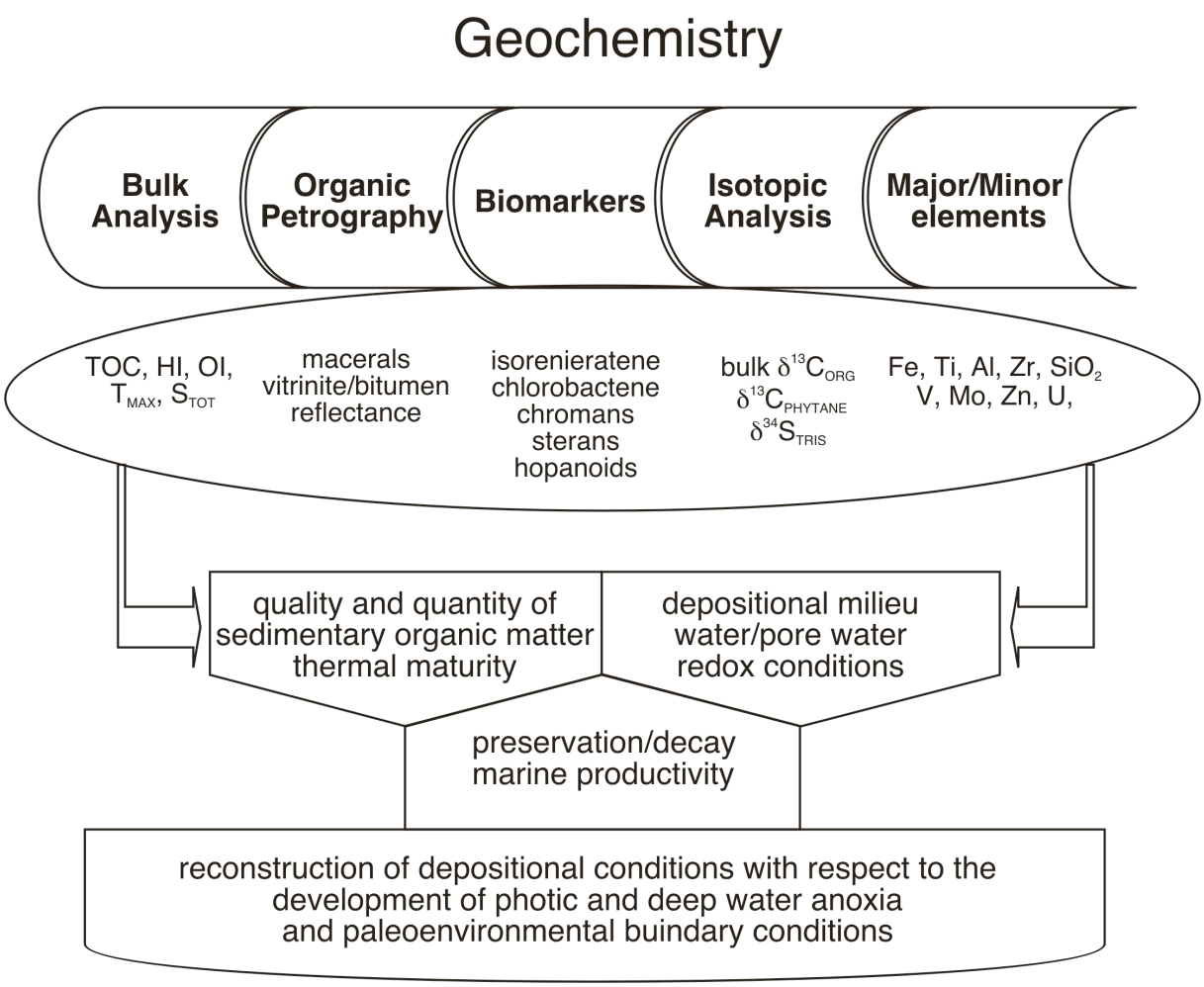

Figure 3. Schematic flow chart for analysis of investigated black shales

Wells S13, S57 and S75 were drilled by the Moroccan State Oil Company ONAREP and SHELL, and samples were kindly made available from the SHELL Core Depository in Rotterdam.

Organic and inorganic geochemical analyses were mainly performed at the Faculty of Geosciences at Bremen University and at the Netherlands Institute for Sea Research (NIOZ) on Texel (Netherlands). Additional geochemical analyses were performed at the Institute for Chemistry and Biology of the Marine Environment (ICBM) in Oldenburg (Germany), at the Max Planck Institute for Marine Microbiology (MPI), Bremen and at Department of Earth Sciences at the University of

Oxford. For detailed description of the methodologies applied, see Chapters 4,5 and 7. In Figure 3, a schematic flow chart summarizes the multidisciplinary approach I adopted, which combined organic and inorganic geochemical analyses, as well as stable carbon and sulphur isotope techniques.

Within the analytical scheme, special emphasis was given to biomarker investigations which were performed during a 9 month stay at the NIOZ under the supervision of Dr. Jaap Sinninghe Damsté. To obtain information on water column anoxia and the position of the chemocline, the biomarker approach was focused on the identification of specific bacteriochlorophylls such as isorenieratene and vhlorobactene. Isorenieratene and chlorobactene are carotenoid pigments exclusively biosynthetisised respectively by the brown- and greencoloured strain of the green sulphur bacteria Chlorobiaceae, [e.g., *Madigan et al.,* 2000]. As strict anaerobes, these bacteria require free hydrogen-sulphide in the water column and light of a specific wavelength in order to carry out photosynthesis. At the present day, these conditions are restricted to a few isolated marine basins, such as the Black Sea, where Chlorobiaceae thrive near the sulphide/oxygen interface (i.e. the chemocline) at light levels of less than 1% of surface irradiance (or <0.5 μE) [van *Gemerden and Mas,* 1995]. In general, Chlorobiaceae from the green strain require higher light intensity and therefore thrive even at shallower depth (~15m water depth) then Chlorobiaceae from the brown strain (~30-150m). Since Chlorobiaceae fix carbon through the reverse tricarboxylic acid cycle (TCA) their biomass is consequently enriched in $\delta^{13}C$. Therefore, biomarker derivatives of Chlorobiaceae show a typical 10-15‰ $\delta^{13}C$ enrichment relative to biomarkers originating from other primary photoauthotrophs [e.g. *van der Meer et al.,* 1998]. A prerequisite for the presence of isorenieratene and chlorobactene in the sediment is an anoxic water column rich in reduced inorganic sulphur species that readily react with functionalised lipids (including isorenieratene and chlorobactene) which then become sulphur-bound during early digenesis (so-called "natural sulphurisation") [see *Koopmans et al.,* 1996ab and *Sinninghe Damsté et al.,* 2001 for review]. In addition, these molecular fossils are very labile compounds which do not readily survive long-distance transport, and are therefore indicators of a local (autochtonous) marine source. It has been reported, however, that anoxic sediments containing isorenieratene derivatives were eroded and subsequently redeposited during late Quaternary "Heinrich" events in oxic parts of the Atlantic Ocean [*Rosell-Malé et al.,* 1997]. Such a mechanism is not expected for the Tarfaya-LaAyoun Basin, since it was a relatively shallow water depth basin (~500m deep) on the NW African continental margin.

1.7. Scope and framework of this thesis

The research presented here consisted of two stages. Initially, regional distribution maps and tectono-depositional models were compiled for individual black shale systems based on an integration of published and accessible unpublished data (Chapter 2 and 3). Though time-consuming, the reviews helped to minimize duplication of research efforts. In the second stage, specific studies were designed and carried out to test existing models (and fill data gaps) identified during the review stage. These studies are presented in Chapters 4,5,6 and 7.

- **Chapter 2** gives an overview of the lithological characteristics, regional distribution, ecology, depositional models and economic significance of C/T black shales in N Africa. Based on a review of published and unpublished information, the distribution and organic-richness of C/T strata throughout the whole region is reported. A general decrease in peak organic richness and black shale thickness is documented to occur from west to east, partly as a result of upwelling along the Moroccan Atlantic coast and the absence of upwelling in the Eastern Mediterranean area. Also, in the confined Central Atlantic, the OMZ reached down in many places to the deep sea floor (3-4 km); while the lower limit of the OMZ along the N African Tethys was much shallower and underlain by oxic water masses. As documented by high-resolution biostratigraphic and chemostratigraphic data, C/T black shale deposition in most areas outside the upwelling zone were restricted to a marked latest Cenomanian transgressive phase. Triggered by this eustatic sea-level rise, the OMZ impinged onto the N African continental shelf and the margins of intrashelf basins which had mostly formed as halfgrabens during the Early Cretaceous. Important units containing organic-rich C/T strata in the region are the Atlantic Tarfaya black shales (Morocco, Western Sahara); black shales and phtanites in the Moroccan and Algerian Atlas; the Bahloul Formation in the SE Constantine Basin and in northern and central Tunisia; the Etel Formation in the Sirte Basin (Libya); the Al Hilal Formation in Cyrenaica (Libya); the Abu Roash Formation in the Abu Gharadig and Fayium Basins (Western Desert, Egypt); the

Daliyya Formation along the NE Sinai-Palestine-Israel coast; and the Shueib Formation in West Central Jordan.

- **Chapter 3** proposes the Tarfaya-LaAyoune Basin as a key location in N Africa for the analysis of oxygen-depleted shallow-marine sedimentary rocks. The Cenomanian to Campanian record of predominantly laminated biogenic sediments, deposited with sedimentation rates exceeding 10 cm/ky during transgressive phases, comprises a unique archive of the Late Cretaceous paleoceanographic and climatic events which led to the deposition of these highly oil-prone source rocks. Furthermore the record in the Tarfaya-LaAyoune Basin has the potential to be correlated with globally recognized paleoceanographic events (i.e. isotope excursions, extinctions, "anoxic events") and to a Milankovitch framework, which will assist their precise dating and assessment of their duration.
- **Chapter 4** details the geochemistry of the C/T black shales in the Tarfaya-LaAyoune Basin and introduces aspects of regional petroleum geology. The Observed large variations in bulk and molecular geochemical compositions in general reflect changes in the quantity and quality of the organic matter. As indicated by organic petrological studies and Rock-Eval pyrolysis, black shales from the Tarfaya Basin consist dominantly of marine algal/bacterial organic matter. Kerogen is characterised by a brightly fluorescing groundmass with lamalginite and bituminite particles, indicating kerogen which would generate petroleum at low temperatures, similar to the kerogen from the Miocene Monterey Formation. Biomarker and kerogen analyses show that the Tarfaya Basin black shales are rich in organic sulphur compounds, from which it can be inferred that natural sulphurization played a key role in the formation of these hydrogen-rich source rocks. Additional inorganic geochemical data indicate that sulphurization of organic matter occurred in response to the enhanced availability of metabolizable organic matter and limitation of iron in the presence of free sulphide in the water column. The C/T succession is organic rich in various parts of N Africa, and may be a hydrocarbon source where sufficiently mature, for example offshore Morocco and in northern Algeria, Libya and the Egyptian Western Desert.
- **Chapter 5** considers whether the uranium content of a shale, as indicated by spectral gamma response, can be used as a measure of the TOC content. This achapter reviews the U/TOC relationship in a range of black shale systems, mostly in N Africa and western Europe, for which appropriate data is available. Published data from the literature is used, to which is added new analytical data from my own field investigations. In general, the data only permit qualitative characterizations of the U/TOC relationships to be made. However, visual inspection of the gamma and TOC profiles presented shows that correlations can range from "good", through "fair-to-good", to "poor". Obviously a close correlation is required if the relationship is to be used predictively, and factors which may influence the development of a stable U/TOC relationship are briefly reviewed. Among these are the complex and poorly understood role played by sorbents in uraium concentration and release, together with syndepositional factors (e.g. sedimentation rate, anoxia) and diagenesis. Furthermore, it is proposed that the U-peaks may be used as correlation horizons within the C/T succession between Tunisia and Jordan. A larger-scale correlation between the two countries, however, cannot be documented.
- **Chapter 6** presents detailed carbon-isotope records for bulk carbonate, TOC and S-bound phytane from three key-sections spanning the C/T boundary interval (Eastbourne, England; Gubbio, Italy; Tarfaya, Morocco), with the purpose of establishing a common chemostratigraphic framework for the OAE2. Evaluation of data is undertaken on the premise that an oceanic anoxic event such as the OAE2 is, by definition, a perturbation of the global marine inorganic/organic carbon reservoirs due to excess burial of OM. Therefore, such an event must be reflected in the isotopic record of the respective sedimentary products, as long as post-depositional processes or local effects have not obliterated the preservation of the primary chemical signals. It appears that the two most conspicuous features of all isotopic profiles, namely the onset of the excursions and of the plateau of maximum $\delta^{13}C$ values, are sufficiently reproducible across the individual sections to allow a reasonably objective stratigraphic definition to be compiled at least for the beginning and the maximum isotopic expression of the OAE2.
- **Chapter 7** discusses high-resolution geochemical records from a depth transect across the Tarfaya-LaAyoun Basin. These multi-proxy records reveal long-term and high-frequency fluctuations in the burial of OC, biomarkers indicative of photic zone euxinia (PZE), and redox-sensitive trace elements which are closely associated with the evolution of the OAE2, sea-level rise and short-term climate variability. High amplitude variations in all proxy records suggest a dynamic depositional

setting where wind-driven fluctuations in upwelling, marine productivity, and photic zone and deep-water euxinia record distinct changes at orbital or even higher-frequency time scales. As such, the Tarfaya-LaAyoun Basin is suggested as a type example of a highly productive Mesozoic continental margin which was strongly affected by the global C/T OAE.

Part II:

Results

Chapter 2

An integrated depositional model for the Cenomanian/Turonian organic-rich strata in North Africa

Chapter 2.

An integrated depositional model for the Cenomanian/Turonian organic-rich strata in North Africa

Authors*: Lüning, S., S. Kolonic, E.M. Belhadj, Z. Belhadj, L. Cota, G. Baric, and T. Wagner*

Status: in press Journal: *Earth Science Reviews*

Abstract

During the Late Cenomanian–Early Turonian (C/T) Oceanic Anoxic Event (OAE2), organic-rich strata was deposited in rift shelf basins and slopes across North Africa and in deep-sea basins of the adjacent oceans. Based on a review of published and unpublished information, this paper documents the distribution and organic-richness of C/T strata across the whole region within a palaeogeographic framework and systematically analyses the conditions and processes, which controlled their deposition. Previously, the C/T in North Africa has been most intensively studied in southern Morocco (Tarfaya) and Tunisia. Only little data is availabe for other parts of North Africa, namely Algeria, Libya and Egypt, because distribution of C/T Corg strata there becomes more patchy. A general decrease in peak organic richness and black shale thickness occurs from west to east, partly as a result of upwelling along the Moroccan Atlantic coast and the absence of upwelling in the eastern Mediterranean area. Furthermore, in the confined central Atlantic, the oxygen minimum zone (OMZ) in many places reached down to the deep-sea floor (3–4 km), while the lower limit of the OMZ along the North African Tethys was much shallower and underlain by oxic water masses. As documented by high resolution biostratigraphic and chemostratigraphic data, C/T black shale deposition in most areas outside the upwelling zone are restricted to a strong, eustatic, latest Cenomanian transgressive phase. Triggered by this sea-level rise, the OMZ impinged onto the North African continental shelf and the margins of intrashelf basins, which mostly formed during the Early Cretaceous as halfgrabens. Important units containing C/T organic-rich strata in the region are the Atlantic Tarfaya black shales (Morocco, Western Sahara), black shales and phtanites in the Moroccan and Algerian Atlas, the Bahloul Fm. in the SE Constantine Basin and in northern and central Tunisia, the Etel Fm. in the Sirte Basin, the Al Hilal Fm. in Cyrenaica (Libya), the Abu Roash Fm. in the Abu Gharadig and Fayium basins (Western Desert, Egypt), the Daliyya Fm. along the NE Sinai–Palestine–Isreal coast and the Shueib Fm. in west central Jordan.

Keywords: Cenomanian–Turonian; anoxia; black shale; North Africa; petroleum source rock

2.1. Introduction

The Cretaceous period is characterised by a series of marine anoxic phases [*Schlanger and Jenkyns,* 1976] associated with widespread organic matter (OM) burial and black shale deposition. Among these is the oceanic anoxic event (OAE) at the Cenomanian–Turonian boundary (C/T), which is the most pronounced and best studied (OAE2, CTBE and CTOAE: [J*enkyns*, 1985; *De Graciansky et al*., 1986; *Arthur et al.,* 1987, 1990]; Bonarelli Event: [*Schlanger et al.,* 1987] but still of controversial origin. Deposition of C/T organic-rich sediments took place in many parts of the world (Fig. 1) and in a variety of palaeobathymetric settings, ranging from deep ocean basins to shallow shelfal seas [*Schlanger and Jenkyns*, 1976]. Parts of North Africa (i.e., the proto southern North Atlantic and eastern Tethys) were also oxygen-deprived, especially the shelf and slope regions along the Moroccan Atlantic coast (Agadir, Tarfaya) and the northern parts of Morocco, Algeria and Tunisia (Fig. 1) resulting in the deposition of organic-rich shales, marls and limestones with TOC contents of locally up to 40% [*Herbin et al.,* 1986]. The C/T organic-rich strata in Tarfaya and Tunisia have been studied in great detail in the past (Morocco: e.g., [*Wiedmann et al.,* 1978; *Leine*, 1986; *El Albani et al*., 1999a,b; *Kuhnt et al.,* 1997; *Kolonic et al.,* 2002]; Tunisia: e.g., [*Robaszynski et al.,* 1993a,b; *Maamouri et al.,* 1994; *Accarie et al.,* 1996; *Nederbragt and Fiorentino,* 1999; *Abdallah et al.,* 2000]) and syntheses including NW Africa have been published by *Herbin et al.* [1986], Kuhnt et [1990] and *Kuhnt and Wiedmann* [1995]. While high-resolution data is available for some selected organic-rich C/T localities in North Africa, a comprehensive discussion of the lateral distribution of organic-rich and organic-poor strata within a palaeogeographic, tectonic and sequence stratigraphic context does not exist for the region and, hence, is attempted here. The present study aims to

- map areas with organically rich and organically poor C/T strata;
- determine potential tectonic control on distribution of organically rich C/T strata;
- predict the distribution of organic-rich C/T strata in areas where only little data exists (e.g., Algeria, Libya, Egypt);
- better understand the depositional conditions by studying the lateral distribution of C/T Corg strata (see also [*Kuhnt and Wiedmann,* 1995], p. 226);
- differentiate between the two potential driving mechanisms (a) primary productivity [e.g., *Parrish,* 1995] and (b) preservation/stagnation [e.g., *Tyson,* 1995] for different parts of North Africa; and
- compare and integrate biostratigraphic and carbon isotope excursion data across North Africa, and from this identify trends, synchronities and diachronities.

An improved depositional model may allow refined organic/non-organic facies predictions in North Africa, which is important for a more effective interpretation within a regional context of the 1-D high-resolution data from individual sections. Furthermore, Mid-Cretaceous organic-rich strata worldwide have sourced almost one-third of the world's hydrocarbon reserves [*Klemme and Ulmishek*, 1991] and also in North Africa they play an important role [*Ziegler and Roure,* 1999]. About 70% of the total world petroleum resources are concentrated in the Tethys realm [*Ulmishek and Klemme,* 1990], including North Africa.

2.2. The Cenomanian–Turonian Oceanic Anoxic Event

Oceanic anoxic events represent intervals of globally increased organic carbon (OC) storage. Traditionally, the term OAE, proposed by *Schlanger and Jenkyns* [1976], explained the seemingly global distribution of black to grey laminated organic-rich shales (>1 wt.% TOC) in pelagic sequences of Aptian–Albian and Cenomanian/Turonian age. For the Cretaceous, a total of six OAEs have been recognized representing episodes of globally widespread black shale deposition in marine environments that correlate closely with transgressions. The C/T oceanic anoxic event is marked by a characteristic positive excursion in the 13C record of carbonates and OM, usually with a sharp base and a ~2 shift in bulk carbonate and 3–6 in organic carbon [*Schlanger and Jenkyns*, 1976; *Arthur et al.,* 1988; *Arthur and Sageman,* 1994 and *Jenkyns et al.,* 1994] that was associated with enhanced burial of OM. This sharp increase in the carbon isotope ratio at the C/T boundary is observed in

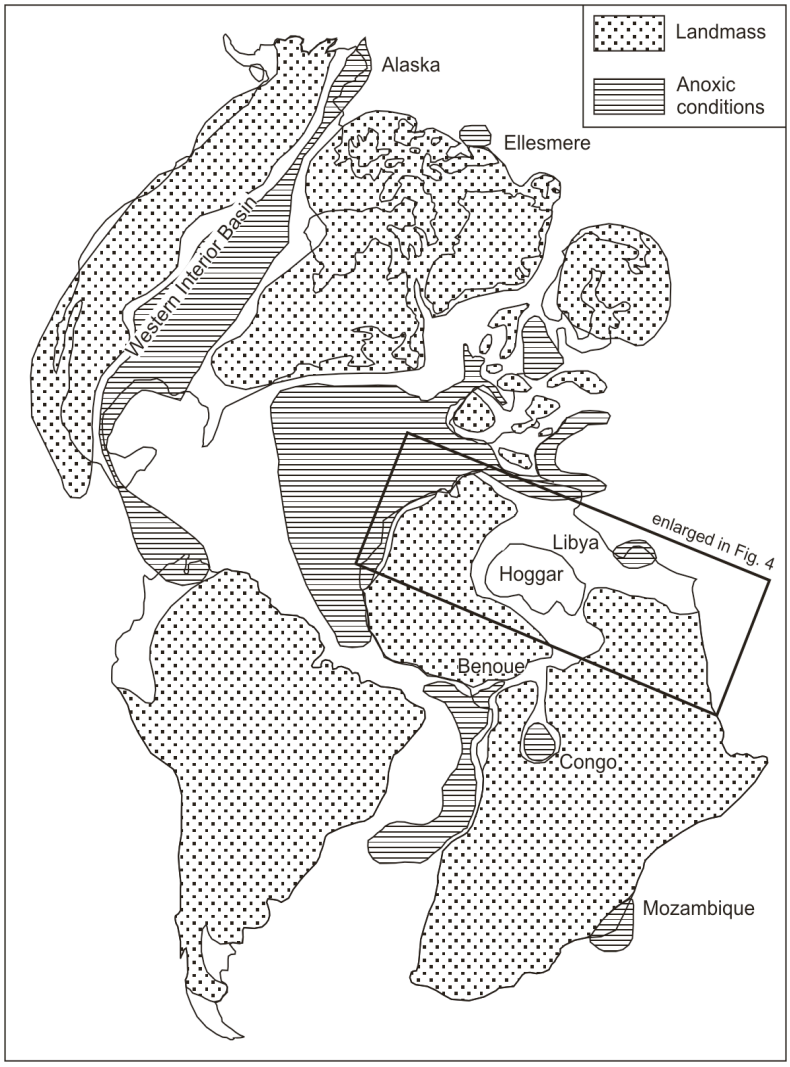

Figure 1. Geographical extent of C/T organic-rich deposits in the Atlantic and adjacent areas [after *De Graciansky et al.*, 1986].

various parts of the world and is used as a stratigraphic tool for high-resolution correlation [*Gale et al.,* 1993] and *Hasegawa,* 1997]. Especially the isotopic excursion recorded in OM provides a reliable time marker [*Arthur et al.,* 1988] while the trend in carbonates is often subject to more short-term variability [e.g., *Paul et al.,* 1999]. The rapid initial rise in 13C values occurred during the latest part of the *Rotalipora cushmani* Zone in the Cenomanian, usually followed by a series of three (A, B and C) or more subcycles on a plateau with maximum 13C values during the lower part of the *Whiteinella archaeocretacea* Zone [*Pratt and Threkeld,* 1984; *Lamolda et al.,* 1994] (Fig. 2). The decrease to pre-excursion values took place within the *W. archaeocretacea* Zone near the C/T boundary. Cyclostratigraphic data from chalk/limestone couplets from Canada [*Prokoph et al.,* 2001] and Morocco [*Kuhnt et al.,* 1997] indicate a duration of ~320 and ~240 ka, respectively, for the worldwide synchronous C/T OAE. However, the effective duration of anoxic conditions varies in different places and can be much longer or even shorter, depending on the local setting.

The large scale burial of OC during the C/T OAE also may have led to a significant reduction in atmospheric CO2 concentrations (and hence temperature) [*Kuypers et al.,* 1999], with CO2 values during the Mid Cretaceous generally at 2–3 (according to some authors up to 10) times above present levels [*Berner,* 1983, 1993, 1994; *Caldeira and Rampino*, 1991]. An open debate exists whether the C/T OAE is associated with (1) enhanced preservation of organic matter at the sea floor as a result of oxygen-depleted deep-water masses (e.g., offshore NW Africa: Sinninghe Damsté, 1998) or (2) by an unusually high flux of organic matter to the sea floor with the rate of burial exceeding the rate of oxidation and biogenic recycling at the sea floor and within the sediments (Moroccan Atlantic coast: e.g., [*Wiedmann et al.,* 1978]). Some authors already differentiate between regions where either the stagnation model or the productivity model dominates organic-matter deposition [*Kuhnt and Wiedmann,* 1995].

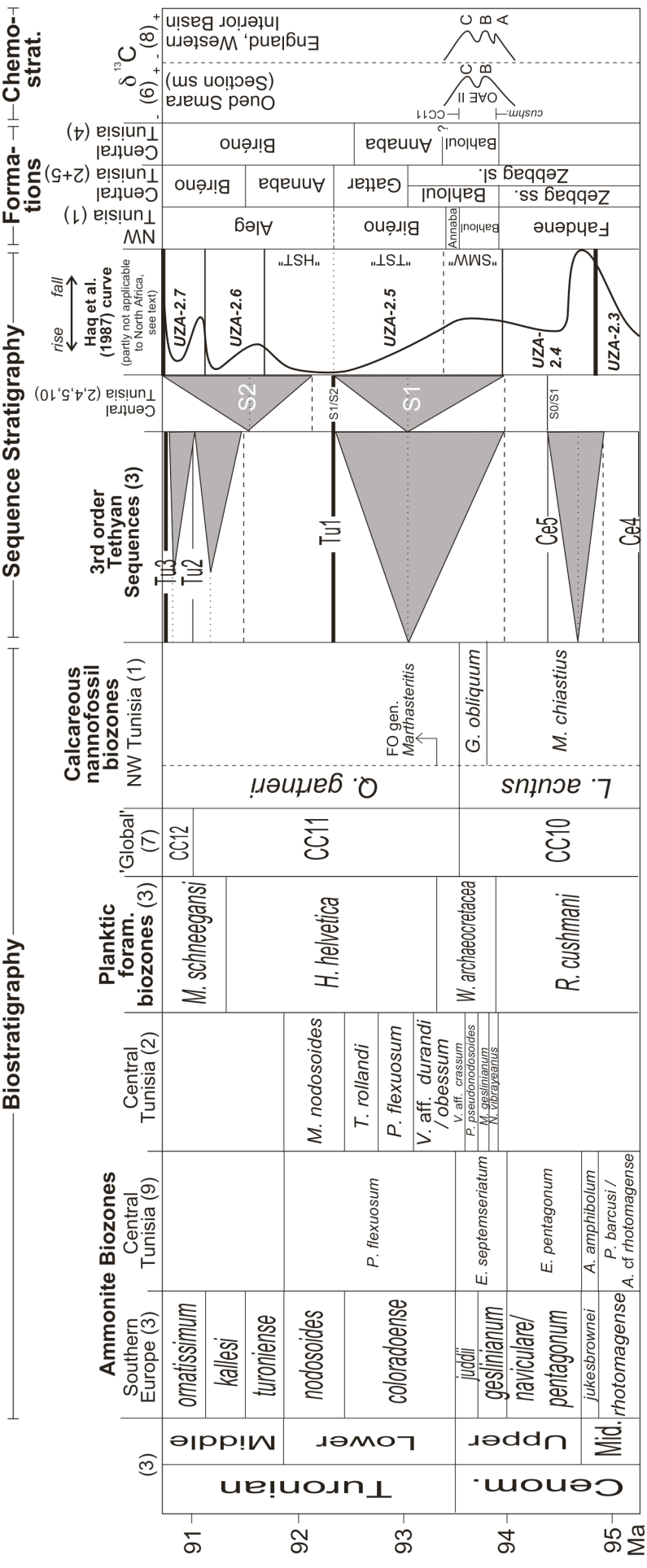
Biostratigraphy
Sequence Stratigraphy
Forma-tions
Chemo-strat.
Ammonite Biozones
Southern Europe (3)
Central Tunisia (9)
Central Tunisia (2)
Planktic foram. biozones (3)
'Global' (7)
Calcareous nannofossil biozones NW Tunisia (1)
3rd order Tethyan Sequences (3)
Central Tunisia (2,4,5,10)
Haq et al. (1987) curve
(partly not applicable to North Africa, see text)
rise
fall
NW Tunisia (1)
Central Tunisia (2+5)
Central Tunisia (4)
Oued Smara (Section sm) (9)
England, Western Interior Basin (8)
Cenom.
Turonian
Upper
Middle
Lower
Mid.
Ma
91
92
93
94
95
omatissimum
kallesi
turoniense
nodosoides
coloradoense
juddii
geslinianum
naviculare/ pentagonum
jukesbrownei
rhotomagense
P. flexuosum
E. septemseriatum
E. pentagonum
A. amphibolum
P. barcusi / A. cf rhotomagense
M. nodosoides
T. rollandi
P. flexuosum
V. aff. durandi / obessum
V. aff. crassum
P. pseudonodosoides
M. gesliniarum
N. vibrayeanus
M. schneegansi
H. helvetica
W. archaeocretacea
R. cushmani
CC12
CC11
CC10
Q. gartneri
L. acutus
FO gen. Marthasteritis
G. obliquum
M. chiastius
Tu3
Tu2
Tu1
Ce5
Ce4
S2
S1
S1/S2
S0/S1
UZA-2.7
UZA-2.6
UZA-2.5
UZA-2.4
UZA-2.3
"HST"
"TST"
"SMW"
Aleg
Bireno
Annaba
Bahloul
Fahdene
Gattar
Zebbag ss.
Zebbag sl.
cushm.
CC11
OAE II
A
B
C

Figure 2. Sequence stratigraphy, biostratigraphic schemes and carbon isotope stratigraphy at the Cenomanian–Turonian boundary in North Africa. Data after the following authors: (1) *Nederbragt and Fiorentino* [1999]; (2) *Abdallah et al.* [2000]; (3) *Hardenbol et al.* [1998]; (4) modified after *Saidi et al.* [1997] (little biostratigraphic data); (5) *Razgallah et al.* [1994]; (6) *Accarie et al.* [1996]; (7) *Sissingh* [1977, 1978]; *Perch-Nielsen* [1979, 1983, 1985]; (8) *Lamolda et al.* [1994]; *Pratt and Threkeld* [1984]; (9) *Robaszynski et al.* [1993b, p. 416]; (10) *Maamouri et al.* [1994]. Note that *Prokoph et al.* [2001] recently proposed a significantly older chronostratigraphic age for the OAE II (96.4±1 Ma, in contrast to ~93.5 Ma in the [*Hardenbol et al.,* 1998] chart used here).

2.3. Geological setting North Africa

2.3.1. Palaeogeography

During the Late Triassic–Jurassic, the supercontinent Pangaea began to break up, with the central Atlantic and Neothethys starting to open. By Cenomanian times, opening of the North and South Atlantic commenced and the Neotethys began to close [e.g., *Baudin*, 1995]. The western Tethys and central Atlantic at C/T times are characterised by a sluggish circulation due to the narrow Palaeostrait of Gibraltar, the shallow and partly still closed connections of the Atlantic to neighbouring oceans [*Handoh et al.,* 1999] and the narrowing of the North Apulian seaway in the Tethys (Fig. 3), factors favouring the development of anoxic conditions [*Philip et al.,* 1993, 2000; *Ricou* 1995; *Baudin*, 1995]. Only when the north and south Atlantic fully openend up did deep north–south oxygen-rich currents develop, similar to the ones observed today. These currents replenished oxygen-poor areas of the Tethys [*Herbin et al.,* 1986] and together with atmospheric cooling may be one explanation for the subsequent disappearance of anoxic conditions. Deep-water production is thought to have switched from down-sinking of warm, saline water masses in equatorial regions [*Brass et al.,* 1982] to the formation of significant amounts of cold, high-latitude deep water [*Kuhnt and Wiedmann*, 1995].

2.3.2. Tectonic evolution

From the Late Triassic to about the Cenomanian North Africa was dominated by an extensional regime associated with the opening of the central Atlantic [e.g., *Oyarzun et al.,* 1997] and the separation and northward drift of the Turkish–Apulian Terrane [*Gealey,* 1988; *Guiraud et al.,* 1987]. Around C/T times a general change from extension to compression occurred in North Africa, which was related to the closing of the Neotethys and the onset of North Atlantic rifting. This resulted in the inversion of the former rift grabens from the preceding extensional phase. `Alpine' deformation intensified during the Tertiary, leading to the formation of the Atlas Fold and Thrustbelt. According to *Camoin* [1991, p. 35] deposition of the Mid-Cretaceous succession in general was structurally controlled by

- subsidence of the Saharan margin as a whole and
- differential movements of fault blocks within each segment, between a subsident proximal zone (halfgraben) and an uplifted one (thin sedimentary cover, hiati).

Details of tectonic events affecting deposition of C/T strata will be discussed in the respective country chapters below.

2.3.3. Eustatic sea-level changes

The latest Cenomanian eustatic transgression is thought to have been the most intense Phanerozoic flooding event [*Haq et al.,* 1987; *Thurow et al.,* 1992; *Gale et al.,* 2002]. Maximum sea level during the C/T interval was probably 255 m higher [*Haq et al.,* 1987] and shelf areas were twice as large as those today [*Tyson,* 1995]. High global sea level during the Mid and Late Cretaceous are related to fast Atlantic sea-floor spreading [*Thurow et al.,* 1992, p. 269] and the absence of polar ice caps during the peak of a Greenhouse cycle.

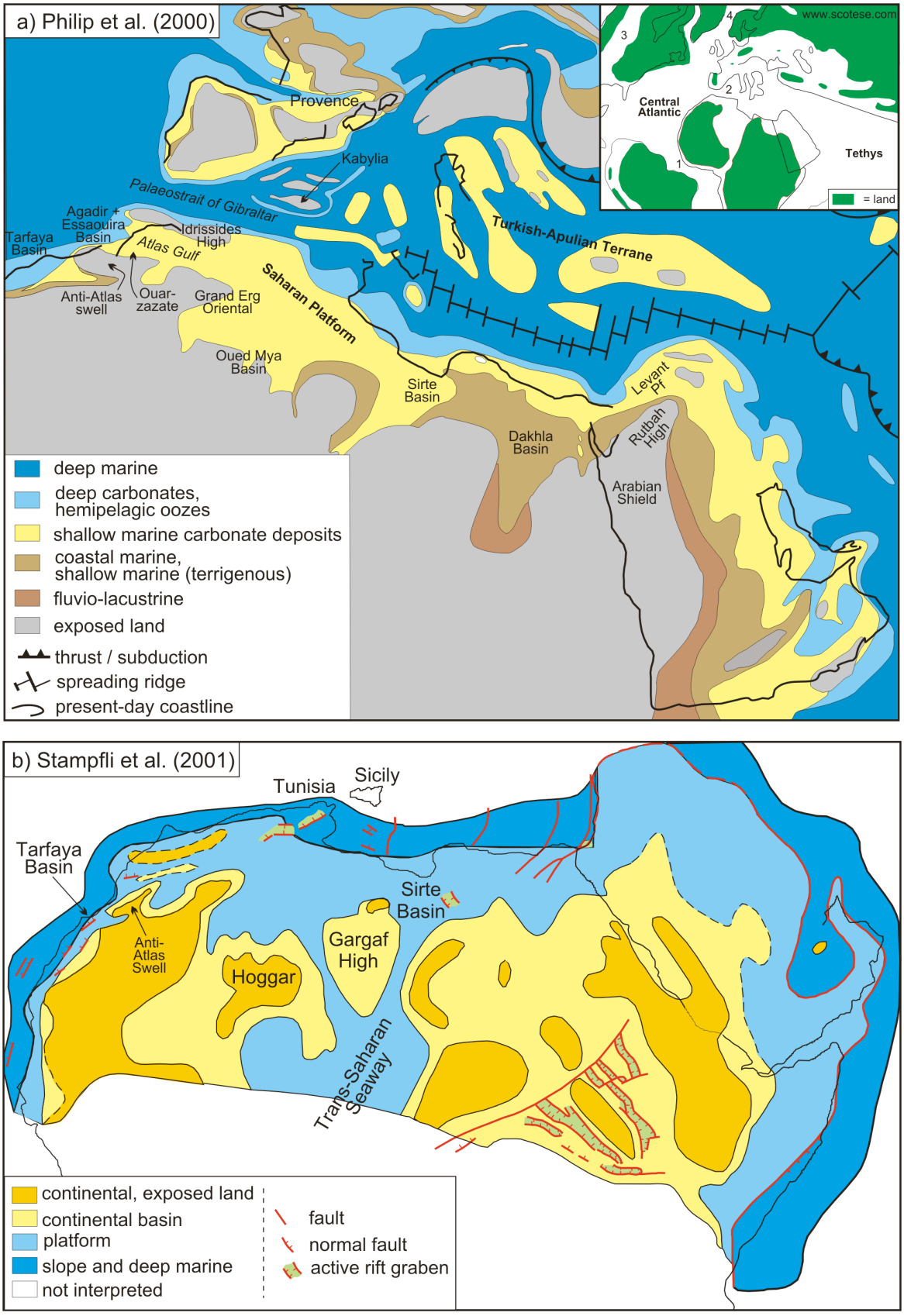

Figure 3. Late Cenomanian palaeogeography of North Gondwana. (a) Late Cenomanian, simplified after *Philip et al.* [2000]. (b) Cenomanian–Turonian, after *Stampfli et al.* [2001]. Plate tectonic reconstruction insert in upper right corner of (a) modified after http://www.scotese.com (2001). (1) Equatorial Atlantic Gateway, (2) Palaeostrait of Gibraltar, (3) Western Interior Seaway, (4) Norwegian Seaway, (5) Transsaharan Seaway.

This latest Cenomanian transgression corresponds to the post-Ce5 transgressive surface (TS) in the Tethyan eustatic sea-level chart of *Hardenbol et al.* [1998] (Fig. 2). The maximum flooding surface of this third-order cycle is developed around the mid Lower Turonian, with the succeeding sequence boundary in the upper Lower Turonian (Fig. 2). Notably, significant differences in timing of the systems tracts boundaries seem to exist in comparison with the eustatic sea-level curve of *Haq et al.* [1987] (Fig. 2).

An important palaeoceanographic event during the C/T flooding was the establishment of a marine connection between the Tethys and the opening South Atlantic via the Trans-Saharan Seaway [e.g., *Collignon and Lefranc*, 1974; *Reyment*, 1980; *Reyment and Dingle*, 1987] (Fig. 3b). This connection may have been active as early as the Late Cenomanian *Neolobites vibrayeanus* Zone [*Reyment,* 1980; *Abdallah and Meister,* 1997).

2.4. Material and methods

The database for this study consists mainly of published data, which is based on field studies, petroleum exploration wells and DSDP/ODP scientific deep-sea drilling wells. In contrast to the abundant data from the Atlantic sea floor, the C/T interval in the southern Mediterranean DSDP/ODP well locations is usually not preserved (e.g., hiatus in DSDP well 127A; Fig. 4). An exception is ODP well 967E on the Eratosthenes Seamount, south of Cyprus (Fig. 4) where the C/T interval has been penetrated and described (see below).

In addition to published data, other sources for this synthesis are proprietary petroleum company archives and our own field studies. The compilation of such data of various origins was facilitated using a special GIS North Africa database, including topographic and geological maps and well locations.

2.5. Cenomanian–Turonian organic-rich deposits in North Africa

2.5.1. General remarks

The C/T organic-rich strata in North Africa has been most intensively studied in Morocco (Tarfaya, Rif) and Tunisia (northern and central parts) where also the highest organic richnesses are reached (Fig. 4). In contrast, very little data is available for the other parts of North Africa, e.g., Algeria, Libya and Egypt. Distribution of C/T organic-rich strata here becomes more patchy and TOC concentrations are significantly lower in these black shales. The individual country C/T descriptions below are arranged geographically from west to east, structured after the following themes:

- Documentation of the likely topographic relief during C/T flooding through analysis of the regional structural evolution.
- Overview of marine C/T lithostratigraphic units and their organic matter content.
- Mapping of maximum C/T TOC values.
- Integration of carbon isotope chemostratigraphic and TOC data.
- Compilation of biostratigraphic data.
- Interpretation of the data within a sequence stratigraphic framework.
- Palaeoecological interpretation.
- Geochemical characterisation.
- Significance of the C/T as potential hydrocarbon source rock.

2.5.2. Morocco

2.5.2.1. Structural setting

Morocco's bathymetry during C/T times is a late product of the Late Triassic–Early Jurassic initial opening of the north Atlantic Ocean and the associated `failed' Atlas rifting. The Upper Triassic–Lower Jurassic synrift sediments are composed mainly of evaporites and terrigenous clastic sediments, while the postrift/passive margin sedimentation along the Moroccan Atlantic coast from

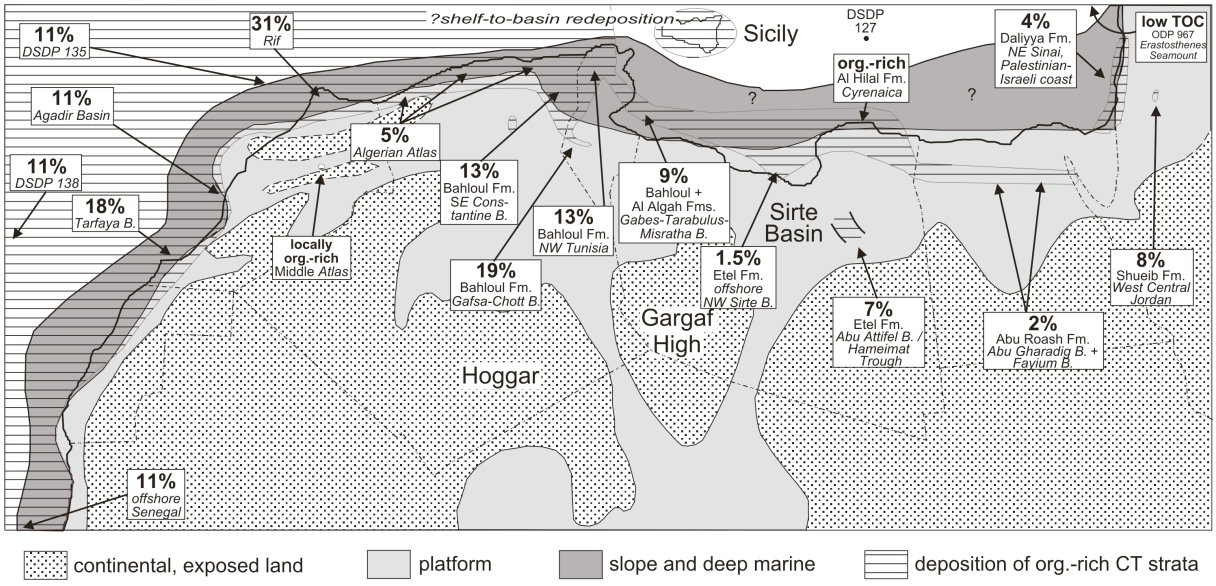

Figure 4. Deposition of organic-rich strata in North Africa during the Late Cenomanian–Early Turonian (for data references, see text). Percentages indicate known maximum TOC values. A general decrease in organic richness from west to east occurs. Palaeogeographic base map modified after *Stampfli et al.* [2001].

Middle Jurassic–Lower Cretaceous consisted of deltaic/paralic carbonates, clastics and evaporites [*Heyman*, 1990; *Ranke et al.,* 1982]. In the Tarfaya–Aaiun Basin (Fig. 5) (but uncommon in the Moroccan basins further north) the massive Lower Cretaceous deltaic deposits were subject to continued Cretaceous rotation of growth-fault structures (Fig. 6), which might also have locally affected C/T deposition and eventually led to erosion of Cretaceous strata in some areas (Fig. 6) [*Heyman,* 1990]. The diapiric rise of Triassic/Jurassic evaporites commenced as further Jurassic/Cretaceous sedimentation increased the overburden, which also could have affected C/T facies distribution in some areas within the `salt province', which is located offshore along the Moroccan Atlantic coast from Rabat to Tarfaya, around the Canary Islands and in onshore Essaouira Basin [*Stets and Wurster*, 1982]. Open-marine conditions with deposition of pelagic limestones and marls were established in the Mid Cretaceous as waters from the proto-Atlantic flooded the Triassic–Early Jurassic-created rift basins of Morocco that coincide with the coastal sedimentary basins of Morocco (e.g., Aaiun, Tarfaya, Souss-Agadir, Essaouira and Doukkala basins) [*Heyman,* 1990].

During the C/T interval, a large marine seaway existed in central Morocco representing a failed rift arm of the North Atlantic Rift System. This seaway, the so-called `Atlas Gulf' (Fig. 3) is bordered by the Anti-Atlas to the south and the Moroccan Meseta to the north, and is characterised by abrupt changes in Cretaceous thickness across normal faults, evidencing syndepositional activity [*Wurster and Stets,* 1982; *Stets and Wurster,* 1982]. Pre- and synsedimentary C/T halfgraben tectonics in the area of the Atlas orogenic system have been also described by *Ensslin* [1992] and *Charrière* [1996] (extensional Infracretaceous tectonics), resulting in fragmentation into disparate small tectonic blocks. In spite of high and differential subsidence rates, the general sedimentation pattern seems to have been mainly controlled by eustatic fluctuations of the sea level [*Ensslin,* 1992]. Structural inversion commenced in the post-Turonian and lasted until the Quaternary [*Wurster and Stets,* 1982; *Stets and Wurster,* 1982].

2.5.2.2. Distribution and characteristics of C/T Corg strata

Organic-rich C/T strata were deposited in several parts of Morocco, in particular along the Atlantic coast in the Tarfaya–Aaiun Basin, in the Agadir and Essaouira basins, along the Palaeostrait of Gibraltar and, very locally, in the Atlas Gulf (Fig. 3 and Fig. 5). In addition, C/T black shales also occur in the neighbouring Atlantic regions, as recorded in exploration and deep-sea DSDP/ODP wells

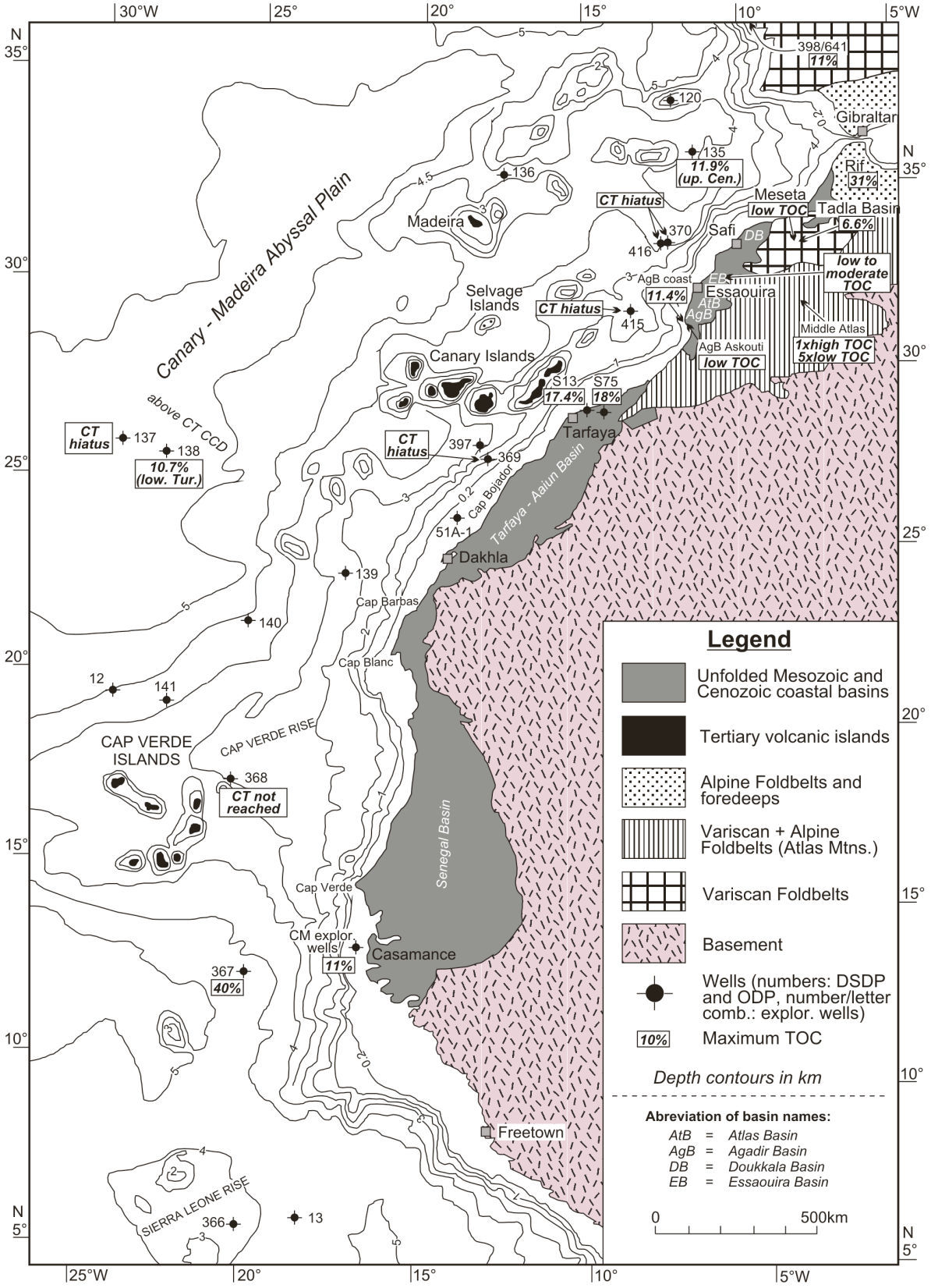

Figure 5. Maximum organic richness of C/T deposits in Morocco and neighbouring areas, including DSDP/ODP wells in the NW African Atlantic. Base map modified after *Ranke et al.* [1982]. TOC data sources: Agadir Basin/AgB [*Herbin et al.,* 1986], Askouti [*Wurster and Stets,* 1982, p. 445], Casamance [*Kuhnt et al.,* 1990; *Holbourn et al.,* 1999b], DSDP 135/137/138/367 [*Herbin et al.,* 1986; *De Graciansky et al.,* 1986], Essaouira Basin/EB [*Wiedmann et al.,* 1982, p. 478], Meseta [*Wiedmann et al.,* 1982, p. 480], Middle Atlas [*Charrière et al.,* 1998], Rif [*Herbin et al.,* 1986; *Kuhnt et al.,* 1990; *Thurow and Kuhnt,* 1986], S13 [*Kuhnt et al.,* 1990, 1997] and S75 [*Luderer,* 1999].

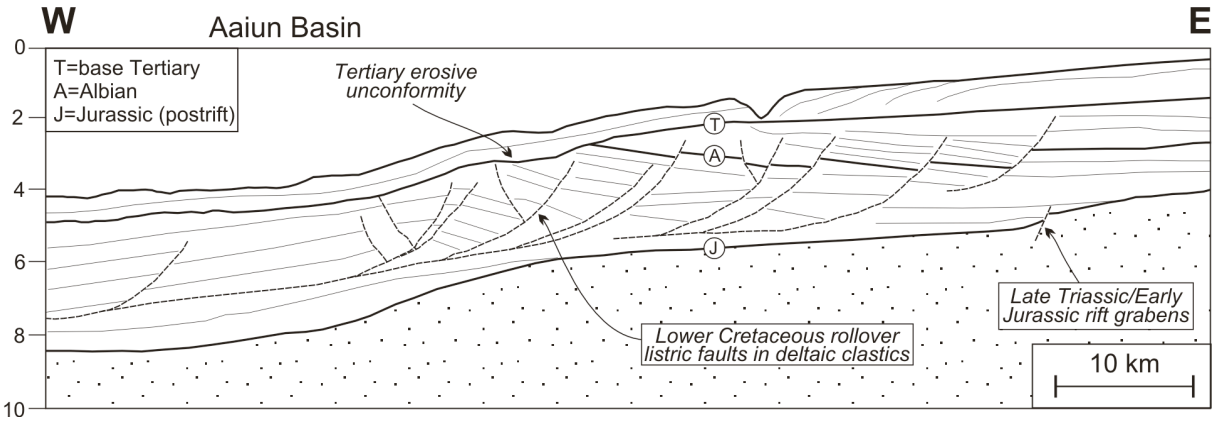

Figure 6. Sketch of the Atlantic margin Aaiun Basin (S-Morocco/Western Sahara) based on seismic (from [*Heyman,* 1990]). A Late Triassic/Early Jurassic halfgraben relief is overlain by Jurassic carbonates and Early Cretaceous deltaic clastics in which syndepositional rollover structures are developed. The Cenomanian–Turonian interval is located somewhere between the Albian (A) and base Tertiary (T) reflectors, and its deposition may still have been affected by the Early Cretaceous rollover halfgraben relief.

(e.g., offshore Senegal, Cape Verde Basin, Galicia margin, Subbetic/Penibetic in southern Spain) (Fig. 5). The duration of the oxygen-poor phase and the organic-matter accumulation rates reach their maximum along the Atlantic coast between the Cap Verde and Tarfaya basins [*Kuhnt et al.,* 1990; *Kuhnt and Wiedmann,* 1995] (Fig. 5). In the other localities mentioned above, the period of the OM accumulation was much shorter and organic-rich units much thinner, although the maximum TOC content remained high [*Kuhnt and Wiedmann,* 1995] (Fig. 5 and Fig. 7).

2.5.2.2.1. Tarfaya basin

The Cenomanian to Campanian succession in the hemipelagic Tarfaya Basin contains an exceptionally thick (700–800 m) unit of potential petroleum source rock [*Leine,* 1986] exhibiting the world's highest accumulation rates of organic matter for the Cenomanian–Turonian [*Kuhnt et al.,* 2001]. Within the C/T, peak TOC values of up to 18% are reached within the C/T isotopic excursion, although organic-richness is high also in the Cenomanian and Turonian strata under-and overlying the OAE (e.g., up to 6–12% in the *helvetica* Zone) (Fig. 7). The C/T deposits in the Tarfaya Basin consist of dark brownish-grey, laminated, kerogenous chalks, alternating with non-laminated lighter coloured, often nodular limestones containing a lower kerogen content. Intercalated are concretions and lenses of chert and siliceous limestone. Main components of the kerogen-rich chalks are faecal pellets containing abundant coccoliths, tests of foraminifera, kerogen-flasers and a carbonate-matrix mainly composed of coccoliths and micrite [*Leine,* 1986]. The strata was subdivided into various different microfacies by *El Albani et al.* [1999a].

2.5.2.2.2. Agadir and Essaouira basins

Organic-rich marls, limestones and siliceous C/T strata with up to 11% TOC (immature OM; [*Herbin et al.,* 1986]) occur at outcrop in the Agadir Basin just north of the town Agadir [*Wiedmann et al.,* 1978, 1982). The unit contains several characteristic m-to dm-scale shell beds, turbidites and slumping features. An outer shelf or deeper environment is assumed [*Wiedmann et al.,* 1978, 1982]. Only 20 km to the east, at the Askouti section, organically poor, inner shelf deposits occur which consist predominantly of monotonous, hard calcareous marls and oyster beds [*Behrens et al.,* 1978; *Stamm and Thein*, 1982; *Wurster and Stets,* 1982; *Stamm,* 1981], evidencing the rapid eastward shallowing here. The organic richness of the C/T interval also decreases northwards from the Agadir Basin towards the Essaouira Basin. There, the strata is characterised by only moderate to low organic values with fossils mostly absent [*Wiedmann et al.,* 1978, 1982] (Fig. 5).

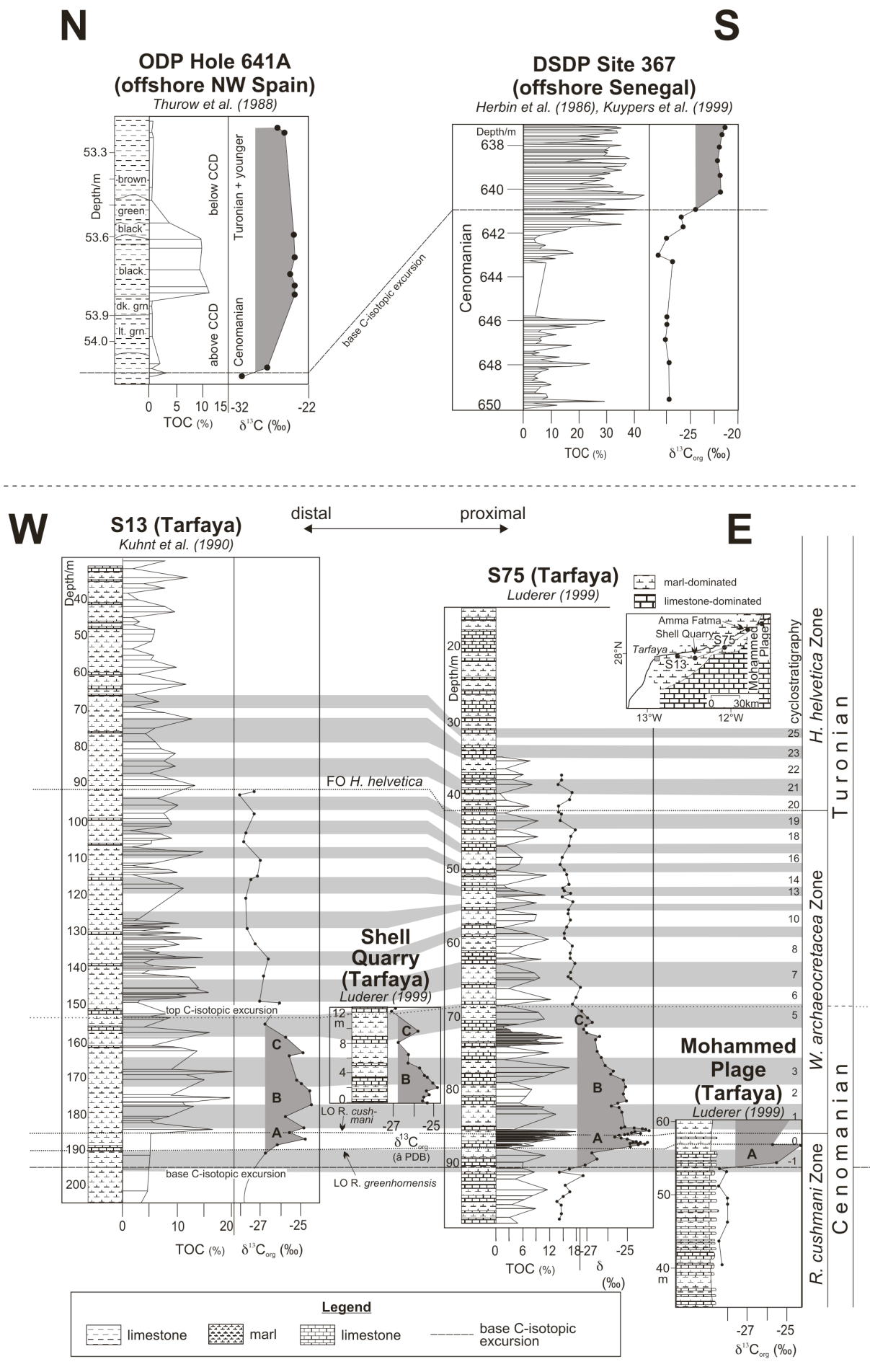
N
S
ODP Hole 641A
(offshore NW Spain)
Thurow et al. (1988)
DSDP Site 367
(offshore Senegal)
Herbin et al. (1986), Kuypers et al. (1999)
Depth/m
53.3
53.6
53.9
54.0
brown
green
black
black
dk. grn
lt. grn
below CCD
above CCD
Turonian + younger
Cenomanian
base C-isotopic excursion
TOC (%)
δ13C (‰)
Depth/m
638
640
642
644
646
648
650
Cenomanian
TOC (%)
δ13Corg (‰)
W
E
distal
proximal
S13 (Tarfaya)
Kuhnt et al. (1990)
S75 (Tarfaya)
Luderer (1999)
marl-dominated
limestone-dominated
Amma Fatma
Shell Quarry
Tarfaya
S75
S13
Mohammed Plage
28°N
13°W
12°W
30km
cyclostratigraphy
FO H. helvetica
top C-isotopic excursion
base C-isotopic excursion
Shell Quarry (Tarfaya)
Luderer (1999)
LO R. cush-mani
LO R. greenhornensis
δ13Corg (à PDB)
Mohammed Plage (Tarfaya)
Luderer (1999)
H. helvetica Zone
W. archaeocretacea Zone
R. cushmani Zone
Turonian
Cenomanian
Legend
limestone
marl
limestone
base C-isotopic excursion

Figure 7. Distribution of organic matter within the C/T-boundary interval in Morocco and the NW African Atlantic in relation to available biostratigraphic data and the characteristic C/T carbon isotope peak. Cyclostratigraphy and Tarfaya correlation from *Luderer* [1999]. Facies distribution Tarfaya after *Kuhnt and Wiedmann* [1995]. Location map for DSDP/ODP Sites 367/641 in Fig. 5. Tarfaya base map from *Luderer* [1999].

Wiedmann et al, [1978, 1982] assumes a middle shelf setting without major upwelling for the Eassaouira Basin.

2.5.2.2.3. Atlas Gulf, Meseta, Tadla Basin

Within the Atlas Gulf area, *Charrière et al.* [1998] studied several C/T sections in the southern Middle Atlas and the High Moulouya where an infralittoral setting on a proximal carbonate patform existed (Fig. 3). In most sections, the C/T interval consists of shallow marine bioclastic limestones, gypsum and marls. Only in one section (C3 of [*Charrière et al.,* 1998]) organic-rich marls of *W. archaeocretacea* Zone age occur, which are overlain by lean calcareous marls with bivalves. The organic-rich interval is characterised by increased numbers of planktic foraminifera, possibly indicating a local deepening in combination with reactivation of the nearby southern Middle Atlas Fault [*Charrière et al.,* 1998, p. 560] with subsidence in the form of synsedimentary halfgraben tectonics [*Ensslin,* 1992 and *Charrière,* 1996], as e.g., contemporaneously in Tunisia (see below).

A similar case of local black shale development in the Atlas Gulf within a predominantly organically lean, dolomitic inner shelf setting is developed about 100 km to the south near Ouarzazate [*Stamm and Thein,* 1982, pp. 462, 468]. Here, a Turonian, biostratigraphically poorly dated, euxinic lagoonal facies with dolomitic laminites occurs (Fig. 3). This facies however is essentially different from the pelagically influenced laminites of the Atlantic coastal region because at Ouarzate the facies is mainly dolomitic, partly even extremely saline, however, frequent (radiolarian?) chert layers and nodules, as well as dubious relics of foraminifers indicate some kind of pelagic realm also for this area [*Stamm and Thein,* 1982]. On the other hand, plant debris may have played an important role in the deposition of organic material, which unfortunately is no longer directly demonstrable because of alteration due to weathering. Nevertheless, numerous indications, such as missing benthos, pseudomorphs of limonite after pyrite and marcasite, silicification and very high concentrations of typical trace elements such as Mo (up to 24 ppm), may be regarded as remnants of a bituminous facies [*Stamm and Thein,* 1982].

The northeastern part of the Atlas Gulf (Fig. 3) is located in the Meseta and Tadla Basin which are both characterised by only gently deformed Meso- and Cenozoic strata. In the Meseta, the facies consists generally of inner to middle shelf, organic-poor, biodetrital, dolomitic limestones and silty marls [*Busson,* 1984; *Wiedmann et al.,* 1978; *Thein,* 1988] (Fig. 5). However, from the Tadla Basin, which is part of the Meseta (Fig. 5), ONAREP reported occurrences of organic-rich, though thermally immature C/T deposits with TOC of up to 6.6% (www.onarep.com), possibly indicating the local development of anoxic/dysoxic conditions here.

2.5.2.2.4. Rif

In the strongly deformed northern Moroccan Rif and the Gibraltar Arch area, the C/T deposits consist of organic-rich (up to 31% TOC, type II kerogen) black laminites with a strong siliceous component (radiolarites and silifications) due to high biogenous productivity [*De Wever et al.,* 1985; *Herbin et al.,* 1986; *Kuhnt et al.,* 1990; *Thurow and Kuhnt,* 1986]. The strata was deposited in environments ranging from outer shelf, slope, to deep-sea facies, above and below the CCD, and included abundant redeposition, also of organic matter, within a turbiditic deep-sea fan system [*Kuhnt et al.,* 1990]. Notably, organic-rich sedimentation here is not confined to a particular palaeogeographic setting [*Thurow and Kuhnt,* 1986]. As a result of the `Alpidic' deformation, the black shales in this area are thermally highly mature and have partly reached a low-grade metamorphic stage.

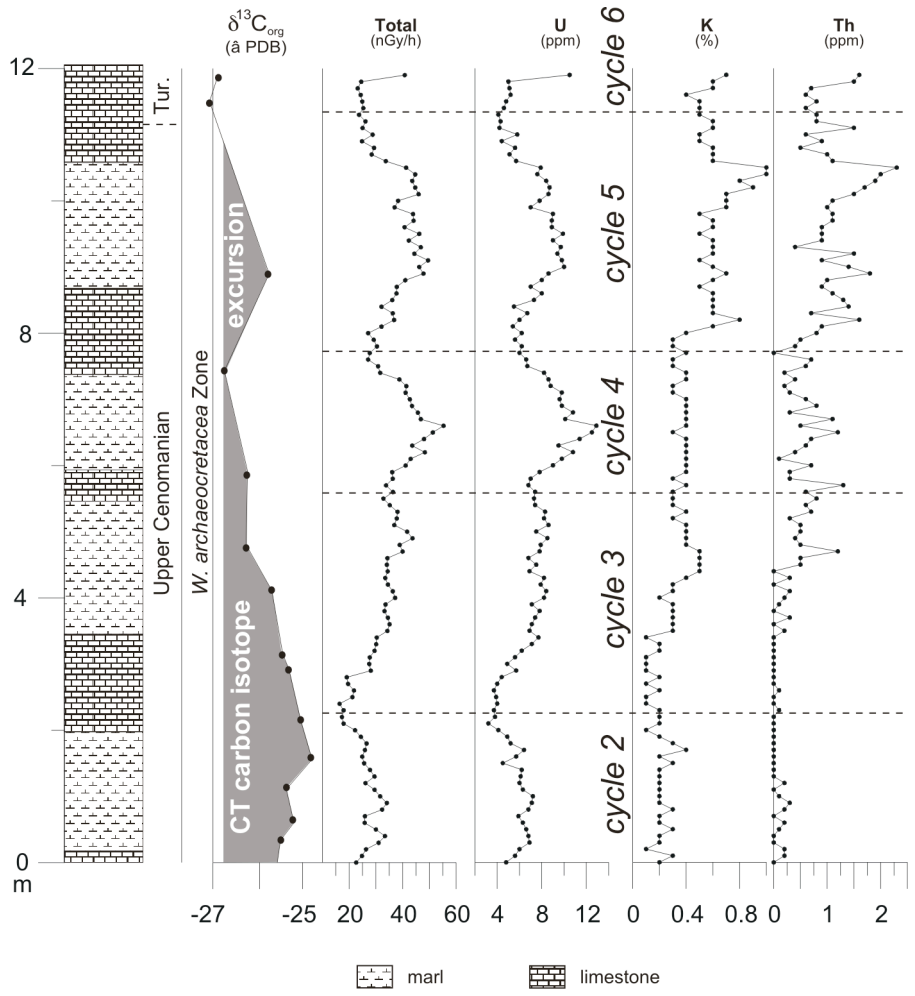

Figure 8. New spectrogamma-ray data from the uppermost Cenomanian limestone-black shale alternation in the ONAREP-Shell-Quarry (30 km E' Tarfaya). The total -ray log shows a characteristic cyclicity, which previously has been interpreted by *Kuhnt et al.* [1997] as a Milankovitch obliquity (39 ka) signal. The spectrogamma data indicates that this cyclicity is mainly due to changes in the (most probably authigenic) uranium content and less so in the potassium and thorium contents. Interestingly, the latter two elements become gradually more abundant upsection and may reflect a progressive increase in detrital material in the middle and upper part of the CTBE here.

2.5.2.2.5. NW African Atlantic margin

Organic-rich C/T strata occurs in several DSDP/ODP wells in the Atlantic at the NW African margin, including DSDP Site 367 (Cape Verde Basin; also in offshore Senegal exploration wells), DSDP Site 138 (500 km west of Canary Islands), DSDP Site 398 and ODP Site 641 (Galicia Margin) (for locations and references, see Fig. 5). Organic-richness reaches its optimum in Site 367 with a maximum TOC of 40 wt.%, while peak TOC values in the other wells lie around 11 wt.%. The C/T black shale at the Galicia Margin is extremely thin (30 cm, abundant radiolara; [*Thurow et al.,* 1988; *Thurow,* 1988]), while at Sites 138 and 367 a thick black shale column exists in the Cenomanian–Campanian, comparable to the Tarfaya basin (see above).

2.5.2.3. Biostratigraphy, cyclostratigraphy and sequence stratigraphy

In the hemipelagic sections of Morocco, the C/T carbon isotopic excursion can be best dated by planktonic foraminifera and is located in the interval from the uppermost *R. cushmani* Zone to the lower *W. archaeocretacea* Zone (Fig. 7). The *R. cushmani* Zone can be further subdivided using the last occurrence of *R. greenhornensis*, which is a distinct datum in the upper part of the *R. cushmani* Zone and is located in the ascending limb of the C/T carbon isotopic excursion [*Kuhnt et al.,* 1997;

Luderer, 1999] (Fig. 7). In Tarfaya, the C/T succession is characterised by the alternation of OC-rich chalks and OC-poorer limestone beds, which is clearly reflected on density and -ray log data. This cyclicity has been used for cyclostratigraphic subdivison of the C/T interval (`zone R', [*Leine*, 1986]) and has been interpreted by *Kuhnt et al.* [1997] and *Luderer* [1999] as a Milankovitch obliquity (39 ka) signal. Notably, recent results now seem to favour a precessional origin of these cycles (own unpubl. data, Sadat Kolonic).

These cycles are also reflected in a high resolution spectrogamma-ray data set (Fig. 8) recently recorded in the Shell Quarry, about 30 km east of Tarfaya (Fig. 7), where an alternation of C/T boundary organic-rich marls and marly limestones is exposed. The spectrogamma data indicates that this cyclicity in the total -ray intensity is mainly due to changes in the (most probably authigenic) uranium content and less so of the potassium and thorium contents.

Reconstruction of the sequence stratigraphic history in hemipelagic areas, including the Tarfaya Basin during the Cenomanian–Turonian [*El Albani et al.,* 1999b], is complicated because of monotonous lithologies, lack of subaerial exposure during sea-level lowstands and absence of sequence stratigraphic geometries [*Lüning et al.,* 1998a]. Identification of sea-level changes is easier in shallower facies where, however, preservation of fossils is often poor and hence biostratigraphic data scarce. In Morocco, the shallow marine Atlas Gulf provides important information about the C/T sea-level changes. *Charrière et al.* [1998] studied the C/T in the Middle Atlas and the High Moulouya and found a strongly diachronous onset of deposition during the C/T transgressive systems tract (TST) (post-Ce5 TS; Fig. 2), ranging from the Late Cenomanian to the Early Turonian (*N. vibrayeanus* Zone to *W. archaeocretacea* Zone; Fig. 2). *Charrière et al.* [1998] interpret the diachronous onset of the flooding as a result of intense palaeotopographic variations due to halfgraben tectonics. The earliest initial flooding date (*N. vibrayeanus* Zone, around planktonic foraminiferal zonal boundary of *cushmani* and *archaeocretacea*, Late Cenomanian) most probably reflects the flooding of the deepest palaeodepressions/halfgrabens and must be considered to provide an approximate or at least youngest age for the base of the transgressive systems tract in the Moroccan sequence stratigraphic development, including hemipelagic areas such as the Tarfaya Basin.

This age of *N. vibrayeanus* Zone in Morocco corresponds well with the age of the latest Cenonmanian transgressive surface in Tunisia (post-Ce5 TS) as well as with the 3rd order Tethyan sea-level chart [*Hardenbol et al.,* 1998] (Fig. 2). Furthermore, also the stratigraphic position of the maximum flooding surface (mfs) in Morocco seems to be comparable to the one in Tunisia and in the Tethyan sea-level chart. This interpretation is based on the occurrence of an extraordinary horizon with meter-size nodules in the Amma Fatma section in the Tarfaya Basin, the origin of which *El Albani et al.* [1997] assume to be linked to minimum sedimentation and maximum concretionary growth. Biostratigraphically, this horizon in the Amma Fatma section lies within the *coloradoense* Zone (ammonites)/*H. helvetica* Zone (plankt. foraminifera) [*Holbourn et al.,* 1999a], which corresponds well with the mfs interpreted in Tunisia and in the eustatic Tethyan sea-level chart of *Hardenbol et al.* [1998]. Based on the good match of the Moroccan sea-level development with the Tunisian and Tethyan ones, we therefore assume that the *Hardenbol et al.'s* [1998] Tethyan curve documents well the C/T sea-level history in all of west and central North Africa, and possibly even in eastern North Africa.

As a result of apparent global-scale variations in timing of sequence stratigraphic events and other inconsistencies [e.g., *Miall,* 1991, 1992], the original Cretaceous `eustatic' sea level curve of *Haq et al.* [1987] has been refined and separate charts developed for the Tethys region (Fig. 2) and the boreal North America/Europe [*Hardenbol et al.,* 1998]. While the biostratigraphic ages of the Turonian sequence boundaries are similar in both the Boreal and Tethyan charts, a major diachroneity seems to exist for the Late Cenomanian sequence boundary Ce5 and the subsequent transgressive surface and maximum flooding surface (Fig. 2). The `eustatic' third-order sequence boundary (at the base of UZA-2.5, about *N. vibrayeanus* Zone) is several hundred thousand years younger than the `Tethyan' one (Ce5, *E. pentagonum* Zone) and roughly coincides with the transgressive surface in the `Tethyan' chart (Fig. 2). While the `Tethyan' chart correctly reflects the major transgression around the C/T boundary in Morocco and interprets the maximum flooding surface somewhere in the middle of the *coloradoense* Zone, the `eustatic' chart contains a long period of a slowly falling sea level and the onset of transgression only in the uppermost *archaeocretacea* Zone (lowermost Turonian), which does not match with the observations from Morocco and Tunisia. Also, the timing of the subsequent sb

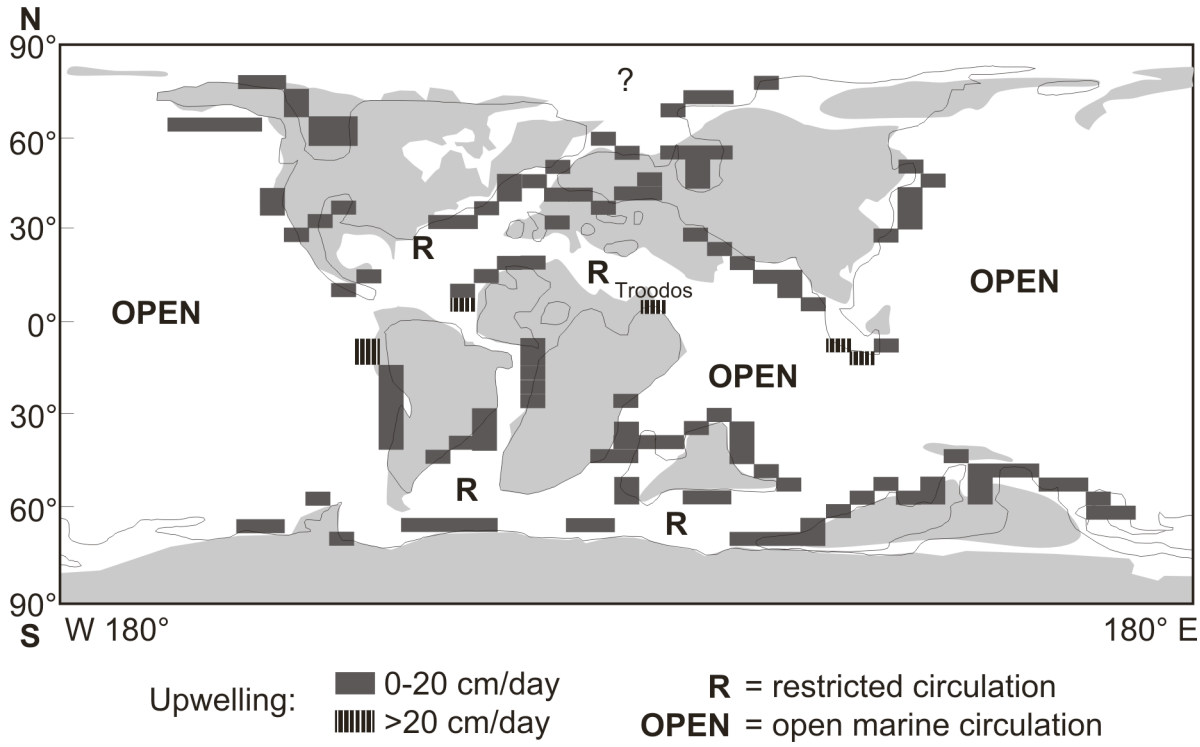

Fig. 9. Simulated mean annual Mid-Cretaceous coastal upwelling [after *Kruijs and Barron*, 1990].

does not match in the `eustatic' and `Tethyan' charts (Fig. 2); notably, the age of the latest Cenomanian sequence boundary in the *Haq et al*. [1987] sea-level curve represents the boreal development and does not characterise the North African development.

For this reason, regional European sea-level curves are not considered to properly reflect the North African sea-level history. Previously, *Kuhnt et al.* [1997] have interpreted large scale (20–120-m-thick) density log cycles in the Tarfaya Basin to be a consequence of sea-level changes, based on correlation with a C/T sea-level curve from the Paris Basin [*Juignet and Breton,* 1992]. The Paris Basin curve includes an additional sequence boundary at the C/T boundary, which, however, seems to have no expression in North Africa, according to available data. Rather than being controlled by sea-level and forming a link between Cretaceous sea-level and climate, as was suggested by *Kuhnt et a*l. [1997], the large scale density cycles may be a record of climatic trends, in the same way as the superimposed higher-frequency Milankovitch cycles. Although a climato-eustatic coupling for orbitally induced high frequency sea-level changes has been described for the Cretaceous [*Jacobs and Sahagian,* 1993], the associated sea-level amplitudes of several meters should be too small to be detected in the hemipelagic [*Quesne and Ferry*, 1995; *Glancy et al.,* 1993; *Strasser,* 1994; *Batt,* 1996]. In further contrast to *Kuhnt et al.'s* [1997] interpretation for the Tarfaya Basin, we do not assume the anoxia to be restricted to the highstand systems tract (HST) but to be related to higher frequency (sea-level independent) palaeoeceanographic/climatic cycles, as evidenced by the thick black shale succession with repetitive high values, alternating with lower ones throughout at least the upper Cenomanian to middle Turonian (Fig. 7). In shallower facies (e.g., Agadir Basin), we consider black shale deposition to be predominantly related to the basal TST and not to the HST (see below).

In contrast to the black shales restricted to the C/T boundary, the shallower, coastal (biostratigraphically poorly dated) Turonian organic-rich deposits in the Atlas Gulf at Ouarzazate are considered by *Stamm and Thein* [1982, p. 468] to have been deposited around the mfs (maximum transgression, uppermost TST).

2.5.2.4. Carbon isotope chemostratigraphy

A high-resolution correlation of four characteristic C/T sections and wells from the Tarfaya Basin based on carbon isotope data, (Milankovitch) cyclostratigraphy and biostratigraphy has been compiled

by *Luderer* [1999] (Fig. 7) to which published and hitherto unpublished TOC data was added. According to *Luderer* [1999], the C/T carbon isotope excursion includes six obliquity cycles, together representing 234 ka.

The threefold subdivision, recorded in the 13C curves of the Western Interior Basin and England [*Pratt and Threkeld,* 1984; *Lamolda et al.,* 1994], also appears to be developed in the majority of the studied Moroccan C/T sections (marked A, B and C in Fig. 7). Another, possibly less equivocal, method of correlation is based on the phases of `initial strong increase' (base C-isotopic excursion in Fig. 7, latest *R. cushmani* Zone) and `terminal gradual decrease' (top C-isotopic excursion in Fig. 7, Early Turonian) of 13C values to pre-excursion values.

Although maximum TOC values in almost all Tarfaya sections are reached within the carbon isotope excursion, the vertical trends in the isotope and TOC profiles in general do not match. This underlines the stratigraphic character of the carbon isotope distribution, rather than being controlled by local geochemical processes.

2.5.2.5. Palaeoecology

2.5.2.5.1. Larger-scale NW Africa

Morocco and the NW African Atlantic margin provide the opportunity to study C/T deposits along a depth transect, with a bathymetric range from shallow marine (Atlas Gulf), over hemipelagic shelf (Tarfaya Basin) to the deep sea (e.g., DSDP 367). Furthermore, the northernmost and eastern parts of Morocco lie in a transition zone between the North Atlantic and Tethys regimes, where the exchange of water masses between these two oceanographic systems was probably hampered by the Palaeostrait of Gibraltar and the shallow Atlas Gulf (Fig. 3) [*Philip et al.,* 2000; *Stampfli et al.,* 2001). Although a first deepwater connection between Central and South Atlantic was slowly beginning to form during the Cenomanian [*Wagner and Pletsch*, 1999], the proto North Atlantic during the C/T must generally still be considered as a marginal oceanic basin with limited connections to other oceans [*Thurow et al.,* 1992] (Fig. 3). An intense upwelling regime for the eastern Atlantic margin, extending from about Senegal in the south to Morocco in the north, was modelled by *Kruijs and Barron* [1990] (see also, their Fig. 8) ([*Thurow et al.,* 1992], Fig. 9). Palaeoecological analysis of benthic foraminifera faunas along the NW African margin confirm the substantially enhanced primary productivity that has existed there in outer shelf to upper slope settings in Cenomanian–Turonian times and, in fact, during most of the Cenomanian–Coniacian ([*Kuhnt and Wiedmann*, 1995; *Wiedmann et al.,* 1978, 1982; *Einsele and Wiedmann*, 1982]; in contrast to views of, e.g., [*Brumsack and Lew*, 1982; *Bralower and Thierstein*, 1984, 1987; *Sinninghe Damsté and Köster*, 1998] who assume a non-elevated productivity setting). Part of the evidence is that the Tarfaya und Agadir basins are characterised by a `*Gabonita* benthic foraminiferal biofacies', which is regarded as a typical assemblage of high-productivity zones [*Kuhnt and Wiedmann,* 1995]. The coastal belt from northern Morocco (Rif), Algeria to Tunisia, however, is characterised by the `*Tappanina* biofacies', which is thought to indicate only slightly enhanced phytodetritus flux and oxic or mildly dysaerobic bottom waters [*Kuhnt and Wiedmann*, 1995; *Holbourn et al.,* 1999a]. The maximum northward extension of this high productivity (`*Gabonita* biofacies') zone in the eastern Atlantic was reached during the Early Turonian, coinciding with maximum sea level and the highest atmospheric temperature in the Late Cretaceous. A contraction of this zone to equatorial latitudes took place in the Early Campanian [*Holbourn et al.,* 1999a] where deposition of organic-rich strata continued throughout the Upper Cretaceous and into the lower Palaeogene [e.g., *Wagner and Pletsch,* 1999].

The upwelling regime has to be regarded as the basis for deposition of the thick upper Cretaceous black shale succession along the Atlantic Moroccan margin. In other areas, away from this upwelling zone (e.g., ODP 641 at the Galicia Margin), the formation of potential petroleum source rocks is restricted to a short time span of a few hundred thousand years at the C/T boundary, and OM accumulation may have been largely controlled by favourable preservation conditions as based on trace metal patterns [*Brumsack and Thurow*, 1986, *Holbourn et al.,* 1999a]. Also, a drastic change from the dominance of terrestrial organic matter in pre-C/T times to marine organic matter during the

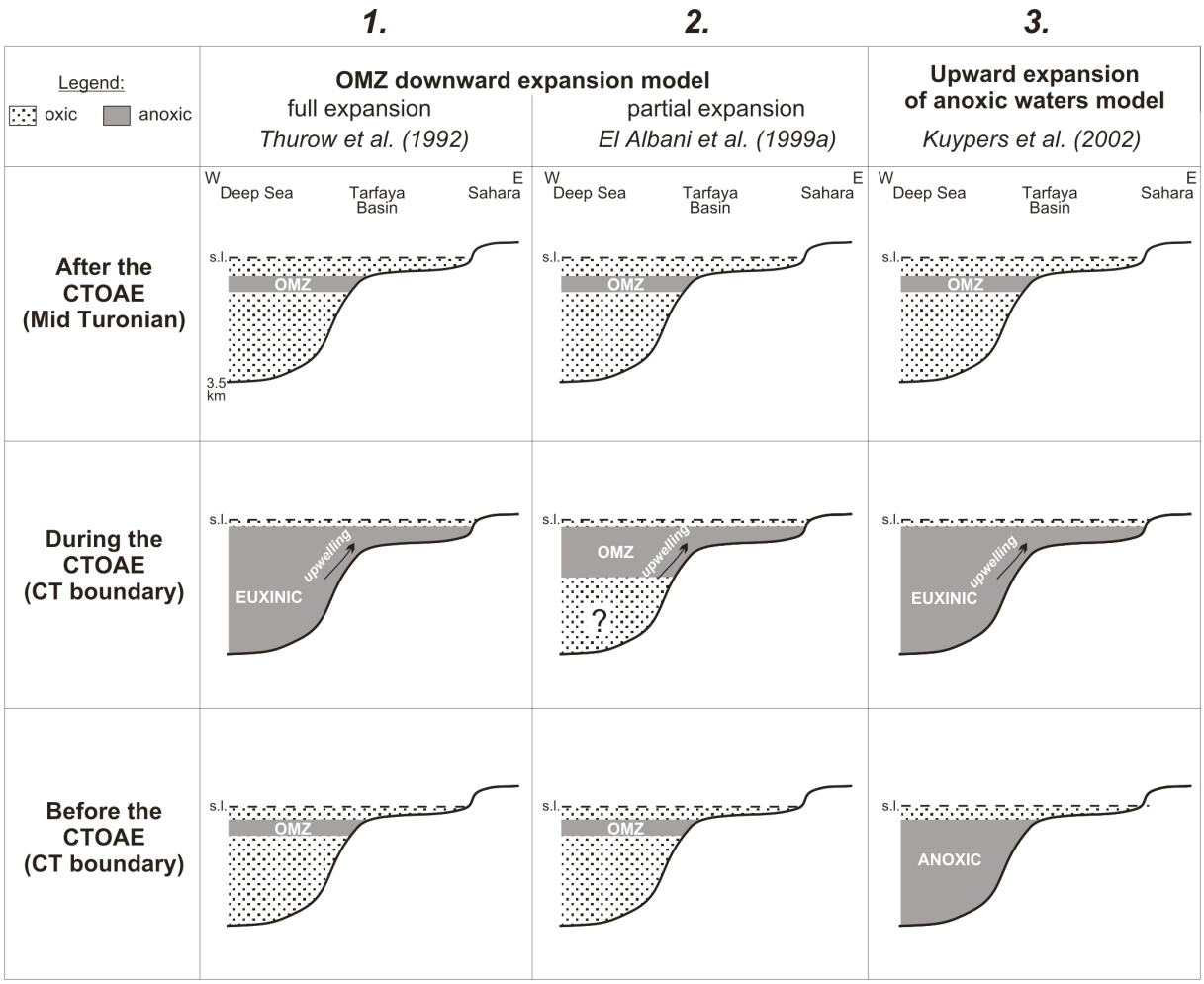

Figure 10. Overview of the main palaeoceanographic models discussed in the literature for the C/T anoxic event at the Moroccan Atlantic margin.

C/T occurred at the Galicia Margin [*Stein et al.,* 1988]. The short-lived C/T event is, therefore, masked by the thick black shale packages in the high productivity zones and complicating identification of the global (vs. regional) mechanisms for the origin of the C/T event along the NW African coast.

The three main oceanographic models discussed for the C/T OAE at the Moroccan Atlantic margin are summarized in Fig. 10. The first two models assume an expanded oxygen minimum zone (OMZ) during the C/T OAE, which invaded the shelf as a result of the latest Cenomanian transgression. In the first model, the OMZ expanded downwards to the deep-sea floor to depths of up to 3500 m [e.g., *Thurow et al.,* 1988; 1992], whereas in the second model only part of this depth is reached, whereby the OMZ overlies an oxic water mass [*El Albani et al.,* 1999a]. The third model, in contrast, proposes during the C/T event an upward expansion of an anoxic water mass that had already existed before the event but was limited to greater depth [*Kuypers et al.,* 2002]. The presence of a euxinic water column in the proto southern North Atlantic during the C/T extending from the sea floor up into the photic zone (as included in models 1 and 3) is indicated by the presence of molecular fossils from photosynthetic green sulphur bacteria in (bacteriochlorophyll pigments *Isorenieratene*, e.g., *Koopmans et al.,* 1996b]) reported from North Atlantic deep-sea wells (e.g., DSDP Site 367) [*Sinninghe Damsté and Köster,* 1998] and the Tarfaya Basin [*Kolonic et al.,* 2002].

2.5.2.5.2. Moroccan coastal basins

Molluscs, microfaunal assemblages and (up to 80%) smectite-dominated clay mineral assemblages in the C/T sections of the Tarfaya Basin indicate outer shelf to upper bathyal depth of the order of 200–300 m [*Einsele and Wiedmann,* 1982; *Kuhnt et al.,* 1990; *Holbourn et al.,* 1999a; *El Albani et al.,*

1999a]. The sediments here were partly affected by storm wave and current activity, as evidenced by occasional hummocky cross stratification in the carbonates and millimeter-scale erosional features. Cyclical changes of anoxic and more oxygenated sea floor conditions are indicated by the presence of alternations of laminated, kerogen-rich chalks and light coloured kerogen-poor limestone beds (thicknesses centimeter- to meter-scale) and, on a finer scale, alternations of dark and light-coloured submillimeter- to millimeter-scale laminae [*Leine,* 1986; *Kuhnt and Wiedmann,* 1995; *Luderer*, 1999]. Many of the darker, organic-rich beds are benthos-free, but planktic foraminifera are always present [*Kuhnt et al.,* 1997; *Luderer*, 1999].

The sedimentation rates in the Tarfaya C/T black shales were relatively high, namely 6.4–8.0 cm/ka in the proximal part of the basin and 11.8 cm/ka in the distal part (S13 well) and may indicate a high productivity setting [*Leine,* 1986; *Kuhnt et al.,* 1997]. Calculations by *Luderer* [1999] based on a cyclostratigraphic timeframe show that the highest palaeoproductivity regime existed during the carbon isotope excursion, with the exception of the lowermost part. The same author also demonstrated that with increasing OC accumulation rates the percentage of heterohelicids of the total planktic forams also increases. In contrast, the planktic foraminifera faunas of organically poorer strata are dominated by the genus *Hedbergella* [*Luderer*, 1999, p. 49]. *Da Gama et al.* [2000] and *Kuhnt et al.* [2001] found that the distribution patterns of calcareous nannofossils within the Tarfaya Basin C/T strata usually show a noisy signal, except the genera *Eprolithus* and *Biscutum* whose distribution seems to follow the 2-m scale light/dark cyclicity.

Based on oxygen-isotope data from planktonic foraminifera sea surface palaeotemperatures in the Tarfaya Basin increase constantly during the Cenomanian, reaching a maximum at the last occurrence of *R. cushmani*, then remaining high for 156 ka before decreasing constantly in the Middle Turonian [*Luderer,* 1999]. New spectrogamma-ray data from the Shell Quarry (Fig. 7 and Fig. 8) show a clear and gradual, nevertheless subtle, increase of K and Th across the middle and upper parts of the C/T carbon isotope excursion, possibly indicating an increased input of aeolian dust from the NW African Continent, resulting from a C/T climatic change and associated intensification of NW African wind systems [*Kolonic et al.,* 2001]. In the modern world, iron from Saharan dust is known to be occasionally blown to the west Florida coast where it fertilises the water, triggering toxic algal blooms (`red tides') [*Lenes et al.,* 2001; *Goudie and Middleton,* 2001].

The bioprovincial affinities of ammonites and bivalves along the Moroccan Atlantic coast was studied in detail by *Wiedmann et al.,* [1978, 1982] and *Einsele and Wiedmann* [1982] and their trends allow important oceanographic insights. While the faunas in the Tarfaya Basin in the south of the studied basin transect are almost exclusively north-boreal in character (with most Mediterranean elements absent; with a similar trend in the calcareous nannoflora; [*Kuhnt et al.,* 2001]), the Meseta to the north is dominated by Mediterranean elements. The Agadir Basin, located between these two areas (Fig. 5), hosts a mixed boreal and Mediterranean ammonite fauna [*Wiedmann et al.,* 1978, 1982; *Kuhnt et al.,* 2000]. The north boreal faunal elements, according to *Wiedmann et al.* [1982], are linked to Atlantic cold, upwelling water masses (Tarfaya Basin), while increasing dominance of Tethyan elements indicates decreasing intensity of upwelling and increasing proximity to the Atlas Gulf, which forms one of the connections between the Atlantic and the Tethys (Fig. 3).

In the deep-sea fan systems in the Rif and Gibraltar Arch area in the extreme north of Morocco the C/T event is characterised by a significant radiolaria bloom and coincides with several important events in the evolution of planktic foraminifera (e.g., first appearance of the genus *Whiteinella*, new species of *Praeglobotruncana*, extinction of the genus *Rotalipora*, radiation of double-keeled genera *Marginotruncana* and *Dicarinella*; [*Thurow and Kuhnt,* 1986, p. 439]).

2.5.2.6. Bulk and molecular geochemistry

Publications on the organic geochemistry of Moroccan C/T black shales are limited to the Tarfaya Basin, including papers by *Leine* [1986], *Halim et al.* [1997], *Kuypers et al,* [1999], *Kuypers et al.* [2002] and *Kolonic et al.* [2002]. For the other C/T Moroccan sites, no detailed organic geochemical investigations have been published up to now.

2.5.2.6.1. Type and origin of organic matter

A detailed and comprehensive description of the OM composition in the Tarfaya black shales is given in *Kolonic et al*. [2002]. The Tarfaya black shales are characterised by high TOC contents of up to 20% and kerogen type I/II with hydrocarbon indices of up to 900 mg HC/g TOC that qualifies these laminated black shales as excellent oil-prone source rocks. Low *T*max values (below 425 °C) obtained from Rock-Eval pyrolysis strongly suggests a consistently immature nature of the OM which has barely reached the top of the oil window. Slightly enhanced thermal maturation towards the central part of the Tarfaya Basin is indicated by the presence of extended unsaturated hopanoids (e.g., hopenes), which were released by thermal degradation of sulphur-bound hopanoids. However, a significant hydrocarbon generation has not yet occurred as indicated by fairly constant low production indices obtained from Rock-Eval pyrolysis.

The total lipid analysis performed after desulfurisation of the total extract shows that the biomarkers predominantely comprise of short-chain *n*-alkanes (C16–C22) and long-chain (C25–C35) *n*-alkanes with no obvious odd-over-even predominance, steranes, hopanoids and acyclic isoprenoids indicating predominantely marine OM. High abundances of algal biomarkers, such as cholestanes, 24-methyl-cholestanes and 24-ethyl-cholestanes, relative to typical biomarkers of membrane lipids derived from cyanobacteria, argue for an algal rather than a cyanobacterial source for the OM.

Detailed organic petrological studies preformed on these black shales support these observations. The kerogen is characterised by unstructured OM (classified as bituminite type II) and lamalginite layers embedded in a brightly reddish–yellowish fluorescing groundmass. According to *Kolonic et al*. [2002], the formation of unstructured OM in the Tarfaya black shale is most likely related to intensive restructuring of labile biopolymers (lipids and carbohydrates) through incorporation of sulphur into the kerogen during early diagenesis. These authors assume that an early break-down of relatively weak C–S and S–S bonds would have facilitated thermal degradation of the Tarfaya kerogen thus generating oil at relatively low temperatures similar as in the Monterey Formation.

Detrital vitrinite and inertinite is only rarely observed in these sediments. Some terrigenous admixture, however, may have taken place based on compound-specific carbon isotope signatures from leaf wax *n*-alkanes in DSDP Site 367 off the coast of NW Africa [*Kuypers et al.,* 1999]. Their presence at DSDP Site 367 testify a probably eolian supply of terrigenous organic matter to the eastern low latitude Atlantic. This mechanism is in agreement with high-resolution iron and titanium XRF-scanning records from two Tarfaya drill sites (S75 and S57) as well as results from recent C/T global climate modeling [*Flögel,* 2002], both proposing orbital-driven fluctuations in African climate aridity/humidity and subsequent eolian export.

2.5.2.6.2. Kerogen

The kerogen fraction of the Tarfaya C/T black shales has been characterized and classified based on potassium permanganate degradation oxidation products [*Halim et al.,* 1997] and flash pyrolysis GC-MS analysis *Kolonic et al.* [2002]. GC and GC-MS analysis of acid oxidation products and products of controlled alkaline potassium manganese degradation of high-molecular weight acids indicate a dominantly aliphatic (56.6%) and aromatic (36.3%) composition of the oxidation products in agreement with results from NMR studies [*Halim et al.,* 1997]. Investigation of each kind of aliphatic and aromatic acids has shown that the kerogen network is formed by aliphatic, cross-linked chains with inserted aromatic structures, which is substantially substituted by aromatic moieties and alcyl chains acting as monosubstituents. Results from flash pyrolysis GC-MS of kerogen support these results by indicating a dominant aliphatic nature of the bulk organic carbon [*Kolonic et al., 2002*]. Accordingly, the vast majority of pyrolysis products generated from the kerogen are sulphur-containing components such as alkylthiophenes, alkenylthiophenes and alkybenzothiophenes, whereas C7–C15 isoprenoidal alkenes/alkanes constituents are only present in relatively low amounts. Non-sulfur containing pyrolysis products are mainly composed of alkylbenzenes and homologous series of *n*-alkenes and *n*-alkanes, the latter components most likely originating from marine algaenans [e.g., *De Leeuw et al., 1991*; *Derenne et al.,* 1992; *Gelin et al.,* 1996]. Phenols and methoxyphenols, pyrolysis products of lignin evidence higher plant biopolymers [*Saiz-Jimenez and de Leeuw,* 1984, 1986] and are only present in trace amounts in the flash pyrolysates that are also supporting a marine nature of the organic matter.

2.5.2.7. Potential for C/T-sourced hydrocarbons

The Mid-Cretaceous Tarfaya-Layoune Basin is one of the largest oil-shale deposits on the NW African continental margin [*Amblés et al.,* 1994] and a major exploration campaign in the Tarfaya Basin was carried out during the early 1980s by Shell and the Moroccan State Oil ONAREP to evaluate the suitability of this strata for open-pit-mining [*Leine,* 1986]. The campaign included the drilling of 55 shallow boreholes, including the S-wells in Fig. 7, and tests in an Oil Shale Quarry (Fig. 7 and Fig. 8) near the village of Tarfaya. The total volume of oil contained in the area in the C/T interval (zone R; [*Leine,* 1986]), that is located at depths shallower than 125 m below the surface, was estimated at 5 billion barrels [*Leine,* 1986] or 73 Gt yielding 5.7 wt.% oil according to *Halim et al*. [1997]. However, economic calculations at the time indicated that production would have been non-commercial, so the project was terminated.

Although the onshore C/T interval of the Tarfaya Basin is thermally immature and maximum depth of burial has probably never been more than 500–600 m [*Kolonic et al.,* 2002], the C/T strata has to be regarded as an important potential petroleum source rock in deeper parts of the offshore NW African shelf. Enterprise Oil considered the deepwater extension of the Tarfaya Basin to possess good potential to become a major hydrocarbon province off-shore NW Africa [*Jarvis et al.,* 1999]. Shell estimates the C/T interval in the Agadir deepwater basin to be thermally mature over large areas [*Truempy and Reeve,* 2001]. The recent Woodside Petroleum oil discovery in a Cretaceous reservoir in offshore Mauritania emphasizes the viability of NW African Cretaceous offshore plays.

2.5.3. Algeria

2.5.3.1. Structural setting

Structurally, Algeria is composed of the Atlas Fold-and Thrustbelt to the north and the Saharan Platform to the south of the South Atlas Fault (Fig. 11). In general, Cretaceous sedimentation on the Saharan Platform was little affected by tectonic (or halokinetic) movements [*Busson, 1998*], with the exception of local strike-slip movements. In the Atlas belt, however, deposition was strongly influenced by synsedimentary extensional and compressional phases. An exception is the Aptian compressional phase that also affected the Saharan Platform (e.g., Berkine Basin) and resulted from transpression along a large-scale, N–S trending Transaharian fracture system [*Maurin and Guiraud*, 1993].

During the Albian–Turonian a major extensional regime existed in NE Algeria, resulting in the formation of graben and halfgraben systems, which controlled the distribution of carbonate platform and deeper basin facies, and therefore also of facies and organic richness of the C/T interval [*Guiraud*, 1990; *Camoin*, 1991; *Aris et al.,* 1998; *Herkat and Delfaud,* 2000; *Herkat,* 2001]. The grabens experienced individual subsidence histories that later resulted in different maturation histories of the organic-rich C/T strata.

Mid-Cretaceous extension was most intense in the SE Constantinois Basin, influenced by the two main extensional systems, the NE-SW trending Aures-Kef Trough and the NW-SE trending Gafsa Graben (Fig. 12). As in Tunisia (see below) formation of the rift grabens was associated with the opening of the Neotethys to the north [*Grasso et al.,* 1999] and the South and Equatorial Atlantic to the southwest [*Maurin and Guiraud,* 1993]. Some authors assume that around the C/T period a change from synrift (mechanical subsidence) to post-rift (thermal subsidence) movements occurred and that extension was associated with a horizontal component in movement (transtension/pull-apart) ([*Laville,* 1985; *Kazi-Tani,* 1986]; R.S. Zazoun, Sonatrach, 2002, personal communication).

In addition to tectonic extension, halokinetic movements occurred in the region, e.g., in Aures and the Hodna Mountains [*Camoin,* 1991, p. 32] (Fig. 12). Following the Mid-Cretaceous extension, compressional phases in NE Algeria occurred in the Mid Santonian [*Guiraud et al., 1987,* p. 439] and from the latest Maastrichtian [*Aris et al.,* 1998].

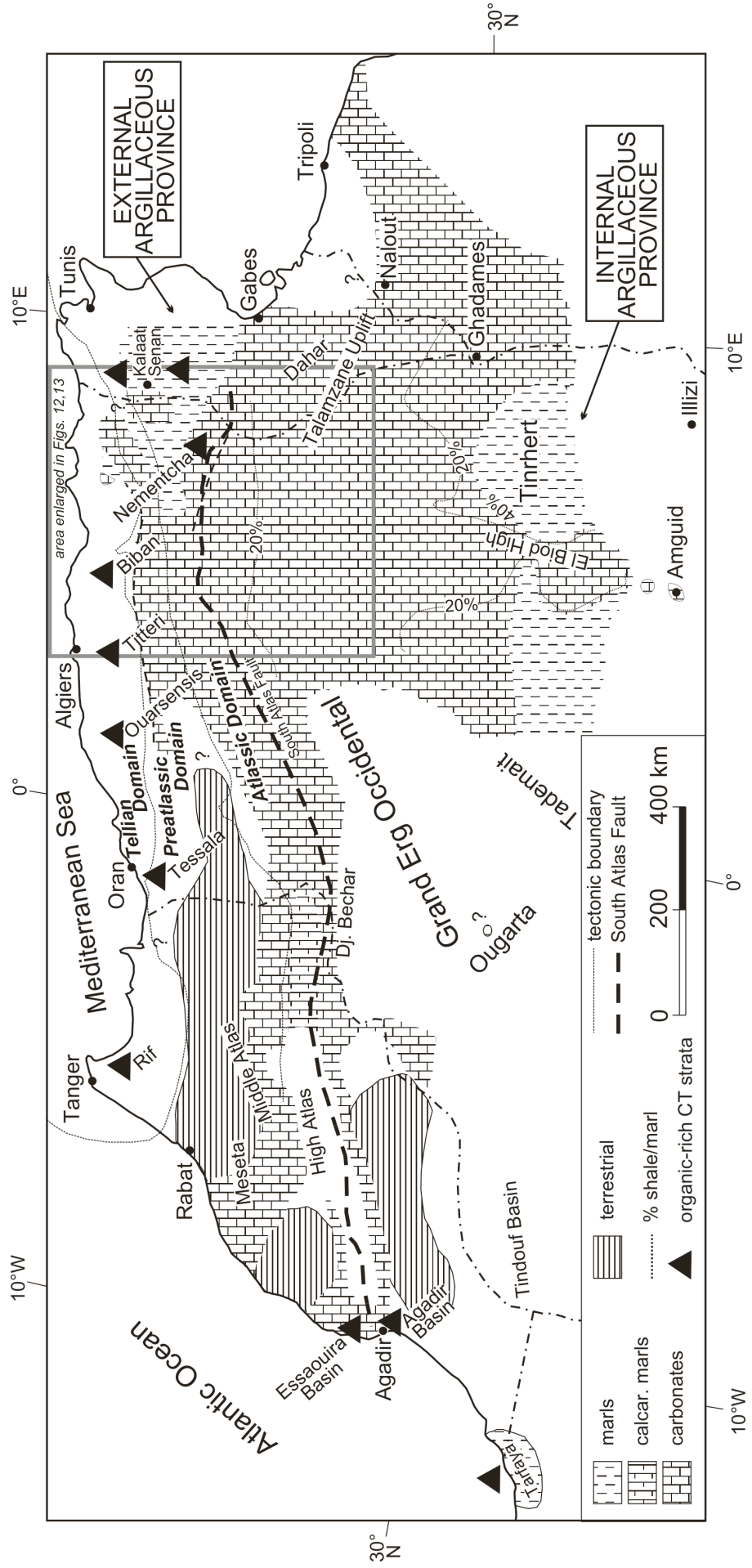
EXTERNAL ARGILLACEOUS PROVINCE
INTERNAL ARGILLACEOUS PROVINCE
area enlarged in Figs. 12,13
Tunis
Gabes
Tripoli
Nalout
Ghadames
Illizi
Amguid
Kalaat Senan
Dahar
Talamzane Uplift
Nementcha
Biban
Tittert
Algiers
Tinrhert
El Biod High
20%
40%
Quarsensis Domain
Tellian Domain
Preatlassic Domain
Atlassic Domain
South Atlas Fault
Grand Erg Occidental
Tademait
Oran
Tessala
Dj. Bechar
Ougarta
Mediterranean Sea
Tanger
Rif
Middle Atlas
Meseta
High Atlas
Rabat
Tindouf Basin
Agadir Basin
Essaouira Basin
Agadir
Atlantic Ocean
Tafaytal
10°W
0°
10°E
30° N
tectonic boundary
South Atlas Fault
0
200
400 km
terrestrial
% shale/marl
organic-rich CT strata
marls
calcar. marls
carbonates

Figure 11. Late Cenomanian–Early Turonian facies distribution and main occurrences of organic-rich C/T strata in NW Africa [after *Busson and Cornée,* 1996; *Busson et al.,* 1999]. Note the development of marl-dominated facies in parts of eastern Algeria ("external" and "internal argillaceous provinces"). Boxed area enlarged in Fig. 12 and Fig. 13.

2.5.3.2. Distribution, characteristics and sea-level control of C/T organic-rich strata

Organic-rich and siliceous C/T strata are reported from many places in Algeria north of the South Atlas Fault, including (from east to west) Nementcha, the Tell constantinois, Tell algérois (Algiers area) and Tell oranais (Oran area) (Fig. 11 and Fig. 12; Table 1) [*Busson and Cornée,* 1996; *Busson et al.,* 1999]. This organic-rich facies very likely formed a continuous band along the Middle Cretaceous North African shelf edge from Tunisia in the east to the Moroccan Prerif Zone in the west [*Kuhnt et al.,* 1990]. Characteristic C/T lithologies include laminated black limestones and marls (e.g., SE Constantinois Basin; [*Askri et al.,* 1995]) and black cherts (e.g., near the city of Constantine; [*Vila,* 1980; *Busson and Cornée,* 1996]) (Table 1; Fig. 11). Fish skeletons and biosiliceous intercalations (radiolarian sands) were commonly observed within the dark laminated sediments [*Mattauer,* 1958; Wildi, 1983].

The organic-rich and siliceous strata was deposited in various tectonic and bathymetric settings (Fig. 3) [*Busson and Cornée*, 1996]. Along the deeper parts of the Tellian margin in northern Algeria, Middle Cretaceous organic-rich sediments have been encountered as large olistolites in a slope series of the Monts de Tessala (Fig. 11) [*Fenet*, 1975], which corresponds to the middle part of the North African continental margin [*Wildi,* 1983]. The largest olistolites comprise laminated black shales, more than 2 m thick, with TOC values up to 4.7% [*Kuhnt et al.,* 1990, p. 141]. An enhanced thermal degradation of the OM in this area, where Late Cretaceous and Early Cenozoic subsidence was important, and Miocene tectonism led to nappe structures, is indicated by comparatively low HI (about 100 mg HC/g TOC) as well as low OI (7–24) and a high *T*max of about 460 °C [*Kuhnt et al.,* 1990, p. 141]. The strong tectonic deformation also complicates the study of the Cretaceous successions.

The organically richest and, with regards to petroleum exploration, most important C/T deposits are located in the SE Constantinois Basin (95,000 km2, 69 exploration wells; Fig. 12) in NE Algeria where they are grouped into the Bahloul Fm., as in Tunisia (see below) and constitute a good hydrocarbon source rock [*Askri et al.,* 1995]. The black marly limestones are rich in pyrite and contain abundant *Globigerina* and *Pithonella*. Thicknesses reach up to 120 m in the SE of Constantine, in the Aures-Kef Trough and in the Talamzane uplift on the Sahara Platform (Fig. 11 and Fig. 13). In the Biskra area (Djebel Bou Rhezal), in Oued Djelal and to the south of Negrine (Fig. 13), the C/T interval is generally dolomitic and therefore does not have good source rock characteristics [*Askri et al.,* 1995]. Peak TOC values in the SE Constantine Basin reach 13% (Tebessa/Negrine area; [*Nacer Bey* et al., 1995]), with average values of 4% (Fig. 12) [*Askri et al.,* 1995]. Elevated TOC values were also recorded to the north of Batna, in the vicinity of Djebel Chelia (2.7%) as well as in the Hodna region (2%) [*Askri et al.,* 1995] (Fig. 12). The organic matter is essentially amorphous and of sapropelic origin, associated with dinoflagellates and more rarely plant remains. The C/T kerogen is characterised by type II OM with HI of up to 883 and a very high petroleum potential of up to 90 kg HC/t [*Askri et al.,* 1995; *Nacer Bey et al.,* 1995]. Cummulative source rock thicknesses of up to 30 m have been reported from the SE Constantine Basin [*Nacer Bey et al.,* 1995].

The best documented field location of the Bahloul Formation in Algeria is at Djebel Dyr, just north of Tebessa (Fig. 12). *Naili et al.* [1994] studied a series of eight C/T boundary sections in a distance of a few kilometers to each other in which thicknesses of the organic-rich Bahloul Formation varied between 2 and 7 m. Notably, the thickest Bahloul occurs in sections with channels and slumping, possibly associated with synsedimentary graben formation and slumping from the graben slopes. The unit here consists of the characteristic laminated, black Bahloul limestones and marls rich in planktic foraminifera and ammonites [*Benkherouf,* 1987; *Naili et al.,* 1994]. A characteristic lamination formed by white planktonic foraminifera layers and dark organic-rich layers is developed. From the field samples, TOC values of up to 2.7% have been measured. Based on the occurrence of *Pseudoaspidoceras pseudonodosoides* the lower part of the Bahloul is uppermost Cenomanian [*Naili et al.,* 1994]. *Benkherouf* [1987] documented the *cushmani* and *archaeocretacea* zones at Djebel Dyr but did not relate them to the boundaries of the Bahloul Formation. Based on benthic foraminifera

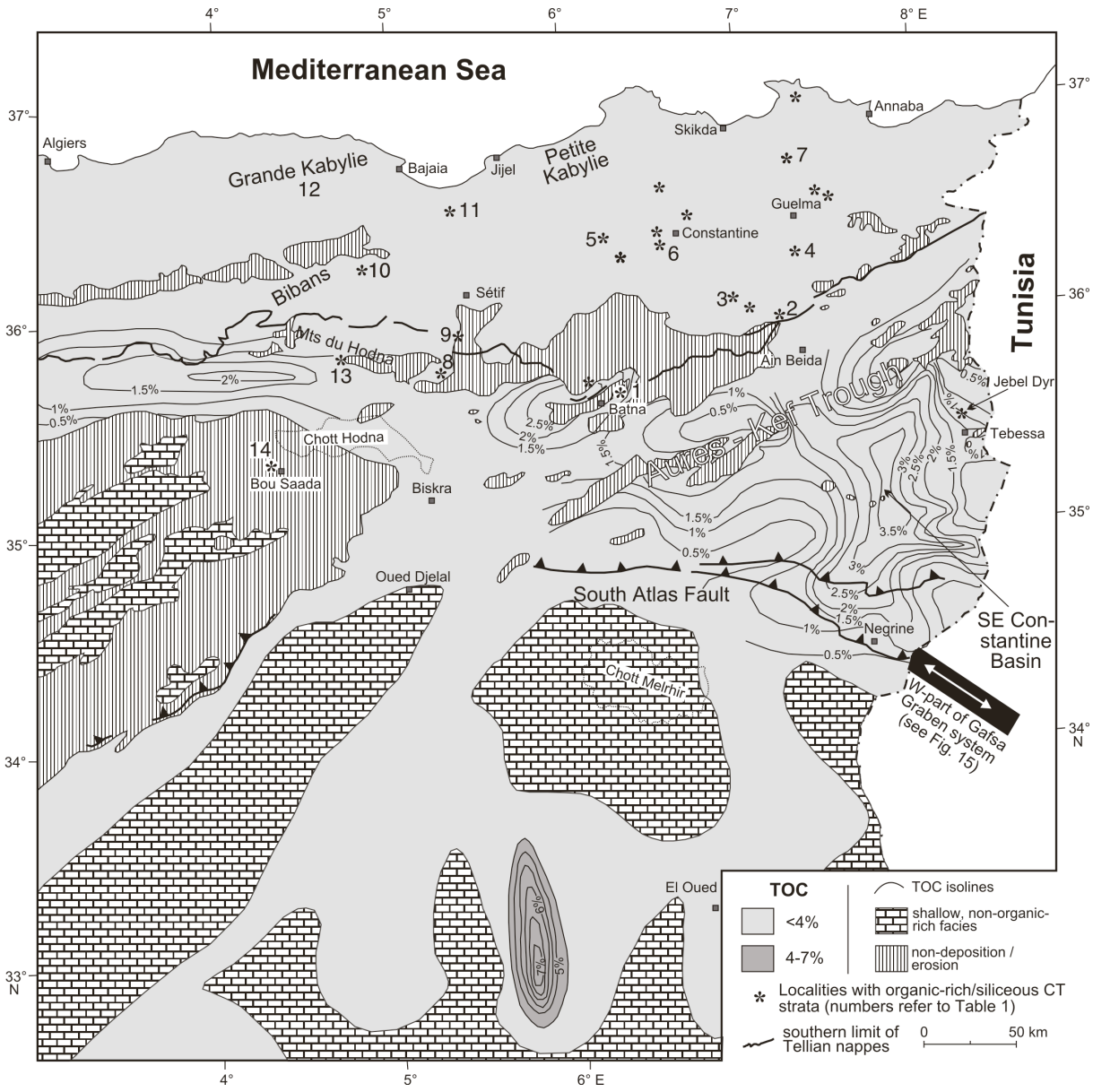

Figure. 12. Distribution and properties of Cenomanian–Turonian organic-rich marls/shales in NE Algeria. Note that also organic-rich Cenomanian/Turonian strata under- and overlying the Bahloul Formation are included here. TOC, contour interval 0.5%. Modified after *Askri et al.* [1995] in *Delsol* [1995]. Contour interval 20 m. Asterisks in the northern part of the illustrated area indicate known occurrences of organic-rich and/or siliceous C/T strata [after *Busson and Cornée,* 1996]. Numbers refer to lithologic description in Table 1.

assemblages almost entirely composed of agglutinated foraminifera, *Benkherouf* [1987] also suggested that reducing sea bottom conditions existed throughout the Middle and Upper Cenomanian. Notably, the rich, planktonic fauna was unaffected by these conditions, indicating well-oxygenated surface waters.

Belhadj et al. [1998] provided a sequence stratigraphic description for the Cenomanian–Turonian deposits in the SE Constantine Basin and interpreted the laminated black Bahloul limestones (also containing glauconite and phosphate) as belonging to the transgressive systems tract, including the C/T boundary (sequence ZC2.5 of *Belhadj et al.* [1998] corresponds to UZA-2.5 in the *Haq et al.* [1987] curve; for eustatic correlation, see also *Herkat and Delfaud* [2000]; Fig. 2). The same authors identified a general facies change across this basin from south to north from evaporites via platform deposits (incl. rudist biodetritic limestones, e.g., wells BGH, DK, Foua) to deeper shelf (Fig. 3). The

1	Djebel Bou Arif	alternating grey marls + whitish marly carbonates	*Vila* [1980]; *Busson and Cornée* [1996]
2	Djebel Hamminat	"black facies"	*Vila* [1980]; *Busson and Cornée* [1996]
3	Djebel Djaffa	biomicrite, dark when freshly broken	*Vila* [1980]; *Busson and Cornée* [1996]
4	Oued Cheniour	blueish marls, platy carbonates without fossils	Blayac [1912]; *Busson and Cornée* [1996]
5	Djebel Kenazaa, Bou Charef	black cherts	*Vila* [1980]; *Busson and Cornée* [1996]
6	Djebel Chettaba	black cherts	*Vila* [1980]; *Busson and Cornée* [1996]
7	Djebel Safia	phtanites	*Vila* [1980]; *Busson and Cornée* [1996]
8	Oued Soubella	siliceous rocks	*Vila* [1980]; *Busson and Cornée* [1996]
9	Dôme de Colbert	carbonates and marls with intercalated cherts	*Savornin* [1920]; *Busson and Cornée* [1996]
10	Colbert / Biban	black platy carbonates, black cherts, pyritic	*Caire* [1957]; *Busson and Cornée* [1996]
11	Djebel Babor (Petite Kabylie)	Organic-rich facies from Vraconian to Cenomanian-Turonian, black Turonian chert	*Obert* (1981); *Vila* [1980]; *Busson and Cornée* [1996]
12	Grande Kabylie	Microbreccia, partly silicified, black and white phtanites	*Gélard* [1979]; *Vila* [1980]; *Kuhnt et al.* [1990]; *Busson and Cornée* [1996]
13	Hodna Mts./Basin	Cenomanian: mostly grey-blue / dark marls late Cenomanian - early Turonian: black limestones + dolomites	*Majoroan* [1987]; *Mekireche et al.* [1998]
14	Bou Saada area	bituminous marls (outer neritic)	*Emberger* [1960]; *Kieken* [1962]; *Guiraud* [1990, 107]
Fig. x34x	Titteri	organic-rich and siliceous facies	*Guillemot* [1952]; *Busson and Cornée* [1996]
	Ouarsenis	organic-rich and siliceous facies	*Mattauer* [1958]; *Polvêche* [1960]; *Kuhnt et al.* [1990]; *Busson and Cornée* [1996]
	Tessala	organic-rich and siliceous facies	*Fenet* [1975]
	Monts des Ouled Naïl	organic-rich and siliceous facies	*Emberger* [1960]

Table 1. Lithologies of reported organic-rich and/or siliceous C/T strata in northern Algeria (numbers refer to Fig. 12 and Fig. 13)

thickness of sequence ZC2.5 varies from south to north in the basin from 35 to 65 m. *Belhadj et al.* [1998] assume that the boundary between anoxic/detric facies zones is controlled by NW–SE trending halfgrabens in association with movements along the South Atlas flexure, which resulted in the formation of enclosed subbasins.

Cenomanian–Turonian marine strata also occurs on the epicratonic Saharan Platform south of the South Atlas Fault (Fig. 3 and Fig. 11); however, organic-rich C/T strata of significant thickness does not occur here. About 100 km to the west of the town El Oued rich but thin layers with TOC values of up to 7% and thicknesses ranging between centimeters and a few meters exist within the C/T interval (Fig. 12). These black shales are associated with evaporites (anhydrite, gypsum) and reflect very shallow marine conditions.

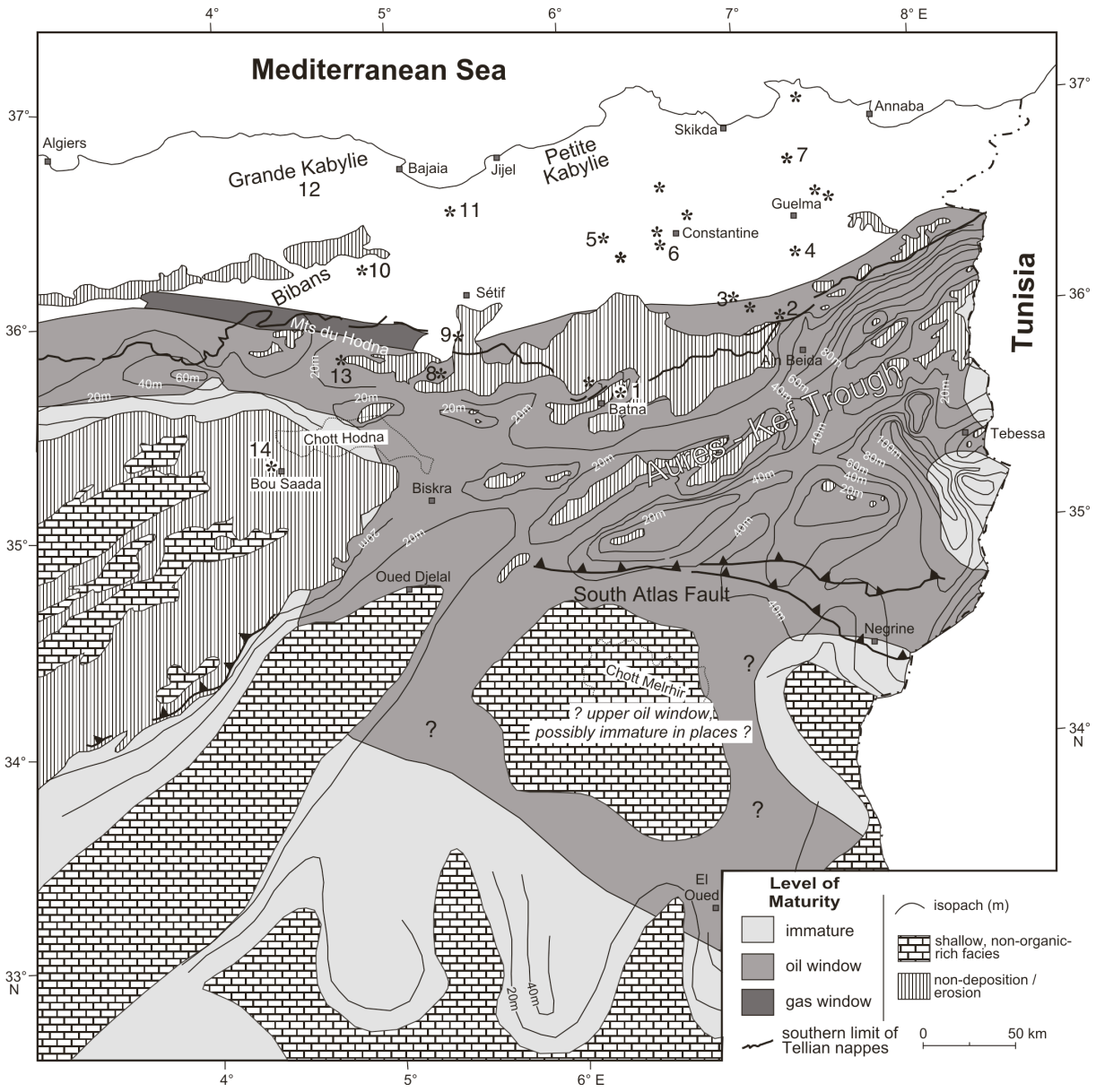

Figure. 13. Distribution and properties of Cenomanian–Turonian organic-rich marls/shales in NE Algeria. Note that also organic-rich Cenomanian/Turonian strata under- and overlying the Bahloul Formation are included here. Cumulative isopach of Cenomanian–Turonian organic-rich strata >1% TOC and level of thermal maturation. Modified after *Drid and Belhadj* [1993] in *Delsol* [1995]. Contour interval 20 m. Asterisks in the northern part of the illustrated area indicate known occurrences of organic-rich and/or siliceous C/T strata [after *Busson and Cornée*, 1996]. Numbers refer to lithologic description in Table 1.

Busson et al. [1999] studied the C/T boundary interval in shallow marine, inter- to subtidal carbonates and marls (`internal argillaceous province'; [*Busson,* 1998; *Busson et al.,* 1999] on the epicratonic Saharan Platform in the Tinrhert area (Fig. 11). In contrast to the majority of mainly dolomitic C/T strata in the Algerian Sahara, the Tinrhert area exposeses a fossiliferous C/T boundary section that *Busson et al.,* [1996, 1999], based on biostratigraphic studies of the ammonite fauna by *Amard et al*. [1981] and *Amédro et al.* [1996], were able to subdivide into six biostratigraphic intervals which are correlatable with standard boreal ammonite zones (Fig. 14). Typically, the succession consists of Cenomanian lacustrine/fluvial gypsiferous marls [*Busson and Cornée,* 1991] that are overlain by Late Cenomanian–Early Turonian marine carbonates and marls, separated by a major marine flooding surface of *C. naviculare* Zone age. This flooding surface correlates well with the latest Cenomanian, third-order transgressive surface in the Tethyan eustatic sea-level model of *Hardenbol et al.* [1998] (post-Ce5 TS; Fig. 2 and Fig. 14). Also, the successive sea

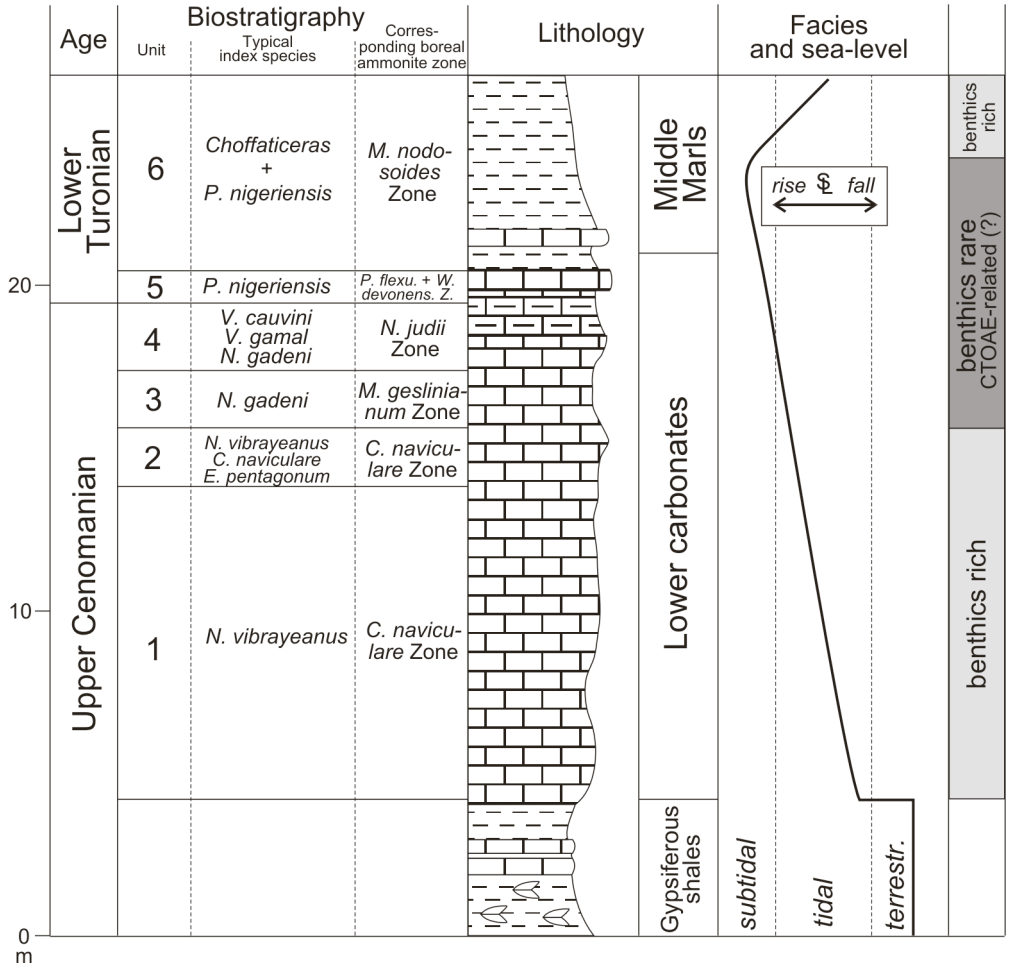

Figure. 14. Late Cenomanian transgression in the Temassinine section in Tinrhert (eastern Algerian Sahara) [after *Busson et al.,* 1999]. Due to the shallowness of the sea, no significant accumulations of organic matter are developed in the CTOAE interval, which, nevertheless, is characterised by rare benthic organisms.

level rise across the C/T boundary up to about the mid Early Turonian is observed in the Tinrhert area and agrees well with the *Hardenbol et al.* [1998] chart. While none of the C/T horizons in the Tinrhert area are organic-rich, a significant drop in benthic diversity and richness has been noted by *Busson et al*. [1999] for the interval from the *geslinianum* Zone to the mid Early Turonian, preceded and followed by benthic-rich units. *Busson et al*. [1999] speculate that this benthic impoverishment may be associated with dysaerobic conditions related to the C/T anoxic phase that was more fully developed in the deeper, more basinal areas to the north, e.g., in northeastern Algeria and northern Tunisia.

2.5.3.3. Potential for C/T-sourced hydrocarbons

In the SE Constantine Basin (Fig. 12), hydrocarbon production exists from Cenomanian, Turonian and Coniacian reservoir horizons [*Nacer Bey et al.,* 1995]. This includes probably C/T-sourced oil production at Djebel Onk, Ras Toumba and Guerguitt El Kihal and probably C/T-sourced gas production at Djebel Foua ([*Dokka et al.,* 1990; *Nacer Bey et al.,* 1995]. however, questioned by other workers who consider the C/T interval immature here). The C/T horizon essentially has been in the oil window since the Paleocene [*Askri et al.,* 1995].

In the Hodna Basin/Hodna Mountains, the C/T interval is organic-rich, 20–40 m thick and mature to overmature [*Mekireche et al.,* 1998]. *Mekireche et al.* [1998] assume a Late Cretaceous main burial and associated HC generation, which unfortunately mostly precedes the main trap formation during the Miocene. Therefore exploration in this area needs to focus on Late Cretaceous structures.

2.5.4. Tunisia

2.5.4.1. Structural setting

As for Algeria, Tunisia can be structurally subdivided into a northern alpine-deformed subsidence zone with thick Mesozoic and Cenozoic strata and a stable Palaeozoic province to the south where Middle Jurassic and younger strata are relatively thin and unfolded (Fig. 15) [*Bishop,* 1988; *Burollet*, 1991]. The C/T organic-rich strata in onshore and offshore Tunisia is mainly found in this northern tectonic province and the distribution and organic content are strongly controlled by Early Cretaceous (pre- and probably even syndepositional) halfgraben systems (Fig. 15, Fig. 16, Fig. 17 and Fig. 18) [*Ellouz,* 1984; *Jongsma et al.,* 1985; *Maamouri et al.,* 1994; *Camoin,* 1991; *Razgallah et al.,* 1994; *Abdallah and Meister,* 1997; *Grasso et al.,* 1999; Bédir et al., 2001], and in some areas by Cretaceous pre- and syndepositional Triassic salt diapiric movements [*Perthuisot,* 1981; *Orgeval*, 1994] (Fig. 19).

As in Algeria, formation of the Tunisian rift grabens was associated with the opening of the Neotethys to the north [*Grasso et al.,* 1999] and the South and Equatorial Atlantic to the southwest [*Maurin and Guiraud,* 1993]. Notably, this rifting in onshore Tunisia and on the Tunisian Shelf did not commence before Late Jurassic/Early Cretaceous [*Grasso et al.,* 1999, p. 247]. Late Triassic–Early Jurassic rifting associated with the separation of the Turkish–Apulian Terrane [*Sengör,* 1985 and *Flexer et al.,* 1986] along the leading edges of the African Plate was restricted to an area well north of Tunisia.

Two Mesozoic rifting events occurred in onshore Tunisia, namely (1) from the Late Jurassic to Early Aptian, associated with E-W-trending halfgrabens and volcanism in the Pelagian sea, and (2) from the Late Aptian to Early Cenomanian, associated with NW–SE trending halfgrabens [*Guiraud and Maurin,* 1991] (Fig. 15, Fig. 17 and Fig. 18). The two extensional phases were interrupted by a regional Mid-Aptian uplifting phase which formed the typical unconformity resolved in seismic data (Fig. 17) [*Guiraud and Maurin,* 1991; *Ibouh and Zargouni*, 1998]. The general graben trends are locally complicated by other faults (NNE–SSW in the Cenomanian, ENE–WSW in the Turonian) which have partly dissected graben segments into a mosaic of rather independent smaller blocks [*Camoin*, 1991]. The maximum width of the graben systems is only a few tens of kilometers [*Grasso et al.,* 1999]. Maximum thickness and peak organic-richness of the C/T strata are usually reached within the graben systems, most clearly documented in NW Tunisia (Fig. 15, Fig. 16 and Fig. 18). Rift movements had ceased [*Grasso et al.,* 1999] or were subtle [*Camoin,* 1991, p. 35] during deposition of the C/T deposits. Major uplifting occurred only from the latest Cretaceous onwards [*Soyer and Tricart*, 1989; *Grasso et al.,* 1999] and, hence, did not affect facies distribution of the C/T strata in Tunisia. A major elongated high, the so-called `North–South Axis', existed in Central north Tunisia during C/T times (Fig. 15) and is characterised by thickness reduction and local instability since the Jurassic, probably related to deep-seated faults separating basement blocks [*Perthuisot,* 1981, p. 234].

In parts of Tunisia, Cretaceous diapiric movements of Triassic salt locally also played a role in controlling C/T-deposition, e.g., in northern [*Perthuisot,* 1981] and central Tunisia [*Bédir et al.,* 2001] and on the Pelagian Shelf [Camoin, 1989, 1991]. In the vicinity of diapirs, the peridiapiric series is characterized by a marked thickness reduction, mainly in the marly members, and partly by development of a detrital facies (sandstones, conglomerates) [*Perthuisot,* 1981]. The Albian to Middle Eocene diapiric rise was probably continuous, but it increased during periods of tectonic instability [*Perthuisot,* 1981; *Grasso et al.,* 1999].

2.5.4.2. Distribution and characteristics of C/T Corg strata

During the Late Cenomanian–Early Turonian, Tunisia was characterised by a generally northward dipping slope at the southern Tethyan margin, including a complete facies transect ranging from terrestrial (southern Tunisia), over lagoonal, shelfal (central Tunisia) to bathyal (northern Tunisia) (Fig. 3). The general facies trend was complicated by a complex tectono-halokinetic palaeorelief (see above) which resulted in strong lateral thickness and facies variations of the C/T strata [*Bishop,* 1975, 1988] (Fig. 15 and Fig. 16).

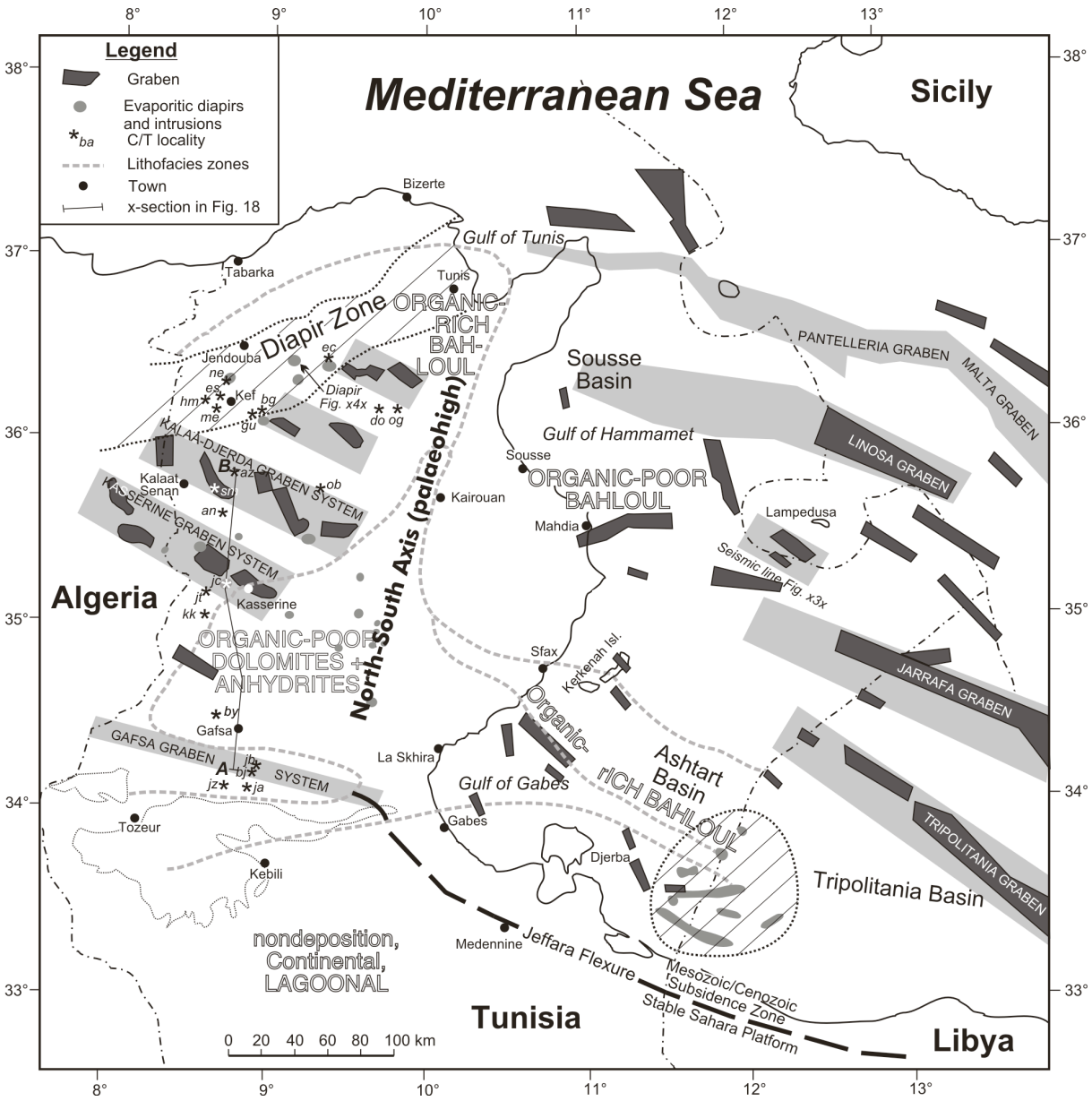

Figure 15. Locations of Early Cretaceous graben systems and syndepositionally active diapirs in relation to the C/T-facies distribution. Locations of grabens and diapirs after *Perthuisot* [1981], *Bishop* [1988], *Camoin* [1991], *Orgeval* [1994] and *Grasso et al.* [1999]; facies zones modified after *Bishop* [1988] (see also Fig. 16). For legend for codes of sections, see Table 2. Cross-section A–B is illustrated in Fig. 18.

Organic-rich C/T strata occur in many places in northern, central and offshore Tunisia and are grouped into the Bahloul Formation that was originally defined by *Burollet et al.* [1954] and *Burollet* [1956]. The thickness distribution of the Bahloul Formation in Tunisia is illustrated in Fig. 16 [after *Ben Ferjani et al.,* 1990]. Also shown in Fig. 16 is the regional distribution of the four main C/T facies types, modified after *Bishop* [1988], which also includes the distinction of an organic-rich and an organic-poor Bahloul facies. The organic-rich Bahloul exists in three regions, namely in onshore NW Tunisia, in a SE–NW trending belt in the Gulf of Gabes and locally in the Gafsa–Chott graben system (Fig. 20). Available well and outcrop data confirm the organic-rich provinces of *Bishop* [1988] (Fig. 20 and Fig. 21), however, the exact boundaries still remain unclear, especially north of the Gulf of Gabes belt, due to the non-availability of well data.

A comparison with the palaeogeographic map (Fig. 3) suggests that the distribution of the organic-rich Bahloul is restricted to intermediate waterdepth and may represents the impingement of an OMZ onto the southern Tethyan margin (Fig. 22) [*Robaszynski et al.,* 1990; *Barrett,* 1998]. A similar

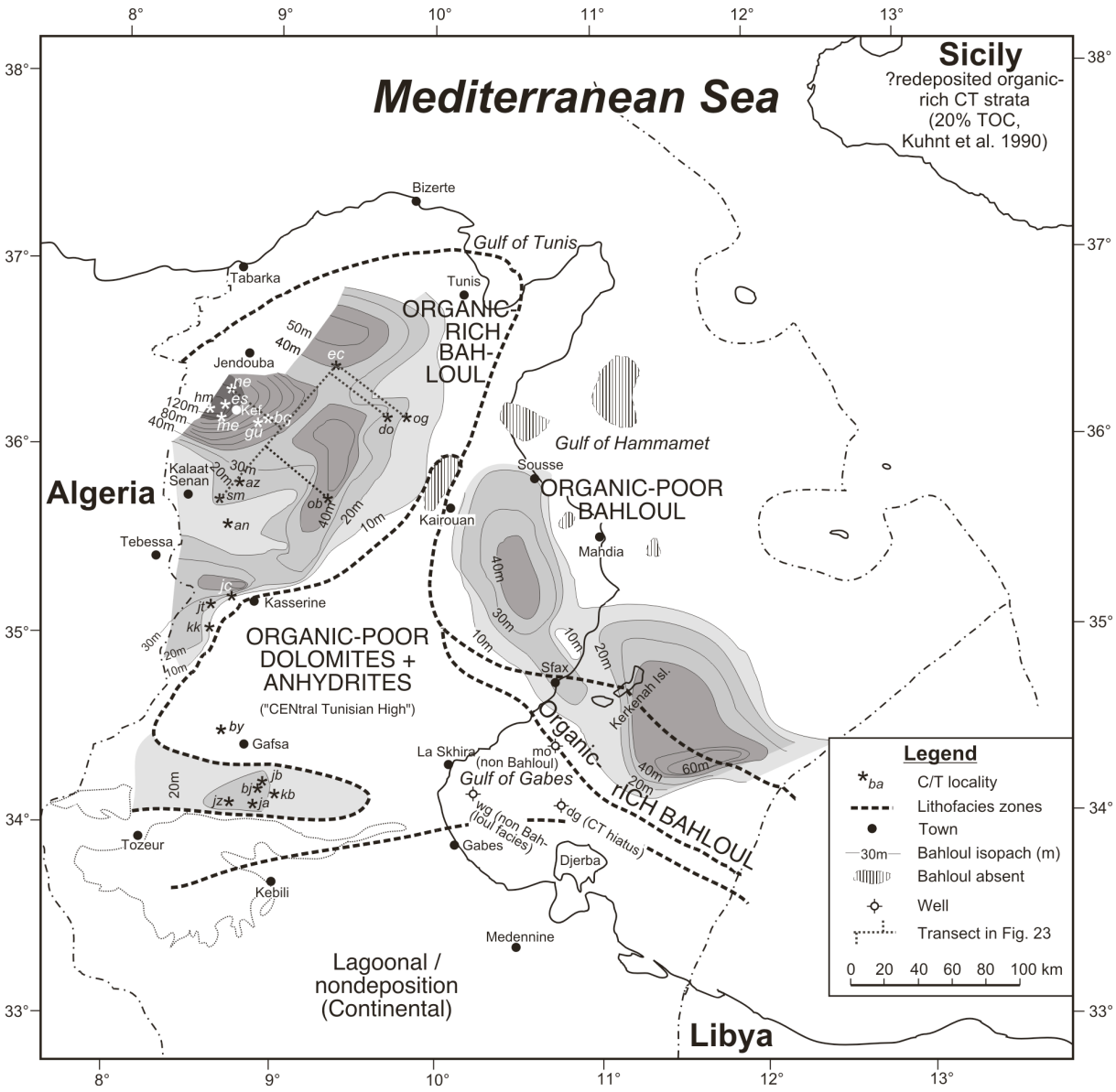

Figure 16. Facies and thickness of the Late Cenomanian–Early Turonian Bahloul Formation and age-equivalent units in Tunisia. Base map and isopach data modified after *Ben Ferjani et al.*. [1990]; facies zones modified after *Bishop* [1988]. For legend for codes of sections, see Table 2. Transect in northern Tunisia refers to sections in Fig. 23. Note that the isopach trends illustrated are simplified and short-distance thickness, and facies changes occur, related to the complex tectono-halokinetic palaeorelief at the time (see Fig. 15).

model seems to apply to the age-equivalent organic-rich deposits at the northwest Australian continental margin [Thurow et al., 1992]. Detailed mapping of the OMZ in Tunisia may help with better predictions of the distribution of C/T organic-rich strata.

In the field, the Bahloul Fm. is usually more resistant to erosion than the marly sections below and above and forms prominent ridges in the landscape [*Robaszynski et al.,* 1993b]. The Bahloul Formation is commonly a few tens of meters thick, with a maximum thickness of 120 m in the NW Tunisian depocentre (Fig. 16), and consists of a regular alternation of laminated and nodular black and greyish limestones and marls with TOC values of up to 13% [*Schlanger et al.,* 1987; *Caron et al.,* 1999; *Abdallah et al.,* 2000] (Fig. 20). A single 19% TOC value was reported by *Abdallah et al.* [2000] from the Gafsa–Chott area. The vertical distribution of limestone vs. marl in the different localities depends on the position on the palaeoshelf/-slope, generally with more carbonate-rich deposits in more proximal and marl-dominated deposits in distal settings. Curiously, in the Nebour section (ne)

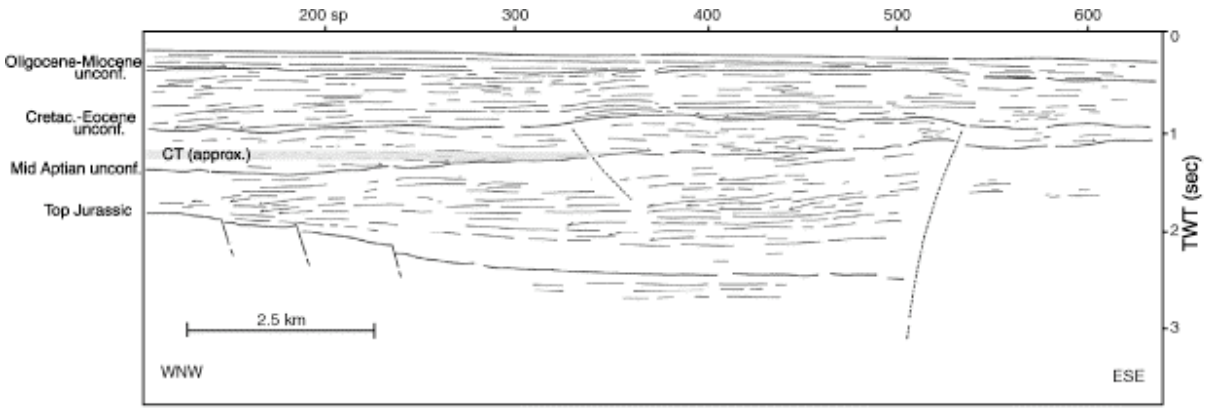

Figure 17. Early Cretaceous halfgraben controlling deposition of C/T strata on the Tunisian shelf near Lampedusa. Note onlap of Albian and upper Cretaceous strata. Position of C/T strata only approximated. For location, see Fig. 15. Drawing based on seismic line (modified after [*Grasso et al.*, 1999]).

Nederbragt and Fiorentino [1999] noted that the TOC values in laminated beds generally are not higher than in surrounding nodular, bioturbated levels.

The vertical TOC patterns vary significantly in different localities in Tunisia (Table 2). Typical patterns observed include (1) a `sine shape' gradual increase and decrease of values within the C/T interval (e.g., Oued Smara/sm section), (2) rather monotonous distributions without major variations in organic content (e.g., Bou Grine/bg section) and (3) short-term TOC spikes with significantly higher TOC than the background values within the C/T column (e.g., Nebour/ne and Oued Bahloul/ob sections) (Fig. 23).

The spiky TOC pattern in combination with typical alternations of dark, organic-rich beds with light beds highlights the importance of repetitively alternating anoxic and dysaerobic environments during deposition of the Bahloul C/T deposits [*Robaszynski et al.,* 1993b; *Abdallah and Meister,* 1997; *Caron et al.,* 1999]. *Caron et al.* [1999] interpreted such dark/light cycles of a few meters thickness in the Bahloul Type Section (ob in Fig. 16) as precession cycles of 20 ka and postulated that the organic-rich strata was deposited under arid and the organically leaner strata under sub-humid conditions.

The apparent cyclicity in oxygenation also exists on a shorter-term scale, expressed by mm-scale laminites with alternating black and light laminae [*Robaszynski et al.,* 1990, p. 221]. Most sections exhibit a sudden increase in TOC at the base, indicating an abrupt aerobic–dysaerobic transition [*Nederbragt and Fiorentino,* 1999] (Fig. 23). In parts of northern Tunisia (e.g., Djebel Fkirine, Zaghouan area, near sections do/og in Fig. 16), the uppermost Cenomanian–lower Turonian black limestone facies continues up to the lower Coniacian [*Salaj,* 1978, p. 385], possibly attributable to local upwelling conditions as in Morocco.

Section ec (Fig. 16 and Fig. 23) is characterized by low TOC values throughout, because the basal (usually organic-rich) part of the C/T interval (and apparently most of the 13C excursion) is not exposed at this locality [*Barrett,* 1998]. The low TOC values of less than 1% may be linked to the rather distal and organically leaner location of the section to the NW on the Tunisian palaeoshelf/slope and underneath the OMZ.

Notably, basinal black laminated shales occur in the Sicily basinal area for which *Kuhnt et al.* [1990] assume a deep-sea fan facies (Fig. 4). Such an environment is prone to redeposition so that potentially the OM may have originated from North African shelfal positions areas and has not necessarily formed in situ (e.g., in the Atlantic: [*Summerhayes,* 1981; *Arthur et al.,* 1984; *De Graciansky et al.,* 1986; *Katz and Pheifer,* 1986]).

2.5.4.3. Biostratigraphy and sequence stratigraphy

The Bahloul Formation was deposited during the latest Cenomanian (uppermost *Rotalipora cushmani* Zone) to earliest Turonian. Especially the upper limit of the unit is known to be diachronous and its

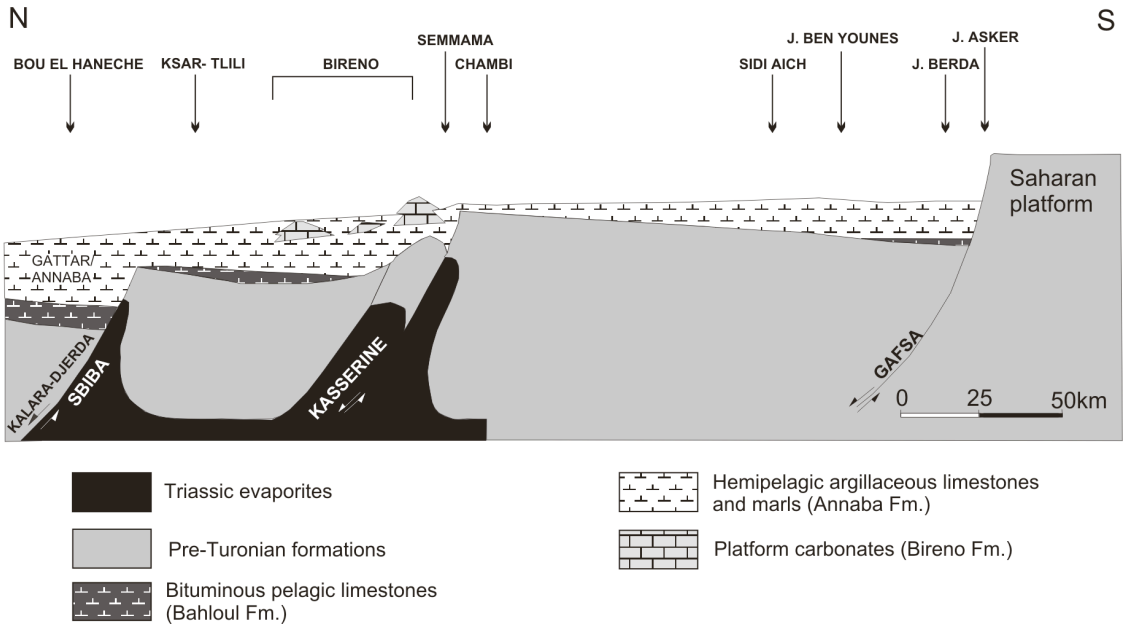

Figure 18. Halfgraben-controlled deposition of C/T strata in central Tunisia [after *Camoin*, 1991; *Abdallah et al.*, 2000]. Location of cross-section A–B in Fig. 15.

age ranges from the *W. archaeocretacea* Zone (e.g., Nebour section/ne; [*Nederbragt and Fiorentino*, 1999]) to the lower *H. helvetica* Zone (e.g., sections es and hm; [*Maamouri et al.,* 1994, p. 42]). *Robaszynski et al.* [1993a,b] originally assumed that the Bahloul Formation in the Kalaat Senan area (section sm) was of uppermost Cenomanian age only, however, this stratigraphic interpretation was later corrected in *Accarie et al.* [1996] who by means of bio- and chemostratigraphy demonstrated that the Bahloul in this section also reaches up into the lower Turonian.

According to *Abdallah and Meister* [1997, p. 218] dysaerobic conditions in the Gafsa/Chott area are clearly diachronous at both the base and the top. In general, dysaerobic conditions in the Gafsa–Chott area appear to have begun slightly later than in west–central Tunisia, about 100 km to the north. Within the basin centre of the Gafsa–Chott graben system at Wadi Berda (section jb; Fig. 20 and Fig. 24), oxygen-depletion is assumed to have prevailed during almost all of the Early Turonian, whereas it was limited to the earliest Turonian in the northern range of the Chotts only a few tens of kilometers away (Khanguet Besbessa Sghira section, kb in Fig. 20) [*Abdallah et al.,* 2000]. The minimum duration of the organic-rich facies in the Gafsa–Chott area ranges from the upper part of the *geslinianum* Zone to the middle part of the *coloradoense* Zone (*flexuosum* level), which corresponds to less than 1 million years [*Abdallah et al.,* 2000].

The onset of deposition of the Bahloul Formation in Tunisia generally coincides with the base of the latest Cenomanian TST [*Hardenbol et al.,* 1993; *Robaszynski et al.,* 1990, 1993b; *Razgallah et al.,* 1994; *Saidi et al.,* 1997; *Abdallah et al.,* 2000] of a major third-order Tethyan eustatic sea-level cycle [*Hardenbol et al.,* 1998]. Notably, *Hardenbol et al.'s* [1998] Tethyan sequence chart for the C/T is mainly based on field data from west–central Tunisia [*Hardenbol et al.,* 1993; *Robaszynski et al.,* 1990, 1993b]. In some parts of Tunisia, the lowermost part of the Bahloul may still belong to the lowstand systems tract (LST), such as in the distal/hemipelagic Oued Smara section (sm) (Fig. 16) where *Robaszynski et al*. (1990, p. 222) described the lowermost 5 m of the Bahloul as LST carbonate mass flow deposits, consisting of calcispheres and echinoderms, originating from the higher shelf, in an autochthonous, pelagic matrix. The remaining 18 m of Bahloul deposits in the sm section represent the TST and are composed entirely of pelagic deposits with typically significantly higher TOC values than in the LST [*Robaszynski et al.,* 1990, 1993b]. A similar sequence stratigraphic interpretation was presented by *Maamouri et al.* [1994]. The diachronous upper limit of the Bahloul lies clearly within the TST (mid TST in the ne section, [*Nederbragt and Fiorentino*, 1999]; uppermost TST in the Gafsa–Chott area, [*Razgallah et al.,* 1994; *Abdallah et al.,* 2000]).

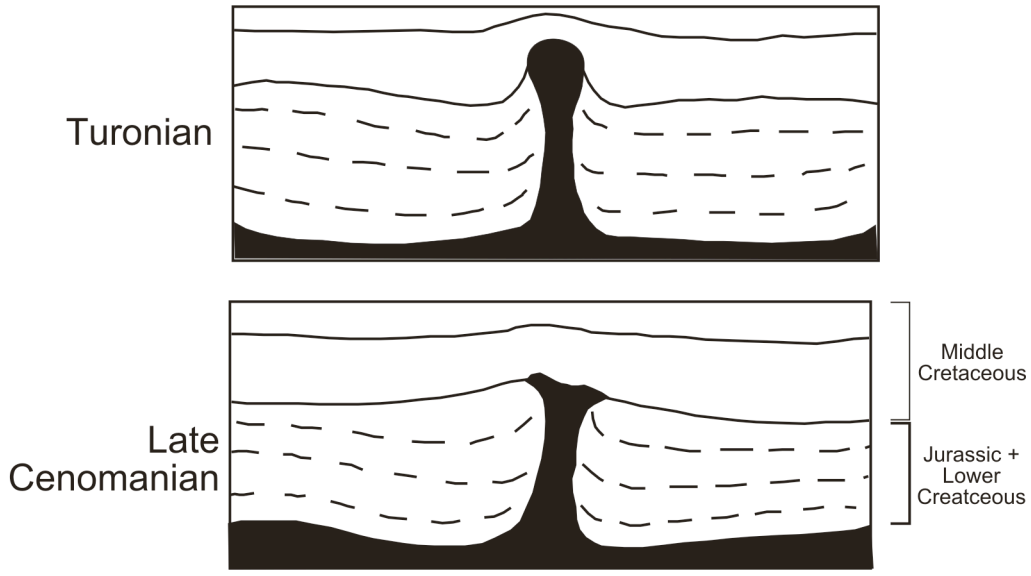

Figure 19. Cretaceous uplift of the Fedj el Adoum diapir in northern Tunisia, affecting distribution and facies of the C/T strata. For location, see Fig. 15. After *Perthuisot* [1981].

The third-order HST overlying the Bahloul TST on the inner Tunisian shelf is generally represented by shallower deposits, such as the shallow marine, bioclastic carbonates of the Gattar Formation and equivalent units [e.g., *Razgallah et al.,* 1994; *Abdallah and Meister,* 1997] (Fig. 2). Strata of a similar facies but older and belonging to the Late Cenomanian–Early Turonian TST was also deposited on the Central Tunisian High (Fig. 15 and Fig. 16) [*Negra et al.,* 1996], implying a pronounced diachroneity of this lithostratigraphic unit. Along the North–South Axis (Fig. 15) and in the offshore the Turonian deposits are locally even missing entirely [*Negra et al.,* 1996; *Bishop,* 1988] due to the presence of pronounced palaeohighs and horst uplifting [*Bishop,* 1988]. Continuous hemipelagic sedimentation occurred during the Turonian in the deeper water facies further north (Razgallah et al., 1994).

2.5.4.4. Carbon isotope chemostratigraphy

A correlation of carbon isotopic data from nine Tunisian C/T sections, complemented by TOC and biostratigraphic results, is illustrated in Fig. 23. As in Morocco (see above) a threefold subdivision based on subcycles appears to be developed in the majority of the ^{13}C curves of the studied Tunisian C/T sections, e.g., sections ob, bg, ne and do (Fig. 23). In the Oued Smara section (sm), only two peaks are fully developed [*Accarie et al.,* 1996], which may correlate with peaks B and C from England and the Western Interior Basin. In all of these sections, peak B occurs slightly above the last appearance of *Rotalipora cushmani* and peak C just below the first appearance of *Q. gartneri* (CC11). The C/T boundary usually lies slightly above the maximum ^{13}C value [*Jarvis et al.,* 1988; *Accarie et al.,* 1996]. Slight discrepancies between the biostratigraphically and isotopically constrained positions of the C/T boundary do, however, partly occur, such as in the Nebour section (ne) of *Nederbragt and Fiorentino* [1999]. As in Morocco (see above) the ^{13}C subpeaks in Tunisia do not correlate with the TOC maxima (Fig. 23) and confirm the excursion's worldwide stratigraphic significance. In Tunisia higher TOC values generaly develop well after the onset of the ^{13}C excursion, a C/T phenomenon observed also in other parts of the world [*Keller et al.,* 2001]. The detailed individual form of the ^{13}C C/T excursions, however, depends on a variety of parameters, including local sediment accumulation rates and sampling density (Barrett, 1998). In C/T sections, with reduced or increased numbers of subcycles within the ^{13}C excursion, the attribution to peaks A, B, C is not always straightforward, leaving room for potential miscorrelations. For example, interpretation of the C peak in the Nebour section (ne, [*Nederbragt and Fiorentino,* 1999]) is complicated by the occurrence

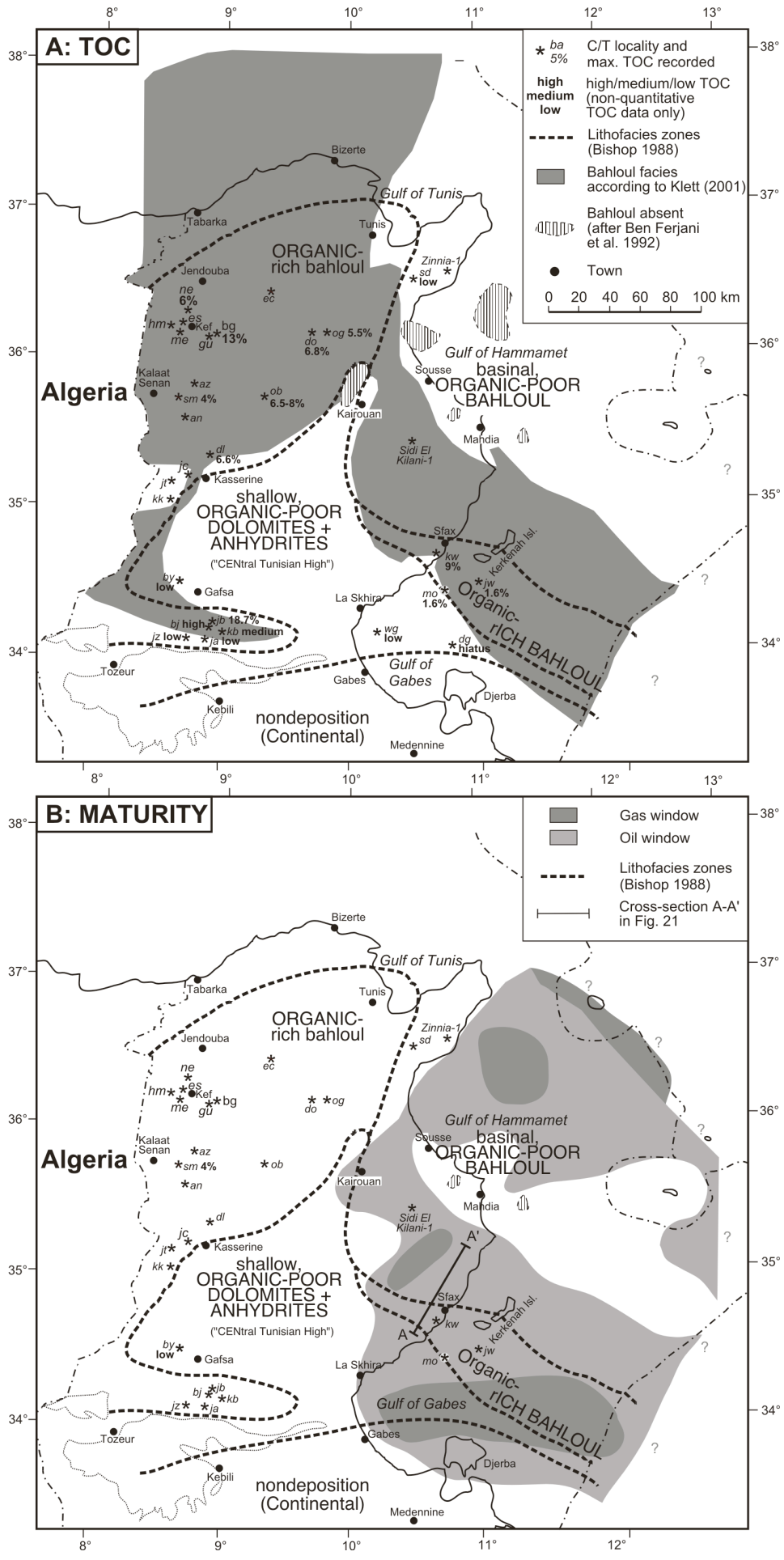
A: TOC
ba 5% C/T locality and max. TOC recorded
high medium low high/medium/low TOC (non-quantitative TOC data only)
Lithofacies zones (Bishop 1988)
Bahloul facies according to Klett (2001)
Bahloul absent (after Ben Ferjani et al. 1992)
Town
0 20 40 60 80 100 km
Algeria
ORGANIC-rich bahloul
shallow, ORGANIC-POOR DOLOMITES + ANHYDRITES
("CENtral Tunisian High")
Gulf of Hammamet basinal, ORGANIC-POOR BAHLOUL
Organic-rICH BAHLOUL
nondeposition (Continental)
Gulf of Tunis
Gulf of Gabes
Kerkenah Isl.
Bizerte
Tabarka
Tunis
Jendouba
Kef
Kalaat Senan
Kairouan
Sousse
Mandia
Sfax
Gafsa
La Skhira
Tozeur
Gabes
Djerba
Kebili
Medennine
Zinnia-1
Sidi El Kilani-1
ne 6%
ec
hm
me
gu
bg 13%
do 6.8%
og 5.5%
az
sm 4%
ob 6.5-8%
an
dl 6.6%
jc
jt
kk
by low
bj high
kb medium
jz low
ja low
kw 9%
jw 1.6%
mo 1.6%
wg low
dg hiatus
8°
9°
10°
11°
12°
13°
38°
37°
36°
35°
34°
B: MATURITY
Gas window
Oil window
Lithofacies zones (Bishop 1988)
Cross-section A-A' in Fig. 21
A
A'

Figure 20. (A) Maximum TOC values in the Cenomanian–Turonian Bahloul Formation in Tunisia (sources of TOC data: section bg: [*Bechtel et al.,* 1998]; bj, by, ja, jb, jz, kb: *Abdallah et al.,* 2000; dl: *Hughes and Reed,* 1995; do, og: *Barrett,* 1998; jw, mo: Ben *Ferjani et al.,* 1990; kw: *Bishop,* 1988; ne: *Nederbragt and Fiorentino,* 1999; *Bechtel et al.,* 1998; *Barrett,* 1998; ob: ETAP, unpublished; *Schlanger et al.*, 1987; *Barrett,* 1998; *Farrimond et al.,* 1990; sd: *Touati et al.,* 1995; sm: *Robaszynski et al.,* 1993b; *Accarie et al.,* 1996]). Facies zones modified after *Bishop* [1988]; distribution of the Bahloul Fm. after *Klett* [2001]. (B) Bahloul maturation zones [after *Bishop,* 1988]. For legend for codes of sections, see Table 2.

of several shorter cycles as well as by the existence of a major 13C peak a few meters above the Bahloul Formation (Fig. 23). In condensed sections away from the depocenter, the excursion may consist of fewer subcycles and it may be unclear whether the A or C peak is absent (e.g., og section; Fig. 16 and Fig. 23).

2.5.4.5. Palaeoecology

Detailed palaeoecological investigations in Tunisian C/T sections using microfacies analysis, planktic and benthic foraminifera, calcareous nannofossils and ammonites have been carried out by *Robaszynski et al.,* [1990, 1993a,b]; *Abdallah et al.,* [1995, 2000], *Abdallah and Meister* [1997], *Saidi et al.* [1997], *Nederbragt and Fiorentino* [1999] and others.

The nannofossil assemblage within the C/T sediments in the Bahloul Formation (as studied by *Nederbragt and Fiorentino* [1999] in section ne; Fig. 16) is characterised by a low diversity that was attributed to a combination of hostile conditions and dissolution during deposition. *Watznaueria barnesae* is a significantly solution resistant form and represents one of the most abundant calcareous nannofossil species in the Bahloul Formation in the section but it makes up usually less than 40% of the calcareous nannofossil assemblage. *Roth and Krumbach* [1986] used a value of *greater than* 40% as evidence for strongly modified nannofossil assemblages altered by dissolution. *Nederbragt and Fiorentino* [1999, p. 55] also noted a drop in abundance and diversity of calcareous nannofossils within the organic-rich strata of the Bahloul Formation. Furthermore, they recorded a decrease in abundance of high productivity indicators in the ne section among the nannofossils, that could be real or the result of dissolution. Overall, calcareous microfossils do not show evidence for a major increase in primary productivity during the CTBE while the Mid Cenomanian–Mid Turonian section as a whole indicates moderately high productivity.

The planktic foraminiferal fauna in the Bahloul Formation (as studied by *Robaszynski et al.,* [1990], p. 221 in the Kalaat Senan area) is composed of globular forms, dominated by the most primitive morphotypes that lived in the uppermost layer of the ocean (ca. 0–50 m). Their diversity is low but their productivity high, characteristic of a colonizer fauna [*Robaszynski et al.,* 1990]. Sub-horizontal bioturbations are the only evidence for the presence of macroorganisms. In the burrows echinoderm debris, phosphate and glauconite grains are concentrated, indicating an increase in energy. On occasions the water stratification must have been disturbed by some ventilation which brought enough oxygen to the water/sediment interface to allow the development of burrowing organisms [*Robaszynski et al.,* 1990].

In contrast to the planktonic organisms, the Bahloul evidences a severe drop in the benthonic biomass, as described by *Abdallah and Meister* [1997] from the Gafsa/Chott area. An anaerobic water/sediment interface has to be assumed (Fig. 22). Following deposition of the Bahloul Formation a gradual relaxation of the hostile oceanic conditions occurred, resulting in diversification of the planktonic/benthonic foraminifera and nannofossil populations.

2.5.4.6. Bulk and molecular geochemistry

Detailed and comprehensive organic geochemical description of the C/T Bahloul Formation were given by *Farrimond et al.* [1990], *Montacer et al.,* [1986, 1988, 1989], *Montacer* [1995], *Orgeval* [1994], *Bechtel et al.* [1998], *Hughes and Reed* [1995], *Barrett* [1998] and *Caron et al.* [1999]. The organic-rich Bahloul Formation is characterised by marine-derivered algal/bacterial type II

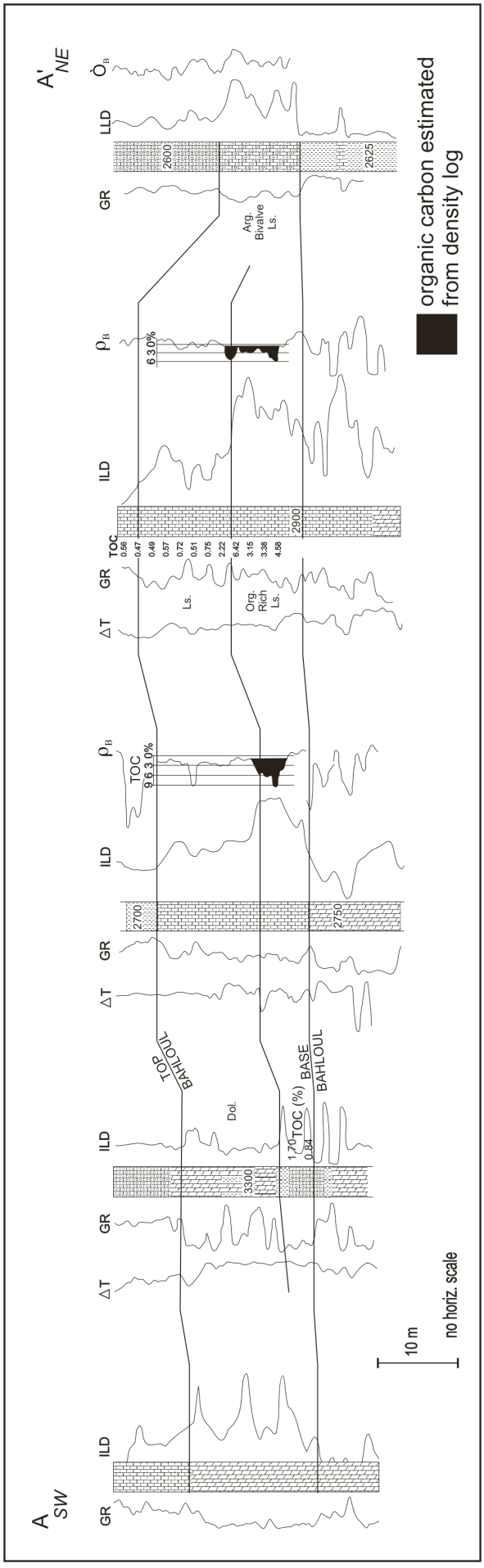

Figure 21. Cross-section of the Bahloul formation in east–central Tunisia [from *Bishop*, 1988] (see Fig. 20B for location of the A–A' transect). GR=γ-ray, T=sonic, ILD=induction log, LLD=laterolog deep, B=bulk density; shaded areas on bulk density curves show estimated organic carbon content using resistivity data as described in *Meyer and Nederlof* [1984].

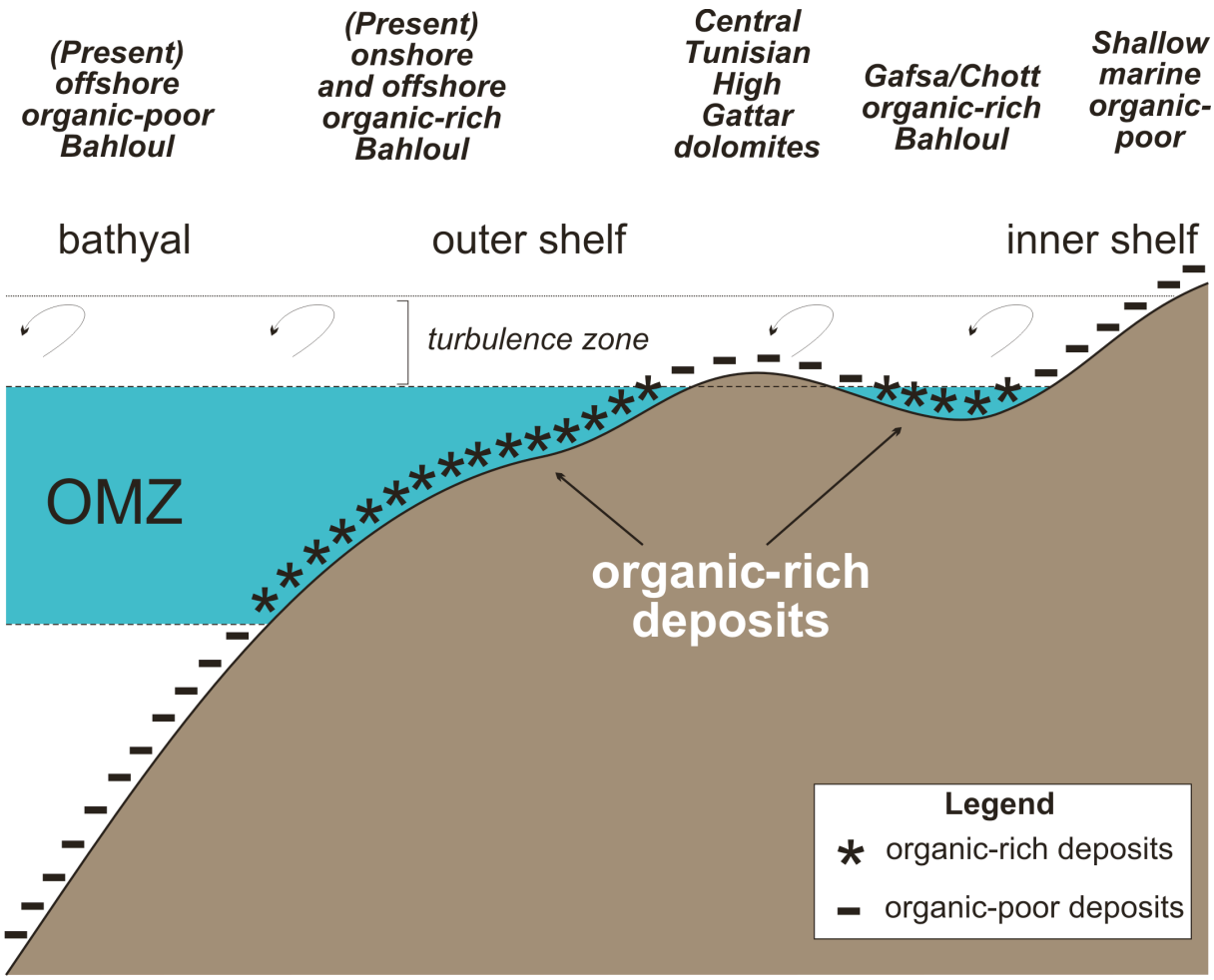

Figure 22. Assumed Cenomanian–Turonian impingement of the OMZ onto the Tunisian shelf controlling the distribution of C/T organic-rich strata (based partly on *Bishop* [1988], *Barrett* [1998] and *Peypouquet et al.* [1986]).

kerogen (HI between 200 and 700 mg HC/g TOC) with TOC concentrations of up to 10%, indicating excellent source rock qualities for oil and gas if buried to a suitable depth. An early maturity level of these laminated black shales is confirmed by *T*max values nearly constant between 420 and 430 °C in places. Organic petrological studies on these sediments indicate kerogen dominated by yellow-orange to bright yellow-orange fluorescing amorphous organic matter (AOM), some palynomorphs, including dinoflagellate cysts. Terrestrial macerals are found as detrital vitrinite and inertinite and are only subordinate in these sediments. Biological marker distribution is typically characterised by short and long chain *n*-alkanes, steranes, hopanoids and acyclic isoprenoids indicating predominantely marine algal/zooplankton OM. In addition, 4-methylsteranes reflect a significant input from dinoflagellates. Methylhopanes indicative of an input from cyanobacteria or methylotrophs are abundantly present in these sediments. The occurrence of bisnorhopane in the Bahloul black shales reflects a specific bacterial source possibly associated with a highly reducing sulphur-rich depositional environment [*Farrimond et al.,* 1990]. It is reported that this compound is found in very high concentrations in petroleum as a free hydrocarbon [*Peters and Moldowan,* 1993]. However, stable carbon isotope investigations of bisnorhopane in the Miocene Monterey Formation suggest that the biological precursor was probably a sediment-dwelling chemo-autotrophic bacterium, utilizing porewater CO2 as a carbon source [*Schouten et al.,* 1998]. Notably, similar observations are reported also from the Tarfaya Basin where this desmethyl hopane occurs in high abundances associated with trace elements characteristic for extremely reducing bottom-water conditions [*Kolonic et al.,* 2002]. This suggests that bisnorhopane is biosynthesised as such by a specific organism only occurring under very extreme palaeoenvironmental conditions.

Code	Locality	Region	Coordinates	References
an	Fej el Annaba	Kalaat Senan		Section 'ana' in *Robaszynski et al.* [1993a], section 'KSn' in *Maamouri et al.* [1994]
az	Azreg	Kalaat Senan		Section 'az' in *Robaszynski et al.* [1993a]
bg	Bou Grine	NW		*Bechtel et al.* [1998], section 'BG' in *Maamouri et al*. [1994]
bj	Jebel Bou Jarra	Gafsa-Chotts		*Abdallah et al.* [2000: p. 52[
by	Jebel Ben Younès	Gafsa-Chotts		*Abdallah et al.* [2000: p. 66]
dg	Degla-1 well	Gulf of Gabes	34°02'N, 10°50'E	own data
dl	Douleb	Kasserine		*Hughes and Reed* [1995]
do	Dir Oulad Yahia	NW	36°6'N, 9°40'E	Section 'DOY' in *Barrett* [1998: p. 96]
ec	Ech Cheid	NW	36°24'N, 9°20'E	Section 'EC' in *Barrett* [1998: p. 92]
es	Jebel Es Seif	NW		Section 'ES' in *Maamouri et al.* [1994]
gu	Koudiat Guenaoua	NW		Section 'G' in *Maamouri et al.* [1994]
hm	Hammam Mellègue	NW		Section 'HM' in *Maamouri et al.* [1994]
ja	Jebel Askar	Central		*Abdallah et al*. [2000: p. 39]
jb	Jebel Berda	Gafsa-Chotts		*Abdallah et al.* [2000: p. 57]
jc	Jebel Chambi	Kasserine		*Saïdi et al.* [1997: p. 67]
jk	Jebel Khechem el Kelb	Kasserine		*Saïdi et al*. [1997: p. 68]
jt	Jebel Tella	Kasserine		*Saïdi et al.* [1997: p. 70]
jw	Jawhara-1 well	Gulf of Gabes	34°22'N, 10°59'E	*Ben Ferjani et al.* [1990:121]
jz	Jebel Zitouna	Gafsa-Chotts		*Abdallah & Meister* [1997: p. 203]
kb	Khanguet Besbessa	Gafsa-Chotts		*Abdallah & Meister* [1997]
kw	Kerkennah West Permit	Sfax		*Bishop* [1988]
me	Melalis	NW		Section 'ME' in Maamouri et al. (1994)
mo	Morjane-1 well	Gulf of Gabes	34°18'N, 10°48'E	*Ben Ferjani et al.* [1990:121], own data
ne	Nebour	NW	36°15'N, 8°36'E	Section 'N' in *Barrett* [1998: p. 102], *Nederbragt & Fiorentino* [1999], *Bechtel et al*. [1998]
ob	Oued Bahloul	NW	35°42'N, 9°20'E (Barrett 1998 section)	Section 'OB' in *Barrett* [1998: p. 86], section 'blb' *in Robaszynski et al.* [1993a], section 'OB' in *Maamouri et al.* [1994], *Schlanger et al.* [1987], *Farrimond et al*. [1990]
og	Oued El Gsab	NW	36°06'N, 9°48'E	Section 'OG' in *Barrett* [1998: p. 99]
sd	Sidi Djedidi-1 well	NE		*Touati et al*. [1995]
sm	Oued Smara	Kalaat Senan	35°45'N, 8°28'E	Section 'sm' in *Robaszynski et al.* [1993a,b], section 'NH' in *Maamouri et al.* [1994], *Accarie et al*. [1996]
wg	West Gabes-1 well	Gulf of Gabes	34°04'N, 10°14'E	own data

Table 2. Abbreviation codes and references of Tunisian C/T localities (Fig. 15, Fig. 16 and Fig. 20)

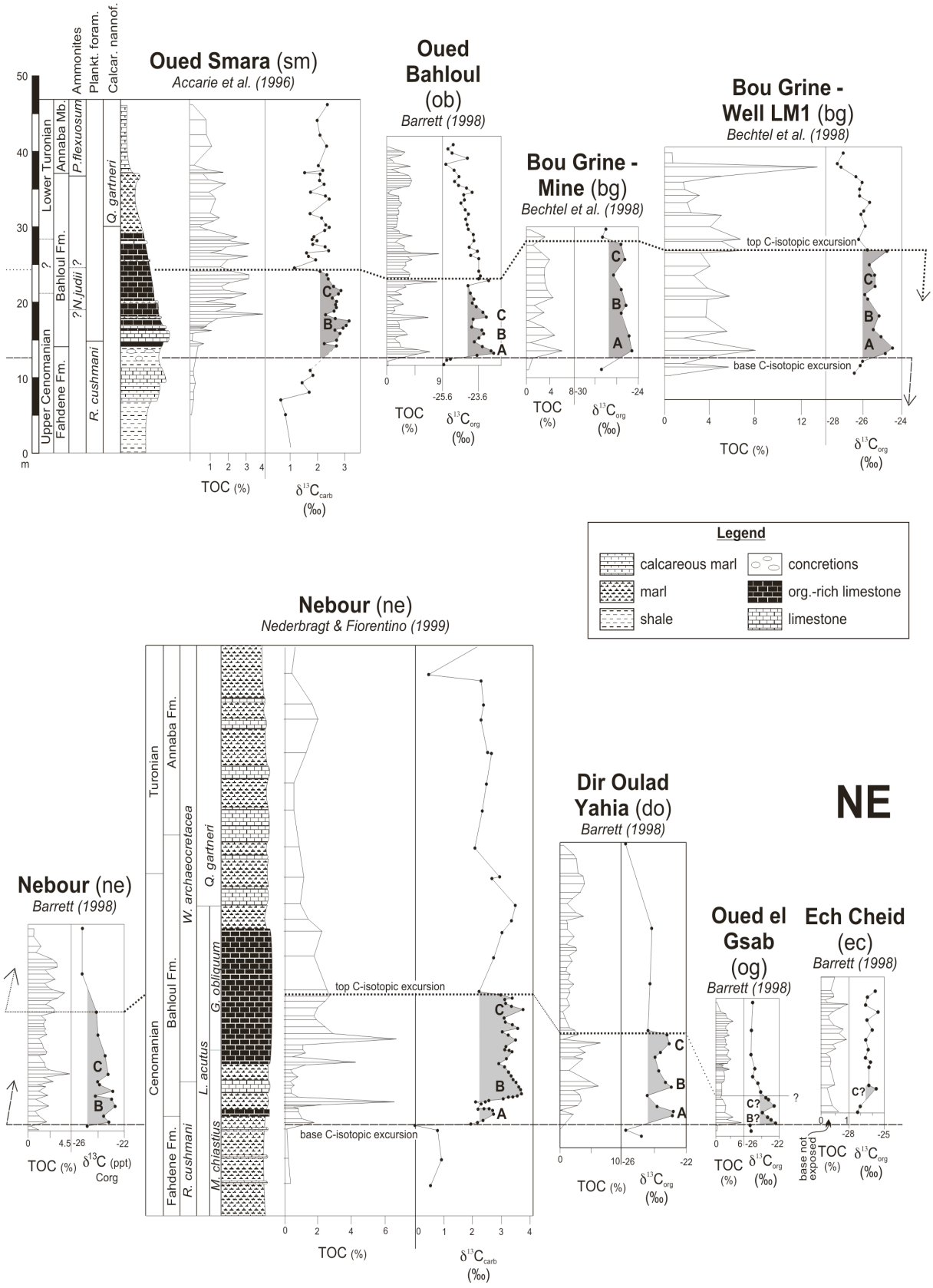

Figure 23. Distribution of organic matter within the C/T-boundary interval in northern Tunisia in relation to available biostratigraphic data and the characteristic C/T carbon isotope peak. SW-NE transect is illustrated in Fig. 16. Data compiled after *Accarie et al.* [1996], *Barrett* [1998], *Bechtel et al.* [1998] and *Nederbragt and Fiorentino* [1999].

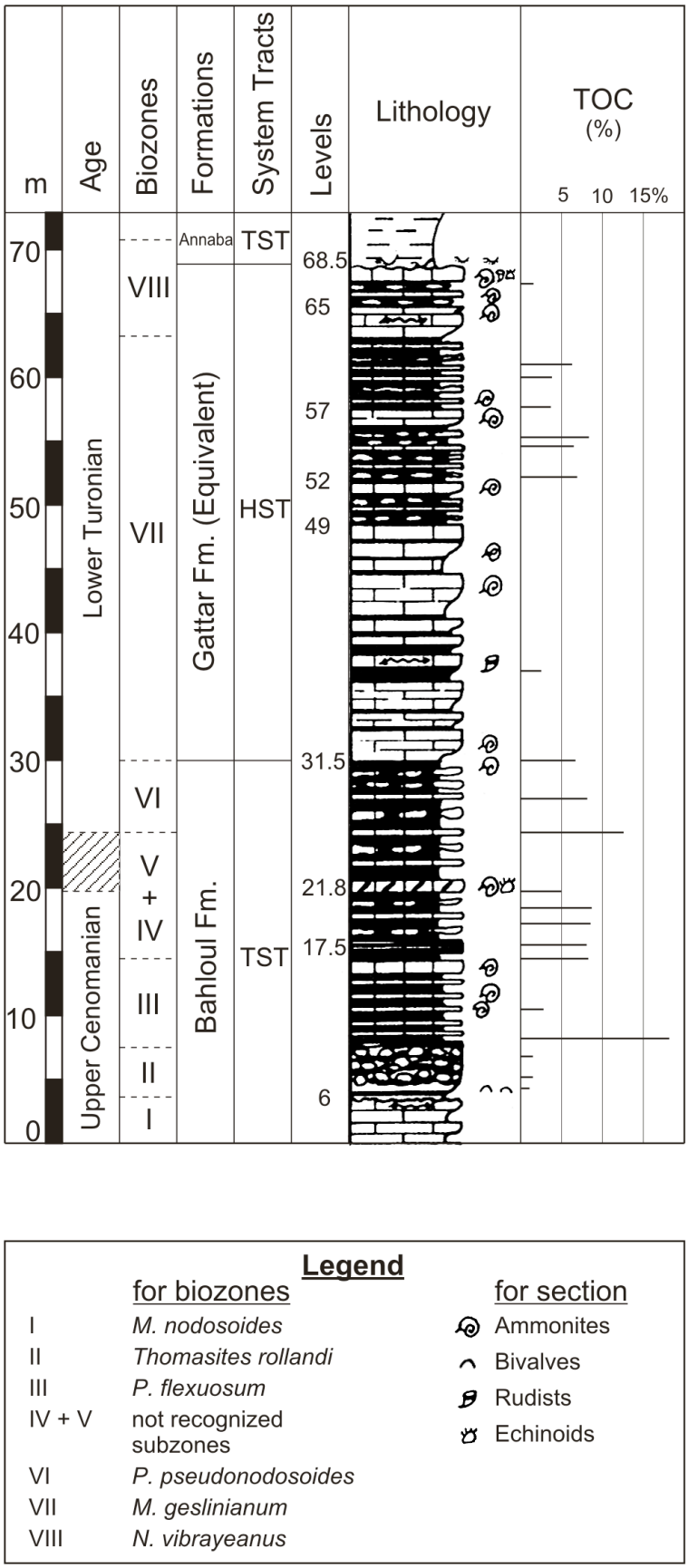

Fig. 24. Biostratigraphy, sequence stratigraphic interpretation and organic richness of the Upper Cenomanian–Lower Turonian in the Jebel Berda section (Gafsa-Chott graben; Fig. 15) [after *Abdallah et al.*, 2000; Abdallah, personal communication].

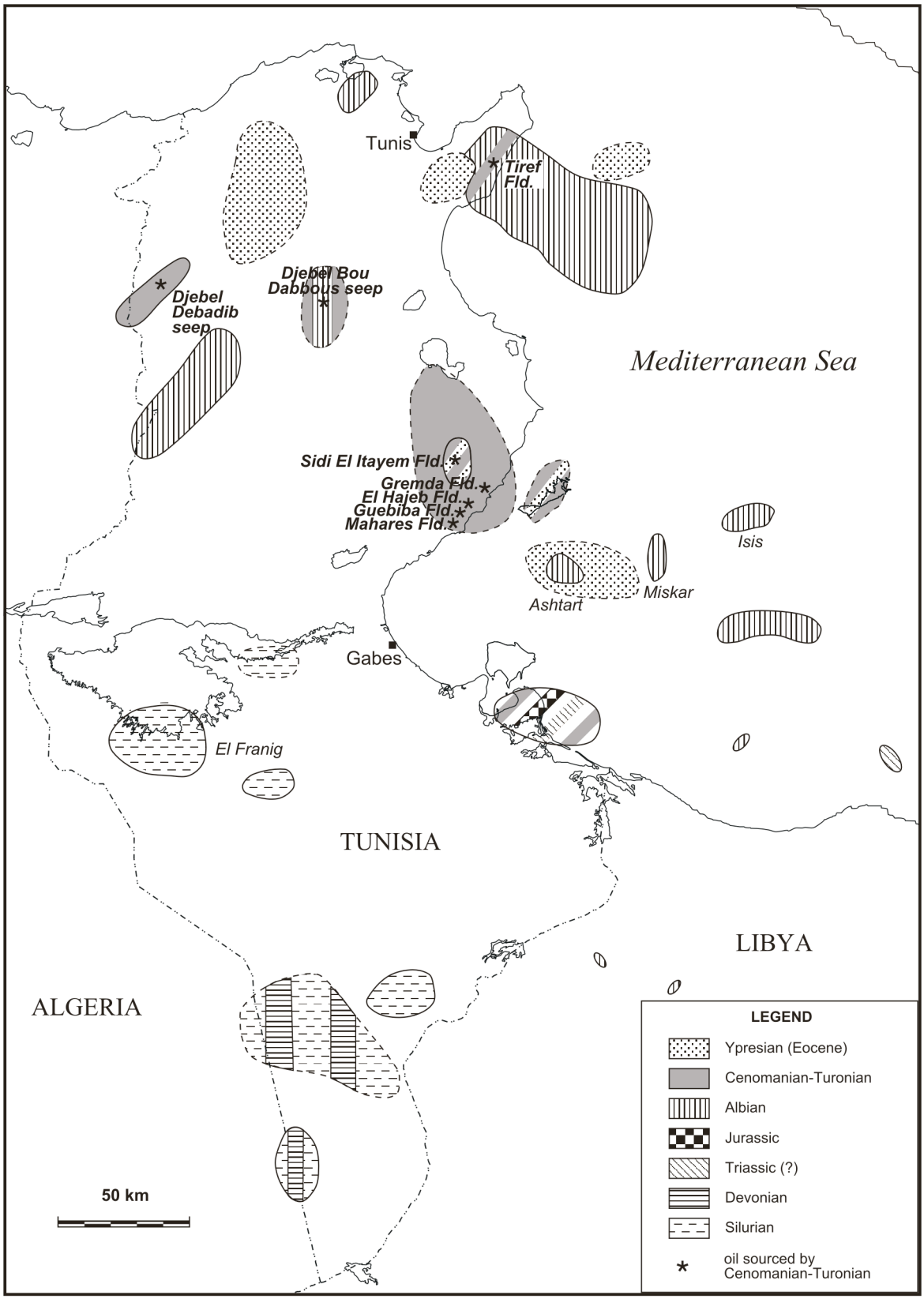

Fig. 25. Oil-source rock correlation in Tunisia [after *Gaaya and Ghenima*, 1998; *Hughes and Reed*, 1995]. C/T-sourced hydrocarbons are known mainly from onshore northern Tunisia.

2.5.4.7. Kerogen characterisation

Barrett [1998] gives a detailed description of the kerogen from the organic-rich Bahloul formation. Accordingly, the organic-rich Bahloul black shales exhibit relatively aliphatic-rich kerogens but contain a relatively higher amount of sulphur aromatic compounds compared to other C/T sections from the Tethyan realm. Similar to the Tarfaya kerogens the vast majority of pyrolysis products generated from the Bahloul kerogen are sulphur-containing components such as alkylthiophenes, alkenylthiophenes and alkybenzothiophenes. Isoprenoidal alkenes/alkanes constituents are only present in relatively low amounts and non-sulphur containing pyrolysis products are mainly composed of alkylbenzenes and homologous series of *n*-alkenes and *n*-alkanes. Higher plant biopolymers are only present in trace amounts in the flash pyrolysates supporting a marine nature of the OM from the Bahloul Formation.

2.5.4.8. Potential for C/T-sourced hydrocarbons, minerals exploration

The Bahloul horizon is one of the main potential source rocks in Tunisia, particularly in the central eastern part of the country (Fig. 25) [*Ben Ferjani et al.,* 1990]. According to a geochemical study by *Hughes and Reed* [1995], the Bahloul is a proven source for oil fields in the onshore Gulf of Gabes Guebiba, Gremda, Mahres and El Hajeb fields, the onshore Gulf of Hammamet Tiref field and an oil-stained outcrop in Djebel Debadib. The respective carbonate reservoir units are mostly in the Cretaceous (e.g., Zebbag Formation, Turonian) and the Eocene (e.g., Metlaoui Formation and equivalent units, earliest Eocene) [*Bishop,* 1988; *Montacer,* 1995]. Apart from the C/T Bahloul Formation, the other important petroleum source rocks in north and central Tunisia are the Albian Mouelha Formation and the Eocene Bou Dabbous Formation [*Hughes and Reed,* 1995]. In some areas, a mixture of oils appears to be present, derived from the C/T interval in combination with either the Albian (Sidi El Itayem field) or Eocene (Djebel Bou Dabbous seep) source rock horizon [*Hughes and Reed*, 1995].

In the Tunisian offshore, the hydrocarbons discovered to-date are believed to have been sourced almost exclusively by the Albian and Eocene source horizons (Fig. 25). The widespread Eocene (Bou Dabbous) source for the Tunisian offshore oils implies either (1) the absence of a Cretaceous-based petroleum system or (2) the presence of an effective seal which prevents Cretaceous derived oils from reaching Tertiary reservoirs in the Gulf of Gabes [*Hughes and Reed*, 1995]. The occurrence of C/T-derived oils immediately onshore suggests the seal scenario is the case and makes pre-Tertiary reservoirs attractive targets in the offshore [*Hughes and Reed*, 1995].

In northern Tunisia, little petroleum exploration on Bahloul-sourced plays has been carried out so far, despite several known oil seeps there [*Montacer,* 1995]. Although *Touati et al.* [1995] eliminated the C/T interval as a potential source in the Sidi Djedidi well (Cap Bon Permit; Fig. 20) on grounds that the C/T there is characterised by low TOC and poor hydrocarbon generating potential, possible better quality C/T source rocks may occur nearby. This is, firstly, because strong graben-related variations in the local palaeorelief have to be assumed (Fig. 15) and, secondly, the Sidi Djedidi well is located in the basinal organic-poor Bahloul facies, but according to *Bishop* [1988] only a few kilometers to the east the organic-rich Bahloul facies occurs (Fig. 20).

Areas where the Bahloul has reached the maturation depth of the oil and gas windows, respectively, are mapped in Fig. 20. Onshore in the so-called Bahloul-Block, the Bahloul Fm. (70 km west of Kairouan) is estimated to have entered the oil window during the Late Cretaceous with peak generation during Eocene–Miocene times (ETAP, 2000, unpublished data).

Besides being a petroleum source rock in parts of Tunisia, the organic-rich Bahloul deposits also play an important role in the genesis of Zn/Pb ore deposits in northern Tunisia (e.g., Bou Grine; [*Orgeval,* 1994; *Bechtel et al.,* 1998]) and in eastern Algeria. The origin of these Zn/Pb ore deposits is related to hypersaline basinal brines, made of ground water and dissolved Triassic evaporites, that leached metals from the Triassic–Cretaceous sediments. The ore deposition happened when these metal-bearing solutions mixed with microbially reduced sulphate solutions that were associated with the organic carbon of the C/T Corg-strata [*Orgeval,* 1994; *Bechtel et al.,* 1998].

2.5.5. Libya

2.5.5.1. Structural setting

Following the Late Triassic–Early Jurassic separation of the Turkish–Apulian Terrane [Sengör, 1985; Flexer et al., 1986] from northern Gondwana, Libya became part of the North African passive continental margin that was affected by Neocomian (Early Cretaceous) to Eocene rifting phases of a failed arm of the Sirte Triple Junction and subsequently by Eocene to Middle Miocene compression due to subduction along the Afro–Eurasian subduction zone [Jongsma et al., 1985, p. 177]. The detailed Cretaceous structural history in Libya was more complicated, of course, with multiple alternations of compressional and extensional regimes.

Early Cretaceous rifting offshore Sirt created a series of half grabens with Neocomian to Albian sediments in a belt which runs broadly parallel to the present-day coastline from Benghazi to Sirt [Smith and Karki, 1996] (Fig. 26). This includes the NW trending Tripolitania and Jarrafa troughs (Fig. 26), which served as depocentres characterised by relatively deeper water sediments such as shales, marls and calcareous oozes [Jongsma et al., 1985, p. 174].

During the Late Cretaceous, active rifting ceased and a passive infill of mud, sand and carbonate occurred across the entire offshore Sirt Basin [Smith and Karki, 1996]. An important compressional event in Libya occurred during the Mid Cenomanian ("Mid-Cenomanian Event"), which partly inverted the horst and graben structures, caused erosion and led to the development of an irregular landscape [Wennekers et al., 1996]. During the Cenomanian transgression, this palaeotopography gradually became submerged, forming peninsulas and islands. Facies and thickness distribution of Upper Cretaceous units in Libya is controlled to a great extent by this marked palaeotopography, as evidenced by characteristic onlap features [Wennekers et al., 1996, pp. 25–26]. Erosion of uplifted highlands resulted in deposition of basal sandstone and conglomerates (Bahi Formation; Fig. 27) in many places [Wennekers et al., 1996].

Tectonic activity in Libya apparently commenced again during the Late Cretaceous [Wennekers et al., 1996: 26]. For example, very active synsedimentary Cenomanian–Turonian faulting from the eastern Sirte Basin was reported by Barbieri [1996, p. 191]. Another significant uplift phase occurred during the Late Turonian (`Sub-Hercynian Event'), which eroded Turonian and older strata in the central and southern parts of the Sirte Basin [Wennekers et al., 1996; Hallett, 2002].

2.5.5.2. Sea-level control, distribution and characteristics of C/T Corg strata

Major transgressions occurred during the Middle and Late Cenomanian in Libya, culminating in the Late Turonian, initiating the onset of marine sedimentation in large parts of northern Libya [Barr, 1972; Barr and Weegar, 1972; Reyment, 1980; Wennekers et al., 1996; El-Bakai, 1997; Selley, 1997]. In onshore northern Libya (e.g., Jebel Nafuhsa south of Tripoli), the facies of most Cenomanian–Turonian deposits ranges between lagoonal to inner shelf / ramp and consist of sandstones and conglomerates (Bahi Fm.), dolomites, marls, shales, sandstones, anhydrites (Sidi As Sid Fm. with Ain Tobi and Jefren Members, Lidam Fm., Nalut Fm., Etel Fm., Qasr al Abid Fm.) [Klen, 1974; Röhlich, 1974; Megerisi and Mamgain, 1980; Belhadj, 1996; El-Bakai, 1997; Heselden et al., 1996; Hammuda et al., 2000; Tawadros, 2001] (Fig. 26, Fig. 27 and Fig. 28). Towards the offshore, deeper shelf facies occur, such as laminated dolomitic marls containing miliolid and pelagic foraminifera and rudist material of the Alalgah Formation in the Gabes–Tarabulus–Misratah (Tripolitania) Basin [Hammuda et al., 1985] (Fig. 28). The miliolids and rudists are thought to be derived from higher up the slope near the crest of the uplift. The pelagic foraminifera are more typical of this environment [El-Bakai, 1997, p. 25]. The outer shelf/ramp environment is only known from a few Libyan offshore wells (e.g., K1-137, H1-137, L1-137, J1-NC35A) which reached the Cretaceous. Rusk [2001, p. 444] reported the Bahloul-equivalent strata to have an average thickness of 35 m in the Tripolitania Basin. In NE Libya, the Cenomanian is partly represented by brownish/greenish-grey, pyritic deep-water shales of the Al Hilal Fm., rich in planktic foraminifera [Barr and Hammuda, 1971; Megerisi and Mamgain, 1980; Duronio et al., 1991; Wennekers et al., 1996].

Organic-rich strata of Cenomanian–Turonian age is less common in Libya than, for example, in neighbouring Tunisia, nevertheless, C/T strata with an elevated organic content has been reported

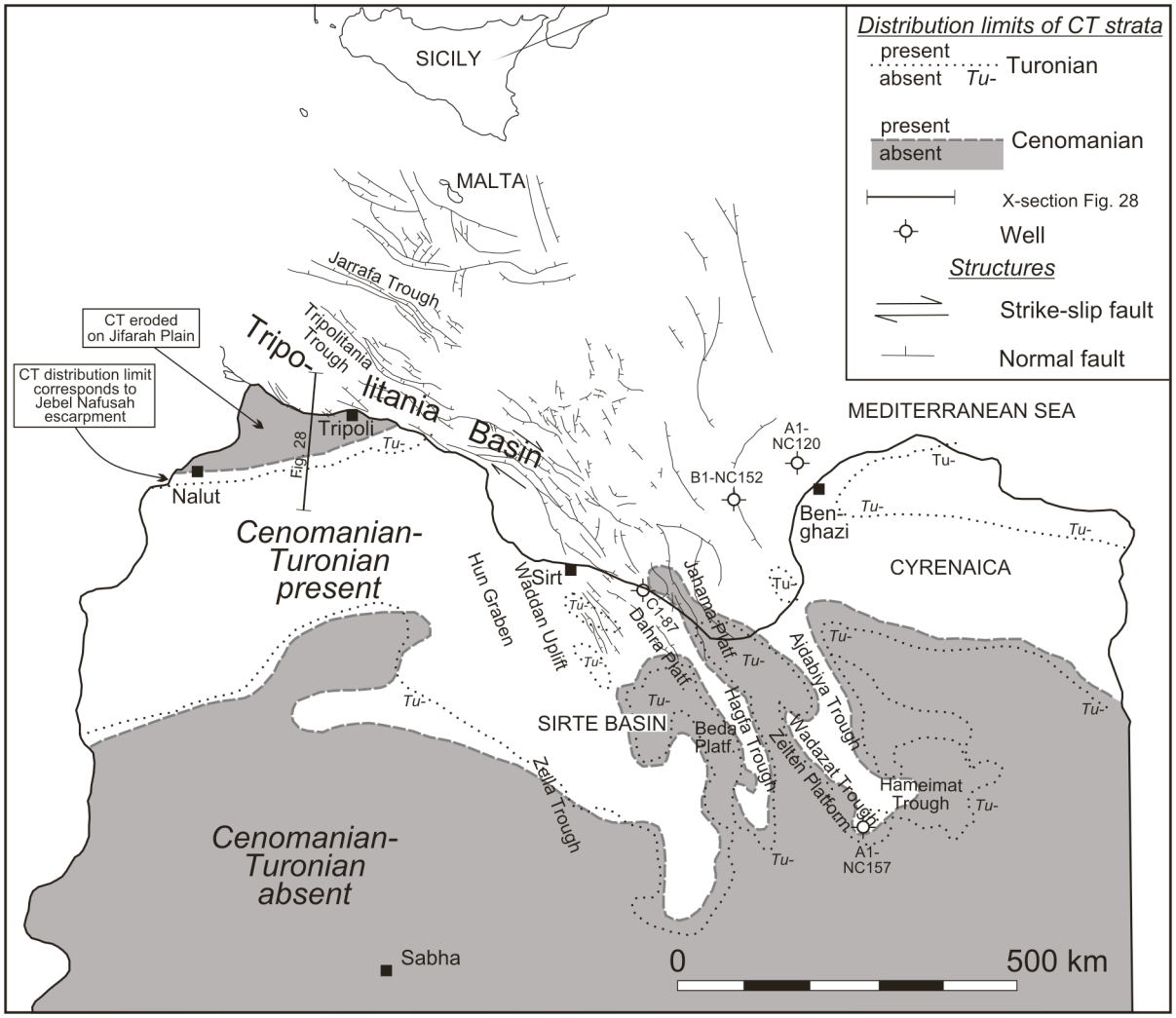

Figure 26. Present-day distribution of Cenomanian and Turonian strata in Libya [after *Wennekers et al.*, 1996]. Also shown are major fault systems on top of the Cretaceous (after Ziegler [1978] in *Jongsma et al.*, [1985]: their Fig. 15).

from parts of northern onshore and offshore Libya, in both lagoonal/inner shelf and deeper shelf settings. It may be assumed that deposition of C/T organic-rich strata in the shallower settings may have occurred preferrably in partly isolated palaeodepressions formed by Early Cretaceous halfgrabens. One of these settings is the Hameimat (=Abu Attifel) Trough/Basin in the eastern Sirte Basin (Fig. 26) where the upper Cenomanian–Turonian Etel Formation has TOC values of up to 6.5%, containing predominantly amorphous and algal type II kerogen [*El-Alami,* 1996]. The base of the Etel Fm. is thought to have been deposited during the beginning of the latest Cenomanian transgression and consists of variable lithologies with dark shales dominating [Barbieri, 1996: p. 191]. A low diversity assemblage occurs, characterised by smooth ostracods and quinqueloculinids, indicating a muddy lagoonal environment that was largely isolated from open marine circulation [*Barbieri,* 1996; *El-Alami,* 1996; *Gras and Thusu*, 1998]. In the basin's depocentre, the Etel Formation is up to 1000 m thick, with a cummulative thickness of 200 m of source rocks, which are reported to cyclically alternate with more oxic strata [*El-Alami,* 1996]. A net shale isopach map of the Etel Formation in the Sirte Basin is given by *Rusk* [2001, his Fig. 5]. *El-Alami* [1996] considers the waxy crude oil of the Abu Attifel field in the Abu Attifel/Hameimat Basin as having been sourced by the Cenomanian–Turonian, whereas *Burwood et al.* [in press] suggest a different, non-marine source rock for the oils of this basin, based on a highly enriched ^{13}C signature and a low sterane/hopane ratio. The oil from the Messla Field may have been sourced by the C/T ([*Clifford et al.,* 1980], discussed in *Schlanger et al.* [1987]). In other parts of the eastern Sirte Basin, however, for example in well A1-NC157 on the Zelten Platform (Fig. 26) the C/T interval is organically lean [*Baric et al.,* 1996].

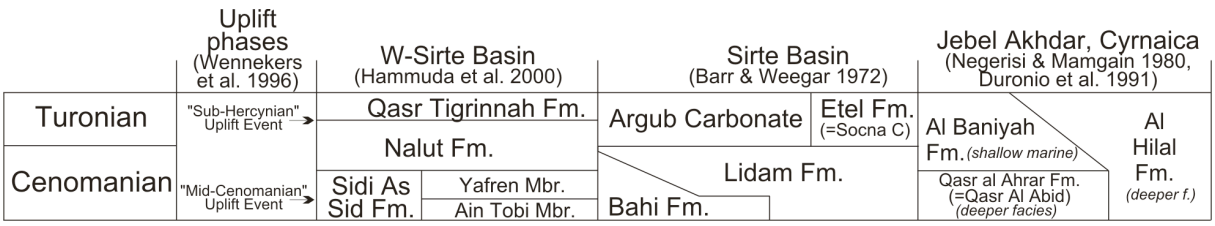

Figure 27. **Correlation of Cenomanian-Turonian lithostratigraphic units in Libya**

From offshore well C1-87 in the northwestern Sirte Basin, *Baair et al.* [2001] described TOC values of 1.39–1.54% from the Cenomanian–Turonian Etel Formation. The organic matter is largely algal in type but also includes minor to significant portions of woody, herbaceous and inertinitic kerogens. HI values range between 250 and 280. This interval apparently consists of fair-poor source rocks (3.48–4.31 mg/g S2) for oil and gas [*Baair et al.,* 2001]. Underneath this unit, two thin organic-rich horizons were identified within the Cenomanian Lidam Formation, namely a shale with 2.19% of good quality (HI=368) organic carbon material (very good source potential, 8.05 mg/g S2) and a shale with 1.52% TOC (HI=279 HI, good source potential, 4.24 mg/g S2).

In deeper shelf settings in the offshore, the undifferentiated Cenomanian Alalgah Formation occurs, which contains black shales and black to greyish brown dolomites interbedded with fossiliferous black shales, argillaceous dolomites and massive and nodular anhydrites [*Hammuda et al.,* 1985; *Tawadros,* 2001; *Hallett,* 2002]. Among oil explorationists the C/T deposits in onshore and offshore Cyrenaica (NE Libya) are known to be organic-rich and laterally extensive but nothing has been published. In the offshore of northwestern Libya also the Turonian–Coniacian Makhbaz Formation is characterised by an organic-rich facies, containing black and dark grey calcareous shales in addition to dolomitic limestones, argillaceous and glauconitic micrites and biomicrites [*Hammuda et al.,* 1985; Tawadros, 2001]. The presence of organic-rich C/T strata in the offshore of Malta is assumed [*Concessions Int*., San Ramon, CA, USA, personal communication].

2.5.5.3. Bulk and molecular geochemistry

A detailed and comprehensive organic geochemical description of C/T organic-rich strata in the Sirte Basin is given by *Robertson Research International* [1979], *Parsons et al.* [1980], *El-Alami et al*. [1989], *Ibrahim* [1991], *El-Alami* [1996] and *Baric et al.* [1996].

The organic-rich sedimentary succession in the Sirte Basin, that is restricted to the so called Etel Formation, is characterized by TOC values ranging between 0.63% and 6.54% with an average value of ~3%. In these sediments, OM consists predominantly of non-fluorescening amorphous kerogen with rarely recognizable morphology of palynomorphs and a minimum amount of exinite. The presence of migrabitumen presumably relates to migrated hydrocarbons originating probably from mature deeper organic-rich intervals of the Etel formation. Kerogen typing reveals a mixture of types II and II/III whereas type II kerogen is most likely attributed to the presence of hydrogen-enriched migrabitumen. Terrestrial macerals are present in form of vitrinite, recycled vitrinite and traces of inertinite and are considered to be of autochthonous or paraautochthonous origin. Rock-Eval pyrolysis supports the visual examinations of the kerogen with hydrogen indices ranging between 260 and 612 mg HC/g TOC indicating the fair to very good source rock potential. The obtained pyrolysis Tmax maturation values vary from 414 to 440 °C with maximum values of up to 476 °C in the deeper stratigraphic horizon of the Sirte/Etel formation suggesting middle to late maturity of the kerogen. The lower *T*max values are most likely depressed due to the presence of migrabitumen in these sediments. Vitrinite reflectance measured on these shales support the conclusion of maturity growth with depth. Apparently these source rocks have reached the initial stage of oil generation, i.e., the oil window. Qualitative estimation of the soluble OM from the Etel Shale indicates bitumen with a low content of alkanes and a high ratio of NSO and asphaltene components pointing to a natural migration. The estimated high proportion of organically bound sulphur of up to 1.7 wt.% in the bitumen indicates a kerogen similar to the Tarfaya kerogen that would require a lower activation energy to form hydrocarbons.

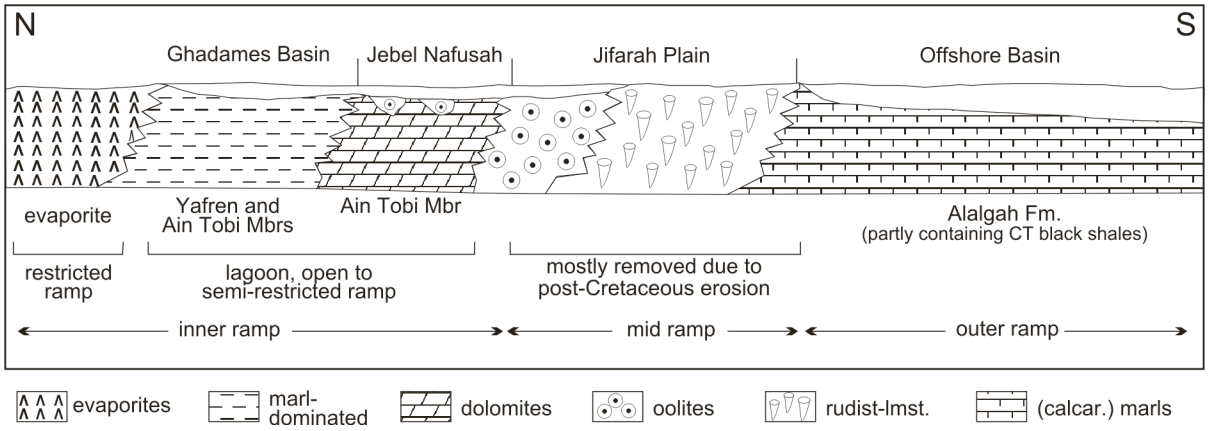

Figure 28. Cenomanian lithofacies transect in NW Libya [after El-Bakai 1997]. The distal Alalgah Formation in the offshore partly contains black shales [Hammuda et al. 1985; Tawadros 2001: 355]. Approximate location of transect illustrated in Fig. 26.

2.5.5.4. Potential for C/T-sourced hydrocarbons

About one-third of Libyan hydrocarbon production is from Cretaceous-aged rocks [*Wennekers et al.,* 1996; *Hallett,* 2002]; however, most of it is sourced from the Campanian Sirte Shale. Locally in the offshore, the C/T may also serve as a source rock (e.g., in the Cyrenaica area). Indications exist in wells A1-NC120 and B1-NC152 (Fig. 26) that hydrocarbons found here originate from a C/T source rock, based on typical Late Cretaceous isotope and sterane configuration data and a high wax contents, characteristic of the Etel Formation. However, an Eocene source is also thought possible [*Burwood et al.,* in press). In large parts of the Tripolitania Basin (Fig. 26), the C/T equivalents of the Bahloul Formation are presently in the oil-and gas window [*Rusk, 2001,* his Fig. 21].

2.5.6. Egypt

2.5.6.1. Structural setting

Following the Late Triassic–early Jurassic break-up of the Turkish–Apulian terrane from Egypt, the northern part of the country was subjected to extensional stress, resulting in the formation of halfgrabens [e.g., *Moustafa and Khalil,* 1990; *Hirsch et al.,* 1995; *Guiraud and Bosworth,* 1999]. This general pre-Turonian extensional regime is thought to have been interrupted by several short-lived compressional phases, e.g., during the Late Cenomanian (Abu Gharadig Basin: EGPC 1992 in *Khaled,* 1999, p. 390]. From about Turonian/Coniacian times onwards, the halfgrabens in Egypt became inverted [e.g., *Lüning et al.,* 1998b]. This intra-plate deformation was a consequence of the beginning collision of Afroarabia and Eurasia along the Cyprus subduction zone and Bitlis-Zagros suture zone.

Tectonic history in the intracratonic Abu Gharadig Basin in the northern Western Desert (Fig. 29) differs from the general development in other parts of northern Egypt because it represents a pull-apart basin related to wrenching along the Trans-African Lineament (TAL) (Pelusium Line) and parallel fault systems, sourced by transpressional stress in the Syrian Arc Foldbelt [*Keeley and Massoud,* 1998]. The Abu Gharadig Basin is composed of E–W trending halfgrabens and was formed during the Albian, reached maximum subsidence in the Late Cretaceous and was subsequently inverted during the Paleocene–Eocene. The Guindi (=Fayium) Basin to the east of the Abu Gharadig Basin is thought to have been located on the other side of the TAL and therefore experienced the opposite sense of movement, resulting in Late Cretaceous uplift and Paleocene–Eocene subsidence here [*Keeley and Massoud,* 1998].

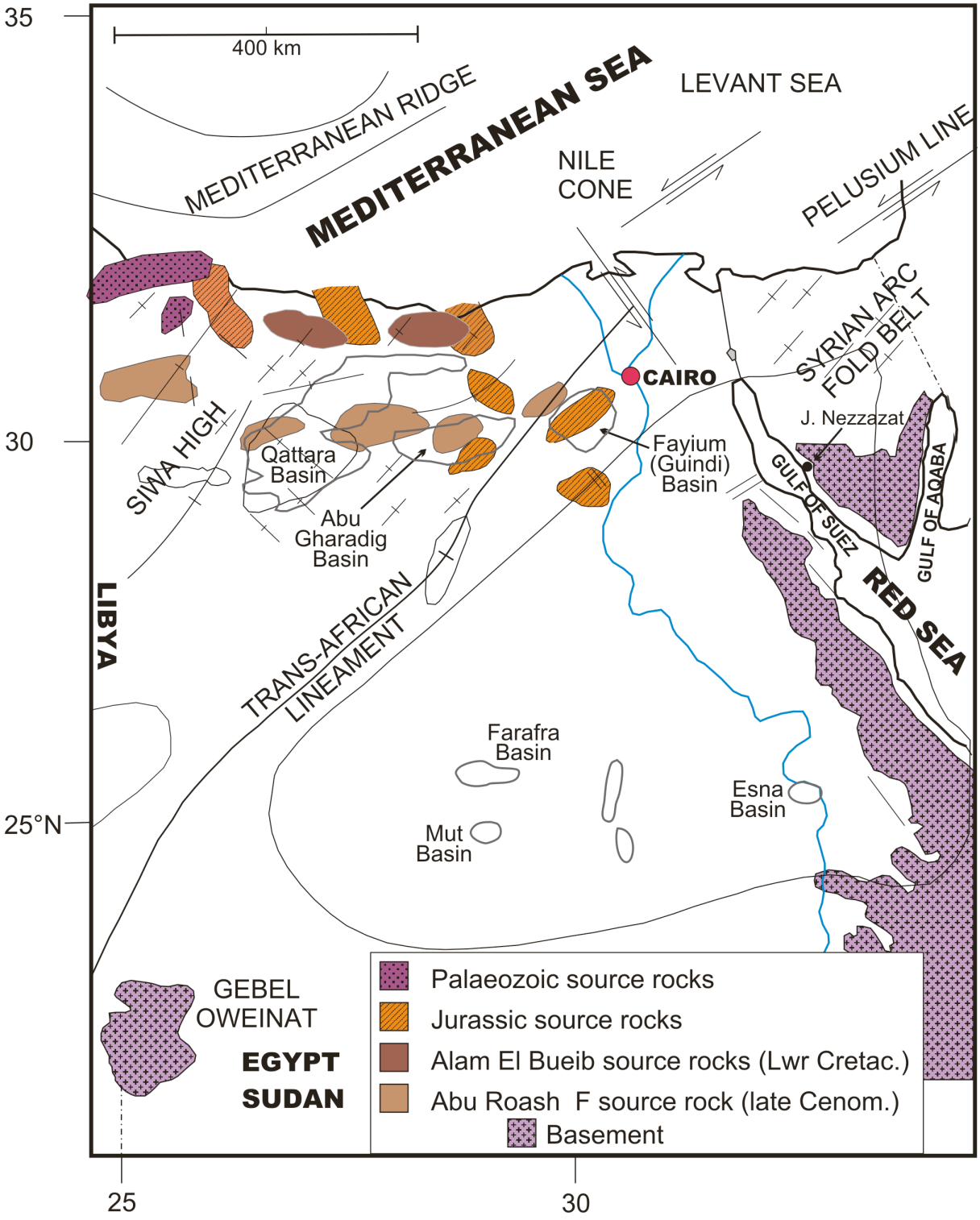

Figure 29. Distribution of the Late Cenomanian Abu Roash F-Member source rock and other source rock units in the Western Desert [after *Meshref,* 1996]. Locations of Cretaceous/Cenozoic sedimentary basins in Egypt after *Tawadros* [2001].

2.5.6.2. Distribution and characteristics of C/T Corg strata

The Cenomanian–Turonian strata in northern Egypt mainly consists of shallow marine carbonates and siliciclastics (Fig. 3), changing southwards into a coastal and terrestrial facies, and subsquently non-deposition [*Kuss and Bachmann,* 1996; *Philip et al.,* 2000; *Stampfli et al.,* 2001]. In large parts

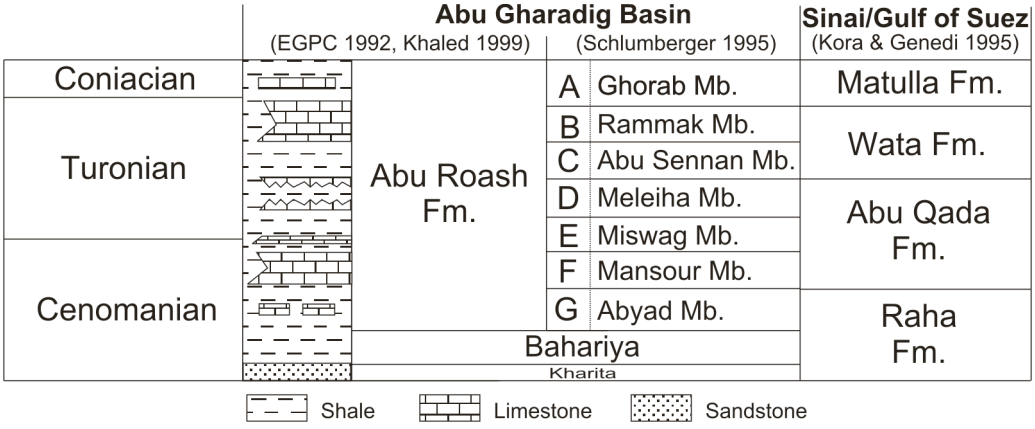

Figure 30. Egyptian Cenomanian–Turonian formations in the Abu Gharadiq Basin and the Gulf of Suez/Sinai. Note that correlation of Abu Roash Members and Abu Qada/Wata formation boundaries is partly uncertain (partly based on [*Tawadros,* 2001]).

of the country, the unit is organically lean, however, in some areas the C/T strata is characterised by TOC values of up to 1.5–2.5% with type I+II kerogen, e.g., in the Abu Gharadig and Fayium basins in the northern Western Desert and parts of the Gulf of Suez (Fig. 29).

In the Abu Gharadig Basin the upper Cenomanian–lower Turonian is formed by the shales, limestones and sandstones of the Abu Roash Formation, which is subdivided into members A–G [*Barakat et al.,* 1987; *Bayoumi,* 1996; *Khaled,* 1999] (Fig. 30). Members E and F straddle the C/T boundary, reach thicknesses of up to several hundreds of meters each and together with member G constitute the most organic-rich horizons (Figs. 31, 32; additional isopach maps of the eastern Abu Gharadig Basin in [*Bayoumi,* 1996]).

An overview of the facies of the Abu Roash members has been given by *Bayoumi* [1996]. In the eastern Abu Gharadig Basin, the clastic-dominated member G exhibits an abrupt upward transition to the carbonate-dominated member F, the latter of which contains dark brown limestones. This contact may be interpreted as transgressive surface which might be correlatable with the post-Ce5 transgressive surface, dated in Tunisia as uppermost *R. cushmani* Zone (Fig. 2). The associated TST is interpreted to include the whole of member F plus the uppermost Cenomanian and lowermost Turonian parts of member E, which are dominated by deeper shelf shales with planktonic foraminifera (Fig. 33). A marked shallowing occurs in the overlying horizons of member E, characterised by organically lean paralic limestones, sandstones and shales [*Bayoumi,* 1996; Fig. 33], possibly representing the lower Turonian post-Ce5 HST (Fig. 2). In the absence of good biostratigraphic data the validity of these interpretations must remain unclear, especially given the fact that tectonic movements have occurred in the basin during this time and might have modified the local sea-level development.

The isopach and average organic content maps published of members E and G by *Barakat et al.* [1987] (Fig. 31) show that organic-rich C/T patches exist around wells Agnes-1, the Abu Gharadig oil- and gasfield and south of Mubarak-1. As illustrated by the isopach distribution, these areas with elevated organic content in the C/T interval partly coincide with sedimentary depocentres and are absent on the flanks of palaeotopographical highs such as the Qattara High [*Barakat et al.,* 1987; *Bayoumi,* 1996]. The trend of the West Halif-1 and Abu Sennan-1 wells (NE–SW) corresponds to the present-day Abu Gharadig Anticline which might have already existed in C/T times and may have acted as circulation barrier in combination with other highs [*Bayoumi,* 1996]. Notably, this trend is characterised by a low organic content, despite a significant thickness of member G, indicating that the distribution of organic-richness seems to be controlled also by parameters other than palaeorelief. Similar observations are made within the Abu Roash formation in the Dabha area (Sirrah-1 well interval 4970–5660 ft, location in Fig. 29). At this site, low organic matter content (TOC<0.6%) has been encountered with a corresponding low generating potential (S2<1.2 mg HC/g rock), thus indicating lack of source rocks potential. Lateral facies changes may have to be considered in

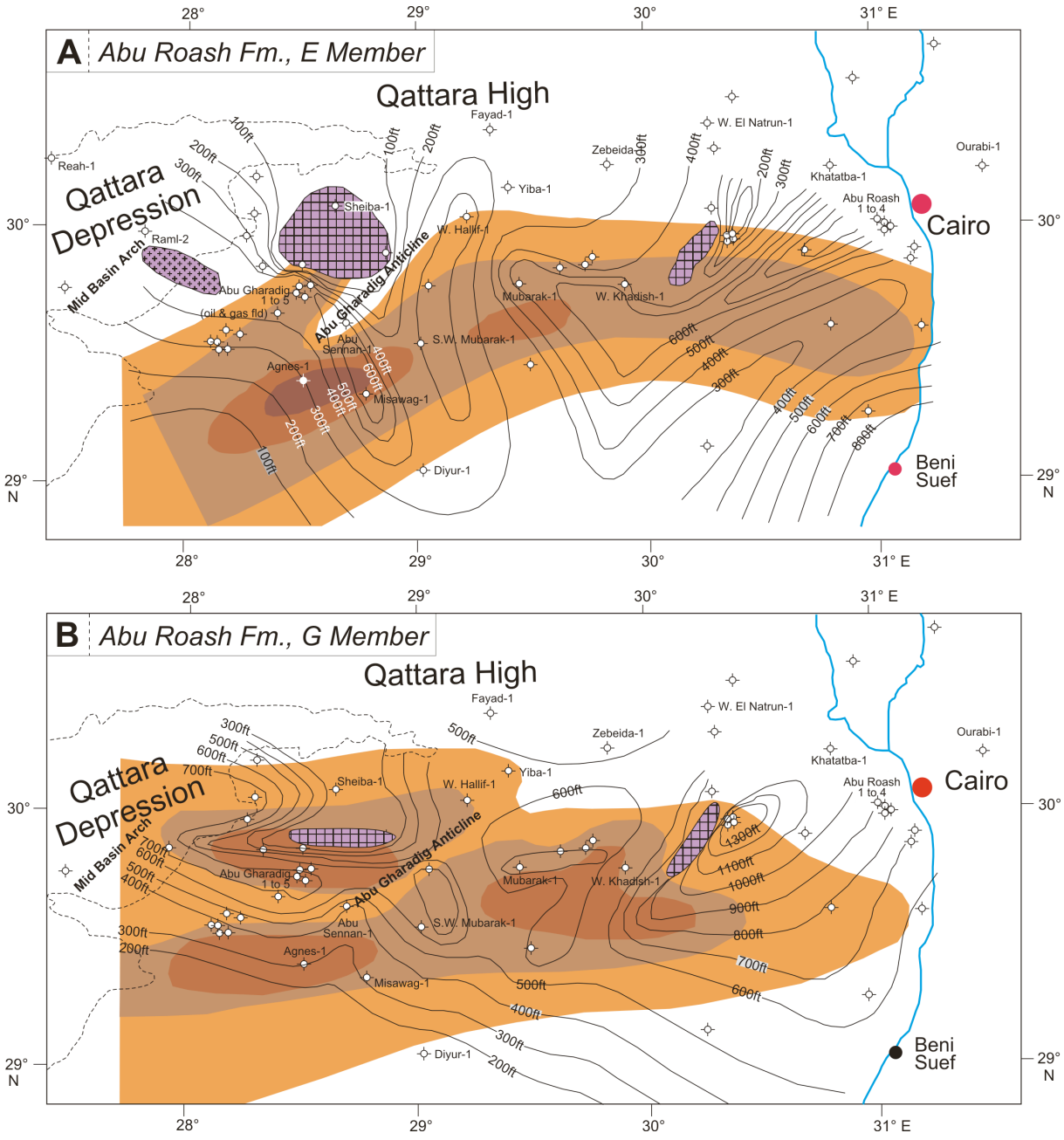

Figure 31. Isopach maps and average organic matter content of the E and G members of the Cenomanian–Turonian Abu Roash Formation (Fig. 30) in the Egyptian Western Desert (after *Barakat et al.*, 1987).

particular. Comparison of the positive organic anomalies in member E shows that they coincide with facies with a high shale content (e.g., Abu Gharadig wells Miswag-1 and Agnes-1; Fig. 31) [*Barakat et al.,* 1987, p. 133]. In limestones of the Abu Roash F member, organic-rich levels are usually reflected on well logs by moderately elevated total gamma-ray and resistivity values [*Bayoumi,* 1996] (Fig. 34).

According to *Khaled* [1999], the Abu Roash E and G members have sourced most of the oil in the Abu Gharadiq fields. *Schlumberger* [1995] consider Abu Roash members E, F and G as the `most prolific and outstanding source rocks in the Western Desert', describing the unit as a good oil source rock in most parts of the Western Desert and moderate quality gas source in the Umbarka area. The Egyptian General Petroleum Corporation (EGPC Homepage, 2001, www.egpc.com.eg) assume the Abu Roash F member to be one of the potential source rocks around Cairo and from here 100 km to the west (including Fayium Basin; Fig. 29).

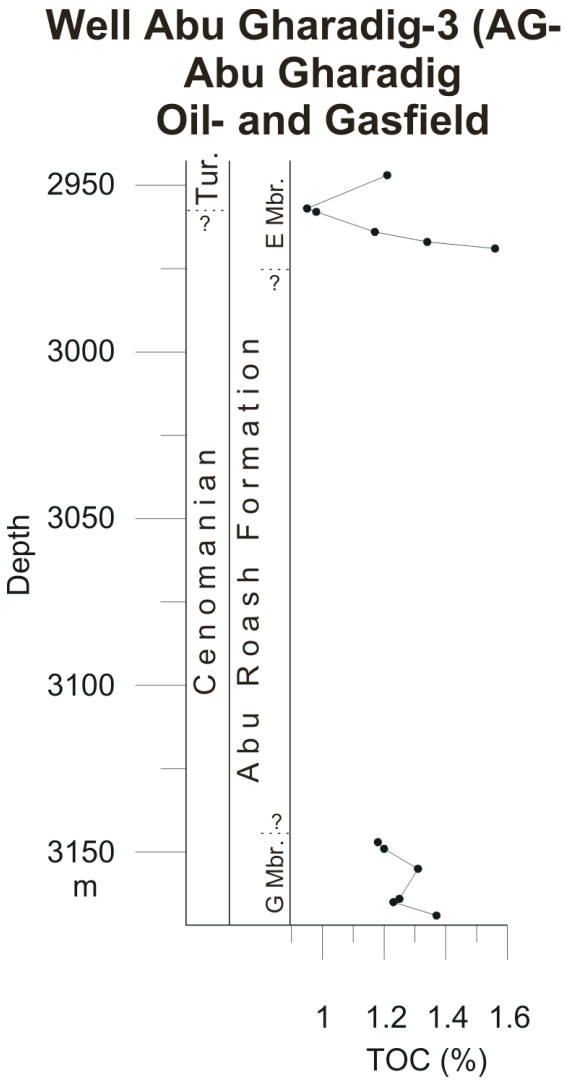

Figure 32. Elevated organic content at the Cenomanian–Turonian boundary in the E and G members of the Abu Roash Formation in well AG-3 in the Abu Gharadig Oil-and Gasfield [after *Khaled*, 1999].

In the Abu Gharadig oil-and gasfield (Fig. 31), the organic-rich intervals are currently mostly in the oil generating window and reaches TOC values of up to 1.5% at well AG-3 ([*Khaled,* 1999]; Fig. 31 and Fig. 32), and up to 2.5% at well BED-16-1 (east of the Abu Gharadig wells, Fig. 31; [*Bayoumi,* 1996]). Thermally immature organic matter is known from the Qatara High wells Raml-2 (interval 3110–4210 ft, members B, F and G) and Reah-1 (interval 4150–4770 ft; members B, F and G), where TOC values range between 0.5% and 3% (well locations in Fig. 31A).

In the Ourabi-1 well 30 km NE from Cairo in the Eastern Desert (Fig. 31), the members E, F and G of the Abu Roash Formation are lithologically similar to the Western Desert equivalents. The transgressive F Member at the C/T boundary contains a brown limestone with shale interbeds interpreted as middle to outer neritic based on foraminifera and ostracod content (unpublished data, INA-Naftaplin). The TOC varies between 0.5% and 1.1% with fair to good hydrocarbon generating potential (S2 pyrolysis yields from 2.6 to 7.1 mg HC/g rock) and high hydrogen indexes (HI 420–670 mg HC/g TOC). Kerogen composition data show that the organic matter is primarily composed of hydrogen-rich unstructured lipids (sapropelic). Notably, the total and uranium (spectro-) gamma-ray values are very low. The overlying E member in this well is a littoral facies with a significant woody, terrestrial input.

In the Gulf of Suez in the Bakr well-12 transgressive sediments near the C/T boundary contain up to 2% TOC (Fig. 35), with HI values as high as 274 [*Mostafa,* 1999, p. 46]. The TOC/HI peak coincides with a high percentage of fluorescent amorphous matter (fluoramorphinite) (Fig. 35). A transgression during deposition of this organic-rich strata is also indicated by molecular biomarker distribution [*Mostafa,* 1999].

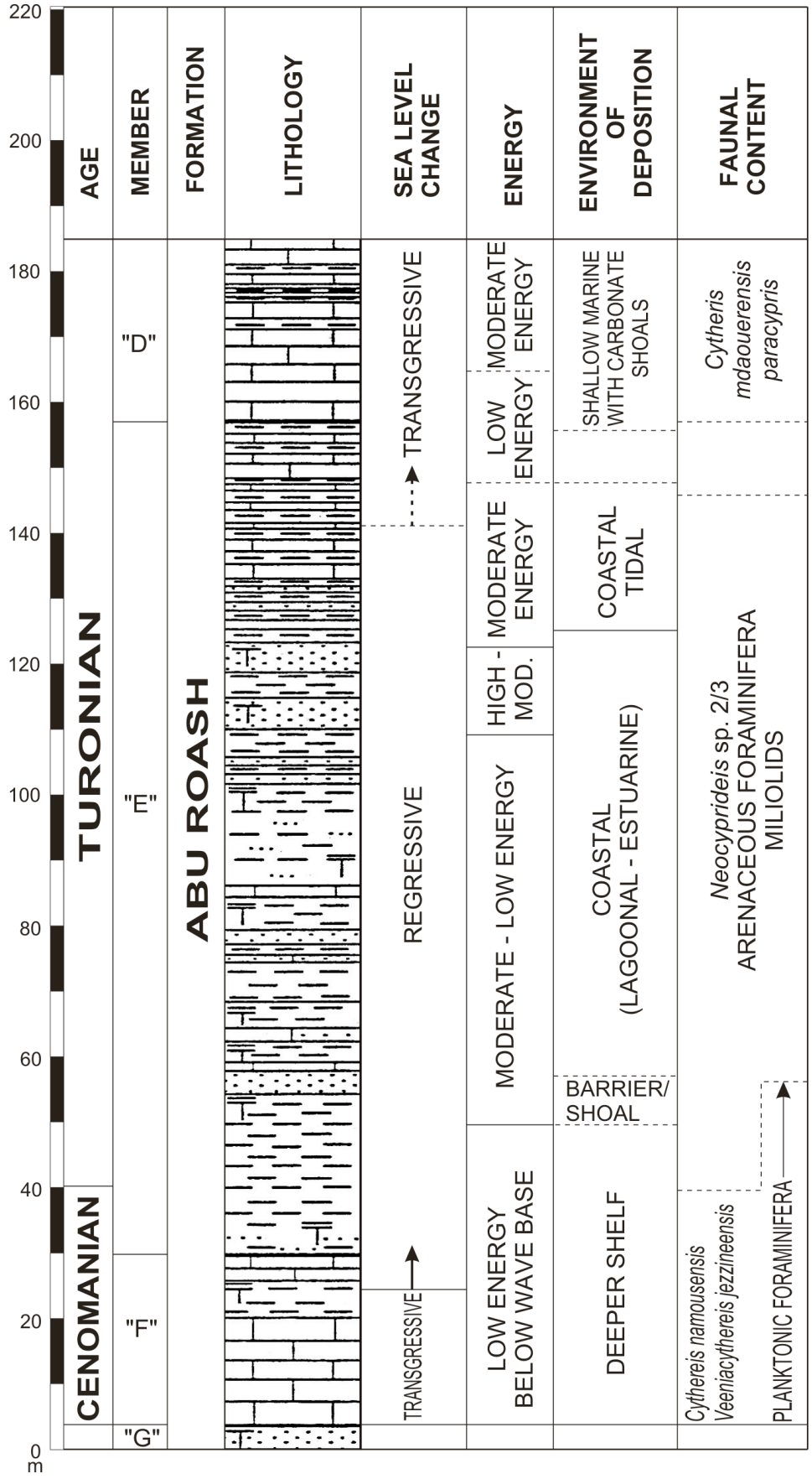

Figure 33. Type section and depositional environments of the Abu Roash members D–F in the Abu Gharadig Basin [after *Bayoumi*, 1996].

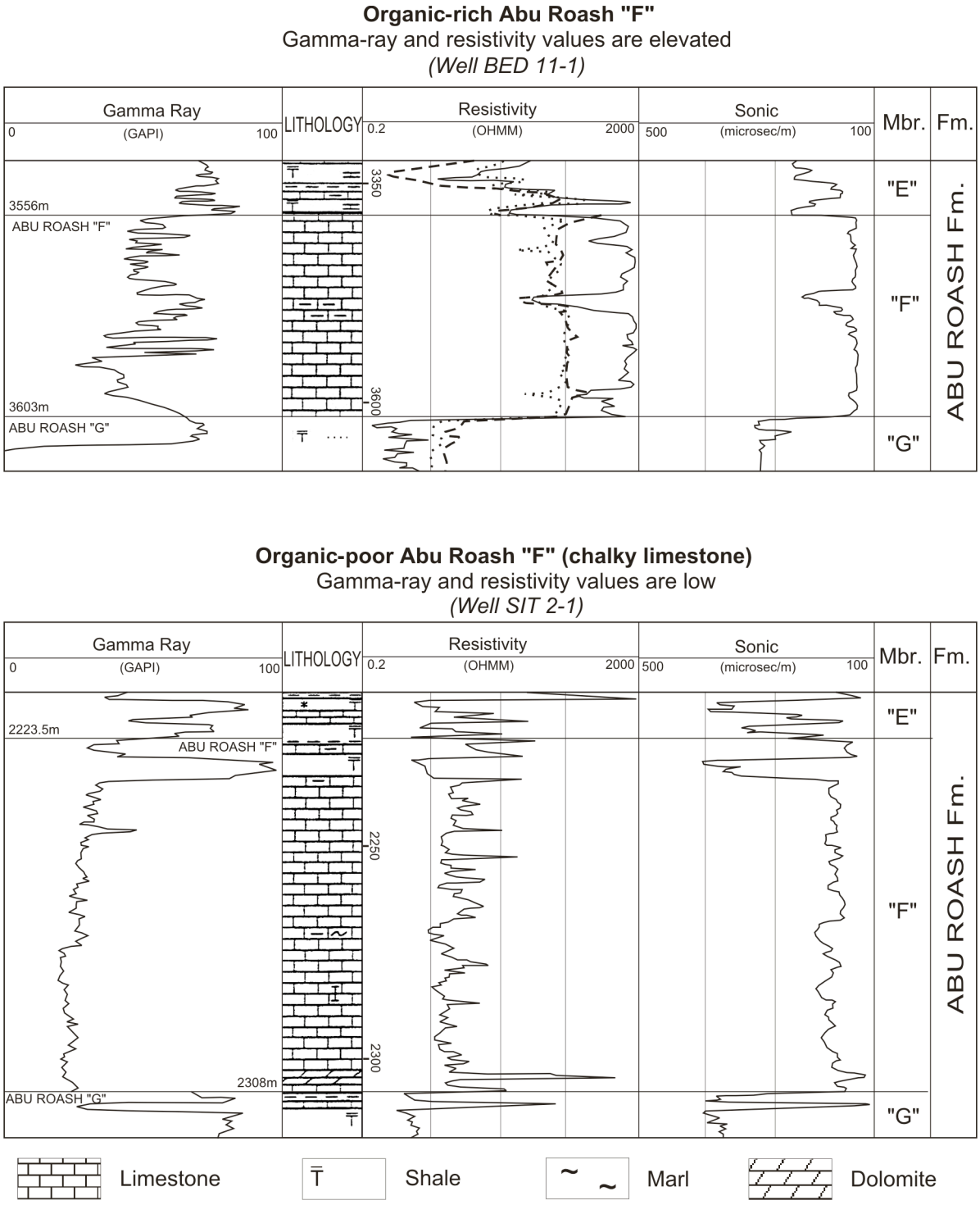

Figure 34. Log characteristics of (A) organic-rich and (B) organic-poor Abu Roash F Member. Gamma-ray and resistivity values are clearly elevated in the organic-rich unit. After *Bayoumi* [1996].

In western Sinai, at the eastern margin of the Gulf of Suez, *Shahin* [1991] studied C/T strata at Jebel Nezzazat (Fig. 29) and recorded the characteristic positive carbon isotope excursion in the Abu Qada Formation (Fig. 36). The peak coincides with a drop in ostracod diversity [*Shahin,* 1991]. The C/T ostracod assemblages in general indicate the presence of a vast palaeogeographical province covering all of North Africa and the Middle East, as well as West Africa which was connected through the Trans Saharan Seaway (Fig. 3b). *Cherif et al.* [1989, p. 255] studied C/T sections in the same area and suggested the presence of topographic relief during deposition of the C/T strata, resulting in strong

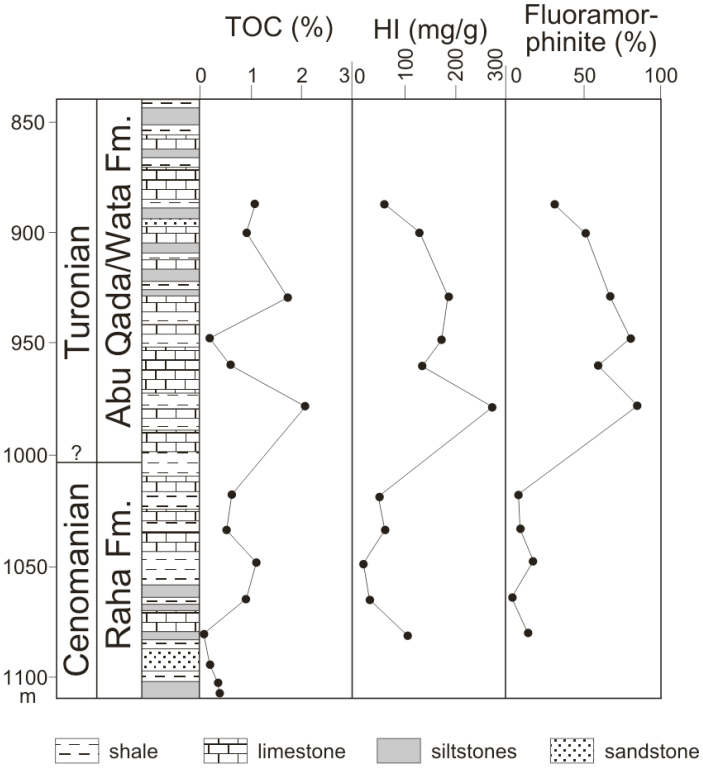

Fig. 35. Organic-rich strata in the C/T boundary interval in the Gulf of Suez (Bakr well-12) [after *Mostafa,* 1999]. Note that the position of the C/T boundary is only a rough estimate due to the lack of good biostratigraphic data.

lateral facies changes of the Abu Qada Formation. Therefore, distribution of C/T strata with elevated organic content may be patchy in the Gulf of Suez/western Sinai area [see also *Bauer et al.,* in press]. In the southern part of the Gulf of Suez [*Mostafa,* 1999, p. 45], parts of eastern Sinai [*Bauer et al.,* 2001, in press] and parts of Palestine/Israel [*Lewy,* 1989; *Buchbinder et al.,* 2000] the C/T strata are absent due to erosion/non-deposition (palaeohighs, subaerially exposed or very shallow marine). Organic-rich C/T strata may exist in the Gaza Basin in NW Sinai because C/T black shales also occur in the nearby Palestinian/Israeli coastal basins (*Lipson-Benitah* et al., 1990) (see below).

2.5.6.3. Bulk and molecular geochemistry

The significance of Mid-Cretaceous source rocks in Egypt gained importance during the last decades, which has initiated a flurry of geochemical examinations especially of the organic-rich formation in the Abu Gharadig Basin and the Gulf of Suez. A detailed and comprehensive overview of Mid-Cretacous source rock geochemistry in the Abu Gharadig Basin is given by *Zein El-Din* [1983], *Shahin et al*. [1986], *Barakat et al.* [1987], *Shahin and Shehab* [1984], *Shimy et al.* [1991], *Hammad et al.* [1992], *Darwish et al.* [1994], *Bayoumi* [1996] and *Khaled* [1999]. Source rock characterizations of Mid-Cretaceous successions from the Gulf of Suez were reported by *Barakat* [1982], *Rhorback* [1983], *Shahin and Shehab* [1984], *Shahin* [1988], *Mostafa and Ganz* [1990], *Mostafa* [1993, 1999] and *Robison* [1995].

The organic richness expressed in terms of TOC for the C/T formation in the Abu Gharadig Basin is fair with highest values of ~2.7 wt.% found for the Abu Roach G Member, while those from the Gulf of Suez have on average lower TOC contents with highest values approaching ~2 wt.% as recorded for the Abu Qada Formation. Optical analysis performed on these shales showed that the OM is mainly composed of marine amorphous sapropelic kerogen (fluoramorphinite) together with structured liptinite (exinite) macerals. The liptinic macerals mostly consist of fresh or brackish macerals (Botryococcus alginite) indicating a fluvial-shallow marine depositional environment. According to *Khaled* [1999], this maceral group is equivalent to the liptikeroginite and mesoliptinite phytoclast group which make up the main components of types I and II kerogens with a high oil and gas source rock potential. This potential is only partly confirmed by the Rock-Eval pyrolysis with

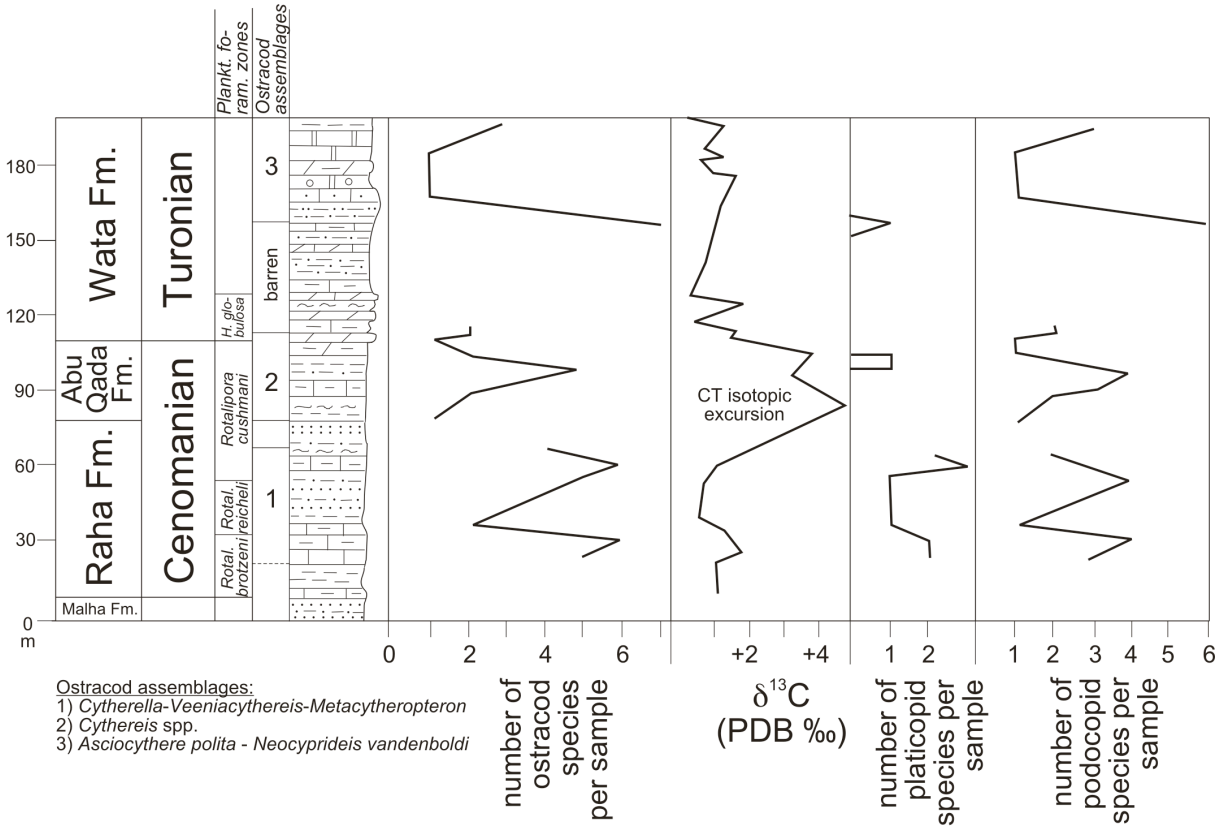

Figure 36. Carbon isotopic excursion and ostracod distribution data in the uppermost Cenomanian shale-dominated Abu Qada Formation in southwestern Sinai (Egypt) [after Shahin, 1991].

hydrogen indices for the Abu Roash and Abu Qada formations ranging in general from 200 to 337 mg HC/g TOC and 132 to 274 mg HC/g TOC, respectively. Exceptionally high hydrocarbon indices of up to 650 mg HC/g TOC are observed within the TOC-rich intervals in wells Raml-2 and Reah-1 (Qatara High, well locations in Fig. 31A) indicating oil prone source rocks.

Corresponding *T*max values for the Abu Roash formation scatter from 440 to 452 °C proposing that the Mid-Cretaceous strata has reached a higher level of thermal maturation in the Abu Gharadig Basin at the zone of oil generation. In the Gulf of Suez *T*max values for the Abu Qada formation range between 407 and 421 °C indicating an immature to very low mature level of the OM. The biomarker distribution in these sediments is typical for type I/II algal/bacterial kerogen compromising of short and long chain *n*-alkanes, sterans, hopanoids and acyclic isoprenoids. Notably in the sediments of the Abu Qada Formation, gammacerane is abundantly present and could be indicative of hypersaline depositional conditions. If this is the case then the organic-rich strata from the Abu Qada formation may have been deposited under a density-stratified water mass and anoxic bottom water conditions.

2.5.7. Neighbouring areas on the Arabian Peninsula

Organic-rich Cenomanian–Turonian strata also occurs on parts of the Arabian Peninsula, e.g., in Israel/Palaestine, Jordan and Lebanon. In the Israeli/Palestinian coastal basins, the C/T boundary interval is represented by up to 30 m thick bituminous marls and black laminated shales of the Daliyya Formation, which were deposited near the Mid-Cretaceous shelf edge and reach TOC values of up to 4% [*Lipson-Benitah et al.,* 1990; *Honigstein et al.,* 1989]. According to ostracod biostratigraphic data deposition of these sediments commenced in the southern Gaza Basin and hereafter dysoxia gradually migrated northwards, associated with the upslope advance of the transgression. High productivity conditions in combination with upwelling are assumed [*Lipson-Benitah et al.,* 1990; *Buchbinder et al.,* 2000]. The Daliyya Formation is considered as a potential source rock for petroleum [*Lipson-Benitah et al.,* 1990]. Nevertheless, oils in the coastal Helez region were typed by biomarker analysis to a Jurassic source rock [*Bein and Sofer,* 1987]. In west central Jordan, several tens of meters of black

marls occur around the C/T boundary in a local basin within the Shueib/Wadi Essir Formation [*Schulze and Kuss,* 2000; unpublished report *FINA* 1988]. TOC values reach up to 8% and are thought to have sourced the Hamzeh Oil Field. C/T strata on the Eratosthenes Seamount, 50 km south of Cyprus, is represented by pelagic chalks which contain varying amounts of pyrite [*Robertson,* 1998], however, apparently no major organic accumulations.

2.6. Depositional model

A predictive depositional model for the C/T organic-rich deposits must explain the following key questions:

- What processes controlled the variations and regional trends observed in C/T organic richness?
- What conditions formed the isolated occurrences of organic-rich C/T strata surrounded by organically lean C/T deposits?
- Does a general relationship between palaeobathymetry and organic-richness exist? For example, do organically lean (hemi-) pelagic deposits exist below a bathymetrically well-defined oxygen minimum zone?
- What is the role of tectonically controlled circulation patterns and which narrow and shallow seaways have to be considered for North Africa?
- In what way was the onset and termination of C/T black shale deposition controlled by the Late Cenomanian–Early Turonian third-order eustatic sea-level cycle?

2.6.1. Oceanic circulation and water mass properties

During C/T times, the Tethys and Central Atlantic were characterised by a sluggish circulation because in the Central Atlantic connections to neigbouring oceanic basins were just establishing [e.g., *Wagner and Pletsch,* 1999] and the Neotethys was beginning to close. The Palaeostrait of Gibraltar was narrow and locally shallow and is interpreted to have served as a barrier hampering the exchange of Atlantic and Tethyan deep-water masses. This separation of oceanic circulations is partly reflected in the generally higher TOC values observed in C/T strata along the NW African Atlantic coast (usually <10% in most slope and deep marine localities), contrasting with generally lower organic richnesses along the Tethyan North African coast (usually <10% TOC, except Tunisia/NE Algeria) (Fig. 4).

Generally, the OAE II has been associated with an intensification of the OMZ and expansion of the OMZ onto the shelves. *Thurow and Kuhnt* [1986] assumed that the anoxic water masses at the NW African Atlantic margin locally reached down to at least 3 km depth. This is in accordance with reconstructions by *Sinninghe Damsté and Köster* [1998] who, based on the presence of molecular fossils, proposed a continuously euxinic water column in the southern North Atlantic during the C/T event (Fig. 10). Other authors previously assumed that the organic matter found in C/T strata in many of the Atlantic deep-sea DSDP wells may have originated in shallower waters prior to downslope redeposition. However, such a mechanism does not need to be invoked in the Atlantic [*Sinninghe Damsté and Köster,* 1998], but it may be applicable at the Atlantic–Tethys boundary in the narrow Gibraltar Palaeostrait area and in Sicily. *Thurow and Kuhnt* [1986, p. 441] assume the C/T organic matter in this area to be more a result of turbidity current-transport than of an in-situ formation due to an expanded OMZ.

The origin of OMZ changes is debated and includes (a) an increase in productivity of oceanic surficial layers ("productivity model") or (b) an increase in thermic or halocline stratification ("stagnation model"). Because of the widespread occurrence of C/T organic-rich strata in a number of poorly interconnected basins (Fig. 1) and in a wide range of bathymetric levels from the deep sea to shelf it seems likely that a common, external trigger for the OAE II exists. During the anoxic event, a significant drop in atmospheric CO_2 concentrations and temperature is assumed [*Kuypers et al.,* 1999], related to the burial of great amounts of organic carbon in marine sediments. The underlying, common cause for this relatively shortlived worldwide climatic and oceanographic change still remains unclear and may be related to fluctuations in the mid ocean spreading rate and associated generation of CO_2 ("Cretaceous Superplume") or other short-term events [*Busson and Cornée,* 1996]. *Sinninghe Damsté*

and Köster [1998] speculated that increased sea-floor spreading, submarine volcanism and hydrothermal activity during the OAE II may have triggered the gradual upward expansion of harmful, oxygen-depleted waters.

A more thorough differentiation between causes and consequences of the C/T event must be attempted, including the thematic separation of unrelated, masking developments. Evidence exists that both the productivity and stagnation models are applicable to deposition of C/T organic-rich strata in different parts of the world, respectively. For example, *Kuhnt and Wiedmann* [1995, p. 225] associated the boreal C/T black shales with the stagnation model, whereas for C/T organic-rich strata in the equatorial Atlantic they assume the productivity model.

2.6.2. Primary productivity

Strong upwelling conditions are thought to have existed along the NW African coast during most of the Cenomanian to Coniacian, as documented by palaeoecological analyses and numerical modelling (Fig. 9) [e.g., *Parrish and Curtis,* 1982; *Kruijs and Barron,* 1990; *Kuhnt and Wiedmann,* 1995; *Bush and Philander,* 1997]. Organic-rich strata were deposited here during this whole interval. Notably, the C/T event in Tarfaya is characterised by TOC values that are only marginally higher than in the under- and overlying strata (Fig. 7), so that intensified E-Atlantic upwelling as an ultimate cause for the shortlived, worldwide OAE II [*Tucholke and Vogt,* 1979; *Summerhayes,* 1981] seems unlikely. Also, *Thurow et al.* [1992, p. 266] noted that, on a worldwide scale, there are too many organic-rich C/T deposits outside of potential upwelling areas for upwelling and related nutrient transport to be exclusively responsible for their origin. Clearly, pronounced upwelling along the eastern Central Atlantic margin existed, however, on the shelves and slopes this process may only mask the processes responsible for the deposition of organic matter during the OAE II event in the deep sea and at the North African southern Tethyan margin.

2.6.3. Preservation/stagnation

In comparison to the longlasting deposition of organic-rich Cenomanian–Coniacian strata along the NW Atlantic margin, the duration of deposition and distribution of C/T organic-rich strata in Tunisia and NE Algeria is considerably less. Importantly, limited (seasonally restricted to January based on modelling results) or no upwelling seems to have occurred along the central North African Tethyan coast [*Kruijs and Barron,* 1990, p. 210; *Nederbragt and Fiorentino,* 1999]. Other authors, in contrast, assume significant upwelling conditions for the C/T in Tunisia [e.g., *Bishop,* 1988; *Barrett,* 1998].

Regardless whether upwelling or not existed during the C/T in northern Tunisia, the data currently available from here indicate that C/T organic-rich strata are limited to a bathymetric belt that may represent the impingement zone of a relatively thin OMZ onto the shelf (Fig. 10 and Fig. 22). The main arguments are organically lean C/T shales which are reported from onshore and offshore NW Tunisia ("basinal organic-poor Bahloul" in Fig. 20) [*Bishop,* 1988; *Barrett,* 1998]. In parts of the Gulf of Hammamet, however, the C/T interval may also be eroded altogether, complicating reconstructions. A similar OMZ with an oxic zone underneath is likely to also have developed further eastwards along the NE African Tethys coast (Fig. 4). Interestingly, the C/T interval on the Eratosthenes Seamount near Cyprus (ODP 967, Fig. 4) does not seem to be organically rich, which provides further evidence that the OMZ in the NE African Tethys did not reach to greater depth as along the NE African Atlantic coast [*Thurow et al.,* 1992, p. 267]. Because of the seamount location, downslope redeposition from shallower, coastal areas could not have taken place at this site. According to *Thurow et al*. [1992], the deep-reaching anoxic water column in the Central Atlantic during the C/T is due to the confined and juvenile nature of the basin, resulting in restricted circulation, a less dense crust and therefore a shallower basin floor. In contrast, the central and eastern North African coast bordered the open Tethyan ocean, which was characterised by full oceanic circulation [*Thurow et al.,* 1992, p. 267] (Fig. 3), consequently the C/T organic-richnesses are also significantly lower than in the Atlantic.

A number of isolated, mostly rift-related organic-rich C/T patches, surrounded by shallower, organically lean C/T strata exist in North Africa, namely in the Moroccan Middle Atlas, NE Algeria, eastern Sirte Basin and Jordan (Fig. 4). Also, the halfgraben systems in northern Tunisia may partly have been only poorly connected, resulting in weak water circulation [*Orgeval,* 1994]. It seems likely that all these little basins reached waterdepths that were sufficiently deep to allow the OMZ to impinge

onto their basin margins [see also *Arthur et al.,* 1987; *Koutsoukos et al.,* 1991]. Restricted circulation within these basins may have further increased oxygen-deficiency, which may be reflected by the maximum TOC values recorded from these isolated basins, for example, in the Central Jordan basin and in the eastern Sirte Basin TOCs are generally higher than in the non-protected, open marine C/T black shale belt (Fig. 4). Another mechanism for some isolated intrashelf basins (e.g., Central Tunisia, Algeria; Fig. 4) may also have been a salinity stratification caused by hypersaline brines fed by dissolving Triassic salt diapirs [*Busson,* 1984; *Orgeval,* 1994; *Abdallah and Meister,* 1997].

2.6.4. Transgression

The latest Cenomanian transgression (post-Ce5 transgressive surface in the Tethyan eustatic sea-level chart of [*Hardenbol et al.,* 1998], Fig. 2) was the ultimate driving force for the raising and expansion of the OMZ onto the North Africa shelves (Arthur et al., 1987). The flooding may have been associated with high spreading rates ("Cretaceous Superplume") resulting in a sea-level rise of 130–350 m [*Kominz,* 1984; *Larson,* 1991a,b]. The great magnitude of this sea-level rise [*Jenkyns et al.,* 1994] resulted in large parts of the shelfal areas to be impinged by the OMZ. The upper 50–70 m in a marine water column are usually well oxygenated by wave and wind action (Nederbragt and Fiorentino, 1999) and less intense transgressions would only lift the OMZ zone to the lower part of the shelfal profile.

The transgression also reduced dilution of the primary organic matter by coarse-grained siliciclastic material in the hemipelagic facies by forcing rivers to adjust their profile, leading to the backstepping of sedimentary bodies. With the exception of the upwelling-related black shales along the NW African Atlantic coast, organic-rich C/T deposits in North Africa are usually restricted to the lower part of the transgressive systems tract (Fig. 2). *Wignall* [1991] classified such black shales as `basal transgressive' (BT), a model which also seems applicable to the majority of lower Silurian black shales in the same area [*Lüning et al.,* 2000].

2.6.5. Palaeorelief

Deposition of organic-rich C/T strata in North Africa was restricted to marine facies of a certain minimum water depth, with shallower facies having been too oxygenated by waves and currents. The distribution of organic matter, therefore, follows closely the palaeorelief that existed during the C/T. Suitable depressions are associated with the North African continental margins (slope/basin; e.g., Libya offshore) and Early Cretaceous and syn-C/T rift grabens and pull-apart basins on the North African shelves (e.g., N-Tunisia, eastern Sirte Basin, Abu Gharadig Basin). Regions dominated by shallow marine C/T facies lack organic-rich deposits and carbonates/dolomites are deposited instead (e.g., Atlas Gulf/Morocco, NW Libya). Some areas even are characterised by a hiatus around the C/T (e.g., Sinai).

Diachronism of C/T Corg strata has been reported [e.g., *Hilbrecht et al.,* 1986; *Hart and Leary,* 1989; *Jenkyns et al.,* 1994). The onset and termination of black shale facies is at least partly controlled by the relief, with more elevated areas being impinged later by the OMZ than lower lying areas.

2.7. Outlook

This synthesis offers a common framework in which to interpret North African C/T black shale parameters and regional trends. More data is evidently needed for some areas such as Tunisia Offshore, the Sirte Basin, Cyrenaica and the Egyptian Western Desert. In a joint effort of the petroleum industry and academia, more C/T data and study material of these regions should be analysed and subsequently be published to infill these gaps. In particular, high resolution biostratigraphic, chemostratigraphic and facies data is needed to allow more precise correlations of onset, intensity and termination of anoxia/dysoxia across the region. Main issues are identification of synchronism of source-rock deposits and a better understanding of their distribution in time and space [*Baudin,* 1995]. Detailed palaeoecological and advanced geochemical studies are needed for central and eastern North Africa to better evaluate to what extent upwelling conditions might have been active or what other mechanisms controlled the intensity, thickness and depth of the OMZ.

Acknowledgements

We would like to thank Dr. J. Bauer, Prof. J. Kuss, F. Schulze, Dr. J. Lehmann (all Univ. Bremen), Dr. R. Burwood (Oxford), Prof. W. Kuhnt (Univ. Kiel), Prof. H. Chellai (Cadi Ayyad Univ. Marrakech), Dr. E.E. Tawadros (Calgary), Dr. Don Hallett, R.S. Zazoun (Sonatrach), Dr. M. Eales (Lasmo-ENI, London), A. Khoja (NOC Tripoli), Dr. M. Kuypers (MPI Bremen) and Dr. M. Martin (ECL) for fruitful discussions. Permissions to present data in this contributions were kindly given by SONATRACH and Prof. W. Kuhnt. We are grateful for technical assistance to INA Naftaplin (Zagreb), Jan Holstein, Katharina Kiesinger and Nergizhan Atli (all Univ. Bremen). The study was funded by the German Research Foundation (grant Lu 654/1). The manuscript benefited from valuable comments by ESR reviewer Dr. P. Wignall (Univ. Leeds). Parts of the GIS North Africa database used for this study can be downloaded at www.northafrica.de/gis.htm.

Chapter 3

Moroccan Basin's Sedimentary Record May Provide Correlations for Cretaceous Paleoceanographic Events Worldwide

Chapter 3.

Moroccan Basin's Sedimentary Record May Provide Correlations for Cretaceous Paleoceanographic Events Worldwide

Authors*: Kuhnt, W., E.H. Chellai, A. Holbourn, F. Luderer, J. Thurow, T. Wagner, A. El Albani, B. Beckmann, J.-P. Herbin, H. Kawamura, S. Kolonic, S. Nederbragt, and C. Street*

Status: published Journal: *Eos Transactions AGU 82, 361-364, 2001*

3.1. Introduction

More than 500 m of Upper Cretaceous laminated biogenic sediments, mainly consisting of calcareous nannoplankton, dispersed biogenic silica, planktonic foraminifers and marine organic matter were deposited in the depocenter of the Tarfaya-LaAyoune Basin, near the town of Tarfaya in southern Morocco, with sedimentation rates exceeding 10cm/ky during transgressive phases. These sediments exhibit the world's highest accumulation rates of marine organic matter for the Cenomanian/Turonian, and allow investigation of paleoceanographic and climate events on a centennial time scale resolution, comparable to global change studies in the Quaternary. Correlation of over 80 cored wells and outcrop sections using orbital cyclostratigraphy, biostratigraphy and high-resolution carbon isotope stratigraphy reveals that the obliquity signal of the Milankovitch frequency band is most prominent in the record of organic matter and carbonate accumulation. Within the laminated sediment, sub-Milankovitch cycles of yet unknown origin with frequencies comparable to Dansgaard-Oeschger oscillations and sunspot cycles are recognized. The record of the Tarfaya-LaAyoune Basin has potential for correlation of globally recognized paleoceanographic events (i.e., isotope excursions, extinction, "anoxic events") to a Milankovitch framework and for assessment of the instantaneity and duration of these events on a centennial and even decadal scale.

Despite this staggering record, geologic research in the Tarfaya-LaAyoune Basin is still in an incipient stage, since outcrops in the basin were totally inaccessible from the early 1970s to the early 1990s, due to the political conflict over the future of the former Spanish Sahara. The Office National de Recherches et d'Exploitations Pétrolières (ONAREP) and Shell Oil Company conducted two oil shale exploration drilling campaigns in the 1970s and early 1980ss. However, most results were kept confidential. Following the companies' release of data and sample material and the settlement of the political conflict, an international team from the Université de Marrakech, the Universität Kiel, the Universität Bremen, University College London and the Université de Poitiers undertook in 1997 - 2000 a new phase of field expeditions. The purpose of this effort was to acquire and integrate new biostratigraphic, geochemical, cyclostratigraphic, and sedimentological data on a basin-wide scale.

3.2. Geological Setting and Facies Succession

Facies distribution patterns, organic matter analyses, micro-fossil assemblages and carbonate microfacies types indicate two distinct depositional environments: one characterizing upper Albian to lower/middle Cenomanian sediments, and the other, upper Cenomanian to Campanian sediments. The first depositional environment is dominated by terrigenous silici- and bioclastic sedimentation with low organic matter content of mainly terrestrial origin. Clay mineral assemblages of the upper-Albian to middle-Cenomanian are characterized by abundant illite and chlorite, eroded from crystalline rocks outcropping in the Anti-Atlas mountains, the Precambrian Reguibat Massif and the paleozoic foldbelt of the Mauritanides, as well as reworked kaolinite indicating active erosion of the relief surrounding the Tarfaya-LaAyoune Basin.

The second depositional environment is characterized by pelagic marls and limestones with a high content of marine organic matter; higher mean content of smectite in clay mineral assemblages, reflecting higher relative sea level; and abundant pelagic macro- and micro-faunas. These Cenomanian-Campanian sediments were probably deposited in nutrient-rich environments as an open-shelf coastal upwelling-system developed [*Einsele and Wiedmann*, 1982].

3.3. Orbital Cyclicity

A series of more than 80 cored exploration wells and outcrop sections in the Tarfaya-LaAyoune Basin reveals cyclic sedimentation patterns of different frequencies in the late Cenomanian to middle Turonian. The cyclicity is mainly controlled by fluctuations in the organic carbon and pelagic carbonate content [*Kuhnt et al.,* 1997]. Two large-scale cycles are observed, which are related to major changes in organic carbon burial and probably reflect third- order sea level fluctuations. Maximum organic carbon burial corresponds to benthos-free, laminated sediments, indicating bottom water anoxia. These periods coincide with sea level highstands of the revised Vail sea level chart.

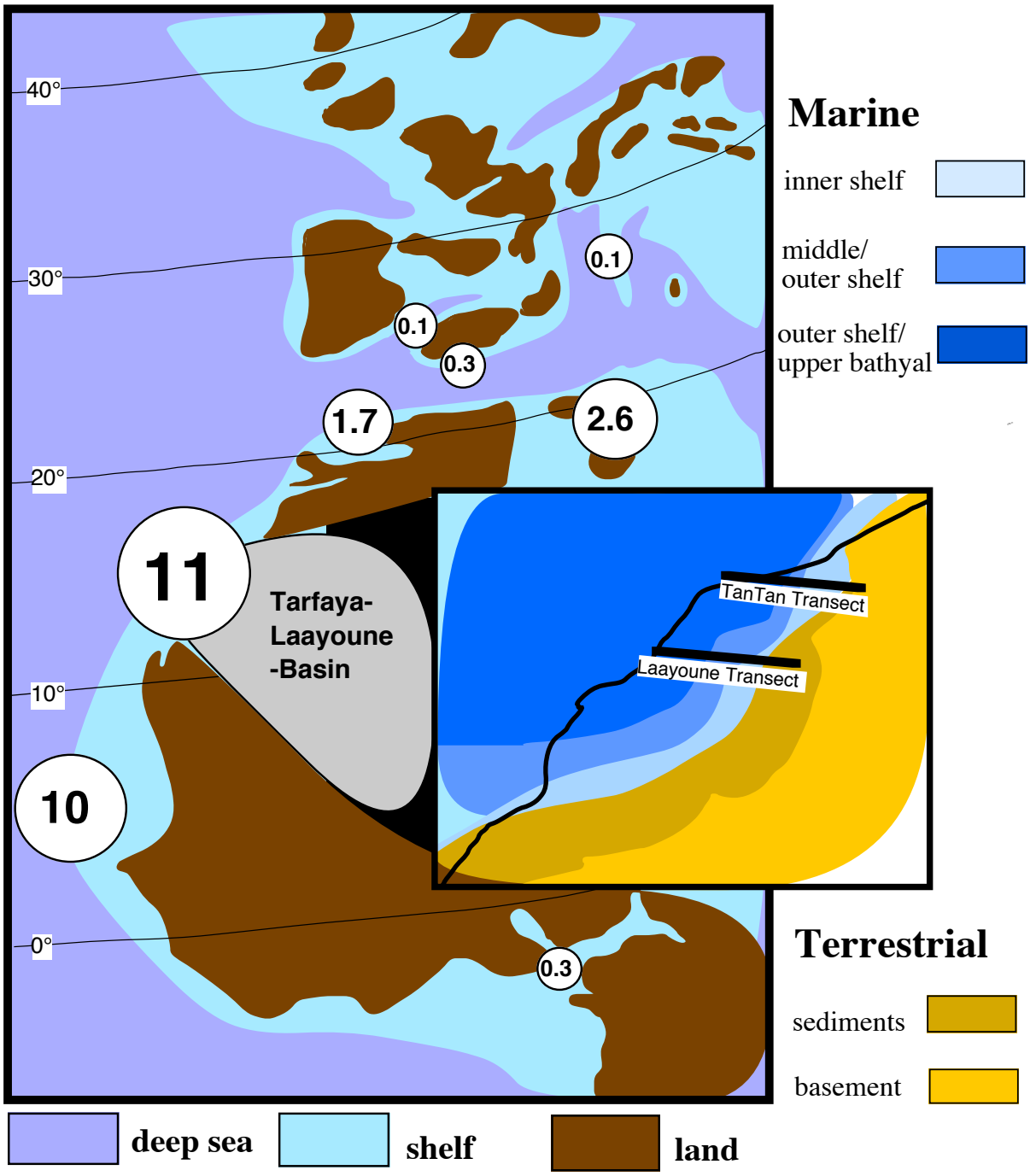

Figure 1: Turonian paleogeography of the Tarfaya-Laayoune Basin (modified from [Kuhnt et al., 1990]) Values in circles are organic matter accumulation rates during the Cenomanian/Turonian oceanic anoxic event (OAE) 2 (in grams per square meter and year).

Superimposed on these large-scale cycles, a Milankovitch-scale orbital cyclicity is observed with frequencies of approximately 100 kyr, 39 kyr, and 19 kyr. The obliquity (39 kyr) signal is the most pronounced of the three frequencies. Individual obliquity cycles have a discrete signature and can be used as correlation horizons within the entire basin (Fig. 3). The Cenomanian/Turonian sedimentation of the Tarfaya-LaAyoune Basin was apparently forced at the same pace and frequency as the Quaternary upwelling system off West Africa [*Tiedemann et al.,* 1994]. This similarity supports trade wind-driven coastal upwelling along the Mid-Cretaceous continental margin off Tarfaya.

Figure 2: Cenomanian sediments exposed along a continuous 20-km long transect reflecting transition from marginal marine to outer shelf paleoenvironments ("Mohammed Plage" coastal section southwest of the mouth of the Chebeika river between Tarfaya and TanTan), the height of the cliff is 30 m).

3.4. Sub-Milankovitch Cyclicity; Origin of Light-dark Laminations

X-ray fluorescence spectrometry (XRF) scanning of major-element concentrations such as silicium, calcium, iron, titanium or manganese and sediment surface color scanning reveal a hierarchy of cycles that is expressed by variations in $CaCO_3$ [NOTE: 3 is subscript] content and visible color changes, within the range of mm-to-meter scale. Sediment color is controlled by variations in total organic carbon and total carbonate content. The organic carbon is predominantly marine in origin and its values match the color cycles closely, while this is less distinct with the $CaCO_3$ [NOTE: 3 is subscript] content. The influence of biogenic silica on overall color can be considered as minor, because it is finely dispersed throughout the sediment even though it can be a significant sediment component (2 - 52%). Individual laminae/thin layers can be exceptionally light because, in addition to the normally dominant background of organic matter and calcareous phytoplankton debris, they contain high concentrations of foraminifera, calcite-replaced radiolaria and/or faecal pellets. Based on the Milankovitch time scale established for the Tarfaya-LaAyoune Basin sediments, we are able to calculate that 0.1mm of sediment represents 1yr in the studied section, assuming an approximately constant sedimentation rate. Based on the counting of distinct bundles of lamina, we hypothesise that decadal sunspot cyclicity represented a signal that is frequently observed in laminated lacustrine sediments and was also described from Holocene marine anoxic basins [*Schaaf and Thurow*, 1997]. The abundant lower-frequency cycles (cm - m) represent centennial-to-millennial signals which are, even for modern environments, not very well established, and do not show a consistent periodic pattern. Further refinement is required via tuning with the sunspot signal.

Abundances of individual nannofossil groups do not reveal any correlation with color cyclicity, with the exception of Eprolithus spp. Furthermore, there is no obvious connection between color cycles, sediment composition, and dissolution resistant/prone calcareous phytoplankton. Typically, warm-water, shelf-dwelling nannoplankton, such as Nannoconus and Braarudosphaera are rare. These findings confirm earlier results from macro-faunal and radiolarian studies, indicating strong, cold, and nutrient-rich water influence in accordance with presumed seasonal upwelling.

The only calcareous nannofossil species paralleling the color trend on a millennial scale, *E. floralis*, has been recognised as indicating high latitude and/or cold/fresh water masses. Its variation in abundance may reflect changes in the intensity of upwelling, especially as this species becomes highly abundant in intervals of high organic matter concentration.

3.5. Rapid global change in the mid-Cretaceous?

The Cenomanian/Turonian (C/T; 93 Ma) event was the most intense of the mid-Cretaceous oceanic anoxic events (OAEs) and is considered as the type example for this phenomenon of organic carbon

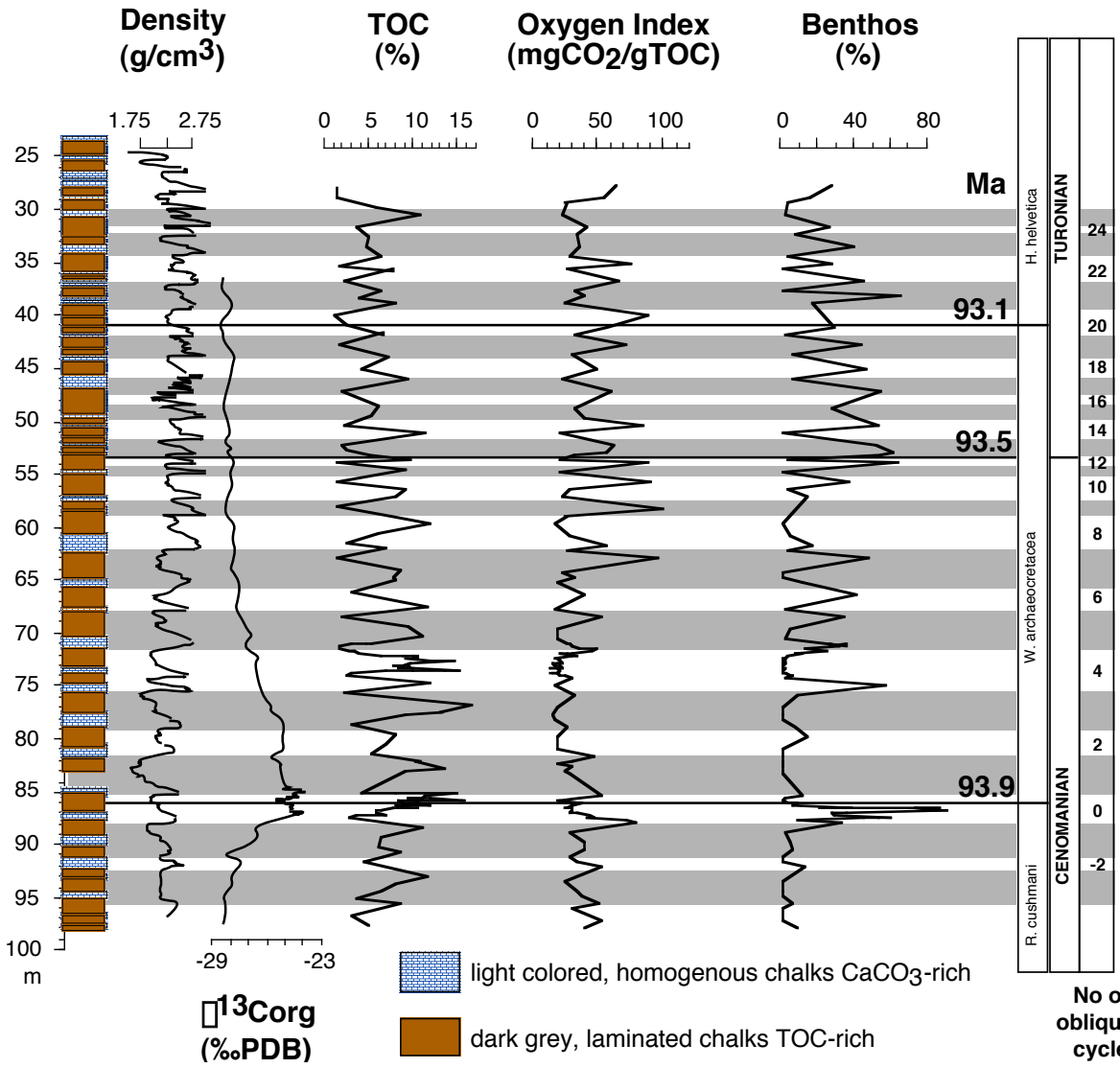

Figure 3: Cyclostratigraphy and the global late Cenomanian δ^{13}Corg excursion in exploration well S75 of the Tarfaya-LaAyoune Basin. Numbered cycles correspond to 39 ky obliquity cycles (data from [*Kuhnt et al.,* 1997 and *Luderer and Kuhnt*, 1997]).

sequestration. Global temperatures at this time were apparently the highest of the last 115 Ma. Most interestingly, the Cenomanian/Turonian OAE is characterised by a large, positive global carbon-isotope excursion in both carbonate and organic matter, caused by a major perturbation of the global carbon budget, most probably due to the extensive burial of organic matter in black shales. Recent evidence indicates that this burial event led to a 40-80% reduction in pCO_2 [NOTE: 2 is subscript] levels [*Kuypers et al.,* 1999], which in turn, had a strong impact on climatic conditions. A major extinction event of marine planktonic organisms occurred at the same time, which was related to either sea level change, global anoxia, or sea water temperature change [*Luderer and Kuhnt*, 1997; *Huber et al.*, 1998].

The entirely cored oil shale exploration wells in the Tarfaya-LaAyoune coastal basin allow the investigation of what is, globally, the highest-resolution record of the late Cenomanian extinction events. The extinction of the planktonic foraminifer *Rotalipora cushmani* is observed within an obliquity cycle of the Milankovitch frequency band ("Cycle 0"), which was examined on a centimeter scale, corresponding to approximately 200 years [*Luderer and Kuhnt*, 1997]. This high-resolution

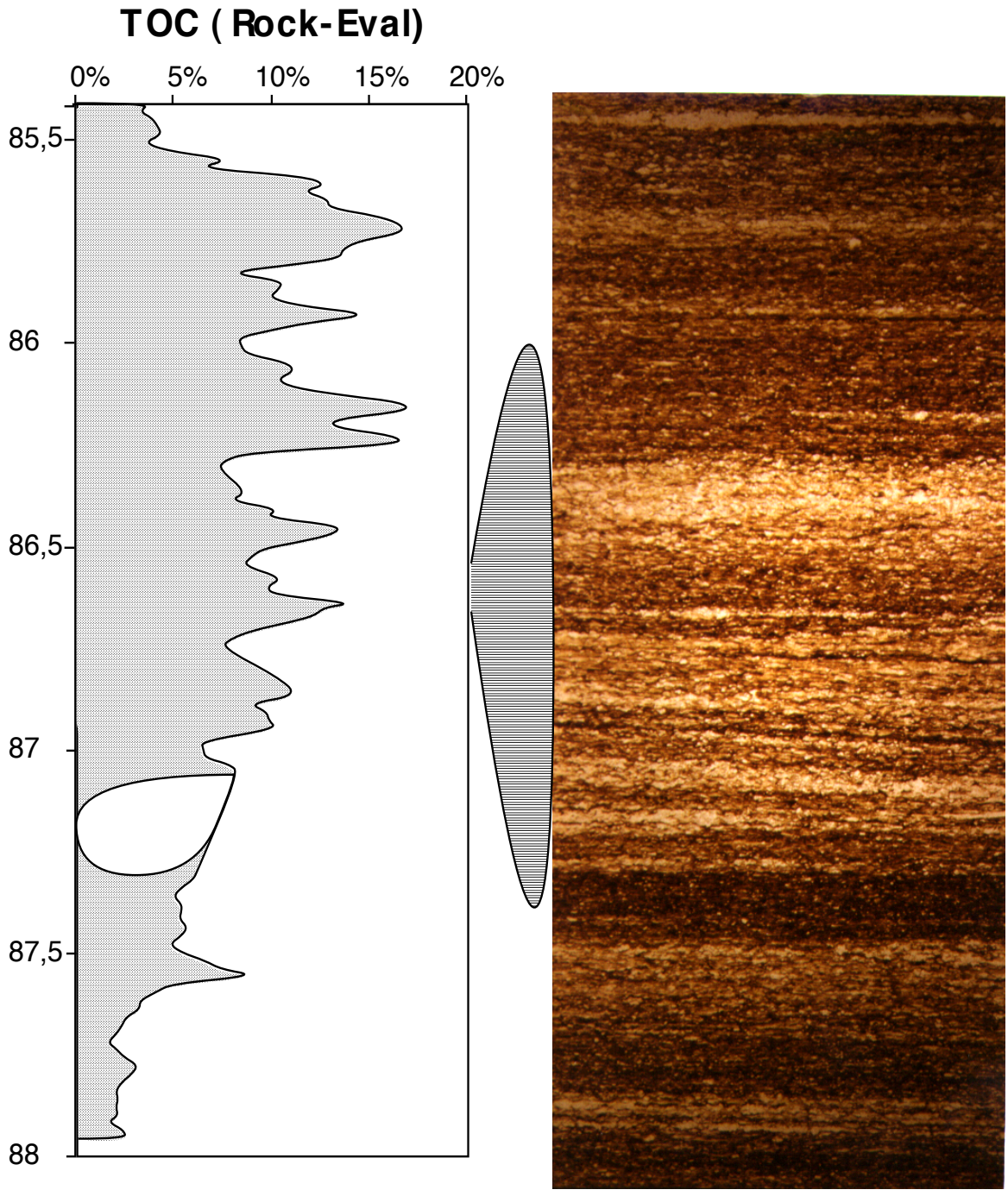

Figure 4. Nested cycles in TOC-content of 3-4 kyr frequency (obliquity cycle 0, late Cenomanian, well S75) and millimeter- to centimeter-scale cyclicity (decadal) within the laminated blackshale (polished rock-slab, well S13, *Whiteinella archaeocretacea* foraminiferal zone; height of the slab is 8 cm)

study revealed no correlation of extinction events to anoxia; i.e., the extinction of *Rotalipora cushmani* is observed within an interval with relatively low total organic carbon and an unusual high percentage portion of benthic foraminifers, indicating at most dysaerobic conditions at the sea floor [*Luderer and Kuhnt*, 1997]. Several thousand years before its extinction, Rotalipora cushmani shows a trend toward development of "atypical" morphotypes, which changes the mode of trochospiral coiling and reduces the thickness of keels. This tendency is paralleled by a trend toward continuously lighter oxygen isotope values or warmer surface water temperatures. The final extinction event occurs at the temperature maximum. The possibility to precisely correlate this major extinction event to a global carbonate isotope curve and an orbitally-tuned time scale makes the Cenomanian/Turonian extinction

event a model case for understanding the spatial and temporal dynamics of extinctions and their relation to global environmental change.

3.6. Organic matter accumulation and seafloor anoxia

In the Cretaceous low latitude Atlantic, boundary conditions for the production and accumulation of organic matter were conspicuously different from those in the modern ocean. Warm, saline bottom waters and high sea levels favored the establishment of widespread oceanic anoxia ("ocanic anoxic events" of [*Schlanger and Jenkyns*, 1976]). Upwelling of nutrient-enriched intermediate waters across the Cenomanian-Turonian boundary specifically favored biological productivity, as well as the preservation of labile organic matter in dysaerobic-to-anoxic marginal basins along the African continental margin [*Kuhnt et al*., 1990].

The Cenomanian/Turonian organic-rich marls deposited in the Tarfaya LaAyoune Basin are extremely rich in organic carbon (approaching 20% total organic carbon in the central part of the basin). Organic matter composition is dominated by kerogen types II and I and the kerogen microscopy shows that the organic matter is dominated by alginite and bituminite, which indicates fully marine conditions with minimal terrestrial influence. Bituminite, being a degradational product of marine phytoplankton, is a proxy for surface water productivity. Therefore, changes in bituminite content, and consequently sediment color, reflect changes in primary productivity. Organic carbon composition remains uniform throughout the sequence and does not show any marked change with the onset the Cenomanian/Turonian oceanic anoxic event.

Across the Cenomanian/Turonian boundary, we observe a general decrease in organic carbon concentration towards the paleo-coastline, whereas anoxia at the sea floor prevailed in the deeper part of the basin. These depositional conditions changed approximately 140 Kyrs after the late Cenomanian carbon isotope excursion, when the re-appearance of large numbers of benthic foraminifers strongly suggests at least periodically better-oxygenated bottom waters.

3.7. Research in Progress

Since the Tarfaya-Laayoune Basin is situated at the margin of the tectonically stable Sahara platform, sea level fluctuation determined in proximal parts of the basin should mainly reflect a eustatic signal. Dating of the onlap of Cretaceous marine sequences on the Sahara platform and mapping of Cretaceous shoreline fluctuations is currently carried out along transects in the north (TanTan transect in Figure 1) and south (Laayoune transect in Figure 1) of the Tarfaya-Laayoune Basin. We observed third-order sea level fluctuations with transgressive phases and highstands (i.e., early Cenomanian, late Cenomanian, late/early Turonian, early Campanian) generally coinciding with high organic carbon accumulation rates. Regressive phases and lowstands (mid-Cenomanian, early Turonian, late Turonian-Santonian) are comparatively organic carbon-depleted. It remains an open question as to whether the observed high frequency facies changes on a Milankovitch frequency band in the distal part of the basin reflect short-term sea level fluctuations, or are entirely productivity driven.

Our current research on Cretaceous rapid global change in the Tarfaya-LaAyoune Basin focuses on three key questions: Was paleoceanographic change (i.e., major isotope shifts) as rapid in the Cretaceous as in the Pleistocene, when major climatic and paleoceanographic transitions took placewithin decades?. Is the temporal and spatial extension of "oceanic anoxic events" precisely correlated to carbon isotope excursions and/or to the frequency and amplitude of Late Cretaceous sea level fluctuations ? And finally, how influential was Cretaceous paleoceanographic change for the evolution of the marine biota (i.e., coccolithophores and foraminifers): Are major speciation/extinction events correlated to excursions of the marine isotopic record?

The unrivalled sedimentary and paleontological record in the Tarfaya-LaAyoune Basin may hold the key to answer these questions.

Chapter 4

Geochemical characterization of Cenomanian/Turonian black shales from the Tarfaya Basin (SW Morocco): relationships between paleoenvironmental conditions and early sulphurization of sedimentary organic matter

Chapter 4.

Geochemical characterization of Cenomanian/Turonian black shales from the Tarfaya Basin (SW Morocco): relationships between paleoenvironmental conditions and early sulphurization of sedimentary organic matter

Authors: *Kolonic, S., J.S. Sinninghe Damsté, M.E. Böttcher, M.M.M. Kuypers, W. Kuhnt, B. Beckmann, G. Scheeder, and T. Wagner*

Status: published Journal: *Journal of Petroleum Geology 25, 325-350, 2002*

Abstract

A Organic geochemical and petrological investigations were carried out on Cenomanian/Turonian black shales from three sample sites in the Tarfaya Basin (SW Morocco) to characterize the sedimentary organic matter. These black shales have a variable bulk and molecular geochemical composition reflecting changes in the quantity and quality of the organic matter. High TOC contents (up to 18wt%) and hydrogen indices between 400 and 800 (mgHC/gTOC) indicate hydrogen-rich organic matter (Type I-II kerogen) which qualifies these laminated black shale sequences as excellent oil-prone source rocks. Low T_{max} values obtained from Rock-Eval pyrolysis (404-425°C) confirm an immature to early mature level of thermal maturation. Organic petrological studies indicate that the kerogen is almost entirely composed of bituminite particles. These unstructured organic aggregates were most probably formed by intensive restructuring of labile biopolymers (lipids and/or carbohydrates), with the incorporation of sulphur into the kerogen during early diagenesis. Total lipid analyses performed after desulphurization of the total extract shows that the biomarkers mostly comprise short-chain n-alkanes (C_{16}-C_{22}) and long-chain (C_{25}-C_{35}) *n*-alkanes with no obvious odd-over-even predominance, together with steranes, hopanoids and acyclic isoprenoids. The presence of isorenieratane derivatives originating from green sulphur bacteria indicates that dissolved sulphide had reached the photic zone at shallow water depths (~100m) during times of deposition. These conditions probably favoured intensive sulphurization of the organic matter. Flash pyrolysis GC-MS analysis of the kerogen indicates the aliphatic nature of the bulk organic carbon. The vast majority of pyrolysis products are sulphur-containing components such as alkylthiophenes, alkenylthiophenes and alkybenzothiophenes. Abundant sulphurization of the Tarfaya Basin kerogen resulted from excess sulphide and metabolizable organic matter combined with a limited availability of iron during early diagenesis. The observed variability in the intensity of OM sulphurization may be attributed to sea level-driven fluctuations in the palaeoenvironment during sedimentation.

4.1. Introduction

The Tarfaya Basin of SW Morocco hosts one of the largest oil-shale deposits in NW Africa [*Amblés et al*., 1994], covering a total area of about 170,000 km2 both on- and offshore. Mid-Cretaceous organic carbon-rich sedimentary rocks reach an exceptional thickness here of up to 800m, and have been intensively investigated by both Moroccan and foreign oil companies [*Leine,* 1986]. The recently-reported discovery of oil in Upper Cretaceous reservoir units in Mauritania, together with a recent offshore geophysical transect (Ifni-Tarfaya-Layoune) by various oil companies (including Enterprise Oil, Shell, Roc Oil, and Kerr-McGee) has emphasized the economic relevance of Cretaceous source rocks throughout the NWAfrican continental margin.

In 1970, Exxon encountered heavy oils in a well in the offshore part of the Tarfaya Basin. Because of its low-API gravity index (average 20°API), these heavy oils were assumed to be sulphur rich. Sulphur in crude oils in the Tarfaya Basin is present in various compounds which were formed during early diagenesis by the interaction of sulphides with functionalized organic compounds [see *Sinninghe Damsté and de Leeuw*, 1990 for a review]. Sulphurization of organic matter (OM) is a process that occurs either at an intramolecular level, forming low molecular-weight organic sulphur compounds (e.g. thiophene, thiolane or thiane moieties); or, the sulphur atoms form (poly)-sulphide bridges between individual compounds resulting in the creation of a macromolecular network [e.g. *Schouten et al.,* 1995a].

Sinninghe Damsté and Köster [1998] identified a fossil pigment derived from anoxygenic photosynthetic green sulphur bacteria in the Tarfaya Basin black shales. This indicates that dissolved sulphide had penetrated into the photic zone during the Cenomanian-Turonian in this part of the southern North Atlantic. Such euxinic conditions, which are comparable to those in the modern Black Sea [*Ohmoto et al*., 1990; *Neretin et al*., 2001], are ideal for early diagenetic sulphurization of OM if the input of reactive iron is limited [*Hartgers et al*., 1997]. Enhanced incorporation of sulphur into organic matter occurs if sulphide is present in quantities which exceed the amount which can be scavenged by pyrite formation.

A number of studies have demonstrated that sulphurization of metabolizable OM can lead to a wide variety of organic sulphur compounds [e.g. *Sinninghe Damsté et al*., 1989a; *Schaeffer et al.,* 1995; *Schouten et al*., 1995b]. Furthermore, it has been shown that natural sulphurization is not only an important sink for excess sulphide, but also that it leads to the enhanced preservation of labile organic compounds such as lipids and carbohydrates [*Sinninghe Damsté and de Leeuw*, 1990; *Sinninghe Damsté et al*., 1998; *Schouten et al*, 1995a]. Geochemical studies on sulphur-rich kerogens from the Kimmeridge Clay Formation [*Boussafir et al*., 1995a,b] showed that natural sulphurization contributed to the formation of orange amorphous organic matter (AOM). These AOM particles were found to be identical to bituminite observed on polished thin sections [*Boussafir and Lallier-Vergès*, 1997]. This type of unstructured OM often represents most of the kerogen in many oil-prone source rocks [e.g. *Tissot and Welte*, 1984]. Similar observations have been made from recent immature deposits along the continental margins of Peru and Oman [*Eglinton et al*., 1994; *Lückge et al*. 1996] where OM is almost exclusively composed of bituminite (up to 98%). Such high proportions of unstructured OM can be explained by high flux-rates of metabolizable OM together with sulphurization processes which transformed the labile OM into non-metabolizable unstructured organic aggegrates [*Lückge et al*. 1996]. Although the chemical pathways of natural sulphurization are now better understood, it is still not clear to what extent the degree or intensity of sulphurization is influenced by (palaeo)-environmental boundary conditions, such as fluctuations in climate, oceanography and sealevel.

The main objectives of the present study were to determine the origin, the formation pathways and the state of preservation of OM in the Tarfaya Basin. We attempt (i) to provide details of the petrography and geochemical composition of the OM, and (ii) to assess spatial and temporal fluctuations in its hydrocarbon potential; finally, (iii) we propose a relationship between palaeoenvironmental conditions and the early sulphurization of sedimentary OM. Particular attention is given to the degree of sulphurization.

4.1.1. Geological Background

The Tarfaya Basin is situated south of the Anti-Atlas Mountains extending into the Palaeozoic

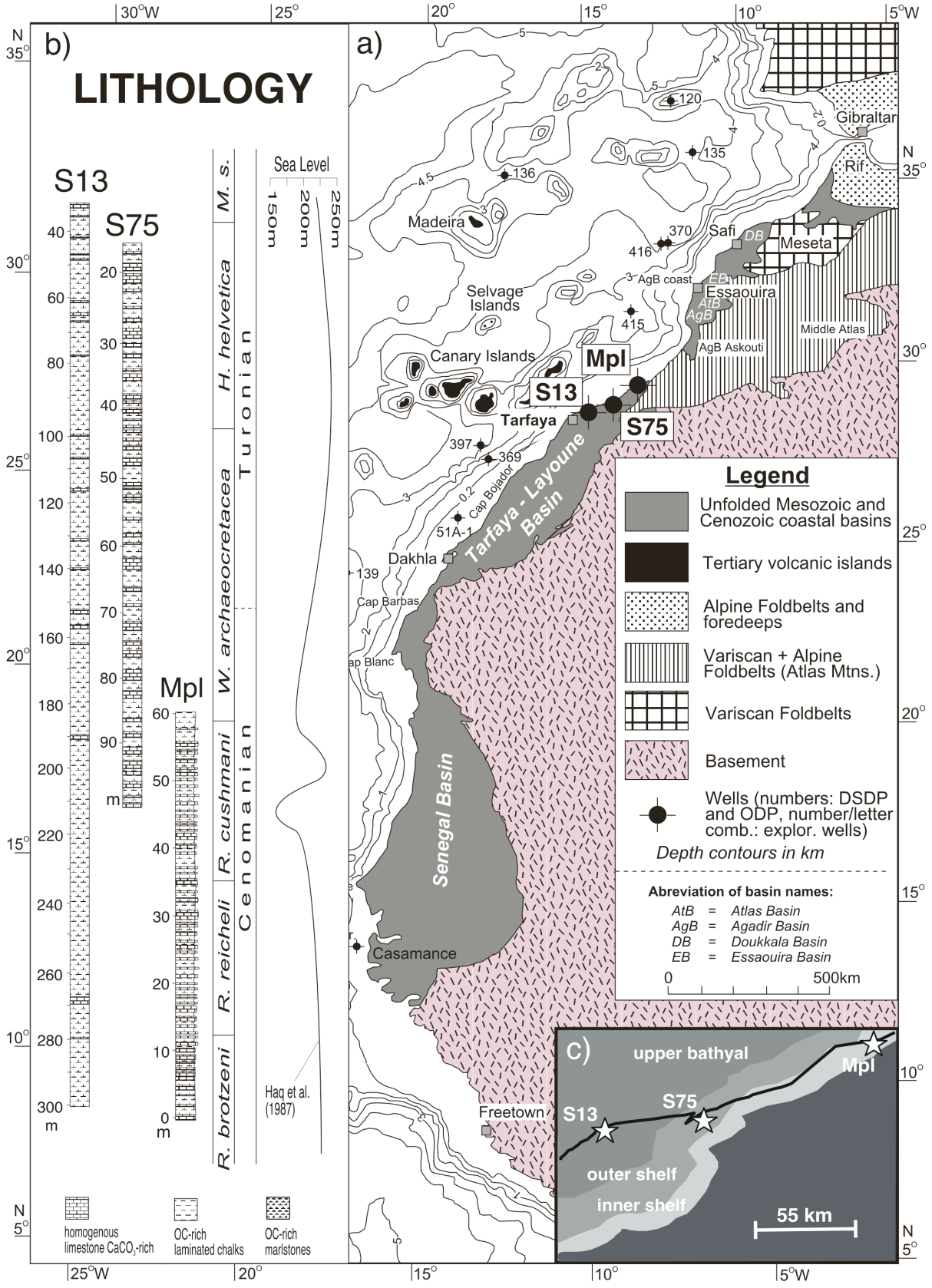

Figure 1a. Map showing the location of the investigated sites (S13, S75 and Mpl) in the Tarfaya Basin, SW Morocco. (b) the stratigraphical ranges of the investigated sections in relation to the relative eustatic sea-level curve of *Haq et al.* [1987]. (c) Palaeogeographic map of the Tarfaya Basin with the palaeo-positions of the studied sites. (Stratigraphy after [*Kuhnt et al.*, 1997], basemap modified after [*Ranke et al.*, 1982]). Abbreviation; M.s.: *Marginotruncana schneegansi* biozone.

Tindouf Basin to the east and the Senegal Basin to the south, while its western margin is defined by the East Canary Ridge (Fig. 1). The basement is composed of folded Precambrian and Palaezoic rocks which are discordantly overlain by Mesozoic sediments whose thickness locally exceeds 12km. Detailed and comprehensive geological descriptions of this area were published by *Martinis and Visintin* [1966], *Viotti* [1965, 1966], *Choubert et al*. [1966, 1972], *Wiedmann et al*. [1978], *von Rad and Arthur* [1979], *von Rad and Einsele* [1980], *Ranke et al*. [1982], *and Heyman* [1989].

In response to early rifting of the central and southern North Atlantic, and a marine incursion into this rift system during the Triassic, a major phase of evaporite deposition occurred in this region. Today, this salt province extends along the NW coast of Morocco, and salt diapirs are important offshore structural elements. The Jurassic was initiated by a major marine transgression and was characterized by high subsidence rates, generally compensated by thick terrigenous clastic sequences and carbonate platform buildups in the shallow-water shelf area. Early Cretaceous (Aptian-Albian) sedimentation was mainly deltaic (e.g. the Tan Tan delta at the northern margin of the Tarfaya Basin), with sediments probably derived from the Tindouf Basin and the African craton to the SE. Aseries of major transgressive cycles in the mid to Late Cretaceous (Albian/Cenomanian, Cenomanian/Turonian, Santonian/Campanian) caused repeated and widespread flooding of the NW African continental margin, and initiated the deposition of more than 800m of laminated biogenic sediments of Cenomanian-Santonian age in the Tarfaya Basin. These sediments consist mainly of calcareous nannoplankton, dispersed biogenic silica and planktonic foraminifera, and have a high content of marine organic matter. Sedimentation rates exceeded 10cm/ky. The sediments were deposited in a nutrient-rich environment in which an open-shelf upwelling system had developed [*Kuhnt et al*., 2001]. During the Miocene, the Upper Cretaceous succession was eroded, and the deposition of the relatively thin Moghrebian Formation took place.

4.2. Material and Methods

Samples used in this study were obtained from three sites along a NE-SW transect through the Tarfaya Basin (Fig. 1). The arrangement of the sites forms a palaeotransect about 175km long from the deepest part of the basin (S13 and S75) towards the palaeocoastline near Mohamed Plage (Mpl). Exploration Wells S13 and S75 were drilled near the village of Tarfaya [*Leine*, 1986]. *S13* is the most distal site and is located approximately 45 km SW of well S75. The *Mpl* profile was recovered from a fresh coastal exposure located about 130km NE of well *S75*. Samples between 2 and 5cm thick were taken from these Cenomanian/Turonian sections at regular intervals of 5-10 cm.

Kuhnt et al. [1990; 1997] used material from wells S13 and S75 to establish a high resolution bio- and isotope stratigraphy for the Late Cenomanian *Rotalipora brotzeni* biozone and the early Turonian *Whiteinella archaeocretacea* biozone (Fig. 1). According to their stratigraphy, the succession at well S13 covers the interval from the lower Cenomanian (*Rotalipora brotzeni* biozone) to the base of the upper Turonian (*Helvetoglobotruncana helvetica* and *Marginotruncana schneegansi* biozone); and that at S75, the interval from the upper Cenomanian to the upper Turonian (upper *Rotalipora cushmani* to middle *H. helvetica* biozone). *Luderer* (1999] concluded that the *Mpl* section represents the interval from the lower Cenomanian (*Rotalipora brotzeni* biozone) to the upper Cenomanian (base of *Whiteinella archaeocretacea* biozone).

4.2.1. Bulk elemental, ICP-AAS, Rock-Eval and petrological analyses

After careful removal of inorganic carbon by 0.25 N HCl, the total amounts of organic carbon (TOC) and sulphur (S_{tot}) were determined with a *LECO CS-300* Carbon-Sulphur analyser. Total reduced inorganic sulphur (TRIS, essentially pyrite) was extracted from the sediment with a hot acidic Cr(II) chloride solution [*Fossing and Jørgensen*, 1989]. The liberated hydrogen sulphide was trapped as Ag_2S and quantified gravimetrically. Iron concentrations were obtained by ICP-AAS analysis using a *Perkin Elmer Optima 3300RL*. Rock-Eval pyrolysis was performed on bulk sediments (Hydrogen Index, Oxygen Index and Tmax) using a Rock-Eval II for the S75 samples and a Rock-Eval VI for the Mpl samples, following the analytical procedures outlined by *Espitalié et al*. [1977]. Rock-Eval data for well S13 were taken from *Kuhnt et al*. [1990]. Maceral compositions were studied on polished blocks using a *Zeiss Axiophot* equipped with incident white and ultraviolet light. The determination and description of maceral compositions followed the standard procedures reported by *Taylor et al*.

[1998]. In this study, observed unstructured OM was defined as bituminite; palynologists who examine isolated kerogen in transmitted light refer to bituminite as AOM particles or amorphogen [e.g. *Boussafir and Lallier-Vergès*, 1997].

4.2.2. Extraction fractionation of extractable organic matter, Raney-Nickel desulphurization and hydrogenation

Pulverized samples (5 to 10g) were extracted with an Accelerated Solvent Extractor (ASE) (tempeature:100°C; pressure: 100psi; DCM:MeOH: 9:1). A part of the total extract was used for direct Raney-Nickel desulphurization [*Petit and van Tamelen*, 1962; *Sinninghe Damsté et al*., 1994] and subsequent hydrogenation in order to analyze both free and Sbound biomarkers in a single analysis. The apolar extract (ca. 20 mg) was dissolved in 4 ml ethanol; an internal standard and 0.5 ml of Raney-Nickel suspension (0.5 g/ml ethanol) were added, and the mixture was refluxed under a nitrogen atmosphere for 1.5 h. During reflux, additional Raney-Nickel suspension (2 x 0.5 g) was added. After desulphurization, ethanol was evaporated and the extract dissolved in 4 ml ethylacetate together with a drop of pure acetic acid and a pinch of PtO_2. Hydrogen gas was bubbled in the solution for 1h, after which the solution was stirred for 24h. The catalysts were removed using a small column packed with Na_2CO3 and $MgSO_4$. The desulphurized and hydrogenated extract was subsequently separated into apolar and polar fractions using a column (20 x 2 cm; column volume (Vo)=35 ml, packed with AlO_2 (activated for 2.5h at 150°C) eluted with hexane/DCM (9:1, v/v; 150 ml) and methanol/DCM (1:1, v/v; 150 ml, respectively). The fractions were evaporated to dryness and dissolved in a small volume of hexane (1 mg extract/1 ml hexane) to be analysed by GC and GC-MS.

4.2.3. Gas chromatography, gas chromatography-mass spectrometry, Curie-point pyrolysis gas chromatography and stable isotope mass spectrometry

Gas chromatography (GC) was performed using a *Hewlett-Packard 5890* instrument, equipped with an on-column injector. A fused silica capillary column (25m x 0.32mm) coated with *CP-Sil 5* (film thickness 0.12 µm) was used with helium carrier gas. Both a flame ionization detector (FID) and a sulphur-selective flame photometric detector (FPD) were used, applying a stream-splitter with a split ratio of FID:FPD = ca. 1:2. Fractions of the extract were injected at 70°C, after which the temperature was raised subsequently at 20°C/min to 130°C and then at 4°C/min to 320°C, at which it was maintained for 20min.

Gas chromatography-mass spectrometry (GC-MS) was performed using a *Hewlett-Packard 5890* gas chromatograph interfaced to a *VG Autospec Ultima Q* mass spectrometer operated at 70eV with a mass range m/z 50-800 and a cycle time of 1.8sec (resolution 1000). The column conditions and temperature programme were the same as described above for GC analyses, respectively.

Curie-point pyrolysis gas chromatography ((Py)-GC) was conducted on a *Hewlett-Packard 5890* series II gas chromatograph fitted with a 25m x 0.32mm *CP-Sil 5* (film thickness 0.45µm) fused silica capillary column and equipped with an FID detector. Samples were pressed on flattened ferromagnetic wires with a Curie temperature of 610°C. The wire was inserted into a glass liner, subsequently introduced into a *FOM-4LX* pyrolysis unit and inductively heated for 10sec. The desorbed fragments were flushed into the capillary column using helium as the carrier gas. The gas chromatograph was equipped with a cryogenic unit and programmed from 0°C (5min) to 320°C (hold time: 10min) at 3°C/min. Helium was used as a carrier gas and the temperature of the FID was 320°C.

Combustion-isotope-ratio-monitoring mass spectrometry: stable sulphur isotope analysis of the pyrite fraction was performed by combustion-isotope-ratio-monitoring mass spectrometry (C-irmMS; [*Böttcher and Schnetger*, 2002]). Silver sulphide was combusted in a *Carlo Erba* elemental analyzer coupled to a *Finnigan* triple collector gas mass spectrometer via a *Finnigan Conflo* interface. Isotope ratios are given in the δ–notation with respect to the SO_2-based V-CDT standard.

4.3. Results and Discussion

4.3.1. Elemental analysis

At well S13 (Fig. 2), the highest total organic carbon (TOC) contents (between 10 and 20%) are

observed in the upper *R. cushmani* to upper *W. archaeocretacea* biozones. Similarly the highest TOC contents at well S75 are observed in the lower to middle *W. archaeocretacea* biozone, with values between 10 and 18% (Fig. 3). Compared to these sites from the central part of the basin, the coastal Mpl section has lower TOC contents, with highest values approaching 10-12 % for the lower *W. archaeocretacea* biozone (Fig. 4). Based on the high resolution bio- and isotope stratigraphy, average sedimentation rates of about 6cm/ky were determined for sites S75 and Mpl, and up to 12cm/ky for site S13 [*Luderer*, 2001]. The organic carbon accumulation rates covary with the TOC content, reaching average values of about 20 $gC \bullet m^{-2} \bullet a^{-1}$; the highest accumulation rates are estimated for the lower to middle *W. archaeocretacea* biozone with values up to 30 $gC \bullet m^{-2} \bullet a^{-1}$ at site S75.

Total sulphur (S_{tot}) contents range between 1-4% for well S75 and 1-3% for the Mpl section; for well S13, S_{tot} data are not available. S_{tot} values remain relatively constant at the Mpl section, while large variations are documented for well S75. Astrong positive correlation between TOC and S_{tot} values is observed for well S75 (Fig. 5) with two distinct populations (for S75 r^2= 0.78 and r^2= 0.81). Most of these samples plot below the range found for "normal marine" sediments (C/S = 2.8 ± 0.8; [*Berner*, 1984]). There is a pronounced shift in TOC/S_{tot} ratios from average background values of 5 covering the lower and upper *W. archaeocretacea* biozone, to higher values of up to 15 within the middle *W. archaeocretacea* biozone. For the Mpl section, a less strong positive TOC/S_{tot} correlation is observed (r^2= 0.78). The iron concentrations for well S75 are relatively low, with values ranging between 3-11 g/kg. Iron data for the Mpl section and well S13 are not available.

4.3.2. Rock-Eval pyrolysis

Interestingly, all three sites show Rock-Eval hydrogen indices (HI) which are fairly high -between 400 and 800 (mgHC/gTOC) - with an S2 pyrolytic yield of up to 140 mgHC/gRock despite their differences in TOC content. A plot of the S2 vs. TOC data (Fig. 6) shows that there is a good correlation for the three sites, indicating that the mineral matrix effect had little influence on pyrolysis. Most values plot on a regression line (HI) that equals 640 mgHC/gTOC (Mpl r^2= 0.95; S75 r^2= 0.94 and S13 r^2= 0.95), identifying Type I/II kerogen and a high oil generation potential [*Tissot and Welte*, 1984].

Plots of HI versus OI (oxygen index) and HI versus T_{max} (Fig. 7) support the latter observation but also point to fluctuations in OI. A persistent low T_{max} between 405-422°C confirms the immature level of thermal maturation throughout the sections at sites S75 (Fig. 3) and Mpl (Fig. 4), whereas site S13 (Fig. 2) exhibits slightly higher T_{max} values of up to 425°C. The S1 pyrolytic yields approach 2.4 mgHC/gRock at site S75, *W. archaeocretacea* biozone (Fig. 3) and 2.1 mgHC/gRock for the upper *R. cushmani* biozone at Mpl (Fig. 4), indicating the presence of abundant volatile hydrocarbons in these black shales.

For well S13, S1 and S3 yields were not available from *Kuhnt et al.* [1990]. Both records were therefore recalculated to provide a complete set of Rock-Eval data. S3 yields were calculated from TOC and Oxygen Indices (OI) using the equation (OI x TOC)/100. Corresponding S1 yields were approximated using Rock-Eval records from the adjacent well S75 assuming a similar OM composition at both sites and therefore a comparable relationship for individual pyrolytic parameters. At site S75, total yields for S1 and S2 are closely correlated (r^2=0.88) especially for samples with S1 yields below 1 mgHC/gTOC (r^2=0.97). Accordingly, both parameters have a more or less constant relationship, which was calculated for each sample from well S75. After grouping these sample-specificrelationships according to stratigraphic biozones, averaged conversion factors were calculated and applied to S2 data from well S13. Averaged conversion factors are 1.34 for the *Helvetica* biozone (based on 19 data points), 1.81 for the *Archaeocretacea* biozone (based on 97 data points), and 1.40 for the *cushmani* biozone (based on 20 data points). The new approximated S1 yields for well S13 were subsequently used to estimate hydrocarbon potential and generation index values. Following this approach, the highest S1 yields are recorded for the *W. archaeocretacea* biozone and reach up to 2.1 mgHC/gRock (Fig. 2).

4.3.3. Organic Petrology

Organic petrological investigations were restricted to the Mpl section and well S75. The sedimentary matrix of organic carbon-rich samples (TOC>2%) is characterized by cloudy, strongly

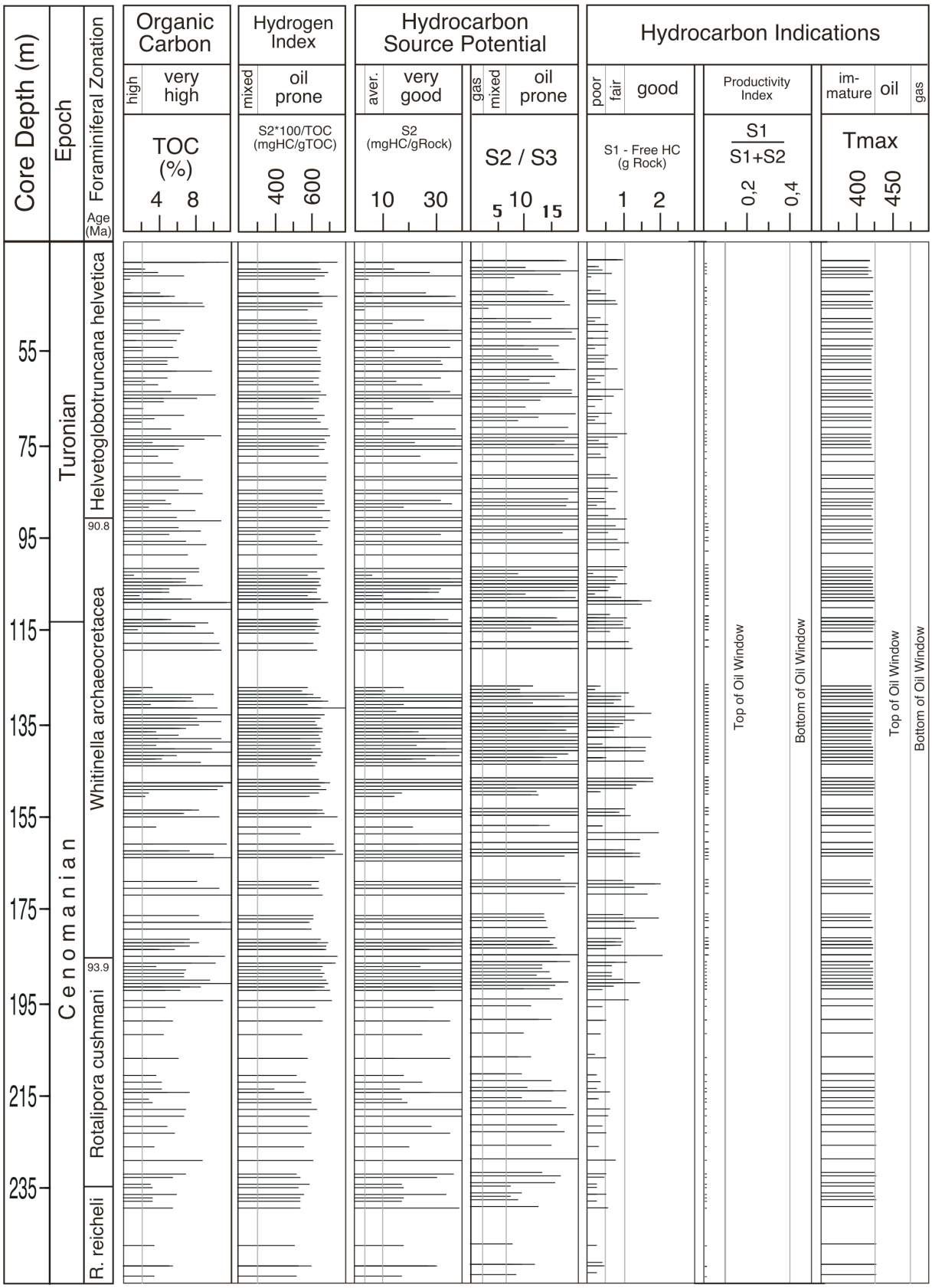

Figure 2. Rock-Eval pyrolysis results for well S13.

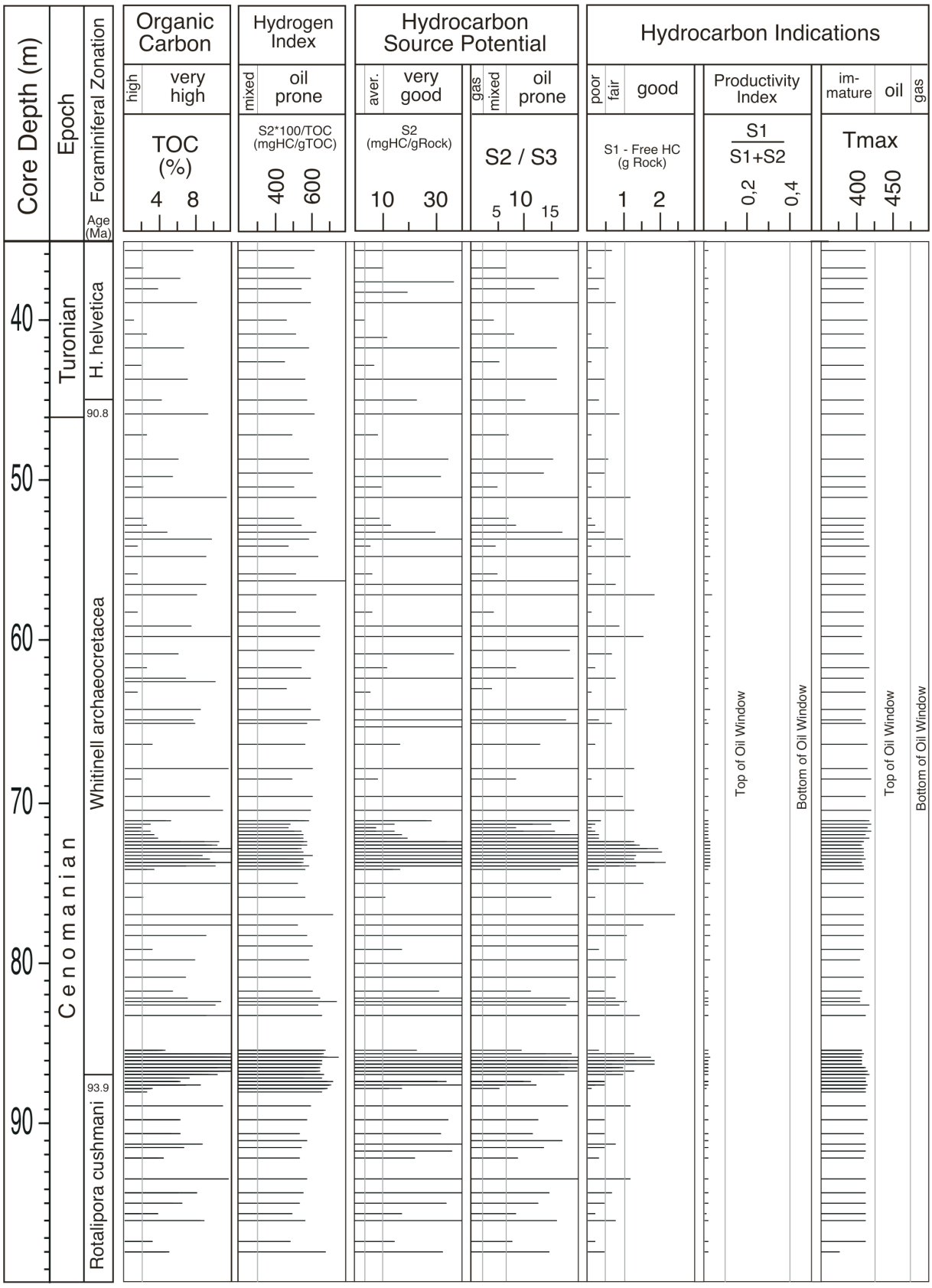

Figure 3. Rock-Eval pyrolysis results for well S75.

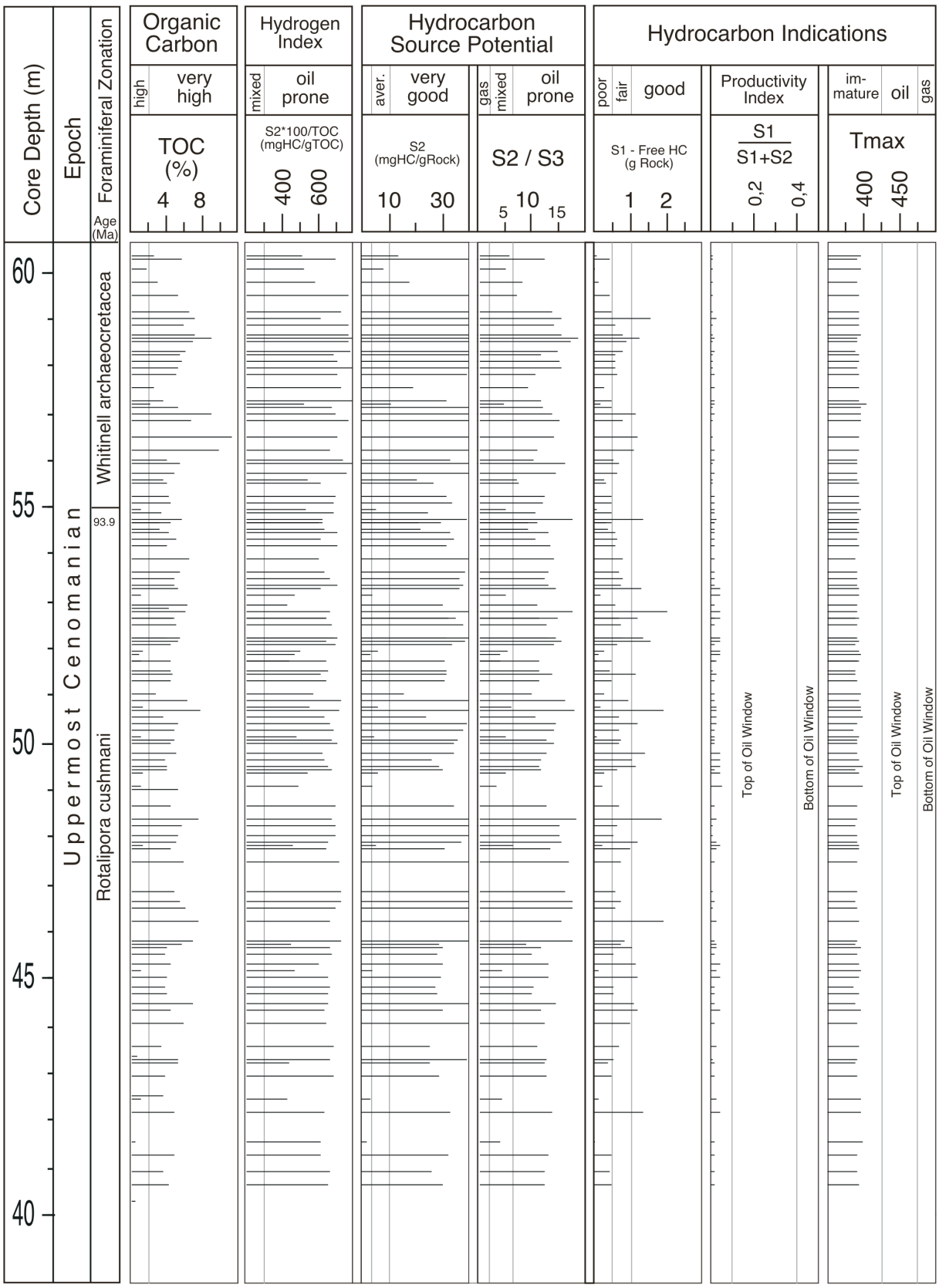

Figure 4. Rock-Eval pyrolysis results for the Mpl location.

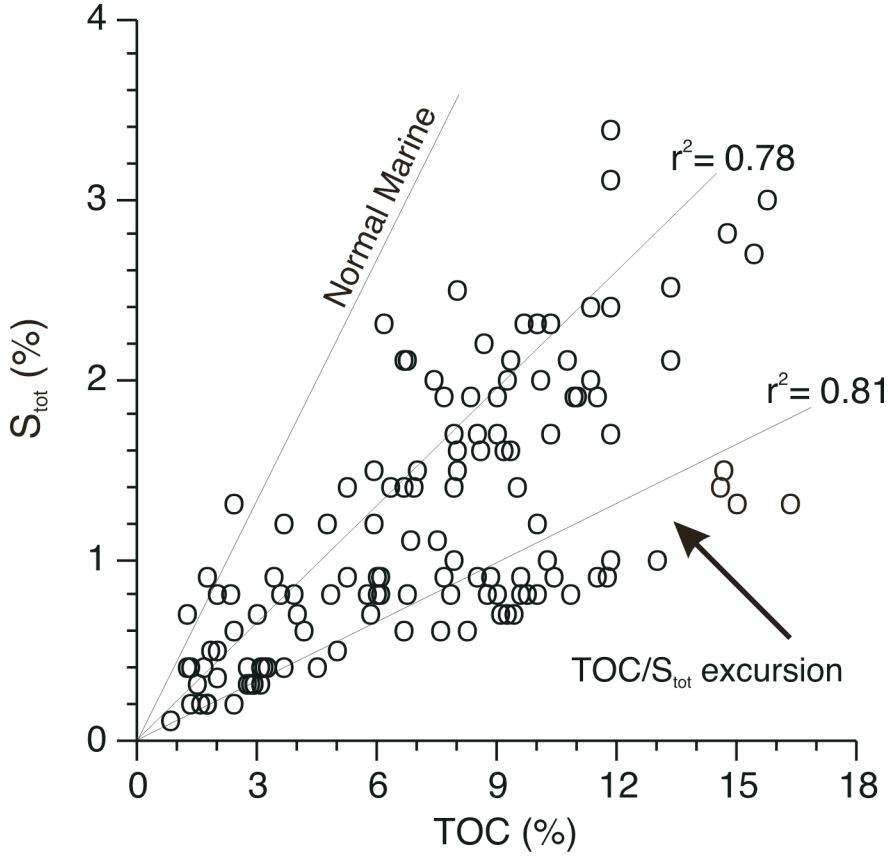

Figure 5. Variation of total sulphur with organic carbon for well S75. Theoretical average line for typical normal marine sediments (C/S = 2.8 ± 0.8) from *Berner* [1984]. See text p. 344 for a discussion of the TOC/S_{tot} excursion.

fluorescent, light red and dark orange to red unstructured OM and lamalginite bodies (Fig. 8). These bituminite particles consist of lenses of variable size (10-100µm) or layers with a length exceeding 150 µm, and differ from other macerals by lacking a welldefined shape that can be related to biological precursors. Lamalginites appear as thinwalled, reddish-orange-yellowish fluorescing macerals, and show a typical lamellar form with little recognizable structure in sections perpendicular to the bedding plane. These hydrogen-rich macerals have often been reported from oil-rich black shales and petroleum source rocks with extremely labile kerogen [*Hutton*, 1987; *Kalkreuth and MacAuley*, 1984; *Stasiuk*, 1994; *Littke and Sachsenhofer*, 1994]. Secondary organic matter, such as pyrobitumen or migrabitumen, was not observed.

By contrast, the maceral composition in sediments with low TOC contents (lower than 2%) show considerably lower matrix fluorescence, and the absence of bituminite particles and lamalginite layers (Fig. 8). In these intervals, the major fraction of liptinic macerals was composed of individual alginite bodies and liptodetrinite. Because of its detrital nature and small particle size, liptodetrinite cannot be assigned to a particular precursor liptinite maceral. Most probably, it was formed by selective preservation of alginite, sporinite or cutinite [*Largeau and Derenne*, 1993]. The recognizable larger alginite bodies showed a strong green-yellow fluorescence colour with sizes that ranged from 10-100µm. Detrital vitrinite and inertinite were only rarely observed in these sediments.

4.3.4. Biomarkers

Large amounts of total extract were recovered from S13, S75 and Mpl black shale samples (average 5-10 mg/g dry sediment). In all of the Tarfaya Basin extracts examined, the apolar fractions obtained after desulphurization showed a very similar biomarker distribution, in general consisting of short-chain (C_{16}-C_{22}) and long-chain (C_{25}-C_{35}) *n*alkanes, steranes, hopanoids and acyclic isoprenoids. Notably, these apolar fractions were dominated by steranes and to a lesser extent by hopanes (Fig. 9a).

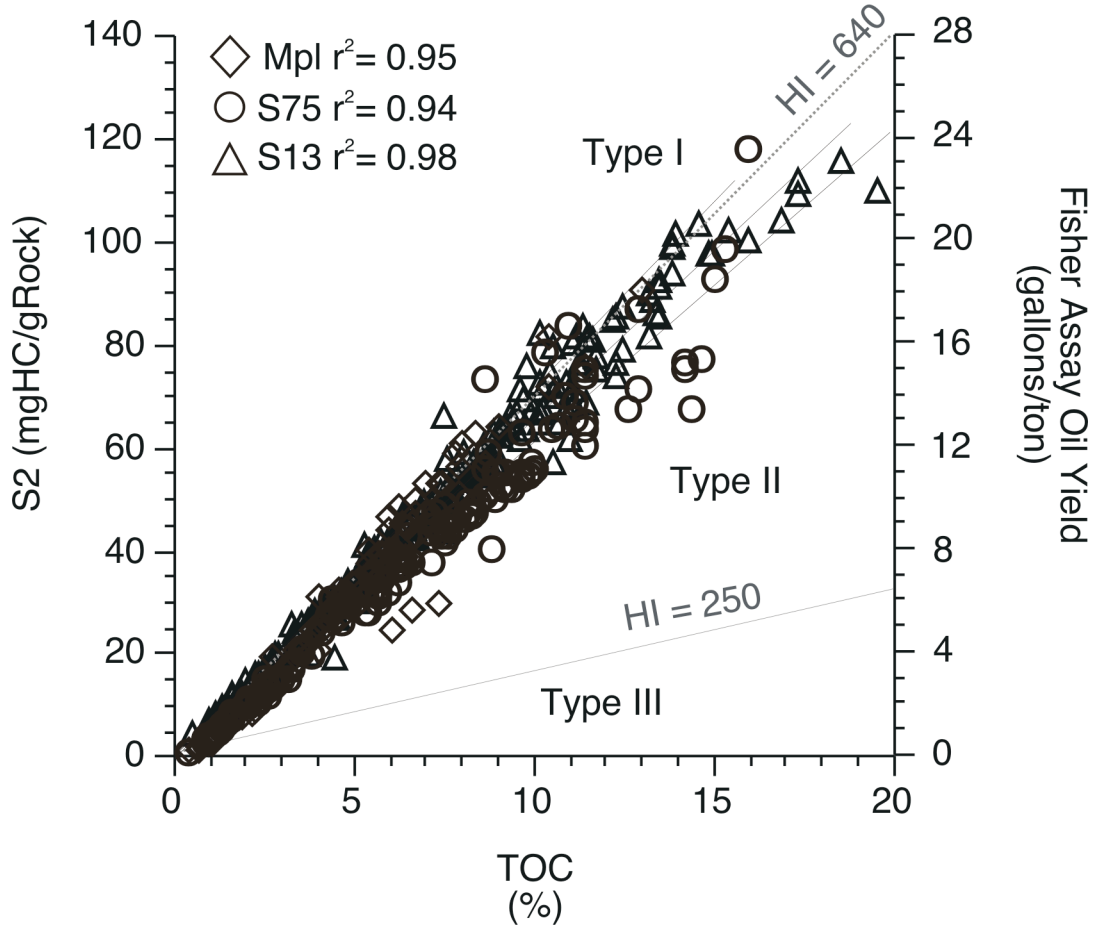

Figure 6. Plot of S2 pyrolytic yield versus % TOC (following [*Langford and Blanc Valleron*, 1990]) for the samples from locations S13, S75 and Mpl in relation to the Fisher Assay Oil Yield, indicating the high oil generation potential of the Tarfaya Basin black shales.

Comparison with extracts which had not been desulphurized indicated that large amounts of these biomarkers were originally present in an S-bound form. The distribution of short-chain (C_{16}-C_{22}) and longchain (C_{25}-C_{35}) *n*-alkanes with no obvious odd-over-even predominance is non-specific, and could indicate derivation from a multitude of algal, bacterial and higher plant sources.

4.3.4.1. Pristane and phytane

The abundance of pristane and phytane was moderate to high, which is typical of marine OM in fossil sediments. Pristane and phytane are most probably derived from either the phytol side-chain of algal or cyanobacterial chlorophyll [e.g. Didyk *et al.,* 1978], from tocopherols (i.e. pristane: [see *Goossens et al.,* 1984]), or from membrane constituents of archaea (for phytane: [e.g. *Brassell et al.,* 1981]). Pristane and phytane skeletons were also released upon desulphurization and probably originate from C_{19} and C_{20} isoprenoid thiophenes, thiolanes and thianes. It has been reported that natural sulphurization favours selective preservation of the phytane carbon skeleton relative to the pristane carbon skeleton [*Sinninghe Damsté et al*., 1986; *ten Haven et al.,* 1987, 1988; *Koopmans et al*., 1996a]. The different potential sources, in combination with selective preservation of the phytane and pristane carbon skeleton through sulphurization, do not allow the use of pristane:phytane ratios to provide further information on redox conditions during deposition of organic matter in the Tarfaya Basin.

4.3.4.2. Steranes

Cholestane, 24-methyl-cholestanes and 24-ethyl-cholestanes are abundant in the black shales from

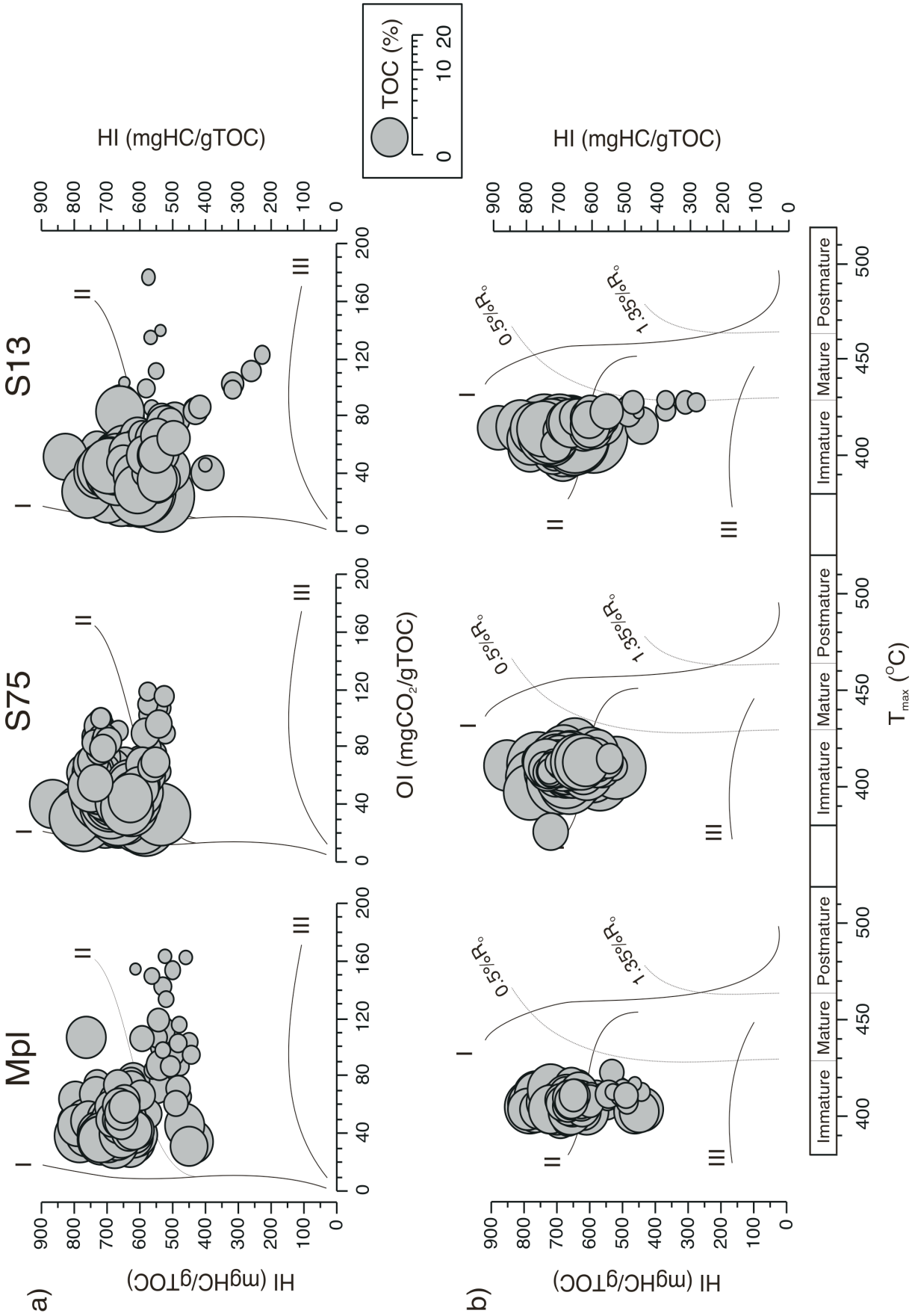

Figure 7a. Plots of OI versus HI and TOC for locations Mpl, S75 and S13 showing relatively homegeneous values around the Type II kerogen field in all three cases. (b) Plots of T_{max} versus HI for the three locations studied.

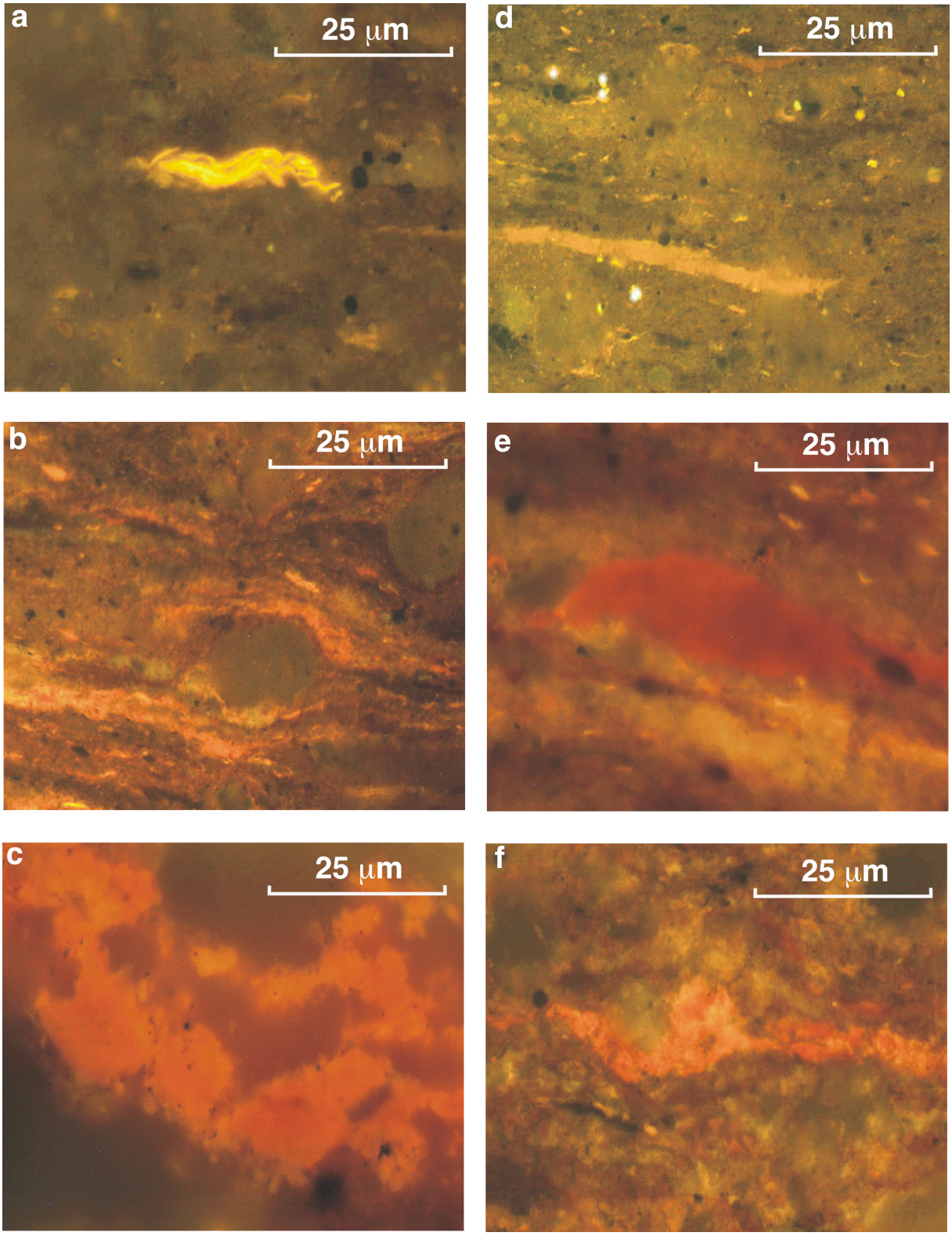

Figure 8. Photomicrographs illustrating the typical maceral composition of sedimentary organic matter in the intervals investigated. (a) Strongly fluorescing algal body and detrital fragments (liptodetrinite). (b) Reddish fluorescing bituminite particles and lamalginite. (c) Brightly reddish fluorescing bituminite particle suggesting lipidic biomass as a precursor. (d) Strongly fluorescing yellow-reddish cutinite and liptodetrinite. (e) Reddish-brown-yellowish unstructured organic matter groundmass around brightly reddishfluorescing bituminite particle and liptodetrinite. (f) Brightly reddish-yellowish fluorescing bituminite particle.

sites S13, S75 and Mpl. Most probably, these steranes were biosynthetisised by various types of marine algae.However, cholesterol and its derivates are also formed by dealkylation of ingested C_{28} and C_{29} sterols by zooplankton living heterotrophically on algal biomass [*Grice et al.,* 1998]. In addition, an input from dinoflagellates to the sedimentary organic carbon is suggested by the presence of 4-methylsteranes [*Mackenzie et al.,* 1982], and is also indicated by the presence of A-ring methylated-sterans and C-ring aromatic-sterans [*Summons et al.,* 1987] (Fig. 9a).

4.3.4.3. Hopanoids

In comparison to steranes, sedimentary hopanoids are less abundant. Hopanoids occur as C_{27} to C_{35} constituents, whereas the hopane distribution with its 17□21□(H)-, 17□21□(H)- and 17□21□(H)-isomers dominate the m/z 191 mass fragmentograms. Hopanoids are probably diagenetic products of diplopterol (hopanes<C30) or bacteriohopanopolyols (BHP), and may originate from cyano-, hetero- or methanotrophicbacteria [*Rohmer et al.,* 1992]. Although significant 2-methyl-hopanes were not observed in the Tarfaya Basin samples, a substantial cynobacterial input cannot be excluded due to the fact that only half of the cyanobacterial cultures investigated by *Summons et al*. [1999] produced 2-methyl-BHPs.

The desmethyl hopane, 28,30–dinorhopane, occurs in high abundances in samples from well S13 which is located in what is thought to have been the deepest part of the Tarfaya Basin. It has been noted that this compound occurrs in sediments and petroleum only as a free hydrocarbon [*Peters and Moldowan*, 1993]. Although its origin is still somewhat enigmatic, there are indications that dinorhopane originates from organisms which only occur in extremely anoxic bottom-water conditions. For example, stable carbon isotope investigations of dinorhopanes in the Miocene Monterey Formation suggest that the biological precursor was probably a sediment-dwelling chemo-autotrophic bacterium, utilizing porewater CO_2 as a carbon source [*Schouten et al*., 1998 a,b].

Futhermore, neohop-13(18)-ene, which is known to occur in high concentrations only in organic matter-rich sediments [*Greiner et al*., 1976, 1977], was identified in the S13, S75 and Mpl samples. It is assumed that these components are derived from bacteria dwelling at or below the chemocline, and that they may therefore be used as indicators of water bodies which were stratified in the past.

4.3.4.5. Isorenieratane

Relatively high concentrations of neohop-13(18)-ene are often accompanied by the presence of isorenieratane derivatives. Isorenieratane, a carotenoid pigment, is exclusively biosynthetisised by the brown strain of the green sulphur bacteria *Chlorobiaceae* [e.g. *Madigan et al.*, 2000]. As strict anaerobes, these bacteria require sulphide in the water column and light of a specific wavelength in order to carry out photosynthesis. At the present day, these conditions are restricted to a few isolated marine basins, such as the Black Sea, where *Chlorobiaceae* thrive near the sulphide/oxygen interface (i.e. the chemocline) at light levels of less than 1% of surface irradiance (van Gemerden and Mas, 1995). Isorenieratane in general is a very labile compound that cannot survive long-distance transport, and is therefore a clear indicator of a local marine source [*Koopmans et al.,* 1996b]. Therefore, the presence of isorenieratane derivatives in the investigated samples (Fig. 9a) provides strong evidence that euxinic conditions must have been present (at least periodically) in the photic zone of the Tarfaya-Basin.

4.3.4.6. Chromans

Finally, methylated chromans were identified in the examined samples. Although their precise biological origin is not known, these compounds are assumed to be derived from photo-autotrophs [*Sinninghe Damsté et al.,* 1987]. The 5,7,8-triMe-MTTC/8-Me-MTTC ratio can be used as an indicator of palaeohypersalinity [*Sinninghe Damsté et al.,* 1993]. However, in the Tarfaya Basin samples, the distribution pattern of methylated chromans is dominated by the presence of 5,7,8-triMe-MTTC suggesting that there was no elevated salinity of the photic zone relative to present-day seawater.

4.3.5. Kerogen characterization

Since extractable biomarkers only represent a relatively small proportion of the total organic carbon content, kerogen analysis was performed using Curie-point pyrolysis. The vast majority of pyrolysis products generated from the kerogen were sulphur-containing components such as alkylthiophenes, alkenylthiophenes and alkybenzothiophenes (Fig. 9b). C_7-C_{15} isoprenoidal alkenes/alkanes were only present in relatively small amounts. Nonsulphur containing pyrolysis products were mainly composed of homologous *n*-alkene and *n*-alkane series and alkylbenzenes. The *n*-alkenes and *n*-alkane doublets most probably originated from marine algaenans. These are insoluble, non-hydrolysable biomacromolecules which are present in algal cell walls [*de Leeuw et al*., 1991], and as such have only been reported from the microalgae *Chlorophyceae* and *Eustigmatophyceae* [*Derenne et al.,* 1992; *Gelin et al*., 1996]. Adominant terrestrial origin for the *n*-alkenes and *n*-alkanes biomarkers (i.e. cutinite) is unlikely since the extractable organic matter contains hardly any higher plant biomarkers (e.g. leaf wax *n*-alkanes or oleananes). Phenols and methoxyphenols, which are pyrolysis products of lignin and thus indicative of higher plant biopolymers [Saiz-Jimenez and de Leeuw, 1984, 1986] were only present in trace amounts in the flash pyrolysates. This also indicates the predominantly marine nature of the organic matter.

4.3.6. The nature of the sedimentary organic matter

The level of organic enrichment and the oil generation potential of these shallow-marine black shales indicates that marine Types I/II and II kerogen occur throughout the studied sections. High S2 hydrocarbon yields and S2/S3 ratios underline the excellent hydrocarbon source potential and oil proneness of the kerogen in the Tarfaya Basin. Observed variations in OI most probably reflect partial oxidation of the marine organic matter (changes in the depositional redox setting) rather than a variable terrestrial contribution. This assumption is based by the cyclic re-appearance of benthic foraminifera coinciding with increased OI [*Kuhnt et al.,* 2001]. Small fluctuations in the OI may also reflect different intensities of carbohydrate sulphurization whereby substantial amounts of oxygen can be introduced into the kerogen [*Sinninghe Damsté et al*., 1998].

The observed low Tmax values at site S75 and the Mpl section strongly indicate the consistently immature nature of the OM which has barely reached the top of the oil window, suggesting shallow burial of the mid-Cretaceous strata. There are regional differences in average Tmax signatures, with slightly enhanced thermal maturation towards the central part (well S13) of the Tarfaya Basin. This is in good agreement with the abundance at site S13 of extended unsaturated hopanoids (i.e. hopenes) which are released by thermal degradation of S-bound hopanoids [*Köster et al*., 1997]. However, significant hydrocarbon generation has not yet occurred. This conclusion is supported by the very low production indices throughout the entire cored interval at wells S13 (Fig. 2) and S75 (Fig. 3) and location Mpl (Fig. 4). Organic-petrological observations for these sites indicate a distinctive maceral composition which suggests intensive sulphurization of OM in the TOC-rich intervals. The sedimentary matrix is dominated by highly fluorescent, unstructured OM aggregates and regularly-spaced lamalginite macerals embedded in a bright yellow fluorescing groundmass. Characterized by its typical yellowish-orange to reddish-orange high fluorescence, these bituminite particles can be classified according to *Teichmüller and Ottenjann* [1977] as bituminite type II. This type of bituminite is reported to be the major constituent of kerogen in the Monterey Formation [*Stankiewicz et al*., 1996] and the dominant AOM maceral in the Kimmeridge Clay Formation [*Boussafir et al.,* 1995a, 1997; *Lallier-Vergès et al*., 1997; *van Kaam-Peters et al.,* 1998].

Conventionally, the formation of unstructured OM has been explained in terms of a restructuring process involving degradation and recondesation reactions of biopolymers [*Welte*, 1974; *Largeau and Derenne*, 1993]. Selective preservation is an important process in the preservation of aliphatic biomacromolecules in fresh-water enviroments, but is less significant in marine habitats where other much more effective mechanisms may operate. In the marine realm, natural sulphurization of reduced sulphur species with functionalized lipids is thought to represent a major sink for labile organic compounds [see *Sinninghe Damsté and de Leeuw*, 1990 for a review]. In particular, carbohydrates, which are usually readily degraded, may escape mineralization due to sulphurization so that they can

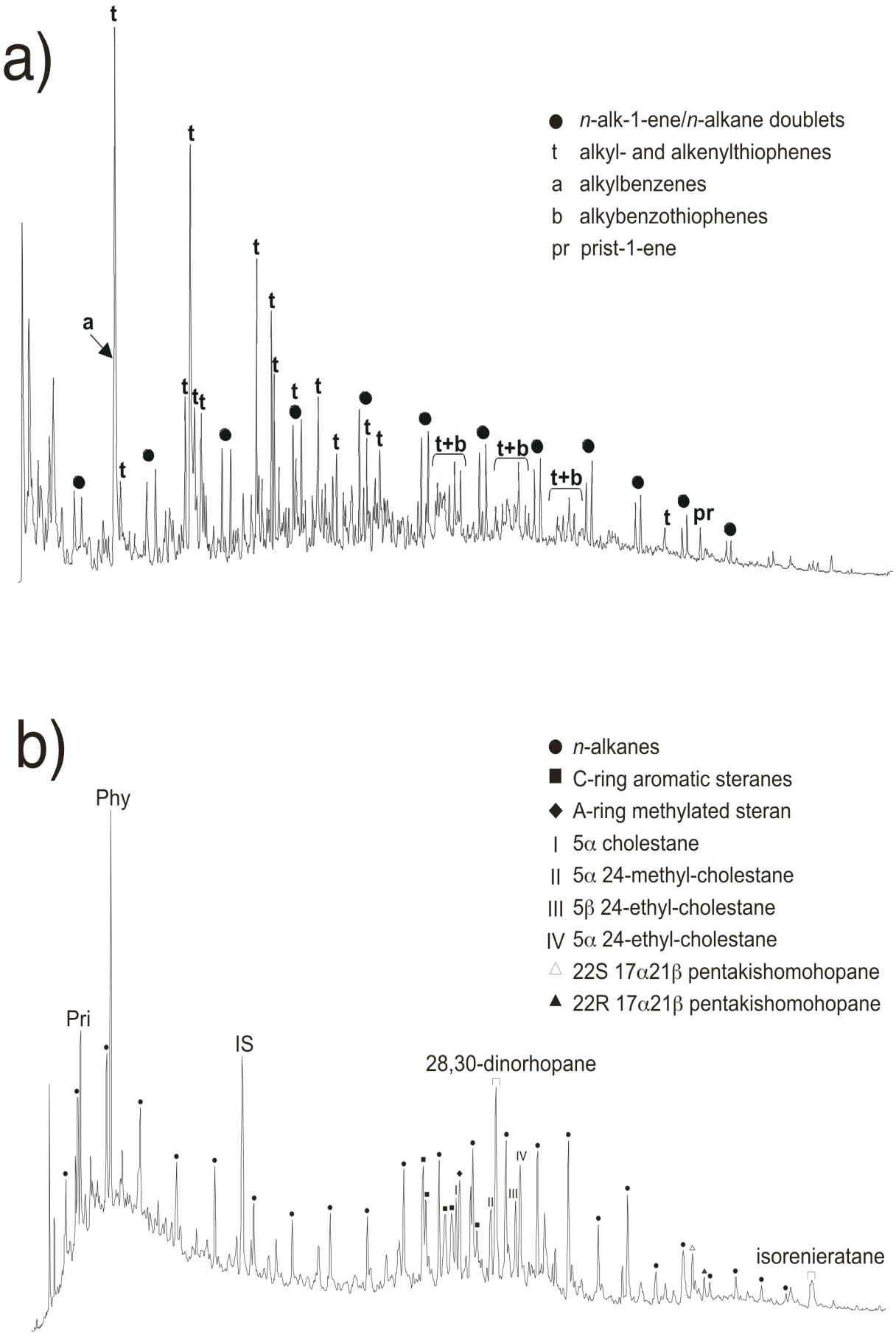

Figure 9. Typical reconstructed total mass chromatograms for (a) desulphurised apolar fraction from the Tarfaya Basin, and (b) flash pyrolysates of kerogen.

potentially form a substantial part of the sedimentary organic matter [*van Kaam-Peters et al.,* 1998]. This mechanism, in which sulphur cross-linked insoluble macromolecular networks of carbohydrate skeletons are formed, is proposed to be a widely occurring diagenetic process. *Stankiewicz et al*. [1996] demonstrated, after isolation by density gradient fractionation and subsequent flash pyrolysis, that the light-red AOM in the Monterey and Duwi Formations is especially enriched in organic sulphur compounds such as alkylthiophenes and thiophenes. Similar observations have been made on Kimmeridgian sediments from the Kimmeridge Clay Formation [*Boussafir et al.,* 1995b; *Lallier-Vergès et al*., 1997; *van Kaam-Peters et al*., 1998], the Orbagnoux Formation [*Mongenot et al.*, 1999] and the Kashpir oil shales [*Riboulleau et al*., 2000], indicating that early sulphurization processes are responsible for the formation of highly flourescent AOM.

It can be assumed that these mechanisms were also responsible for the morphological restructuring of primary marine biomass in the Tarfaya Basin. This assumption is supported by the observed predominance of alkylated thiophenes in the flash pyrolysates, suggesting that they are derived from a quantitatively significant part of the bulk OM. Alkylthiophenes originate from S-bound lipids [*Sinninghe Damsté et al*., 1989b] or carbohydrates [*Sinninghe Damsté et al.,* 1998; *Kok et al*., 2000].The orange AOM from the Kimmeridge Clay Formation is composed of both S-bound lipids and S-bound carbohydrates, of which the latter become increasingly abundant with increasing TOC [*van Kaam-Peters et al.*, 1998].

From the above, it can be assumed that the bituminite particles in the kerogen from the Tarfaya Basin are composed of S-bound lipids and probably also of S-bound carbohydrates. It has been shown that carbohydrate sulphurization may also significantly affect the timing of oil generation from source rocks [*Lewan*, 1998]. From a petroleum geochemical perspective, an early thermal breakdown of relatively weak C-S and S-S bonds would facilitate thermal degradation of the Tarfaya kerogen, thus generating oil at relatively low temperatures.

4.3.6. Relationships between palaeoenvironmental controls and early sulphurization of sedimentary organic matter

Prolific growth of sulphate-reducing bacteria occurs under anaerobic conditions in the water column or in sediment pore waters and in the presence of metabolizable OM, thus promoting the reduction of sulphate to sulphide [e.g. *Madigan et al*., 2000]. Major sinks for sulphide (H_2S or HS-) are the formation of iron-sulphides such as pyrite (e.g. Berner, 1984); and its re-oxidation to elemental sulphur, thiosulphate or sulphate [e.g. *Jørgensen*, 1988]. A proportion of the intermediate sulphur species may be recycled to hydrogen sulphide and sulphate via bacterial disproportionation [*Cypionka et al*., 1998; *Böttcher et al*., 2001]. Another important sink for reduced sulphur is its incorporation into OM [e.g. *Sinninghe Damsté et al*., 1989a,b; *Aizenshtat et al*., 1995; *Hartgers et al*., 1997; *Werne et al*., 2000; *Kok et al.*, 2000]. For the Tarfaya Basin black shales, the dominance of sulphur compounds in kerogen flash pyrolysates, and the fact that most biomarkers occur as S-bound forms, indicate that the OM is sulphurized to a high degree. This conclusion is in general also supported by organic petrological investigations which show variable amounts of unstructured and biodegraded OM. However, the observed differences in the abundance of bituminite particles in the kerogen suggest variable sulphurization intensities of the OM, which, in turn, are most probably related to changes in (palaeo)-environmental boundary conditions.

The occurrence of isorenieratane derivatives in the Tarfaya Basin Cenomanian-Turonian shales indicate that temporarily euxinic conditions occurred during sedimentation, with the presence of sulphide in the photic zone. It is therefore suggested that the degree of OM sulphurization was controlled by the supply of reactive iron, because iron availability is considerd to be a major factor controlling sulphur incorporation into OM [*Bein et al*., 1990; *Zaback and Pratt*, 1992]. Following this mechanism, excess iron results in greater scavenging by pyrite (Raiswell *et al*., 1988), whereas iron limitation results in a higher degree of natural sulphurization [*Hartgers et al*., 1997].

Iron availability at well S75 can be estimated from the Fe-S_{tot} relationship. As illustrated in Fig. 10, most of the recorded data (open circles) do not plot along the stoichiometric pyrite line (S_{tot}=1.15Fe), indicating that not all of the sulphur is fixed in pyrite; this is probably due to a lower flux ratio of reactive iron relative to reactive OM. Interestingly, however, some samples (filled circles) do plot along the pyrite line, which implies that essentially all the iron had been reduced and fixed in pyrite. Accordingly, for samples that plot on the pyrite line, iron availability was not limited during

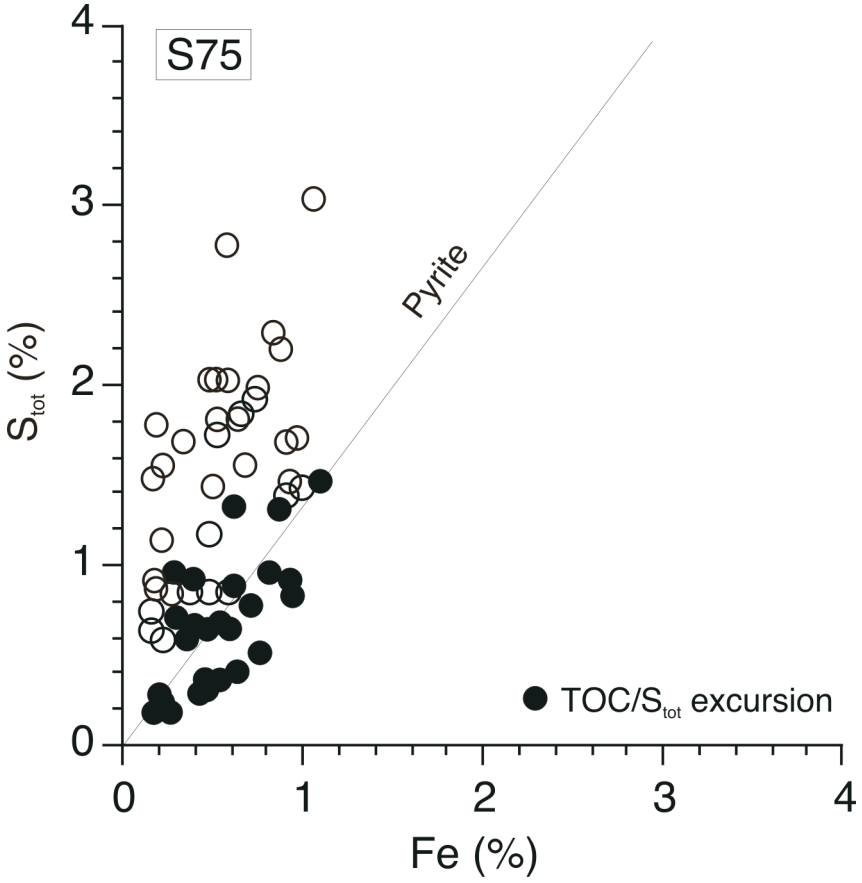

Figure 10. Plot of Fe% versus Stot% for well S75. The absence of a positive correlation suggests persistent iron limitation for the Tarfaya Basin during black shale deposition. Filled circles represent TOC/S_{tot} data points from the part of the *W. archaeocretacea* biozone with enhanced TOC/S_{tot} values.

sedimentation and the degree of natural sulphurization was therefore inhibited. This conclusion is also indicated by first total reduced inorganic sulphur values, which point to a higher proportion of sedimentary sulphides being trapped in pyrite, consequently leading to lower amounts of organicallybound sulphur being formed.

In a stratigraphic context, samples plotting along the pyrite line are derived from the lower to middle *W. archaeocretacea* biozone (62-82m below surface). In this stratigraphic interval, TOC/S_{tot} ratios are dramatically enhanced by a factor of about three compared to the over- and underlying sections, and coincide with the early Turonian sea-level transgression as proposed by *Hardenbol et al*. [1998]. To link the well-documented changes in the carbon-sulphur system in the Tarfaya Basin to fluctuations in the global sea-level, the following considerations can be made. A prominent eustatic sea-level rise in the early Turonian would probably have been accompanied by an inflow of nutrient-rich intermediate waters to the NW African continental shelf. These intermediate waters originated from deep basins in the southern North Atlantic, where extremely oxygendepleted to euxinic conditions have been proposed for the entire Cenomanian/Turonian water column [*Sinninghe Damsté and Köster*, 1998; *Kuypers et al*., 2002]. Mixing of these deep, anoxic waters with shallow-water masses from the African shelf was probably fostered by wind-induced upwelling processes, and could have resulted in (i) enhanced marine productivity across the shelf; and (ii) the establishment of persistent anoxic to severely dysoxic conditions, at least in the deeper parts of the continental shelf. The biomarker records from the Tarfaya Basin even support the temporary establishment of an entirely euxinic water body, from the sea floor to the photic zone.

These extreme conditions must have had a major impact on organic carbon burial during the lower *W. archaeocretacea* biozone, but probably also affected the organo-sulphur cycle and consequently the degree of OM sulphurization. Evidence in support of this conclusion is provided by preliminary

aluminium-normalized vanadium records from the examined sites, which reveal an average ten-fold enrichment of V/Al (up to 180mg/g), Mo/Al (up to 15mg/g) and Cr/Al (up to 54mg/g) ratios compared to the average shale composition after *Wedepohl* [1991], corroborating the progressive establishment of bottom-water euxinia during the lower *W. archaeocretacea* biozone.

This mechanism of sea-level driven changes in the development of bottom and photic zone euxinia is also supported by preliminary sulphur isotope measurements on sedimentary pyrite at site S75, which show $\delta^{34}S$ ratios between –10 and –20 ‰ vs. V-CDT. These variations document fluctuations in sulphur cycling and related overall isotope fractionation. The observed ten-permil shift at well S75 was probably controlled by the balance between total reduced inorganic sulphur and organic matter burial, and may thus indicate that a higher proportion of pyrite was formed following deposition. The sulphur isotope data further indicate sulphate reduction at intermediate cellular microbial sulfate reduction rates [*Chambers and Trudinger*, 1979], and may also include contributions from the oxidative part of the sulphur cycle. Because there is no significant isotope fractionation during the formation of iron sulphides from a sulphidic solution [*Böttcher et al*., 1998], the isotopic composition of pyrite in the Tarfaya Basin sediments reflects that of H_2S. Assuming a sulphur isotopic composition for seawater sulphate during the Cenomanian/Turonian of about +15‰ [*Strauss*, 1999], and that pyrite formed in the water column or close to the sediment-water interface (open system with respect to sulphate; [*Hartmann and Nielsen*, 1969]), overall sulphur isotope fractionation of at least -25 to -35‰ must have occurred in the Tarfaya Basin. This is within the range found in studies of cultured sulphate-reducing bacteria (Chambers and Trudinger, 1979), but is smaller than that found during formation of TOC-rich Pliocene sapropel in the deep Mediterranean [*Passier et al*., 1999a] or the modern Black Sea [*Ohmoto et al.* 1990; *Neretin et al*., 2001].

The stratigraphic trend of the sulphur isotope ratios show that pyrite is more negative (–15‰ to –20‰) within the interval of the TOC/S_{tot} excursion (i.e. in the upper *W. archaeocretacea* biozone) compared to the sections above where less negative sulphur isotopes of about -10‰ were determined. Asimilar trend has been found for sediments from well S13. We relate the most negative $\delta^{34}S$ values to a higher contribution from the oxidative part of the biogeochemical sulphur cycle, which, consistent with *Passier et al*. [1999b], may have been caused by more intense sulphur cycling within the TOC/S_{tot} excurison. More intense sulphur cycling implies enhanced reoxidation of hydrogen sulphide and formation of sulphur intermediates, followed by bacterial disproportionation with associated sulphur isotope fractionation [e.g. *Cypionka et al*., 1998; *Böttcher et al.,* 2001].

4.4. Conclusions

Large variations in bulk and molecular geochemical compositions in general reflect changes in the quantity and quality of organic matter. As indicated by organic petrological studies and Rock-Eval pyrolysis, black shales from the Tarfaya Basin consist dominantly of marine algal/bacterial organic matter. Kerogen is characterised by a brightly fluorescing groundmass with lamalginite and bituminite particles, indicating kerogen which would generate petroleum at low temperatures, similar to the kerogen from the Miocene Monterey Formation. These conclusions are supported by the results of total lipid and kerogen analyses, which consistently document an abundance of marine compared to terrestrial biomarkers and the minor occurrence of lignin pyrolysis products. The abundance of algal biomarkers such as cholestanes, 24-methyl-cholestanes and 24-ethyl-cholestanes relative to typical biomarkers from membrane lipids derived from cyanobacteria is evidence for an algal rather than a cyanobacterial source of OM. The presence of isorenieratane indicates temporary development of photic zone euxinia.

Biomarker and kerogen analyses show that the Tarfaya Basin black shales are rich in organic sulphur compounds, from which we infer that natural sulphurization played a key role in the formation of these hydrogen-rich source rocks. Additional inorganic geochemical data also indicate that sulphurization of organic matter occurred in response to the enhanced availability of metabolizable OM and limitation of iron. The observed variations in the degree of OM sulphurization most probably relate to changes in the depositional conditions, which could be due to the lower Turonian sea-level transgression. Accordingly, enhanced primary productivity resulting from the inflow of nutrient-rich waters led to ecological changes that temporarily influenced the boundary conditions for the carbon-sulphur cycle during the deposition of lower *W. archaeocretacea* biozone.

Acknowledgements

The authors are indebted to the management of ONAREP (Morocco) and Shell Oil (Netherlands) for providing the well materials. We are grateful to El Hassane Chellai (*University of Marakesh*) for assistance during fieldwork in the Tarfaya Basin. We thank Elisabeth Lallier-Vergès, Jim Amstrong and Harilaos Tsikos for constructive reviews of an earlier version of this manuscript. This project was supported by the Deutsche Forschungsgemeinschaft (grants *Wa 1036/6* and *Ku 649/9*). Tabulated data for this paper is available on the web under:
www.pangaea.dePangaVista2?query=kolonics&maxlat=&minlon=&maxlon=&minlat

Chapter 5

Uranium spectral gamma-ray response as a proxy for organic richness in black shales: applicability and limitations

Chapter 5.

Uranium spectral gamma-ray response as a proxy for organic richness in black shales: applicability and limitations

Authors*: Lüning, S. and S. Kolonic*

Status: published Journal: *Journal of Petroleum Geology, 26, 153-174, 2003.*

Abstract

In many organic-rich, low-carbonate hemipelagic shales, there is a stable and close correlation between the uranium and TOC contents. In this paper, we present a number of case studies using our own data and that from previous publications to investigate black shales with (1) good, (2) fair-to-good and (3) poor U-TOC correlations. U-TOC ratios in the different black shale units are compared to each other, and possible reasons for the observed variations are discussed.

In general, the U-TOC ratio in a black shale is controlled by a number of factors which include for example the primary uranium content of the water body, the carbonate content and the sedimentation rate. The development of a stable U-TOC ratio may be inhibited by the presence of phosphate, by a high carbonate or sand content, by dissolution ("burn-down") of uranium during intermittent oxic periods, and by large-scale diagenetic remobilisation of uranium. In suitable black shale systems, vertical variations in organic richness can be approximated by measuring the uranium content using spectral gammaray measurements. This may be especially important in outcrop studies because gammaray logging is a straightforward field technique. Before the uranium content can be used as a proxy for TOC content in a black shale system, however, a thorough calibration of uranium and TOC is necessary, in order to determine the stratigraphic and regional limits of the derived U-TOC ratios and to establish the presence of a stable U-TOC correlation.

5.1. Introduction

Many hydrocarbon source rocks are enriched in authigenic uranium which precipitates at the sediment-water interface under anoxic conditions and accumulates together with organic matter (OM) [e.g. *Schmoker*, 1981; *Meyer and Nederlof*, 1984; *Zelt*, 1985; *Mann et al.,* 1986; *Wignall and Myers*, 1988; *Stocks and Lawrence*, 1990]. Precipitation is triggered by the reduction of the soluble U^{6+} ion in seawater to insoluble U^{4+}. In some black shale systems, a linear relationship between concentrations of TOC and uranium has been reported [e.g. *Bell et al.,* 1940; *Zelt*, 1985], and uranium can therefore here be used as a proxy to predict the TOC content. In these black shales, time-consuming organic geochemical analyses can be replaced by more simple, non-destructive measurement of uranium content using gamma-ray spectrometry, both in wells and at outcrops. This technique had been developed and tested as long ago as the 1940s by several different research groups ([e.g. *Bell et al.,* 1940; *Russell*, 1945]; see *Zelt,* 1985 for an historical overview), and was registered as a US patent by *Supernaw et al.* [1978]. It allows verticallycontinuous logs of organic richness easily to be produced, for example for regional petroleum source rock evaluations and palaeoecological studies [*Fertl and Rieke*, 1980; *Herron*, 1991]. Gamma-ray based isopach mapping of source rocks was conducted by *Schmoker* [1980, 1981], who studied Upper Devonian "hot shales" in the Appalachian Basin; and by *Lüning et al.* [2000; *in press* b] who studied Silurian and Upper Devonian black shales in North Africa.

Where a U/TOC relationship is established, however, it must always be locally calibrated. Also it must be restricted to a geologically uniform environment, because the U/TOC ratio can vary in black shale systems of different ages and in different regions [*Schmoker*, 1980, 1981; *Mendelson and Toksöz*, 1985; *Mann et al.,* 1986; *Herron*, 1991).

The development of a stable U/TOC ratio depends on a number of factors [e.g. *Russel*, 1945; *Myers and Wignall*, 1987; 1988; *Klinkhammer and Palmer*, 1991; *Herron*, 1991; *Van der Weijden et al.,* 1993; *Wignall*, 1994], of which the most important are:

1. The primary concentrations of uranium and OM in the water body;
2. The lithological composition of the sediments (e.g. whether shale or carbonatedominated);
3. The availability and concentration of a sorbent (OM, phosphate), and the type of OM;
4. The sedimentation rate and duration of anoxia;
5. The position of the redox boundary relative to the sediment-water interface; and
6. The degree of thermal maturation.

In this paper, we aim to give an overview of the U/TOC proxy technique and present examples of black shale systems in which the uranium content can easily be used to approximate the TOC. Most of these examples come from Europe and North Africa (Fig. 1). We also discuss black shale systems in which there are fair-to-good and poor correlations between uranium and TOC contents. We attempt to identify depositional environmental, stratigraphic and other parameters controlling black shale systems which are conducive to the development of a close and stable correlation between uranium and TOC.

5.2. Uranium in organic-rich shales and its spectral gamma-ray signature

The uranium content in shales consists of detrital and authigenic components. The "average non-bituminous shale" *sensu Taylor* [1965] and *Wedepohl* [1991] contains about 4 ppm U, which is largely of detrital origin. However, significant variations exist depending on the detrital source material. For example, Silurian and Upper Devonian organicallylean shales from North Africa on average contain 4 ppm U (Fig. 2C), whereas Cretaceous black shales from the same region generally contain less than half this concentration.

Reduction and precipitation of authigenic uranium is an important mechanism in many oxygen-deficient systems and can lead to an increase in the total uranium content of the sediment which may therefore exceed by many times the detrital uranium component [e.g. *Schmoker*, 1981; *Meyer and Nederlof*, 1984; *Mann et al.,* 1986; *Wignall and Myers*, 1988; *Stocks and Lawrence*, 1990]. A gamma-ray spectrometer can be used to measure the abundance of uranium; together with the mostly detrital

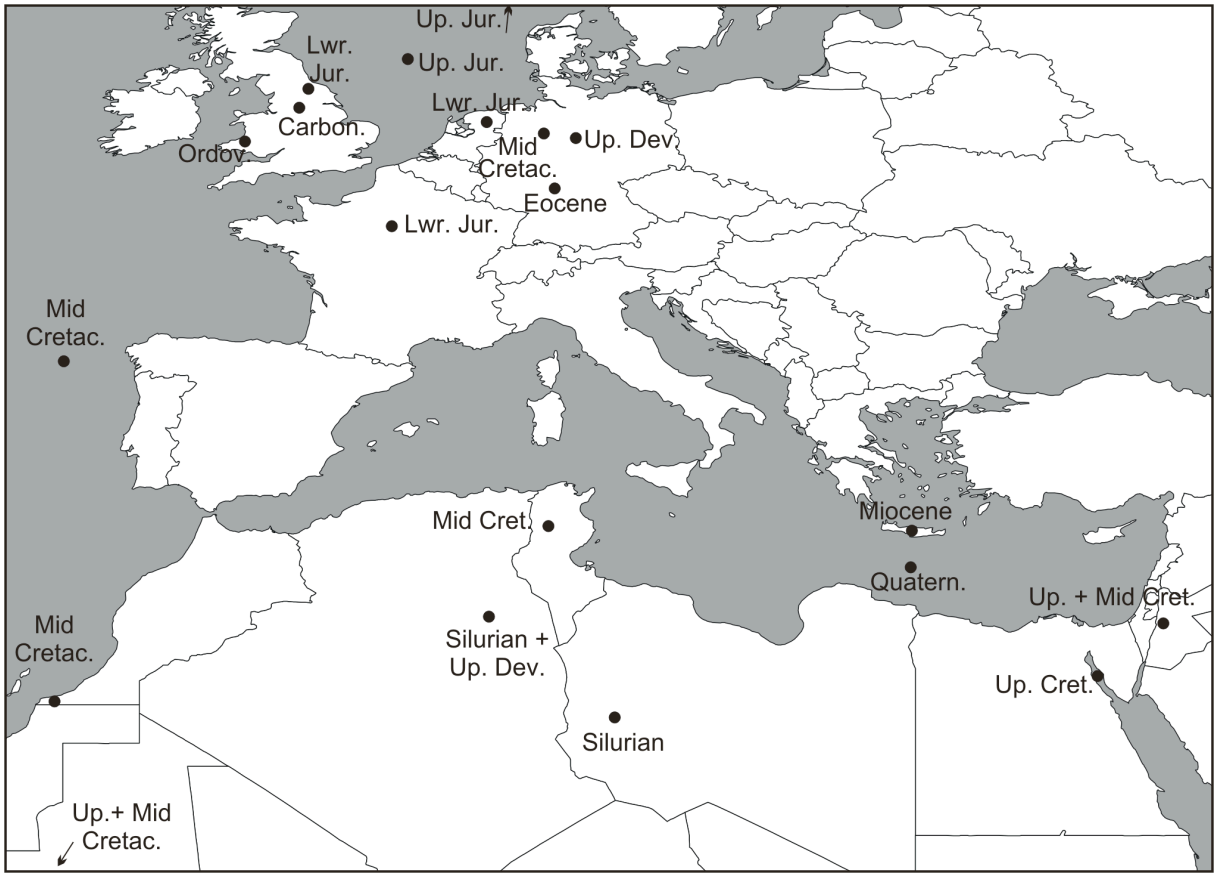

Figure 1. Map showing the location of the European and North African black shale successions referred to in this paper. Additional examples (not illustrated) are taken from North America and Australia.

potassium and thorium, this produces the bulk of the natural radioactivity, and hence gamma radiation, in rocks [*Dypvik and Eriksen*, 1983].

A formula for the calculation of the authigenic uranium content in marine mudrocks from spectral gamma-ray data was introduced by *Wignall* [1994] and takes the form $U_{authigenic}=U_{total}$ - Th/3 (example in Fig. 5E), where Th/3 approximates the detrital U component. Calculation of $U_{authigenic}$ using this formula is most useful in shale successions with variable carbonate contents, which therefore have variable detrital uranium contents. These calculations are less important in pure shale successions with fairly stable detrital compositions.

Due to the high gamma-ray signatures of uranium-enriched black shales, they are often referred to informally as “hot shales”. Typical examples are the Late Jurassic Kimmeridge Clay Formation of the North Sea ([*Zimmerle*, 1995], p. 117; Glennie (Eds.), 1998, p. 437), and the Upper Devonian and Lower Silurian of Central North Africa [*Lüning et al.,* 2000; *in press* b].

5.3. Methods

The data in this paper come from previous publications by the authors [*Lüning et al.*, 2000; *in press* a,b] and other researchers, to which is added new data from the Cenomanian-Turonian oil shales of the Tarfaya Basin in South Morocco (Fig. 1). For the latter, spectral gamma-ray measurements were carried out in the field using a gamma-ray spectrometer (model *GRS 2000*, manufactured by Geofyzika, Brno, Czech Republic). A standard duration of 3 minutes was selected for each measurement, with a spacing between measured points of 10 cm. Natural radioactivity in rocks originates mostly from uranium, potassium and thorium. The spectrometer differentiates between these elements by identifying typical peaks in the gamma-ray energy spectrum.

Geochemical analyses of fresh samples from the coastal Ama Fatma outcrop section (Tarfaya Basin) were carried out at the University of Bremen. The samples were pulverised in an agate mortar.

Organic and inorganic carbon contents were measured using a *LECO CS-300* Carbon-Sulphur analyser (precision of measurements ±3%). For TOC determination, inorganic carbon was carefully removed by repetitive addition of 0.25 N HCl. Calcium carbonate (CaCO3) contents were calculated using the relationship $CaCO_3 = (C_{inorg}-C_{org})$ x 8.33. For total digestion analyses, samples of about 50mg were digested in a mixture of 3ml HNO3 (65%), 2ml HF (40%) and 2 ml HCL (36%) of supra-pure quality at 200°C and 30 kbar in closed Teflon vessels [*Heinrichs et al*., 1986]. After drying by evaporation, the residue was re-dissolved with 0.5ml HNO3 (65%) and 4.5ml deionised water. Resulting solutions were analysed by inductivity-coupled plasma-atomic emission spectrometry (ICP-AES) and inductivity-coupled plasma-mass spectrometry (ICP-MS), respectively. The results were checked with international standard reference materials; relative standard deviations in duplicate measurements are below 3%.

Note that the U^{238} and K values derived from ICP-MS refer to discrete horizons of 1 cm thickness, in contrast to the U and K values derived from spectral gamma-ray logging which are averaged over a 30 cm thick interval. U/TOC ratio data-points illustrated in this paper are either taken directly from the literature or were generated by reading the data pairs from published and unpublished well logs and databases (including interpolation between available TOC data points, if necessary). TOC values used are not averaged but refer to individual measurements. Naturally, ratios derived from smoothed log curves should show less variation then ratios of the same section derived from raw data.

Quality ranking of U/TOC correlations into “good”, “fair-to-good” and “poor” is based on qualitative observations only. This is due to the relative heterogeneity of the underlying data used, so that statistical correlation coefficients are not available for all datasets.

5.4. Black shales with good Uranium-TOC correlations

5.4.1 Lower Silurian of North Africa/Arabia

Silurian and Upper Devonian marine black shales are believed to represent the source rocks for almost all the Palaeozoic-sourced hydrocarbons in North Africa [*Boote et al.,* 1998]. Silurian organic-rich “hot” shales in Algeria, Tunisia and Libya are characterised by high gamma-ray responses of up to 700 API, originating almost entirely from uranium (Fig. 2B) [*Lüning et al.,* 2000, *in press* a]. They contain little carbonate (0.5-7%). In general, the gamma-ray intensity in these shales can be used as a proxy for the organic richness, and 200 API corresponds approximately to 3% TOC for shales just above and within the oil window (Fig. 2A) [*Lüning et al.,* 2000]. As of yet, no combined U/TOC dataset is available for this unit.

5.4.2. Upper Devonian (Frasnian) of Algeria

The TOC trends in the Frasnian “hot shales” of Central North Africa can also be approximated using the shales’ natural radioactivity (Fig. 2C), so that source rock isopach maps can be generated based on total-gamma-ray well logs (Lüning *et al., in press* b). In common with the Silurian black shales in North Africa, the gamma-ray response of the Frasnian hot shales is dominated by U-radiation (Fig. 2C). These shales generally contain little carbonate, although carbonate concretions and nodules are commonly intercalated in the shale succession. The U/TOC ratio is comparatively high and measures 3 ppm U / %TOC (Fig. 5A,L). The U/TOC ratio for the Silurian “hot shales” here may be even higher than this, because in the Frasnian interval 3% TOC corresponds to a gamma-ray reading of only 150 API, compared to 200 API in the Silurian [*Lüning et al.,* 2000; *Lüning et al., in press* b].

5.4.3. Upper Devonian of North America

Marine, organic-rich shales are common in parts of the Appalachian Basin and locally source a number of gasfields [*Schmoker*, 1980, 1981]. The spectral gamma-ray signatures of Upper Devonian black shales in North America generally closely match those in North Africa, with most of the positive total gamma-ray excursions in the shales attributable to increased amounts of uranium (Fig. 2D).

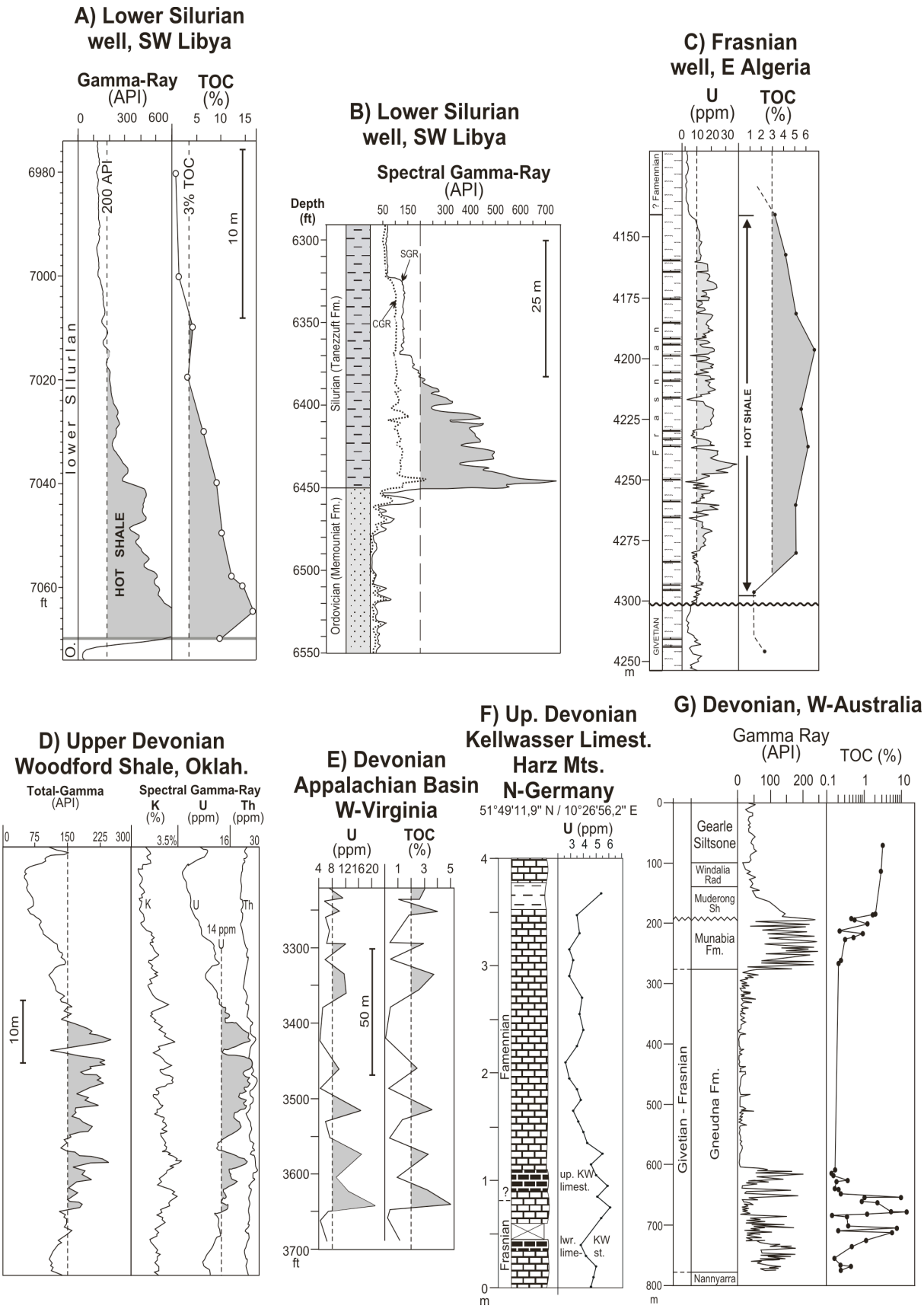

Figure 2. Correlation of total gamma-ray (GR), spectral GR, uranium content and TOC content in Palaeozoic marine black shales. Good GR-U correlations exist in the Lower Silurian and Upper Devonian (Frasnian) of North Africa, while correlations in the Devonian examples from Germany and Australia are less reliable (*see text*). Origin of data: A,F. authors' own data; B. *Lüning et al.* [in press a]; C. *Lüning et al.* [in press b]; D. *Fertl and Chilingarian* [1990]; E. *Fertl and Riek*, [1980]; *G. Ghori* [1999].

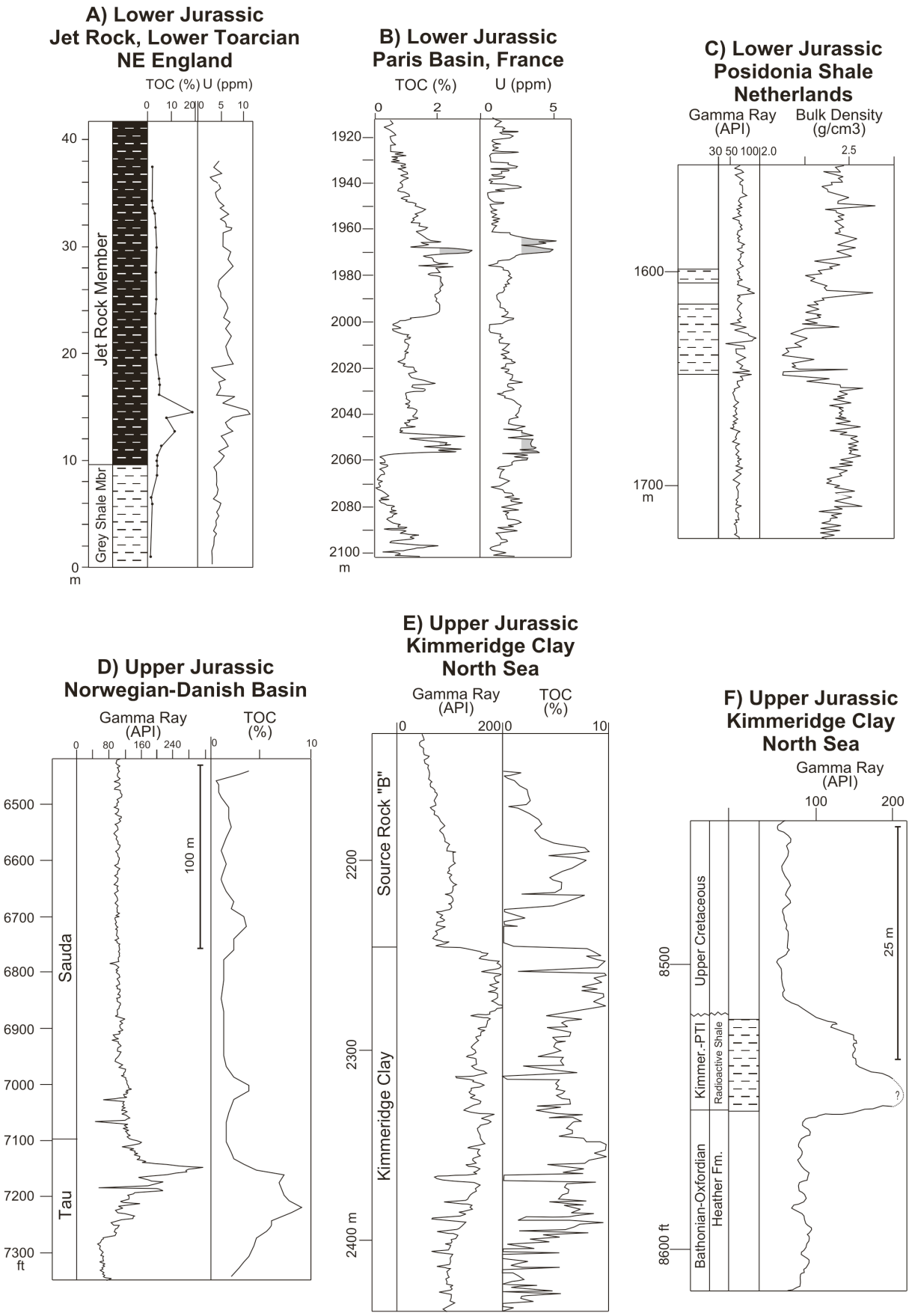

Figure 3. Correlation of total GR, spectral GR, uranium content and TOC content in European Jurassic marine black shales. In many cases, a fair to good GR-U correlation can exists on a large scale while the correlation is often poor on a smaller scale. Origin of data: A. *Myers and Wignall* [1987]; B. *Bessereau et al.* [1995]; C,F. *Meyer and Nederlof* [1984]; D. *Stocks and Lawrence* [1990]; E. *Creaney and Passey* [1993].

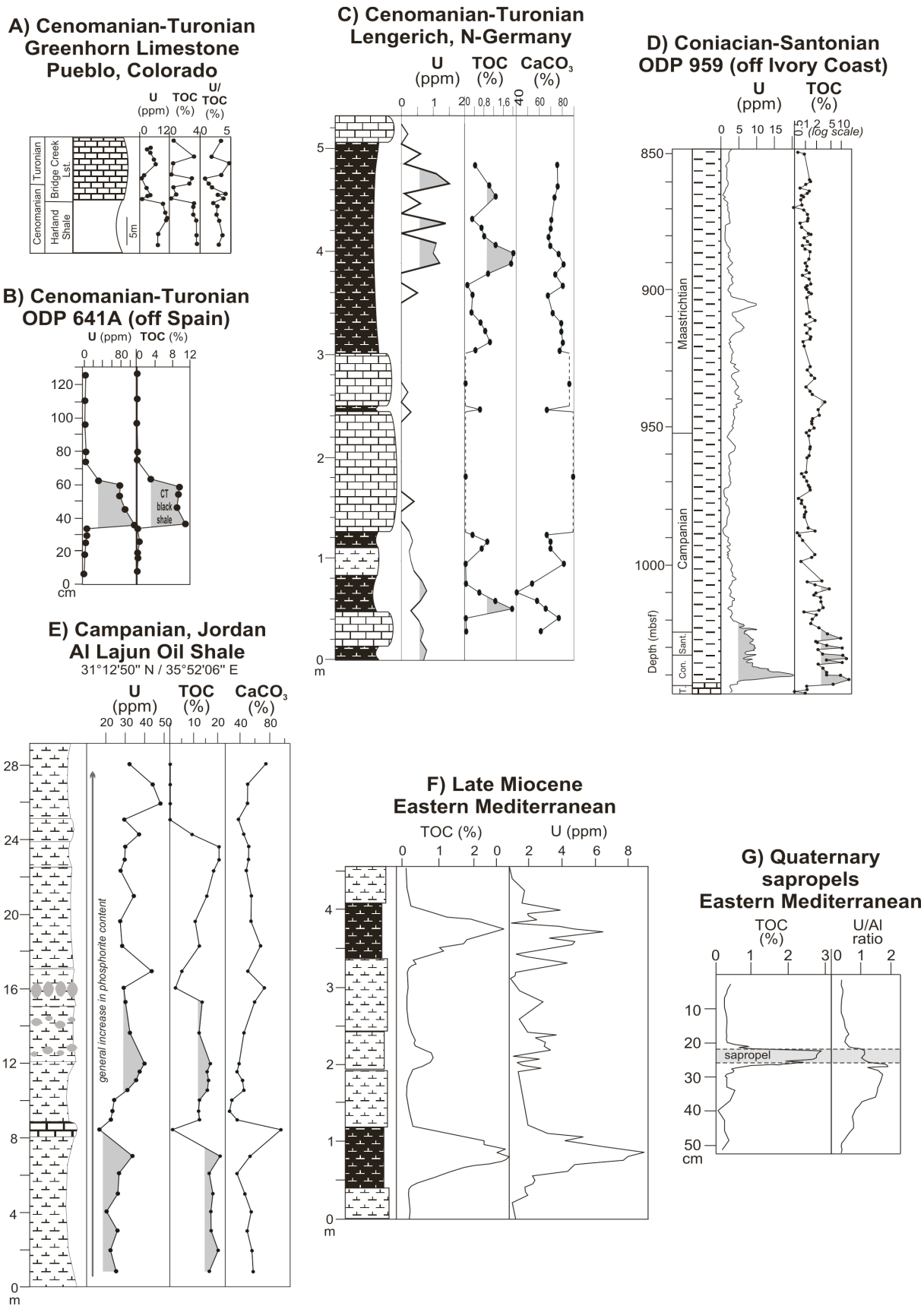

Figure 4. Correlation of total GR, spectral GR, uranium content and TOC content in Cretaceous and Cenozoic marine black shales. Note the good GR-U correlation in the two Cretaceous ODP wells (B, D). See text for detailed discussion. Origin of data: A. *Zelt* [1985]; B. *Thurow et al.* [1988]; C,E. authors' own d ata; D. *Wagner and Pletsch* [1999] and ODP data repository; F. *Ten Veen and Postma* [1996]; G. *Thomson et al.* [1995].

The unit's gamma-ray and organic contents were studied by *Schmoker* [1980, 1981] who found that U/TOC ratios are laterally variable (TOC varies by a few % over a few 100s km) and that careful calibration was necessary to reconstruct organic-richness from gamma-ray logs in different parts of the basin. The U/TOC ratio is generally high, measuring around 5 ppm U / %TOC (Fig. 5L) ([*Fertl and Rieke*, 1980]: their fig. 14; [*Mendelson and Toksöz*, 1985]: their fig. 4). A similarly good correlation between TOC and gamma-ray was also reported from Frasnian basinal shales in the Alberta Basin in Western Canada [*van Buchem et al.*, 2000].

5.4.4. Upper Carboniferous of England

Upper Carboniferous black shales termed "marine bands" occur in northern England and were deposited during transgressive pulses within a deltaic succession [*Maynard et al.*; 1991, *Fisher and Wignall*, 2001). These black shales contain up to 200 ppm U, generally with a good U/TOC correlation (Fig. 5K) [*Fisher and Wignall*, 2001]. These authors found that enriched uranium values were only encountered under specific depositional conditions of low but fluctuating oxygen regime and extremely slow sedimentation rates. Interestingly, truly euxinic facies did not contain high concentrations of U. The U/TOC ratio in this succession is high, averaging 3 ppm U / %TOC.

5.4.5. Upper Cretaceous of the eastern Atlantic margin

A deeper-shelf to bathyal Coniacian-Santonian black shale succession with TOC values of up to 15% occurs in offshore West Africa (Fig. 4D), and was drilled in ODP Site *959*. The anoxia represented by these black shales corresponds to Oceanic Anoxic Event III [*Schlanger and Jenkyns*, 1976]. Uranium and TOC distribution curves correlate well ([*Wagner and Pletsch* 1999; *Mascle et al.,* 1996]; ODP online logging data at *http:// www.ldeo.columbia.edu/ BRG/ODP*). The carbonate content is moderate and up to 15%. The U/TOC ratio is rather low and averages about 0.8 ppm U / %TOC.

5.4.6. Neogene and Quaternary sapropels of the Eastern Mediterranean

Organic-rich deep-marine sediments of Neogene and Quaternary age, known as sapropels, occur widely in the Eastern Mediterranean. They are composed of rhythmically interbedded dark-brown, organic-rich laminites and grey-blue, bioturbated and homogenised marl beds [e.g. *Postma and ten Veen*, 1999]. Reducing conditions at the sea floor were due to low deep-water oxygen levels or high Corg fluxes, in particular during glacial events [e.g. *Mangini et al.,* 2001]. The uranium content in the organic-rich layers reaches up to 50 ppm [*Mangini and Dominik*, 1979; *Mangini et al.,* 2001]. In an Eastern Mediterranean Miocene sapropel succession described by ten Veen and Postma (1996), the U and TOC curves match well (Fig. 4F). Here, the U/TOC ratio averages 1.3 ppm U / %TOC (Fig. 5I) which is intermediate compared to other black shale successions.

Some of these Neogene-Quaternary Eastern Mediterranean sapropels have undergone significant diagenetic alteration which may have modified the original U/TOC relationship. During better ventilated phases partial to full oxidation of the OM in the sapropels occurred. OM and uranium underwent migration or release to solution processes resulting from the oxidation of the uranium from the insoluble U^{4+} ion to soluble U^{6+}, if the sapropel was effected by the downward-moving oxidation "burn-down" front [*Thomson et al.,* 1995; *Mangini et al.,* 2001]. The burn-down depth usually extends less than a few tens of cm below the sediment surface, and depends on the sedimentation rate and the organic richness of the sapropel [*Mangini et al.,* 2001]. With low sedimentation rates and thin sapropels, the uranium originally present may completely disappear under subsequent oxic conditions [*Mangini et al.,* 2001]. Downward remobilisation of uranium from sapropels during betteroxygenated phases is assumed to have occurred in the Eastern Mediterranean, and to be responsible for the formation of a "secondary" U peak below the sapropel, resulting in a poor correlation between Corg and uranium (Fig. 4G) [*Thomson et al.,* 1995].

5.5. Black shales with fair-to-good Uranium-TOC correlations

5.5.1. Neogene and Quaternary sapropels of the Eastern Mediterranean

The Lower Jurassic (Liassic) in various parts of Western Europe is represented by black shales which were deposited in epicontinental seas and whose organic richness can exceed 20% TOC. The quality of the U/TOC relationship varies greatly across the region, ranging from good to poor.

A good U/TOC correlation was recorded for the Posidonienschiefer in a well in the Hils area of northern Germany, where uranium concentrations of up to 12 ppm were observed (Fig. 5B) [*Mann et al.,* 1986]. Poorer U/TOC correlations occurred in fractured horizons, either because of secondary fracture-related uranium enrichement or due to problems with uranium spectral measurements [*Mann et al.,* 1986]. Similarly good to moderate U/TOC correlations were also reported from the Liassic of NE England by *Myers and Wignall* [1987] (Figs. 3A, 5D) and *van Buchem et al.* [1992]. In these examples the U/TOC ratios are low with 0.4-0.6 ppm / %TOC.

In the Paris Basin, the Liassic is represented by mixed shales and carbonates [*Herron and Le Tendre*, 1990; *Bessereau et al.,* 1995]. The organic-rich intervals coincide with mildly elevated uranium contents: maximum TOC is only 3% and the uranium concentrationonly reaches 3 ppm (Fig. 3B). The U/TOC ratio appears to be only slightly higher than that of the Liassic black shales in Germany and England (~1 ppm U/%TOC) (Fig. 5C).

In other parts of Western Europe, however, the U/TOC ratio of Liassic shales is less well developed. In the subsurface in the Netherlands, for example, the bituminous Posidonienschiefer is not correlated with any significant increase in gamma-ray activity ([*Meyer and Nederloff*, 1984], their Fig. 9). A poor and even partly inverse correlation between U and TOC contents has been reported for the Posidonienschiefer of Dotternhausen in southern Germany [*Junghans et al*., in press]. Here, phosphatic fishbones with an associated increase in uranium may have caused some interference.

5.5.2. Upper Jurassic of England and France

The Upper Jurassic Kimmeridge Clay Formation (and equivalents) is the most important source rock in the North Sea [Glennie (Ed.), 1998]. The shale is characterised by gammaray intensities often exceeding 200 API and is therefore informally referred to as a "Radioactive" or "Hot Shale" [*Stocks and Lawrence*, 1990; *Meyer and Nederlof*, 1984] (Figs. 3D, E, F). While large-scale TOC trends in the Kimmeridge Clay are generally well reflected in the total gamma-ray curves (and therefore most probably in the uranium spectral gamma-ray curves), at a smaller-scale the U/TOC correlation turns out to be rather poor (Fig. 3E) [*Myers and Wignall*, 1987; *Creaney and Passey*, 1993; *van Buchem et al.,* 1995].

5.5.3. Cenomanian-Turonian (Upper Cretaceous)

Organic-rich strata deposited during the "Cenomanian-Turonian Oceanic Anoxic Event" occur in many localities and range from deep-sea to shallow-marine deposits. In the Atlantic, the unit reaches TOC values of 10% (ODP *641A*) and 35% (DSDP *367*), respectively. It is strongly enriched in uranium and other trace metals (Fig. 4B) [*Thurow et al.,* 1988; *Arthur et al.,* 1990]. The U/TOC ratios are highly variable and range from high to intermediate; thus, the ratio averages 10 ppm U / %TOC at ODP *641A*, and 1.4 ppm U / %TOC at DSDP *367* (Fig. 5J) [Arthur *et al.,* 1990].

High-resolution spectral gamma-ray and geochemical studies of outcropping lowermost Turonian black marls at Ama Fatma in the Tarfaya Basin (South Morocco) have been carried out by the authors. This basin hosts one of the largest oil-shale deposits in NW Africa [*Leine*, 1986; *Kolonic et al.*, 2002]. The Ama Fatma section is composed of a cyclical succession of limestones and organic-rich marls with TOCs of up to 10%. The uranium content is relatively low, with a maximum of 8 ppm. Most of this uranium is thought to be authigenic, because the shales' low Th and K values (Fig. 6) and high carbonate content (45-75% in the marls) suggest that the detrital uranium component is likely to be low [see *Myers and Wignall*, 1987]. The U/TOC ratio is very low, averaging 0.25 ppm U / %TOC. The absence of major uranium enrichment in this unit is also apparent in the subsurface gamma-ray logs published by *Leine* [1986], which show that maximum values do not exceed 170 API and average values are only around 90 API. The largest part of the total gamma-ray signal originates from uranium radiation, as indicated by the cross-plot in Fig. 7A.

Despite the low total uranium content in this unit, larger-scale TOC trends are well reflected by the total gamma-ray and uranium spectral gamma-ray signatures and by the U^{238} content, as well as by the

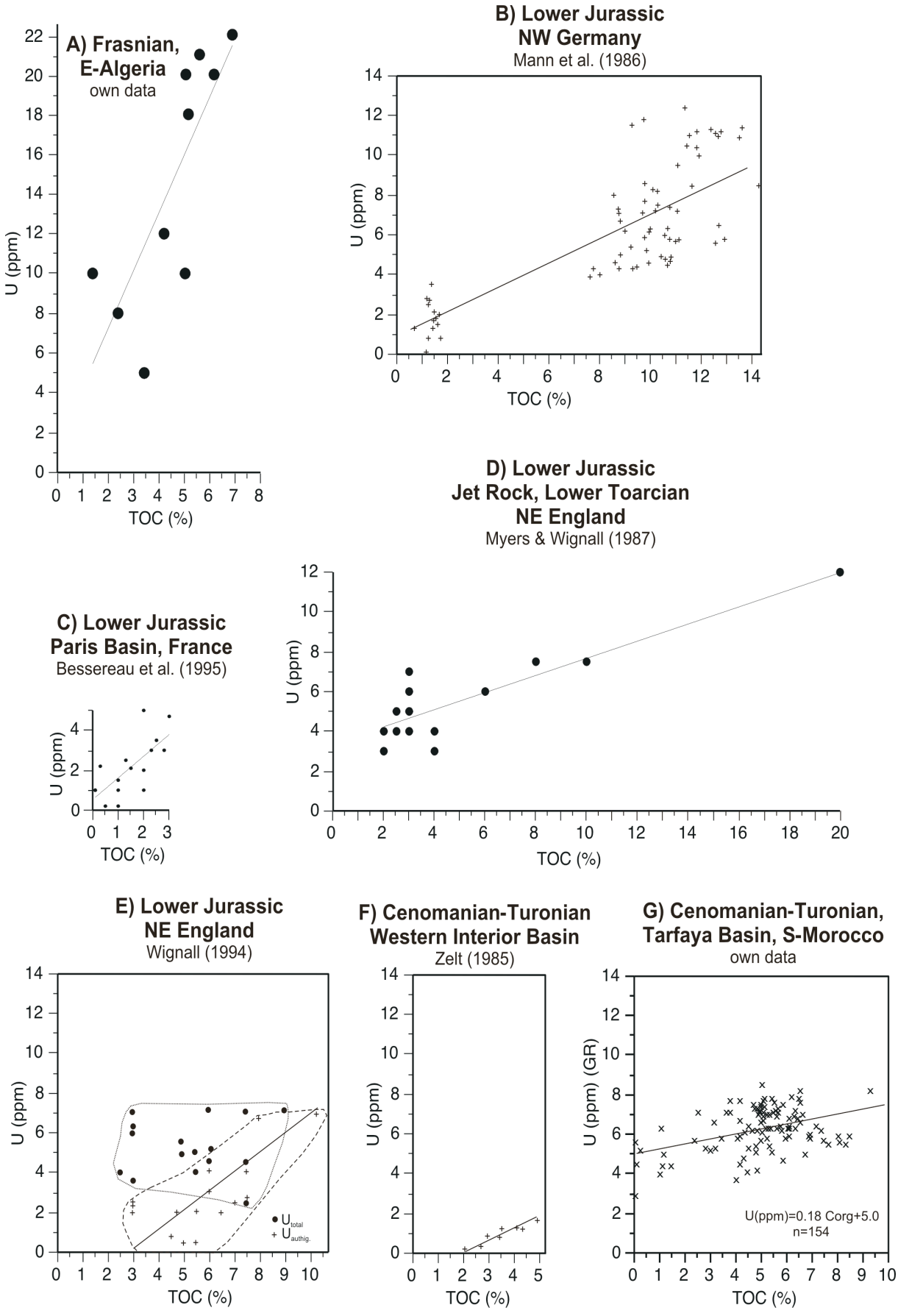

Figure 5. U/TOC cross-plots of selected marine black shales. Figs A-I and J,K have the same scales. A summary of all the regression lines is shown in L. Lettering in (L) refers to examples in Fig. 5A-K; regression lines *m* and *n* in (L) are after *Mendelson and Toksöz* [1985].

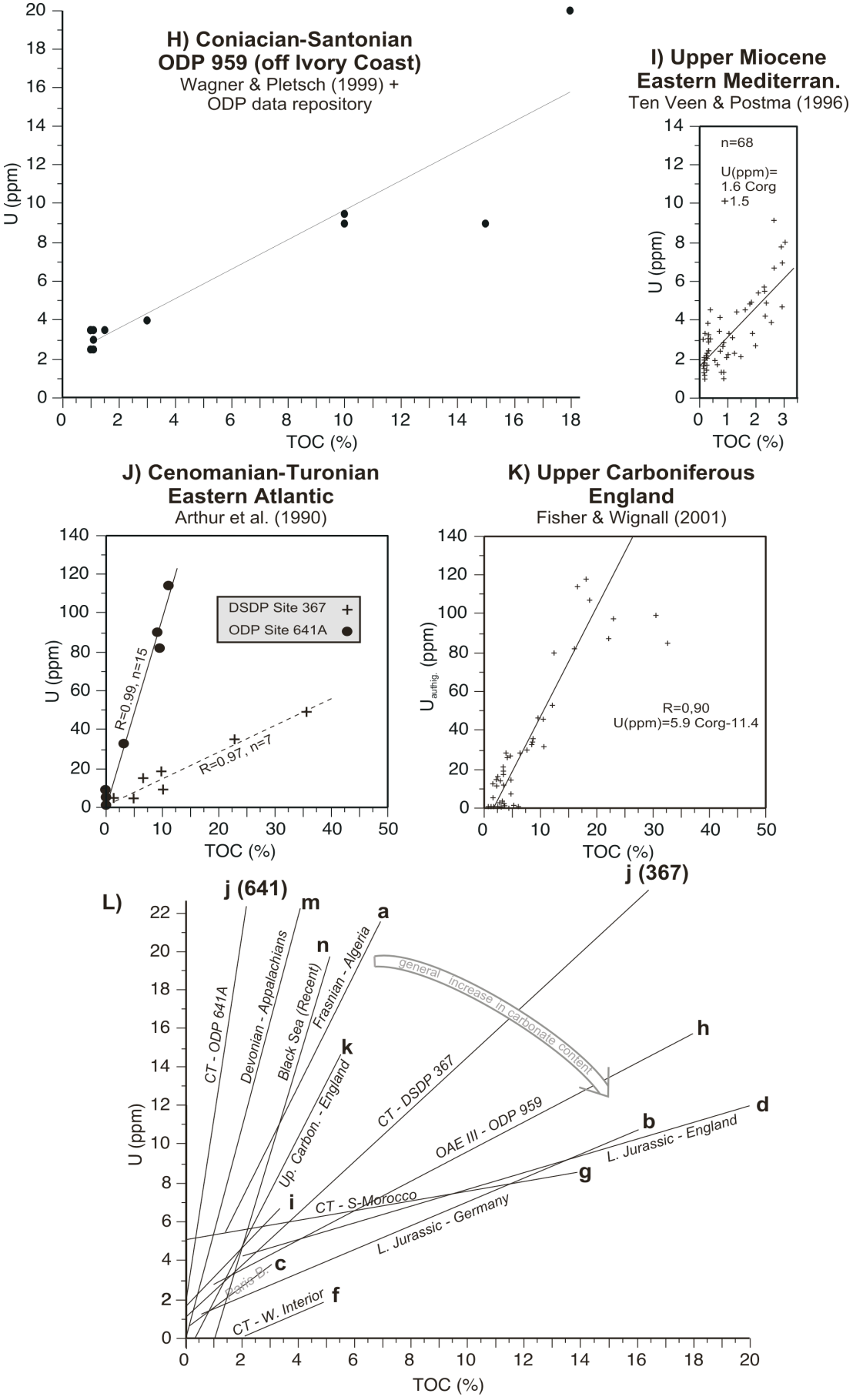

Figure 5. U/TOC cross-plots of selected marine black shales *(contninued).*

concentrations of Ni and other trace elements (trace elements were measured by ICP-MS) (Figs. 6, 7B,D). On a smaller scale, the U^{238} content and the uranium measured by gamma-ray spectrometry may serve as acceptable proxies for the TOC content (Figs. 6, 7B). However, the spectral gamma-ray responses cannot match the precision of the ICP-MS data because gamma-ray data-points were averaged over roughly 30cm thick intervals while the ICP and TOC data refer to more precisely-defined (sub-cm thick) intervals. Consequently, the high-frequency variations in organic richness which were found to be present in the lowermost Turonian Ama Fatma Formation (Fig. 6) cannot be resolved by the spectral gamma-ray technique, but can be using ICP-MS U data (Fig. 7C).

Organic-rich carbonates of similar age in Oman were recently studied by van *Buchem et al*. [2002]. As in the Moroccan example, the large-scale TOC cycles correlate well with the total gamma-ray curve. However, gamma-ray values do not exceed 80 API, even in the organically richest part of the succession (14% TOC) and the U/TOC ratio should therefore be very low.

Cenomanian-Turonian shales in the US Western Interior Basin with TOCs of up to 5% were investigated by *Zelt* [1985] for their spectral gamma-ray response (Fig. 4A). The U/ TOC correlations were fair to good. The U/TOC ratio in one example published by *Zelt* [1985] was low, averaging 0.7 ppm U / %TOC (Fig. 5F).

5.5.4. Campanian (Upper Cretaceous)

The Campanian "Brown Limestone" in the Gulf of Suez contains up to 3% TOC and is marked by strong, uranium-related gamma radiation which in well logs often coincides with a characteristic resistivity peak [*Mostafa,* 1992; *Shahin et al.,* 1999]. Part of this uranium enrichment may, however, be related to the presence of a phosphoritic content, which increases in age-equivalent phosphorites in neighbouring areas. The stability of the U/TOC relationship may suffer from this interference.

5.6. Black shales with poor Uranium-TOC correlations

5.6.1. Ordovician, Welsh Basin

Middle Ordovician black shales in the Welsh Basin contain up to 6 ppm uranium. *Lev et al.* [2000] showed that major late diagenetic redistribution of uranium has taken place in this black shale system, leading to a loss or enrichment of up to 95% of the uranium originally present. In this case, uranium obviously cannot be used as a proxy for TOC [*Lev et al.,* 2000].

5.6.2. Devonian of Germany and Australia

Organically enriched black limestones of latest Frasnian/earliest Famennian age — the so-called Kellwasser Limestones [e.g. *McGhee*, 1996] — were investigated for their spectral gamma-ray response at their type locality in the Harz Mountains (Germany) by the authors (Fig. 2F). The TOC content in this unit ranges between 0.4-1.0% ([*Buggisch*, 1972], p. 34; [*Schindler*, 1990], p. 24), while the over- and underlying grey cephalopod limestones typically contain only 0.05% TOC ([*Schindler*, 1990], p. 24). The upper Kellwasser Limestone is characterized by slightly increased uranium concentrations (by 1-2 ppm), although the uranium peak is rather broad and extends for several tens of cm into the under- and overlying organically-lean limestones (Fig. 2F). Significantly, no uranium peak is developed in the lower Kellwasser Limestone. Note that this unit underwent low-grade metamorphism [*Buggisch*, 1972, 1991] which may have altered the original uranium content; however, this may not necessarily be the case for metamorphic grades up to amphibolite facies [*Dostal and Capedri*, 1978].

From Western Australia, *Ghori* [1999] published the log characteristics of shallowmarine carbonates and fine-grained siliciclastics of Givetian-Frasnian age. Although the organic-rich facies as a whole is marked by increased gamma-ray values, no clear U-TOC correlation appears to exist (Fig. 2G).

5.6.3. Cretaceous of Jordan, Tunisia and Germany

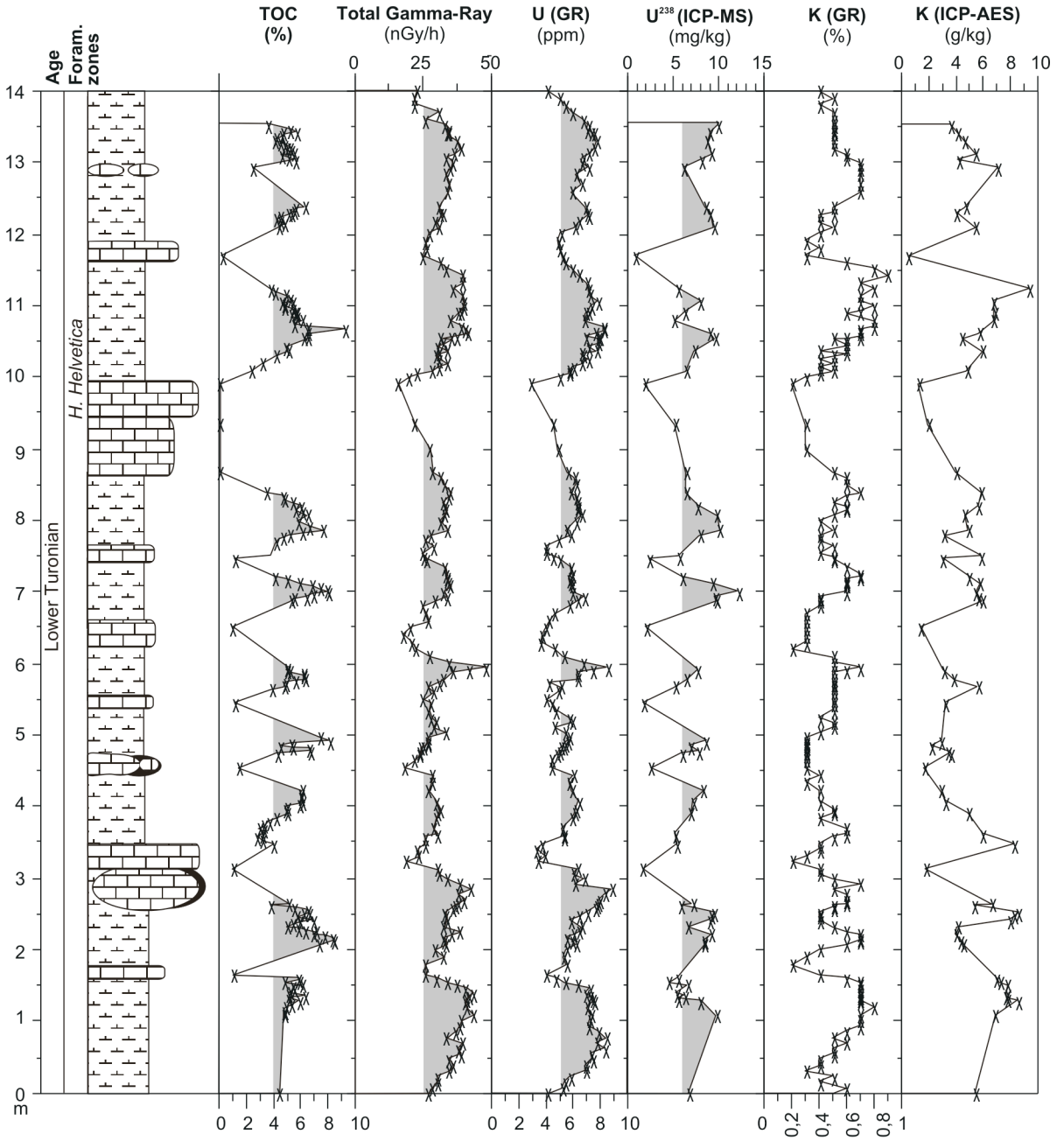

Figure 6. Cenomanian-Turonian black marls, Ama Fatma (Tarfaya Basin, South Morocco): correlation of TOC, spectral gamma-ray and ICP-MS data. In general there is a good correlation between TOC and uranium (both GR and ICP-MS). Differences are partly due to the fact that the gamma-ray tool averages over a larger interval (30 cm) than the geochemical techniques (2 cm).

Cenomanian-Turonian black marls in Jordan (Karak area), Tunisia (Oued Mellegue, Oued Smara) and northern Germany (Lengerich) were studied by the authors. They are characterized by extremely low maximum uranium values, generally less than 5 ppm (Jordan, Tunisia) and 1.5 ppm (Germany), in spite of TOC values of up to 8% (Jordan), 6% (Tunisia) and 2% (Germany) (Fig. 4C). In all three cases uranium and TOC contents appear to be largely unrelated. This contrasts with the rather stable U/TOC ratios recorded in similar, age-equivalent strata in Morocco (see above).

An acceptable U-TOC correlation was derived for the lower part of a Campanian oil shale section studied by the authors in Jordan (Fig. 4E). In the upper part of this unit, however, no U/TOC correlation exists, most likely because of an up-section increase in the phosphate content.

5.6.4. Lacustrine organic-rich strata

Meyer and Nederlof [1984] described examples of organic-rich lacustrine deposits from the Lower Cretaceous of Gabon and the Oligocene of Indonesia. In both cases, organic-rich intervals were not associated with a systematic increase in gamma-ray response. Eocene lacustrine black shales were studied in a 190 m deep well in Messel (Central Germany). No correlation between uranium and TOC contents was observed; the uranium contents plotted rather consistently around 3-4 ppm [*Wonik*, *in press*].

5.7. Discussion

The case studies referred to above suggest that stable U-TOC relationships only develop in certain, suitable organic-rich systems and that U/TOC ratios in different black shales can vary widely. Various factors may influence the relationship between uranium and TOC contents, and these are briefly reviewed below:

5.7.1. Initial uranium concentration

The primary concentration of dissolved U^{6+} in the water plays an important role in controlling the U/TOC ratio preserved in a black shale. Uranium is an order of magnitude less concentrated in fresh water than in sea water; therefore, most lacustrine organic-rich deposits are not enriched in uranium and covariation with TOC generally does not occur [*Broecker and Peng*, 1982; *Herron*, 1991]. Nevertheless, lacustrine U-TOC correlations of "moderate" quality have been recorded [e.g. *Creaney and Passey*, 1993], possibly due to a relatively high content of primary dissolved uranium in the lakes concerned associated with the presence of U-enriched rocks in the drainage basins.

The variability of the marine U/TOC ratios illustrated in Fig. 5L does not reveal a clear trend through the Phanerozoic. Therefore, a systematic gradual reduction of the uranium concentration in anoxic water bodies with time is unlikely. Nevertheless, some general comments can be made on the basis of the data presented. Palaeozoic black shales appear generally to be characterised by higher U/TOC ratios than do Mesozoic shales. However, some non-Palaeozoic black shales (such as the mid Cretaceous black shale in ODP *641A* and the Holocene Black Sea organic-rich mud) also have high U/TOC ratios. Smallerscale trends may also be recognized in some locations and over some stratigraphic intervals. For example, in the Palaeozoic black shales of North Africa, an organic richness of 3% corresponds in the Lower Silurian with a total gamma-ray response of 200 API, and in the Upper Devonian with only 150 API (see above), indicating a reduction in uranium content in shales deposited in similar palaeo-environmental conditions at different times.

5.7.2. Lithological composition and facies

The examples discussed above demonstrate that the lithological composition of an organic-rich unit is one of the most important factors controlling the development of stable U/TOC relationship. Most suitable for the development of a stable relationship are pelagic or hemipelagic shales with little or no carbonate content and little silt or sand content. Examples of little-contaminated shales are the Cretaceous shales of the Atlantic DSD Sites below the carbonate compensation depth, and the shelfal Silurian and Upper Devonian "hot shales" of North Africa (Fig. 5L). In more calcareous hemipelagic organic-rich systems (e.g. the Lower Jurassic in Western Europe, and the Cenomanian-Turonian black marls of south Morocco), a stable U/TOC ratio does exist but values of the ratio are significantly lower (Fig. 5L). Shallow-marine, more calcareous and sandy organic-rich systems are generally characterized by the absence of a stable U/TOC relationship, as evidenced by the Cenomanian-Turonian black marls in Jordan, Tunisia and North Germany.

The greater uranium concentrations in shales compared to carbonates of the same organic richness may be explained by the property of clay minerals to concentrate uranium ions by cation exchange and adsorption.

5.7.3. Sorbent availability

The availability of a sorbent such as organic matter or phosphate is an important prerequisite for uranium precipitation. However, uranium is adsorbed by different types of organic matter with

variable efficiency [*Swanson*, 1960]. Phosphate can also act as a sorbent and trigger the precipitation of uranium, in quantities largely unrelated to the organic richness of the sediment. Development of a stable U/TOC relation in phosphaterich lithologies is therefore complex.

5.7.4. Sedimentation rate and duration of anoxia

Sedimentation rate and duration of anoxic conditions also influence the relationship between uranium and TOC concentrations. In principal, the longer that OM is in contact with sea water, the more uranium can be fixed ([*Myers and Wignall*, 1987], p. 182; [*Arthur et al.,* 1990], p. 99). Low sedimentation rates favour higher U/TOC ratios, e.g. in abyssal compared to hemipelagic settings. *Mangini and Dominik* [1979] demonstrated that the U/ TOC ratio for Mediterranean sapropels tends to be inversely proportional to the sedimentation rate.

The frequency and duration of anoxic episodes or cycles also influences the developement of a stable U-TOC relationship. In mostly oxic environments with only short anoxic phases, uranium may be partly or fully oxidised ("burned down"), remobilised and released to solution [e.g. *Thomson et al.,* 1995; *Mangini et al.,* 2001). In these cases, no stable covariance of uranium with OM can be expected. Environments with longer term oxygen-deficiency are less affected by this diagenetic effect.

5.7.5. Redox boundary

The position of the redox boundary relative to the sediment-water interface also seems to influence the development of interrelated uranium and TOC [*Myers and Wignall*, 1987; *Van der Weijden et al.,* 1993). *Myers and Wignall* ([1987], p. 186) reported that authigenic uranium correlates well with TOC in the Lower Toarcian in Southern England where bottom-water stagnation alone was the controlling factor on the level of organic carbon preserved. They found that the correlation worsens, and eventually disappears, when factors such as surface productivity and sedimentation rate were important in controlling organic carbon preservation (e.g. in the Kimmeridge Clay of southern England).

5.7.6. Diagenetic factors

The degree of thermal maturation and other diagenetic effects can also influence the U-TOC relationship. In general, the organic content of mature black shales is reduced as a consequence of hydrocarbon generation and expulsion, while the uranium content is commonly less effected by this process [*Meyer and Nederlof*, 1984; *Passey et al.*, 1990; *Stocks and Lawrence*, 1990]. The resulting relatively high U/TOC ratios are therefore only of a secondary nature, while the initial U/TOC ratio may have been lower. In some black shale systems, however, changes in the U/TOC ratio with increasing thermal maturity appear to be non-systematic and are therefore hard to predict (see synthesis in [*Zelt*, 1985], p. 2-31). In principal, uranium does not undergo major redistribution during metamorphism up to amphibolite grade [*Dostal and Capedri*, 1978]. However, the uranium chemistry of a shale can undergo diagenetic modification, for example by uranium mobilisation "fronts" (Silurian, Germany) [*Spirakis*, 1996; *Landais*, 1996]. These shales are unsuitable for TOC reconstructions based on uranium content [*Lev et al.,* 2000].

5.7.7. Approximation of the organic-richness in boreholes using combined log data

Because stable U/TOC ratios are not developed in all black shale systems and thorough calibration is necessary in each case, organic richness profiles from well logs are most easily generated at the present-day using combinations of log data. These make use of a black shale's lower density, slower sonic and higher resistivity responses compared to an organically lean shale (e.g. the Älog R Method; [*Meyer and Nederlof*, 1984; *Passey et al.,* 1990; *Herron* 1991]). Density, sonic and resistivity data, however, are difficult to measure at outcrop so that combined subsurface/outcrop studies of certain black shale systems may still benefit from using the conventional U/TOC ratio technique.

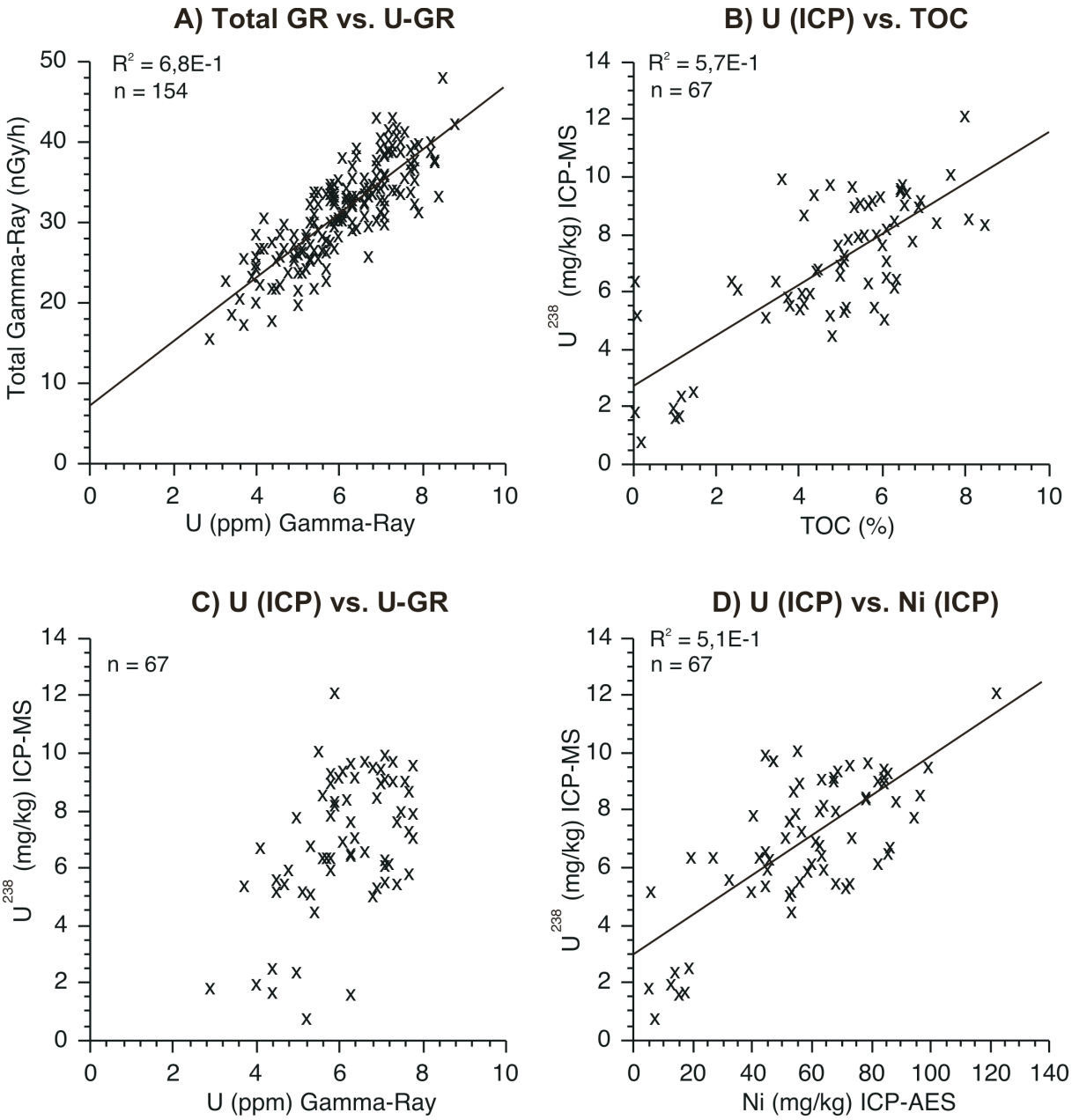

Figure 7. Cross-plots of spectral gamma-ray and geochemical data from the Early Turonian organic-rich marl at Ama Fatma, Tarfaya Basin (Morocco).

5.7.8. Reconstruction of the organic-richness in weathered outcrop sections

The U/TOC proxy technique may be applied to weathered black shale successions in which the initial OM has largely been destroyed. If the uranium content has been preserved, however, the original (pre-weathering) organic-richness may be approximated. An example of this application is given by *Lüning et al.* [*in press,*c] with reference to Lower Silurian shales in Southern Libya.

5.8. Conclusion

1. Many organic-rich, low-carbonate hemipelagic shales are characterized by the development of a stable U/TOC relationship.
2. In these shales, the U/TOC ratio is influenced by a number of factors including the primary uranium content of the water body, the carbonate content and the sedimentation rate. Palaeo-oceanographic conditions, such as primary productivity and water-body stratification, will also

influence the ratio which will therefore vary in different black shale "types".

3. The development of a stable U/TOC relationship may be inhibited by the presence of phosphate; by a high carbonate or sand content in the shale; by dissolution ("burndown") of uranium during oxic periods; and by large-scale, diagenetic uranium remobilisation.
4. In suitable black shale systems, the organic-richness can easily be approximated by measuring the uranium content using spectral gamma-ray techniques. This techniquemay be especially important in combined studies using borehole and outcrop data, because gamma-ray logging tools are simple to use in the field.
5. In all cases, a thorough calibration of the uranium/TOC relationship should to be undertaken, the aim being to determine the stratigraphic and geographic limits of the ratio derived at any location.

Acknowledgments

We would like to thank the following colleagues for their support and discussions during spectral gamma-ray surveys in Germany, Morocco, Tunisia, and Jordan: Frauke Schulze, Jochen Kuss and Thomas Wagner (all University of Bremen); L. Schöllmann (Westphalian Natural History Museum, Münster); T. Wonik (GGA, Hannover); A. Gharaibe (NRA Amman); Hassane Chellai (University of Marrakesh); A. Schmid-Röhl (University of Tübingen); and Uwe Buczko (University of Bayreuth). We are grateful to Sabine Kasten (University of Bremen) for support with the ICP analyses. We acknowledge technical assistance provided by Christian Müller (University of Bremen). The manuscript benefited from useful comments by Thomas Aigner (University of Tübingen), and Frans van Buchem (IFP) who kindly supplied additional data. Funding was provided by the German Science Foundation (DFG grants *Lu 654/1-1, Lu 654/1-2, Wa 1036/6*).

Chapter 6

Carbon-isotope stratigraphy recorded by the Cenomanian/Turonian Oceanic Anoxic Event: correlation and implications based on three key-localities

Chapter 6.

Carbon-isotope stratigraphy recorded by the Cenomanian/Turonian Oceanic Anoxic Event: correlation and implications based on three key-localities

Authors*: Tsikos, H., H.C. Jenkyns, B. Walsworth-Bell, M.R. Petrizzo, E. Erba, I. Premoli Silva, A. Forster, S. Kolonic, M. Baas, T. Wagner and J.S. Sinninghe Damsté*

Status: submitted Journal: *Journal of the Geological Society (London)*

Abstract

We present detailed carbon-isotope records for bulk carbonate, total organic carbon (TOC) and phytane from three key-sections spanning the Cenomanian/Turonian boundary interval (Eastbourne, England; Gubbio, Italy; Tarfaya, Morocco), with the purpose of establishing a common chemostratigraphic framework for Oceanic Anoxic Event (OAE) 2. Isotope curves from all three localities are characterised by a positive carbon-isotope excursion of approximately 4 ‰ for TOC/phytane and ca. 2.5 ‰ for carbonate, although diagenetic overprint appears to have obliterated the primary carbonate carbon-isotope signal in at least part of the Tarfaya section. Stratigraphically, peak $\delta^{13}C$ values for all components are followed by intervals of high, near-constant $\delta^{13}C$ in the form of an isotopic plateau. Recognition of an unambiguous return to background $\delta^{13}C$ values above each plateau is, however, contentious in all sections, hence no firm chemostratigraphic marker for the end-point of the positive isotopic excursion can be established. The stratigraphically consistent first appearance of the calcareous nannofossil *Quadrum gartneri* at or near the Cenomanian/Turonian boundary as established by ammonite stratigraphy, in conjunction with the end of the $\delta^{13}C$ maximum characteristic of the isotopic plateau, provides a potentially powerful tool in delimiting the stratigraphic extent and duration of OAE 2. This Oceanic Anoxic Event is demonstrated to be largely if not wholly confined to the latest part of the Cenomanian stage.

Keywords: Oceanic Anoxic Events**,** Carbon Isotopes, Cenomanian/Turonian, Stratigraphy, Correlation

6.1. Introduction

The concept of Oceanic Anoxic Events (OAEs), as introduced in the mid-nineteen-seventies [*Schlanger and Jenkyns,* 1976], hinged upon the discovery of coeval, organic-carbon-rich sediments deposited across a range of marine settings, from shelf seas to the open ocean. The Cenomanian/Turonian (C/T) boundary interval represents a classic example of an OAE because it is typified by the development of organic carbon-rich deposits on a global scale, with a concomitant positive shift in carbon-isotope values in marine carbonate and marine and terrestrial organic matter [*Arthur et al., 1988; Hasegawa,* 1997]. This positive $\delta^{13}C$ shift is conventionally related to excess burial of organic carbon [*Jenkyns,* 1980; *Scholle and Arthur,* 1980; *Schlanger et al.,* 1987]. The C/T OAE (hereafter referred to as "OAE 2") or Bonarelli Event (named after the Bonarelli level, the characteristic black shale cropping out in the Marche-Umbrian Apennines of central Italy) therefore constitutes an ideal candidate for detailed investigations of the changing environmental conditions behind the establishment of widespread marine anoxia during specific intervals of geological time.

In this paper, we examine the carbon-isotope stratigraphy of three key, outcrop/drill-core sections spanning the C/T interval from England, Italy and Morocco (Fig. 1). High-resolution total organic carbon (TOC) records and stable-isotope data from total carbonate and organic carbon have been obtained on a cm- to dm scale. These records were complemented by compound-specific $\delta^{13}C$ data for free as well as sulphur-bound phytane at lower stratigraphic resolution. Phytane is an organic compound (acyclic isoprenoid) which is predominantly derived from the phytol side-chain of phytoplanktonic chlorophyll-*a*, and therefore represents a useful proxy for the isotopic composition of ancient marine phytoplankton communities [e.g., *Kohnen et al*., 1992; *Kuypers et al*., 1999, 2002]. In comparison with $\delta^{13}C$ data for bulk organic carbon, phytane-based isotope records are to a much lesser extent influenced by changing contributions of isotopically distinct organic matter sources, or by different degrees of organic-matter degradation [e.g. *Sinninghe Damsté et al.,* 1998].

The carbon-isotope curves have been calibrated against new calcareous nannofossil and planktonic foraminiferal biostratigraphy; in a different paper [*Walsworth-Bell et al*., in prep.], we present detailed biostratigraphic and taxonomic data for the same sections. Carbon-isotope profiles are compared with published chemo-and biostratigraphic data from Pueblo (Colorado, USA; Fig. 1), the proposed stratotype section for the C/T boundary [*Kennedy et al*., 2000]. Our objectives are two-fold: (1) to generate a universal chemostratigraphic framework for OAE 2 by comparing and contrasting the various isotopic records from the different sites; and (2) to highlight the advantages and limitations of using detailed isotope stratigraphy as an independent correlative tool for constraining the stratigraphic extent and duration of OAE 2.

6.2. Selected sites and methodology

Three representative sections spanning the Cenomanian/Turonian boundary interval in contrasting palaeoceanographic settings were selected for this investigation, namely Eastbourne (East Sussex, England), Tarfaya (SW Morocco) and Gubbio (Umbria, Italy; Fig. 1). The Eastbourne section was logged and sampled wholly at the Gun Gardens locality between November 2000 and August 2001, and thus represents an improvement on composite sections from the same area published previously [e.g. *Gale et al*., 1993; *Paul et al*., 1999; *Keller et al*., 2001]. A core (S57) representing C/T sediments at Tarfaya (drilled by SHELL during exploration in the late 1970s–early 1980s) was logged and sampled in October 2001 at the Ocean Drilling Program Core Repository in Bremen, Germany, where it is currently stored. At Gubbio, two cores (S2 and S4) were drilled in the Vispi Quarry in the Contessa Valley (Fig. 1) during June 2000. These cores are stored at the Ardito Desio Department of Earth Sciences, University of Milan, and were logged and sampled in October 2000–March 2001. Sampling intervals ranged from 20–40 cm for the material from Eastbourne and Tarfaya, to ca. 10 cm for the limestones from Gubbio, whereas the organic-rich Bonarelli level was sampled on a more detailed cm- to sub-cm scale.

Carbonate (C,O) isotope ratios were determined on powdered bulk-rock samples from all three sites, by reaction with orthophosphoric acid at 90ºC, using a VG Isocarb device and Prism mass spectrometer at the University of Oxford. Normal corrections were applied and the results are reported using the usual δ notation, in ‰ deviation from the VPDB (Vienna Pee Dee Belemnite) standard.

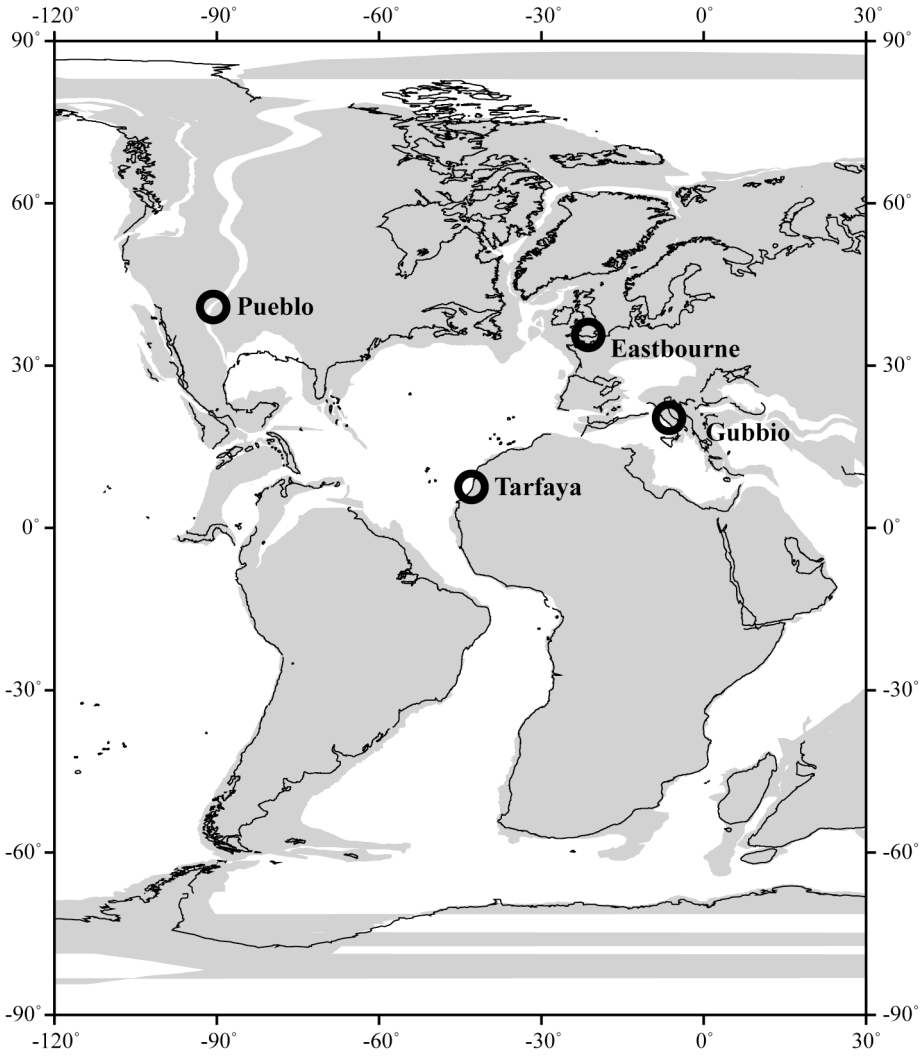

Figure 1. Global palaeogeographic map for the Cenomanian/Turonian boundary interval [after *Hay et al.*, 1999] showing the three sites selected for this paper and the Pueblo locality, the proposed global stratotype for the Cenomanian/Turonian boundary [*Kennedy et al.*, 2000]

Calibration to VPDB was performed via our laboratory standard calibrated against NBS19 and Cambridge Carrara marble. Reproducibility of replicate analyses of standards was generally better than 0.1 ‰ for both carbon- and oxygen-isotope ratios.

Weight-percent total organic carbon (TOC) values were determined on organic-rich samples from the Gubbio and Tarfaya sections, and on a few, organic-lean samples from the Plenus Marls member at Eastbourne, using a Strohlein Coulomat 702 device. Duplicate samples were taken, one of which was roasted at 450ºC overnight to remove organic carbon. Both samples were then roasted at 1300ºC to decompose the calcium carbonate. In a separate operation, the duplicate samples were combusted at 1400ºC and the CO_2 produced was fed into a barium perchlorate solution for total C analyses, with a resultant change in pH. Back titration to the original pH was performed using an electrolytically produced reagent; the quantity of electricity required for this purpose gave an absolute determination of the amounts of carbon present. The difference between the samples that had and had not been roasted at 450ºC gave a measure of the value of TOC. Analytical reproducibility by this method was such that repeat analyses for organic carbon generally differed by no more than 0.02%.

For determinatons of the bulk carbon-isotope composition of the organic matter, the same samples were acidified with dilute HCl at ambient temperature to remove carbonate. Depending on the original TOC contents of each sample, between 5–70 mg of the dried carbonate-free residues were weighed in tinfoil cups and placed in a Europa Scientific Limited CN biological sample converter connected to a 20–20 stable-isotope gas-ratio mass spectrometer. Carbon-isotope ratios were measured against a

laboratory nylon standard, with a $\delta^{13}C$ value of -26.1 ± 0.2‰. Analytical results are presented in the usual δ notation, in ‰ deviation from the VPDB (Vienna Pee Dee Belemnite) standard.

Selected powdered samples from the Tarfaya and Gubbio sections were solvent-extracted with a mixture of dichloromethane/methanol (9:1, v/v), and the total lipid extracts were successively separated by column chromatography, into saturated and unsaturated, apolar and total polar fractions. In the case of the core samples from Gubbio, compound-specific $\delta^{13}C$ measurements on phytane present in the saturated apolar fractions were obtained using isotope-ratio monitoring gas chromatography coupled with mass spectrometry (irm-GC-MS) at the Royal Netherlands Institute of Sea Research (NIOZ). For the Tarfaya core samples, the polar fractions were first treated by *Raney Nickel* desulphurization, in order to release sulphur-bound hydrocarbons, followed by column separation and hydrogenation of the apolar fractions to yield phytane. All compound-specific carbon-isotope measurements were carried out at least in duplicate (σ = ±0.03 to 0.58) and the mean $\delta^{13}C$ values for each sample are presented in the usual δ notation *versus* the VPDB standard. The analytical quality of the irm-GC-MS was monitored by adding an internal standard of known isotopic composition for every individual sample injection.

Nannofossil biostratigraphy was generated using standard techniques [*Bown and Young*, 1998]. Smear slides were studied under the light microscope, and nannofossil abundance and preservation determined using qualitative categories. A more detailed discussion of methods and full documentation of the data can be found in *Walsworth-Bell et al.* [in prep.].

Planktonic foraminiferal biostratigraphy was generated for the Eastbourne Plenus Marls Member (Eastbourne) and Tarfaya sections using washed residues. Samples were soaked in hydrogen peroxide, washed under running water through 63-150 µm, 150-250 µm and >250 µm sieves, and then dried. Ultrasonic treatment was used to clean specimens, facilitating identification. The harder lithologies of the Eastbourne Grey Chalk Member and White Chalk Formation and Gubbio sections, were studied in thin-section.

6.3. Results

6.3.1. Eastbourne, East Sussex (England)

The Gun Gardens section at Eastbourne is the most expanded Cenomanian/Turonian section in the Anglo-Paris Basin, and has variously been the subject of detailed bio- and chemostratigraphic studies [e.g., *Gale et al.*, 1993; *Paul et al.*, 1999; *Keller et al.*, 2001]. The same section has also been proposed as the European reference section for the C/T interval [*Paul et al.*, 1999]. The succession consists of three, broadly defined lithological units, namely (from bottom to top): Grey Chalk Member, Plenus Marls Member and White Chalk Formation (Fig. 2). Lithological variations amongst these three units are essentially related to the interplay of two end-member components, i.e., $CaCO_3$ (mainly as nannofossils) and clay. The Grey Chalk contains common intercalations of thin, marly layers, with omnipresent bioturbation. The Plenus Marls consists of grey marls and clay-rich chalks in the basal part, progressively becoming purer chalk alternating with dm-thick marl layers upwards in the section. The White Chalk comprises hard, nodular to gritty chalk separated by cm-thick flaser marls in the lower parts, with the latter becoming less common stratigraphically upwards.

Results for bulk carbonate carbon and oxygen isotopes across a 27 m-thick outcrop section at Gun Gardens, Eastbourne, are presented in Figure 2. Nannofossil and planktonic foraminiferal biostratigraphy is also provided. The lowermost 6 m (Grey Chalk) are characterised by essentially constant $\delta^{13}C_{carb}$ values of ca. 3‰. A distinct rise in $\delta^{13}C_{carb}$ occurs at the base of the Plenus Marls, with a first maximum of ca. 4.8‰ occurring at approximately 4 m above the contact with the Grey Chalk; this is immediately followed by a small dip in values of ca. 0.5‰. A second, positive isotopic "spike" (ca. 5.4‰) occurs higher in the succession, close to the contact with the overlying White Chalk. The remaining part of the section (White Chalk) records essentially constant values of ca. 4.8‰ for about 4 – 5 m, followed by a smooth decline in the uppermost ca. 8 m, to $\delta^{13}C_{carb}$ values of less than 4‰. Bulk carbonate $\delta^{18}O$ data show considerable variation across the entire stratigraphy, yet they register a drop in $\delta^{18}O$ values near the second $\delta^{13}C_{carb}$ maximum, from ca. -3‰ in the Grey Chalk/Plenus Marls interval, to -3.5 – -4‰ in the overlying White Chalk Formation.

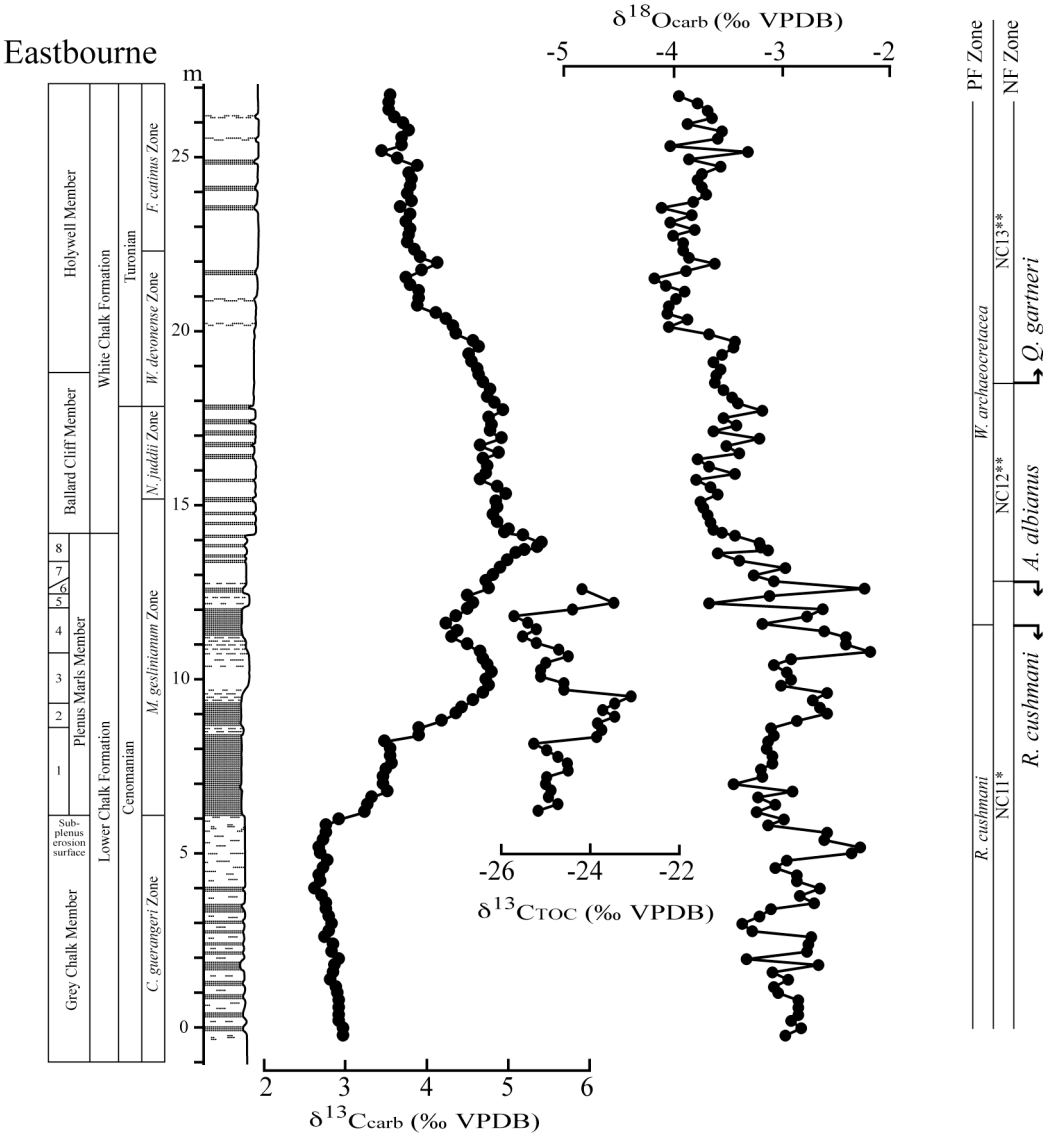

Figure 2. Carbon- and oxygen-isotope stratigraphy and biostratigraphy of the Eastbourne section, England. Chalk intervals are shown as blank, marls as stippled. PF: planktonic foraminiferal; NF: nannofossil. Zone NC11* from the zonation of Bralower *et al*. (1995); NC12 and -13** from that of Walsworth-Bell *et al.* (in prep.).**

The Eastbourne section contains very little organic carbon, in most cases below the detection limit of the instrumental analytical technique used in this study. The Plenus Marls unit was selected for isotopic analyses of its organic-carbon fraction, due to its lower bulk carbonate/clay ratio and thus potentially higher TOC content. Bulk TOC values were nevertheless very low throughout the Plenus Marls interval (0.1– 0.2 wt%) with a maximum of 0.26 wt% (this study) recorded in Bed 6 (Fig. 2) of Gale *et al.* (1993). Bulk organic-carbon $\delta^{13}C$ ($\delta^{13}C_{TOC}$) data presented in Figure 2 were obtained from 31 samples, beginning from the base of the Plenus Marls, up to (and including) one sample from Bed 6. Despite the very low TOC contents, reproducibility of data was in the range ±0.3 to 0.5‰. By comparison with the $\delta^{13}C_{carb}$ data over the same interval, $\delta^{13}C_{TOC}$ values show little similarity, although both record a ca. 2‰ increase at a comparable stratigraphic level to that of the first carbonate carbon-isotope peak. Nevertheless, the possibility exists that such a trend may be related to other causes such as, for example, variable contributions of terrestrial *versus* marine organic matter, changes in the aquatic primary biomass productivity and/or changes in dissolved carbon dioxide content [e.g. *Arthur et al*, 1988].

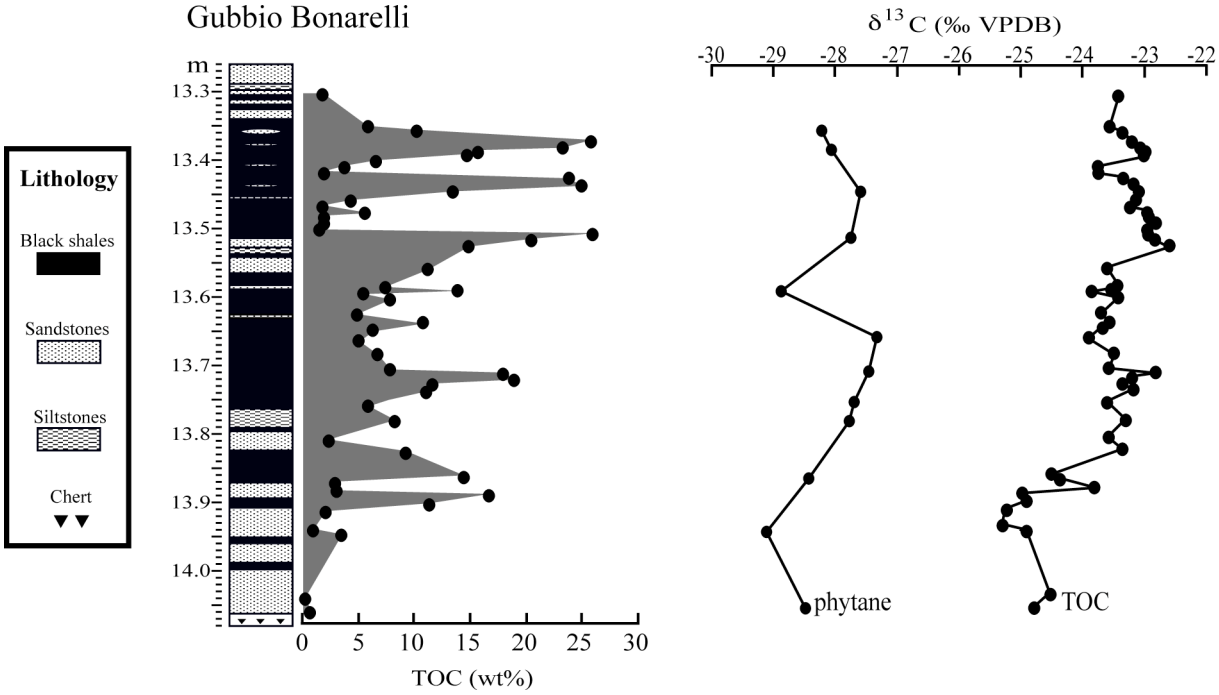

Figure 3. Total organic carbon (TOC), $\delta^{13}C_{TOC}$ and $\delta^{13}C_{Ph}$ stratigraphic profiles across the Bonarelli level, S4 core, Gubbio, Italy.

6.3.2. Gubbio, Umbria (Italy)

The stratigraphically continuous pelagic carbonate succession of the upper Albian to Santonian Scaglia formation (Scaglia Bianca and Scaglia Rossa) has been the subject of several investigations in the past [e.g., *Arthur and Premoli Silva*, 1982; *Jenkyns et al*., 1994; *Stoll and Schrag*, 2000]. The Scaglia Bianca encloses the Bonarelli level, a striking, approximately 1 m-thick black shale unit [*Arthur and Premoli Silva*, 1982] which is the most spectacular sedimentary expression of the OAE 2 known. Gubbio is the type locality for the Bonarelli level.

The Bonarelli level has a thickness of approximately 82 cm in S4, the core which yielded the optimum recovery of this unit. (We take the Bonarelli level, which has not been formally defined, to be the whole limestone-free interval, including the lowermost chert and the uppermost radiolarian sand; *sensu* [*Arthur and Premoli Silva*, 1982]). It comprises largely black, organic-rich siliceous shale, interbedded with cm-thick layers of radiolarian-rich sandstone and siltstone. Stratigraphically, TOC contents vary widely and reach maximum values of up to 25–26 wt% in the uppermost portion (between 10 and 25 cm below the stratigraphic top). Bulk $CaCO_3$ contents throughout the entire Bonarelli level are either very low (<5 wt%) or below the limit of detection.

$\delta^{13}C_{TOC}$ values of ca. -25‰ characterise the lowermost 15 cm of the Bonarelli level, but rise sharply by approximately 1–1.5 ‰ as TOC values reach their first maximum of ca. 15 wt% (Fig. 3). Thereafter, the $\delta^{13}C_{TOC}$ data show little variation throughout the remainder of the unit, apart from a relative minimum between 30–45 cm (Fig. 3). Highest isotopic values (-23.0 to -22.5‰) are observed in the uppermost portion of the Bonarelli level, and coincide with the interval where highest TOC values also occur. Lower-resolution phytane $\delta^{13}C$ ($\delta^{13}C_{Ph}$) data (Fig. 3) essentially mimic the $\delta^{13}C_{TOC}$ pattern, with values of ca. -29‰ in the lower part of the Bonarelli level, progressively increasing to maxima of -28 to -27.5‰ stratigraphically upwards.

The Scaglia Bianca formation, which encloses the Bonarelli level, is a micritic limestone containing abundant solution-welded nannofossils and planktonic foraminifera and common intercalations of chert and local, mm-scale marl seams. Isotopic variations across the 36.64 m-thick S2 core section compare well with previously published curves (e.g., *Stoll and Schrag*, 2000) and are shown in the stratigraphic plots of Figure 4. $\delta^{13}C_{carb}$ values show a first maximum of ca. 3‰, at approximately 20 m below the base of the Bonarelli level, which must correspond to the

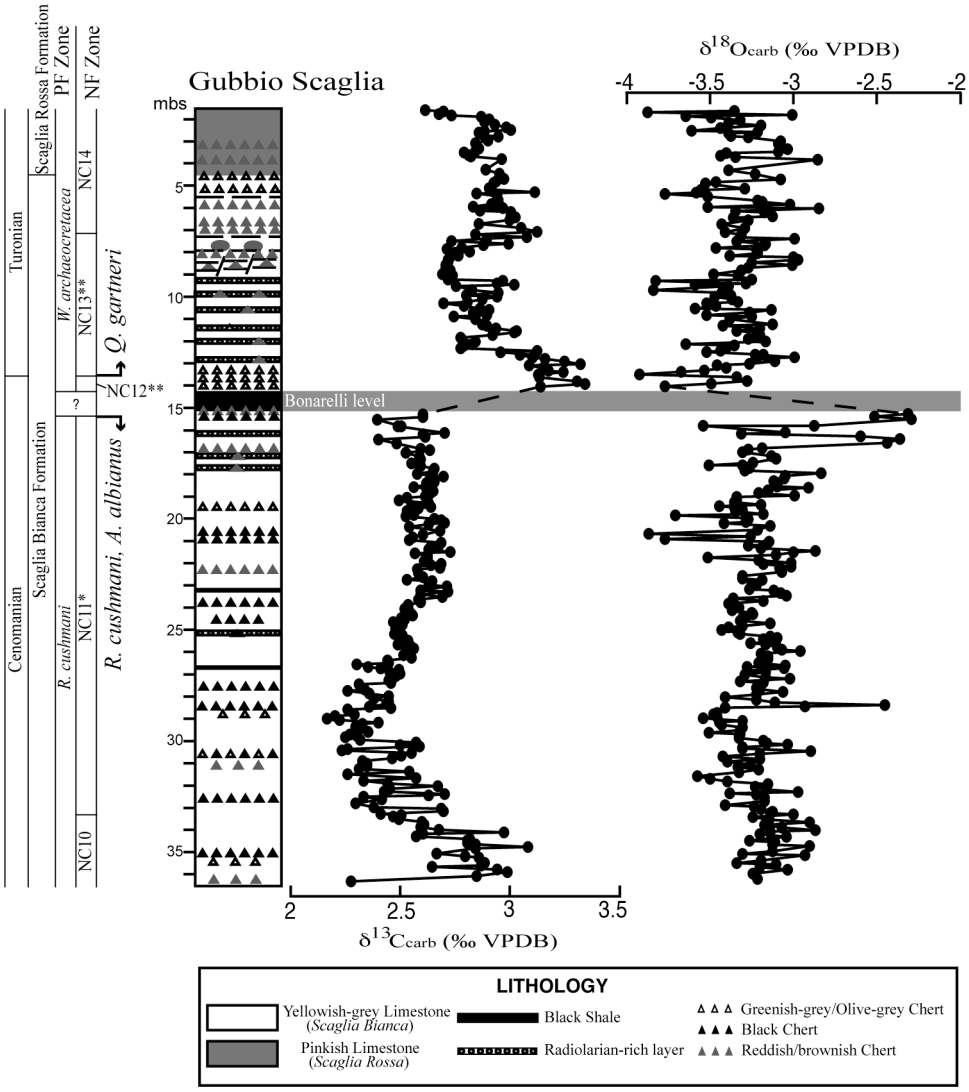

Figure 4. Carbonate carbon- and oxygen-isotope stratigraphy and biostratigraphy of the Scaglia Bianca and Scaglia Rossa formations in the Gubbio S2 core. PF: planktonic foraminiferal; NF: nannofossil. Zones NC10 and -14 from the zonation of *Roth* [1978]; NC11* from that of *Bralower et al.* [1995]; NC12 and -13** from that of *Walsworth-Bell et al.* [in prep.] C/T boundary placed using the first occurrence of the nannofossil *Q. gartneri*.**

"Mid-Cenomanian Event" [*Jenkyns et al*., 1994; *Coccioni and Galeotti*, 2003]. Thereafter, values progressively decline to isotopic minima of ca. 2.3‰ over a stratigraphic interval of 5–6 m, gradually rise to an average value of ca. 2.6‰, and remain essentially constant for the uppermost 10 m of section below the Bonarelli level. Immediately above the latter, $\delta^{13}C_{carb}$ values are the highest seen in the Gubbio section, with an average value of ca. 3.2‰ prevailing over approximately 1.5 m of stratigraphic thickness. Above this interval, values decline to <3‰, and show little variation for the uppermost 10 m of the section, including the transition from the Scaglia Bianca (white limestone) to the Scaglia Rossa (reddish limestone) formations at 4.27 m stratigraphic depth (Fig. 4). Bulk carbonate $\delta^{18}O$ data show considerable scatter throughout the entire Scaglia section, possibly resulting from post-depositional diagenetic modification. Nevertheless, the data do record a slight lowering in average $\delta^{18}O$ values of approximately 0.3‰, between the pre- and post-Bonarelli stratigraphic sediments, which could indicate an overall rise in temperature over this interval (Fig. 4).

Formulation of a complete nannofossil and planktonic foraminiferal biostratigraphy for the Gubbio section is hindered due to the virtual absence of carbonate in the Bonarelli level. As a result, although the key marker species *Axopodorhabdus albianus* (nannofossil) and *Rotalipora cushmani* (planktonic foraminifer) are last encountered immediately below this unit, it is likely that their true last

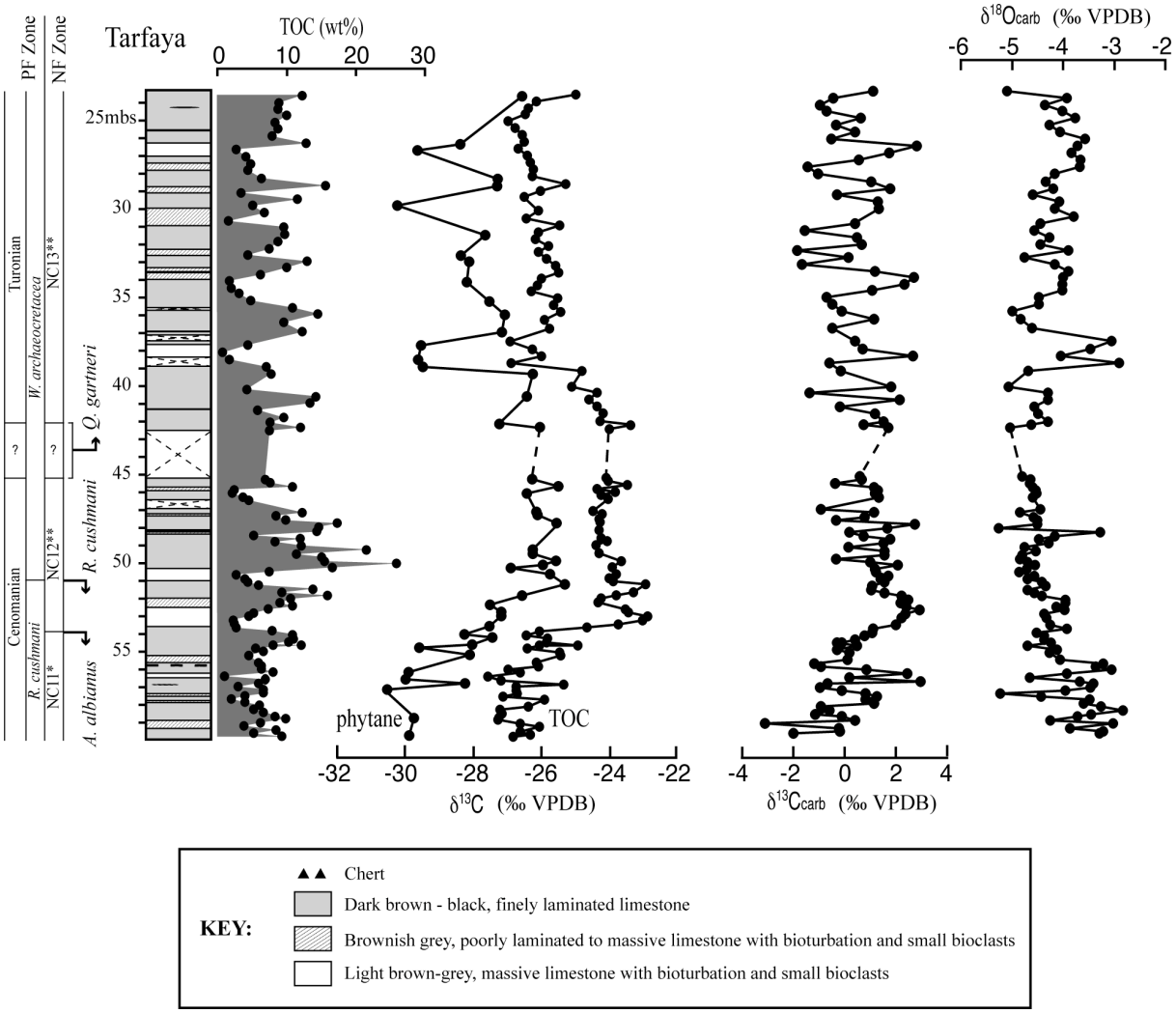

Figure 5. Stable-isotope chemostratigraphy and biostratigraphy of the Tarfaya S57 Core. PF: planktonic foraminiferal; NF: nannofossil. Zone NC11* from the zonation of *Bralower et al.* [1995]; NC12 and -13** from that of *Walsworth-Bell et al.* [in prep.]. C/T boundary placed using the first occurrence of the nannofossil *Q. gartneri*.**

occurrences fall within the black shale itself. The first appearance of the marker nannofossil *Quadrum gartneri* is observed at ca. 1 m above the Livello Bonarelli, and is thus not affected by this preservational problem.

6.3.3. Tarfaya (SW Morocco)

The Tarfaya Basin in SW Morocco is host to an exceptionally thick (up to 800 m) organic matter-rich, shallow-marine sedimentary succession spanning the mid-Cretaceous, including perhaps the most stratigraphically complete C/T interval known [*Luderer and Kuhnt,* 1997]. It has therefore been the subject of several studies in the past [e.g., *Kuhnt et al*., 1997, 2001; *El Albani et al*., 1999; *Kolonic et al*., 2002]. The section investigated here (core S57) comprises ca. 37 m of organic-rich calcareous sediment, characterised by rhythmic alternations of dm-scale, dark- and light-coloured layers separated by gradational contacts. In terms of TOC, individual sample contents vary from less than 1 wt% to higher than 20 wt%, whereas total carbonate and lesser clay are the other dominant components throughout the section.

Bulk-rock TOC and $\delta^{13}C_{carb}$, $\delta^{13}C_{TOC}$ and $\delta^{13}C_{Ph}$ data are shown in Figure 5, along with nannofossil and planktonic foraminiferal biostratigraphy. The $\delta^{13}C_{TOC}$ curve exhibits a characteristic positive excursion, from values between -27 and -26‰ for the lowermost 4 m of the core, to ca. -23‰ at

approximately 53 m below surface. The excursion culminates in two distinct, closely spaced isotopic peaks, separated by a ca. 1‰ "trough". Thereafter, data form an isotopic "plateau" of $\delta^{13}C$ values around -24‰, which spans the portion of the succession wherein a peak in TOC content is also observed. At approximately 9 m stratigraphically above the second isotope spike, $\delta^{13}C_{TOC}$ values begin to decline, and stabilise around the value of -26‰ for the remaining part of the section.

Phytane and, to a lesser extent, total carbonate $\delta^{13}C$ data, show some important similarities with, and differences from the $\delta^{13}C_{TOC}$ curve. Probably the most important reproducible feature in all three curves is the progressive increase in $\delta^{13}C$ values by ca. 4‰ for the phytane, and 2.5 – 3‰ for bulk carbonate, beginning from ca. 56 and 54 metres below surface respectively, and extending for 3–5m stratigraphically upwards. However, these isotopic peaks appear to be slightly offset in relation to those seen in the bulk organic-carbon isotope curve. Furthermore, definition of a true positive excursion plateau in the $\delta^{13}C_{carb}$ curve is clearly problematic, owing to the highly variable nature of the data from both above and below the interpreted isotopic maxima. This ill-defined excursion is possibly a result of later diagenetic overprinting due to the transfer of isotopically light carbon from bacterial degradation of organic matter to carbonate cement [e.g., Scholle *and* Arthur, 1980]. Diagenetic effects are also believed to be responsible for the variable degrees of calcareous nannofossil and planktonic foraminiferal preservation, observed across the entire Tarfaya section. Curiously, although carbonate $\delta^{18}O$ data are known to be most susceptible to diagenetic exchange, the bulk carbonate $\delta^{18}O$ profile shows a consistent upward decrease by ~1.5‰ across the Tarfaya profile, although whether or not these data actually record palaeotemperature trends and/or changes in the evaporation-precipitation balance in seawater is unknown.

With respect to the $\delta^{13}C_{Ph}$ profile, although relatively constant values characterise the interval 51-39 m in concert with the observed plateau of the $\delta^{13}C_{TOC}$ curve, no clear return towards pre-excursion values is observed thereafter. The narrow trough of $\delta^{13}C_{Ph}$ values between 39 and 38 metres below surface, which is also seen in the $\delta^{13}C_{TOC}$ curve, coincides with a corresponding drop in TOC values and suggests a local productivity effect rather than a global signal.

6.4. Synthesis

A compilation of carbon-isotope profiles and biostratigraphic data as presented in the foregoing paragraphs is shown in Figure 6. Of critical importance here is the comparison between our new data and existing chemo- and biostratigraphic information from the proposed stratotype section for the Cenomanian/Turonian boundary at Pueblo, Colorado, USA [*Pratt and Threlkeld*, 1984; *Watkins*, 1985; *Pratt et al.*, 1993; *Gale et al.*, 1993; *Kennedy et al.*, 2000; *Walsworth-Bell et al.*, in prep.]. Special emphasis is placed on the reproducibility of salient features of the isotopic profiles across the different sites, and the importance of these in defining potentially global chemostratigraphic markers, both for delimiting the stratigraphic extent of OAE 2 and for the placement of the Cenomanian/Turonian boundary. Evaluation of data is undertaken on the premise that an oceanic anoxic event such as OAE 2 is, by definition, a perturbation of the global marine inorganic/organic carbon reservoirs due to excess burial of organic matter. Therefore, such an event must be reflected in the isotopic record of respective sedimentary products, as long as post-depositional processes or local effects have not obliterated the preservation of primary marine chemical signals.

Earlier comparisons between the isotope profiles of TOC from Pueblo and total carbonate from Eastbourne [*Gale et al.,* 1993] demonstrated a complex, but broadly comparable $\delta^{13}C$ curve geometry across the C/T boundary interval, comprising three distinct positive isotope spikes. Calibration of both curves using ammonite stratigraphy [*Gale et al.*, 1993] revealed that the Cenomanian/Turonian boundary corresponds to the uppermost of these spikes. Our new, higher resolution isotope profile for Eastbourne compares well with that presented by *Paul et al.* [1999], the most detailed produced to date, in that it shows the curve to be more complex than a simple three-pronged excursion. Instead, we observe an initial rise in $\delta^{13}C_{carb}$ values to form a smooth peak, followed by a slight decline and a further rise to a peak of maximum values that defines the beginning of a broader plateau. These features represent the beginning and maximum isotopic expression of OAE 2, and are followed by a subsequent gradual drop towards pre-excursion values. A re-appraisal of the Pueblo and Eastbourne curves of Figure 6, in conjunction with the existing ammonite stratigraphy indicates that, in relation to

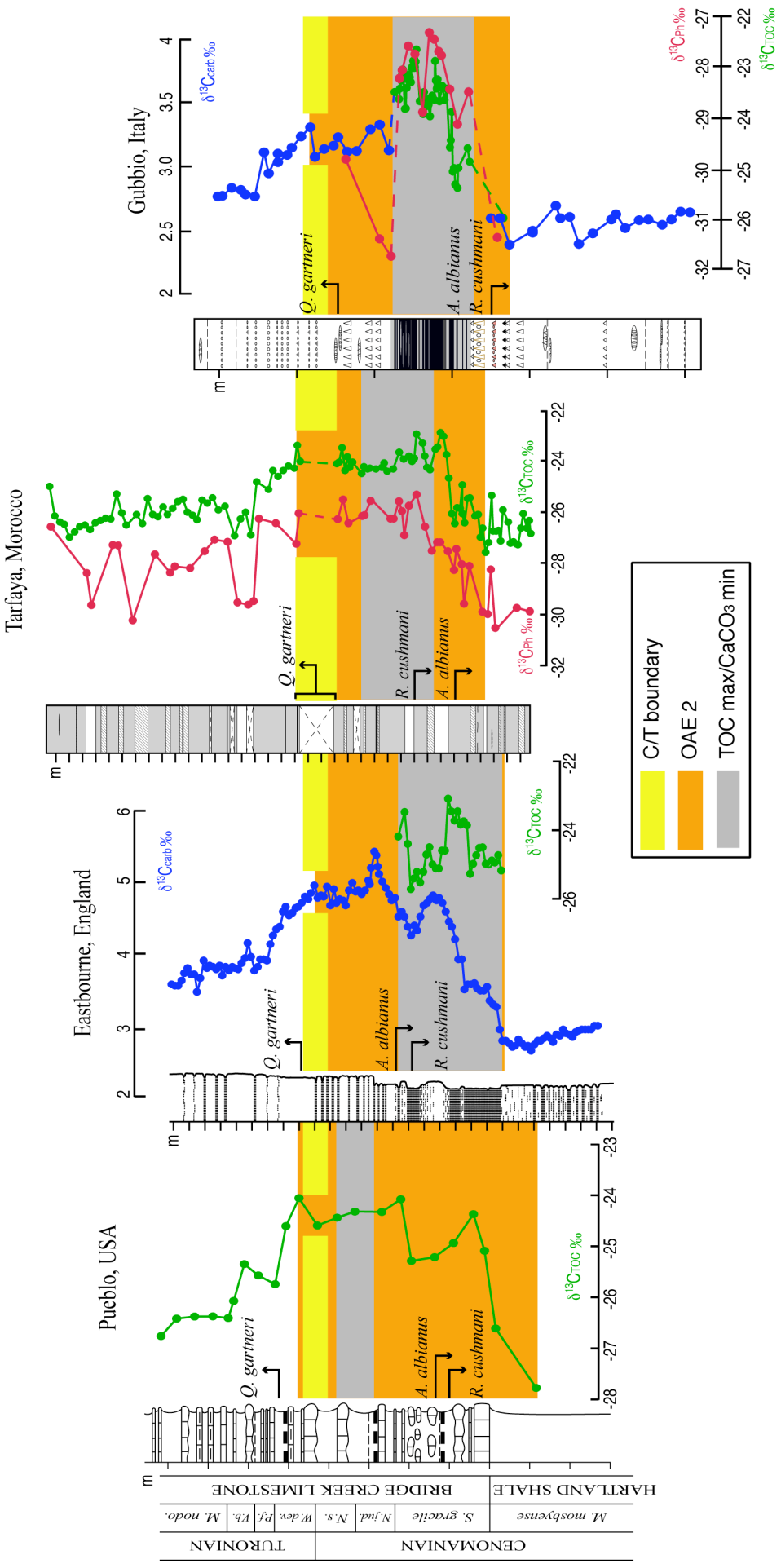
Gubbio, Italy
Tarfaya, Morocco
Eastbourne, England
Pueblo, USA
δ13Ccarb ‰
δ13CTOC ‰
δ13CPh ‰
Q. gartneri
A. albianus
R. cushmani
m
C/T boundary
OAE 2
TOC max/CaCO3 min
CENOMANIAN
TURONIAN
M. mosbyrense
S. gracile
N.jud.
N.s.
W.dev.
Pf.
Vh.
M. nodo.
HARTLAND SHALE
BRIDGE CREEK LIMESTONE

Figure 6. Chemo- and biostratigraphic correlation between the Cenomanian/Turonian sections at Eastbourne (England), Tarfaya (Morocco) and Gubbio (Italy), and the proposed stratotype section in Pueblo, Colorado, USA [after *Pratt et al*., 1993]. C/T boundary at Pueblo and Eastbourne fixed on the basis of ammonite stratigraphy. Pueblo data (except the first occurrence of *Q. gartneri*) from *Kennedy et al.* [2000] and references therein; first occurrence of *Q. gartneri* at Pueblo modified from *Watkins* [1985], by *Walsworth-Bell et al.* [in prep.].

the C/T boundary, a critical point in both isotope profiles is the level coinciding with the stratigraphically highest maximum $\delta^{13}C_{TOC}$ and $\delta^{13}C_{carb}$ value, respectively. This essentially marks the end-point of the main isotopic plateau, which would, in theory, also represent the end of OAE 2, as expressed by the positive carbon-isotope anomaly [see also *Kuypers et al*., 2002].

In the light of the above observations, we have calibrated the isotopic profiles of the remaining two sites (i.e. Tarfaya and Gubbio) against those for Eastbourne and Pueblo. The diverse lithological character of the Gubbio section (i.e. pelagic carbonate enveloping essentially carbonate-free black shale), however, has required a combination of the existing profiles in a composite stratigraphic framework (Fig. 6). Construction of the composite profile has been aided by a few additional TOC and phytane $\delta^{13}C$ data for extremely TOC-lean carbonate samples from within the Scaglia formation, collected immediately above and below the Bonarelli unit (Fig. 6). Interpretations of the composite Gubbio chemostratigraphic profile rest on the assumption that changes in the $\delta^{13}C$ values of marine organic and inorganic materials during OAE 2 largely reflect the isotopic composition of the dissolved inorganic carbon (DIC) reservoir, as controlled by increased global burial rates of isotopically light organic matter. This simplistic assumption facilitates the discussion that follows, but does not take into account other factors that may also affect the composition of bulk organic matter such as, for example, changes in the dissolved carbon dioxide content of the surface ocean [*Pratt* et al., 1988] and/or productivity-related changes in fractionation between DIC and biomass [*Kuypers et al*., 2002].

Figure 6 demonstrates that the Tarfaya and Gubbio isotopic profiles share some important similarities with the profiles from Eastbourne and Pueblo. In both Tarfaya and Gubbio, a sharp rise in $\delta^{13}C$ values of 3–4‰ is now evident for both TOC and phytane, in a similar fashion to the $\delta^{13}C_{TOC}$ record for Pueblo. Furthermore, high $\delta^{13}C_{TOC}$ and $\delta^{13}C_{Ph}$ values with little variation persist in both sections stratigraphically above the early isotopic maxima (spikes), resulting in the development of isotopic plateaus. However, the combination of individual records makes the stratigraphic definition of the end-points of these positive excursions rather unclear. In the Pueblo section, the $\delta^{13}C_{TOC}$ curve appears to return sharply to near pre-excursion values immediately above the C/T boundary, although the available record is of low-resolution and may not have captured the entire isotopic anomaly. All $\delta^{13}C$ records for the Tarfaya section are somewhat inconclusive in defining such a drop at any specific stratigraphic level, and this is particularly the case with the carbonate $\delta^{13}C$ profile. Similarly, the scarcity of $\delta^{13}C_{TOC}$ and $\delta^{13}C_{Ph}$ values above and below the Bonarelli level in the Gubbio section also preclude their use in establishing a concrete stratigraphic marker for the end-point of the isotopic excursion. It is likely, however, that the interval of relatively higher values of $\delta^{13}C_{carb}$ immediately above the Bonarelli horizon represents an extension of the positive isotope anomaly into the limestones above. In that case, the end of the plateau may be tentatively placed at approximately 1m above the stratigraphic top of the Bonarelli level (Fig. 6).

In summary, it appears that the two most conspicuous features of all isotopic profiles, namely the onset of the excursions and plateau of maximum $\delta^{13}C$ values, are sufficiently reproducible across all individual sections (Fig. 6) to allow a reasonably objective stratigraphic definition for at least the beginning and maximum isotopic expression of the Oceanic Anoxic Event. Chemostratigraphic definition of the end-point of the isotopic excursion, however, is clearly more contentious, but it appears that the last $\delta^{13}C$ plateau maximum may well represent the most suitable chemostratigraphic marker. The first appearance of the nannofossil *Q. gartneri*, an independent biostratigraphic marker (Fig. 6), coincides reasonably well in all sections, not only with the proposed end-point of the isotopic excursion, but also with the C/T boundary as defined by ammonite stratigraphy (i.e. first occurrence of the species *Watinoceras devonense*; [*Kennedy et al*., 2000], see Fig. 6). Consequently, this bioevent constitutes a particularly useful supplementary datum for placing both the C/T boundary and the end of OAE 2, especially in those cases where isotopic profiles fail to provide conclusive stratigraphic information.

6.5. Conclusions

Carbon-isotope records for total organic carbon, phytane and total carbonate from three contrasting Cenomanian/Turonian sections at Eastbourne in England, Gubbio in Italy and Tarfaya in Morocco, offer a global chemostratigraphic framework for the C/T Oceanic Anoxic Event. The onset of the isotopic anomaly, representing the initial increase in organic-matter burial rates, is clearly demonstrated by a rapid rise in $\delta^{13}C$ values for TOC/phytane by approximately 4‰, and for total carbonate, by ca. 2.5‰. The development of an isotopic plateau of near-constant, high $\delta^{13}C$ values stratigraphically above the initial excursion is also evident in all sections examined.

It is worth noting that the chemostratigraphic delimitation of the extent of OAE 2 offers a more reliable alternative to the original lithostratigraphic definition [*Schlanger and Jenkyns*, 1976], based on the presence of coeval organic-rich horizons in the C/T interval. The use of carbon isotopes as a proxy for globally enhanced organic-carbon sequestration is applicable to sites not characterised by enrichment in organic matter (e.g., Eastbourne). In addition, when considered against integrated chemo- and biostratigraphy, it is clear that C/T organic-rich and/or carbonate-poor horizons may be significantly diachronous (Fig. 6), probably reflecting the unique interaction between local palaeoceanographic conditions at each site and the global event.

Nevertheless, a number of limitations regarding the use of carbon-isotope profiles as a global chemostratigraphic tool have also been highlighted. Although the carbonate record in Eastbourne seems to be devoid of major post-depositional alteration, diagenetic modification in the isotopic composition of sedimentary carbonate in the Tarfaya section appears to have had a profound effect in obscuring the primary isotopic signal. TOC and phytane $\delta^{13}C$ profiles, albeit showing some similarities, also provide partially inconclusive evidence in terms of chemostratigraphic application. Despite capturing the onset and maximum expression of the positive isotopic anomaly associated with OAE 2, these records preclude formulation of a precise chemostratigraphic definition of the end-point of the excursion, probably as a consequence of local variations in organic-carbon productivity/preservation obscuring the global isotopic signal. The first appearance of the nannofossil *Q. gartneri* near the C/T boundary used in conjunction with the interpreted end-point of the isotopic plateau provides a useful supplementary stratigraphic tool in this regard. Invariably, integration of high-resolution, carbon-isotope records and detailed biostratigraphy will constitute an essential requirement for all future studies, which strive to link worldwide C/T sections under a common stratigraphic framework. In this instance, the OAE can be demonstrated to be largely, if not wholly, confined to the lattermost part of the Cenomanian Stage.

Acknowledgements

This work is supported by the European Unions's Improving Human Potential Program through the project "C/T-Net - Rapid global change during the Cenomanian/Turonian oceanic anoxic event: examination of a natural climatic experiment in earth history", under contract HPRN-CT-1999-00055, C/T-Net. Our results were produced in the wider context of C/T-Net research activities, and the contribution of all other network partners is gratefully acknowledged. In addition, we thank J. Cartlidge, T. O'Conell, R.M. Corfield and S. Wyatt (Oxford) for assisting with the isotopic and bulk TOC analyses, and D. Sansom (Oxford) for the preparation of the Eastbourne stratigraphic log. We are also grateful to SHELL for providing our research group with Tarfaya core S57.

Chapter 7

Mechanisms of black shale deposition at the NW African Shelf during the Cenomanian/Turonian Oceanic Anoxic Event: implications for climate coupling and global organic carbon burial

Chapter 7.

Mechanisms of black shale deposition at the NW African Shelf during the Cenomanian/Turonian Oceanic Anoxic Event: implications for climate coupling and global organic carbon burial

Authors: *Kolonic, S., T. Wagner, A. Forster, J.S. Sinninghe Damsté, B. Walsworth-Bell, S. Turgeon, H.-J. Brumsack, W. Kuhnt, H. Tsikos and M.M.M. Kuypers*

Status: submitted Journal: *Paleoceanography*

Abstract

High-resolution geochemical records from a depth transect through the Cenomanian/Turonian Tarfaya Basin (NW African shelf) reveal high-amplitude fluctuations in accumulation rates of organic carbon (OC), redox-sensitive and sulphide-forming trace metals, and biomarkers indicative of photic zone euxinia. These fluctuations are in general coeval and thus imply a strong relationship of OC burial and water column redox conditions. The pacing and regularity of the records and the absence of a prominent continental signature suggest a dynamic depositional setting linked to orbital or higher frequency forcing. Determining dominant frequency, i.e. obliquity or eccentricity, depends on the definition of the OAE2 and its duration. Both frequencies bear their own justification and thus require the discussion of two alternative orbital scenarios. Wind-driven upwelling of nutrient-rich, oxygen-depleted intermediate waters from the deep Atlantic and the periodic development of photic zone and deep-water euxinia were the prominent mechanisms determining marine sedimentation at Tarfaya. Accumulation records clearly identify the basin centre as the primary site of sediment deposition with highest temporal variability and an up to six-fold increase in OC burial from ~2 $g/m^2 \cdot a$ prior to the OAE2 to ~12 $g/m^2 \cdot a$ (eccentricity model) during the OAE2. Photic zone and bottom water euxinia alternated with periods of greater oxygenation of the water column in response to climate forcing. Assuming equal distribution of OC burial in the C/T ocean an enrichment factor of at least 50 is estimated for the Tarfaya Basin, which outlines the potential importance of this relatively small basins on the global carbon budget during the mid-Cretaceous OAEs.

Index Terms: 4802 Anoxic environments, 4806 Carbon cycling, 4267 Paleoceanography, 1055 Organic geochemistry, 1065 Trace elements
Key words: Cretaceous black shale, oceanic anoxic event, orbital forcing, biomarkers, trace metals, photic zone euxinia, global carbon burial, Tarfaya Basin.

7.1. Introduction

The Cretaceous was an extraordinary period in Earth history, when organic carbon (OC)-rich sediments were repeatedly deposited on a basin-wide or even global scale [e.g. *Hay et al.,* 1999; *Larson and Erba*, 1999; *Jones and Jenkyns*, 2001; *Leckie et al.*, 2002]. Three distinct intervals of particularly high OC burial rates are distinguished in the marine record, occurring during the Aptian-Albian, the Cenomanian/Turonian (C/T) transition, and the Coniacian-Santonian. These periods of enhanced global sequestration of OC, termed "Oceanic Anoxic Events" (OAEs) [*Schlanger and Jenkyns*, 1976; *Jenkyns*, 1980], favoured the formation of petroleum source rocks and affected the mid-Cretaceous climate by effectively reducing atmospheric pCO_2 [*Arthur et al.*, 1988; *Kuypers et al.*, 1999; *Wallmann*, 2001]. Although new insights into the functioning of the mid-Cretaceous ocean-atmosphere system have been gained in recent years [e.g., *Hay et al.,* 1999; *Larson and Erba*, 1999; *Jones and Jenkyns*, 2001; *Leckie et al.*, 2002, *Wallmann*, 2001; *Bice and Norris,* 2002; *Kuypers et al.*, 1999, 2002], the environmental factors that triggered and sustained these OAEs remain controversial. Increased submarine igneous activity associated with the formation of the Caribbean Oceanic Plateau, resulting in enhanced hydrothermal supply of bio-limiting metals and more efficient nutrient cycling due to a breakdown in thermal stratification, has been put forward as one possible trigger mechanism [*Larson and Erba*, 1999]. Meanwhile, *Kuypers et al.* [2002] demonstrated that deep-water black shale formation in the C/T low-latitude N Atlantic most likely resulted from a combination of enhanced organic matter (OM) preservation due to increased anoxia, and increased primary productivity.

The most pronounced OAE (hereafter referred to as the OAE2) occurred ~94 Ma ago, during the C/T transition, and is regarded as the type example of the Mesozoic OAEs. The OAE2 was associated with large and short-term changes in atmospheric pCO_2 [e.g., *Kuypers et al.*, 1999], extinction of marine biota [e.g., *Kuhnt et al.*, 1995; but see *Gale et al.,* 2000], and ocean chemistry turnover [e.g., *Brumsack et al*., 1980; *Kuypers et al*., 2002]. The OAE2 is characterized by a distinct positive excursion in the stable carbon-isotopic record ($\delta^{13}C$) of marine carbonate and marine and terrestrial OM [*Schlanger and Jenkyns*, 1976] This positive $\delta^{13}C$ shift is conventionally related to excess burial of OC [*Schlanger and Jenkyns*, 1976; *Jenkyns*, 1980; *Arthur et al.*, 1988].

The deposition of particularly thick OC-rich black shales indicates that the NW African shelf (Fig. 1) was a major site of OC burial during OAE2 [*Kuhnt et al*., 2001; *Kuypers et al.,* 2002]. The Tarfaya Basin on the NW African Shelf, contains more than 500 m of Upper Cretaceous laminated OC-rich biogenic sediments [*Leine*, 1986]. These black shales were deposited with sedimentation rates exceeding 10 cm/ka [*Kuhnt et al.*, 2001], allowing investigation of paleoceanographic changes and climate events on a centennial time-scale resolution.

This study aims to reassess the stratigraphic extension of the OAE2 in the Tarfaya Basin, and to reconstruct the mechanisms of black shale deposition on the NW African Shelf during the C/T transition with respect to climate coupling and global organic carbon burial. Applying a high-resolution approach to four sites located along a NW-SE depth transect through the Tarfaya Basin, we reconstruct: (1) trends of OC burial before, during, and after the OAE2; (2) the associated development and coupling of deep and photic zone anoxia; and (3) the mechanisms that drove black shale formation in the Tarfaya shelf basin in a spatio-temporal perspective, using organic and inorganic geochemical data. Thus allowing us to assess the importance of the mid-Cretaceous NW African shelf as a primary site of global OC burial.

7.2. Material and Methods

The samples were obtained from four sites along a NW-SE transect through the Tarfaya Basin (Figure 1), establishing a paleotransect of about 120 km in length connecting the deepest part of the basin (Sites S13 and S57) with transitional locations (Site S75) and a proximal location close to the paleocoastline (Mohammed Plage, Mpl). Sample material from S13, S57 and S75 was obtained from cores drilled by the Moroccan State Oil Company (ONAREP) and Shell Oil during the late 1970s and early 1980s [*Leine*, 1986], Sediment slices between 2 and 7 cm thick on average were taken from the investigated C/T core intervals. Mpl material was obtained from a coastal exposure.

All samples were dried and ground in an agate mortar before total (TC) and organic carbon (TOC) contents were measured using a LECO CS-300 carbon-sulphur analyzer (precision of measurements ±3%). For TOC determinations, inorganic carbon was carefully removed by repetitive addition of 0.25

N HCl. $\delta^{13}C$ values (±0.1‰ versus Vienna Pee Dee belemnite, VPDB) were measured on decalcified sediments, using automated on-line combustion followed by conventional isotope-ratio mass spectrometry. For biomarker analysis, pulverized samples (5 to 10 g) were extracted with an Accelerated Solvent Extractor (ASE) (temperature: 100°C; pressure: 100 psi; DCM:MeOH: 9:1). For most samples (i.e. from the S13, S75 and Mpl sites) an aliquot of the total extract was used for direct Raney Nickel desulphurization [*Petit and van Tamelen*, 1962; *Sinninghe Damsté et al.*, 1994] and subsequent hydrogenation in order to analyse both free and S-bound biomarkers in a single step. In the case of S57 extracts were first fractionated into an apolar and polar fraction and the polar fraction was subsequently desulphurized using Raney Nickel [*Kuypers et al*., 2002]. It is likely that isorenieratane and chlorobactane concentrations obtained in this way are lower than those determined after direct desulphurization of the total extract, since upon polar-apolar fractionation a substantial amount (i.e. up to 40% of the total extract) remains on the column. This material likely contains substantial amounts of S-bound aromatic carotenoids [*Koopmans et al*., 1996]. Samples were analyzed by gas chromatography-mass spectrometry (GC-MS) using a Hewlett-Packard 5890 gas chromatograph interfaced with a VG Autospec Ultima Q mass spectrometer operated at 70 eV with a mass range m/z 50-800 and a cycle time of 1.8 seconds (resolution = 1000). Compounds were identified using both GC relative retention times and mass spectra by comparison with literature data and reference standards. For compound specific $\delta^{13}C$ sulphur-bound phytane measurements, the polar fractions were first treated by Raney Nickel desulphurization, in order to release sulphur-bound hydrocarbons, followed by column separation and hydrogenation of the apolar fractions to yield phytane. All compound-specific carbon-isotope measurements were carried out at least in duplicate (s = ±0.03 to 0.58) as described by [*Kuypers et al*., 2002] and the mean $\delta^{13}C$ values for each sample are presented in the usual δ notation versus the VPDB standard. The analytical accuracy of the irm-GC-MS was monitored by adding an internal standard of known isotopic composition to every individual sample injection.

Major, minor and trace element composition was determined using either XRF spectrometry on fused-borate glass beads (S13 and S57) or by inductively coupled plasma-atomic emission spectrometry (ICP-AES; S75 and Mpl). XRF calibration curves were based on international standard reference material. Measured values were within 3% of the accepted value and standard deviation of three replicates was less then 3%. For ICP-AES, about 50 mg of sample was digested in a mixture of 3 ml HNO3 (65%), 2 ml HF (40%) and 2 ml HCl (36%) of supra-pure quality at 200°C and 30 kbar in closed Teflon vessels [*Heinrichs et al.*, 1986]. After drying by evaporation, the residue was re-dissolved with 0.5 ml HNO_3 (65%) and 4.5 ml deionised water. Subsequently, the solutions were analyzed with ICP-AES, and the results checked with international standard reference material; relative standard deviations in duplicate measurements were below 3%.

Sedimentation rates (SR) and mass accumulation rates (MAR) of OC, $CaCO_3$, trace metals, and biomarkers were calculated assuming that SRs were linear within each individual sedimentary cycle. To calculate bulk MARs dry bulk density (DBD) instead of wet bulk density and porosity was used [*Stein*, 1991]. DBD was obtained from core density logs of S13 and S75 and extrapolated to S57 and Mpl [*Leine,* 1986; *Kuhnt et al.,* 1997]. S57 and Mpl densities were determined assuming the same linear relationship between TOC and DBD as observed in S13 and S75 ($r^2 = 0.95$).

7.3. Geological setting, lithology and organic matter composition

The Tarfaya Basin is situated southwest of the Anti-Atlas Mountains. It extends into the Tindouf Basin to the east and the Sénégal Basin to the south; its western margin is defined by the East Canary Ridge. The basement is composed of folded Precambrian and Paleozoic rocks, which are unconformably overlain by Mesozoic sediments whose thickness locally exceeds 12 km [*Heyman,* 1989]. Covering a total area of about 170,000 km^2, the Basin hosts one of the largest oil-shale deposits in the world [*Amblés et al.*, 1994], reaching an exceptional thickness of up to 500 m. Detailed and comprehensive geological descriptions of this area have been provided by *Martinis and Visintin* [1966], *Viotti* [1965, 1966], *Choubert et al.* [1966, 1972], *Wiedmann et al.* [1978], *von Rad and Arthur* [1979], *von Rad and Einsele* [1980], *Ranke et al.* [1982], and *Heyman* [1989].

The C/T black shales of the entire Tarfaya Basin reveal distinct similarities in bedding structures, composition, and cyclicity, which allow basin-wide correlation of individual beds. Sedimentary bedding cycles mainly consist of

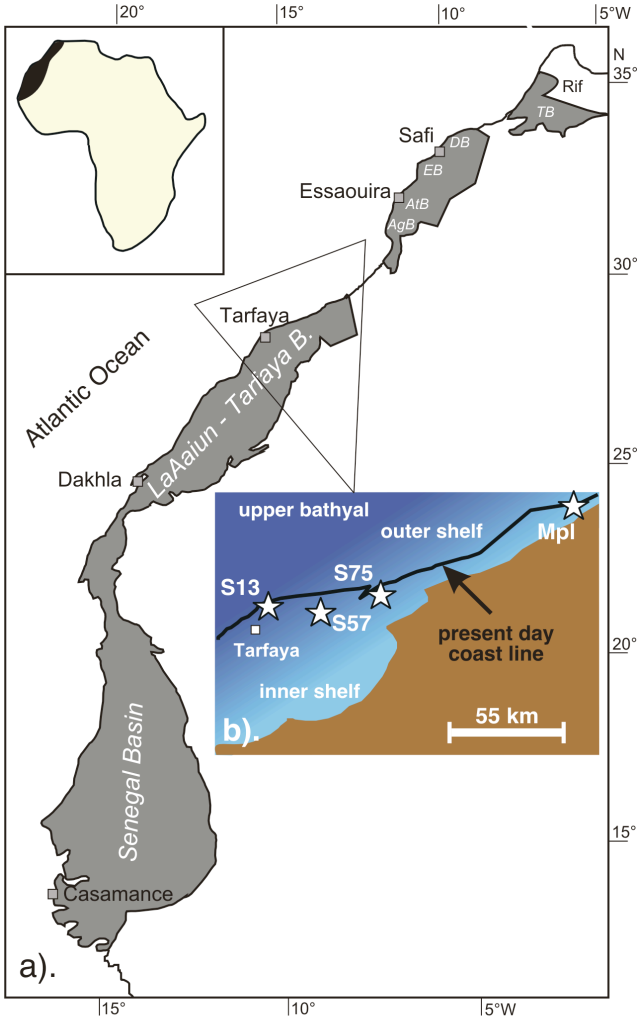

Figure 1. (a) Distribution of unfolded Mesozoic and Cenozoic coastal basins containing OC-rich C/T black shales along the NW African continental margin [modified from *Lüning et al.*, 2003] (b) Paleogeographic map of the Tarfaya Basin with the positions of the studied sites along a depth transect from the basin centre (S13, S75, S57) close to the paleocoastline (Mpl). Abbreviations; AgB.: Agadir Basin, AtB.: Atlas Basin, EB.: Essaouira Basin, DB.: Doukkala Basin, TB.: Taddla Basin.

two types of lithology, i.e. dark brownish-grey, laminated, kerogenous chalks which alternate with non-laminated, lighter coloured, often nodular limestones with lower kerogen contents.Beds with up to meter-size carbonaceous concretions, lenses of chert and siliceous limestone and tempestite beds showing characteristic hummocky cross-stratification structures [*El Albani et al.*, 1999ab] form distinct interlayers, which can be traced over large distances and frequently serve as excellent correlation levels. These main lithologies have been sub-divided into various types of microfacies as proposed by *El Albani et al.* [1999ab].

Main components of the kerogen-rich chalks are fecal pellets containing abundant calcareous nannofossils, foraminiferal tests, kerogen-flasers, and a carbonate-matrix mainly composed of nannofossils and micrite [*Leine*, 1986]. A detailed and comprehensive description of the OM of the Tarfaya black shales is given in *Kolonic et al.* [2002]. Accordingly, the Tarfaya black shales are characterized by high hydrogen indices between 400 and 800 (mgHC/gTOC), indicating a dominant marine origin of sedimentary OM (type I-IIS kerogen). Organic petrological studies confirm the latter conclusion, and show that the bulk sedimentary OM is almost entirely composed of a brightly fluorescing groundmass with high abundances of lamalginite and bituminite, while detrital vitrinite and inertinite are only present in trace amounts. The persistence of low Tmax values obtained from Rock-Eval pyrolysis (404-425°C) supports an immature to very early mature level of thermal maturation in terms of hydrocarbon (HC) generation. Total lipid analyses performed after desulphurization of the total extract show that biomarkers mostly comprise short-chain (C_{16}-C_{22}) and long-chain (C_{25}-C_{35}) *n*-alkanes with no odd-over-even predominance, together with steranes, hopanoids and acyclic isoprenoids [*Kolonic et al.,* 2002]. Flash pyrolysis GC-MS analysis of the kerogen confirms the aliphatic nature of the bulk OC. Phenols and methoxyphenols, both pyrolysis products of lignin and thus indicative of higher plant biopolymers [*Saiz-Jimenez and de Leeuw*, 1984, 1986], are only present in trace amounts [*Kolonic et al.,* 2002].

7.4. Basin biostratigraphic framework and cyclostratigraphy

This study focuses on the chronostratigraphic interval between ca. 92 and 95 Ma BP and spans three planktonic foraminiferal zones (PFZs; Fig. 2), i.e. (a) the early to late Cenomanian *Rotalipora cushmani* PFZ, (b) the late Cenomanian to early Turonian *Whiteinella archaeocretacea* PFZ, and (c) the early to late Turonian *Helvetoglobotruncana helvetica* PFZ [*Obradovich*, 1993; *Gradstein et al.*, 1995]. The planktonic foraminiferal biostratigraphy of *Kuhnt et al.* [1990, 1997, in press] was applied to S13 (top *R. cushmani* to base *H. helvetica* PFZ) and S75 (top *R. cushmani* to base *H. helvetica* PFZ). New planktonic foraminiferal biostratigraphic data were used for S57 (top *R. cushmani* to mid-*W. archaeocretacea* PFZ) [*Tsikos et al.,* Carbon-isotope stratigraphy recorded by the Cenomanian/Turonian Oceanic Anoxic Event: correlation and implications based on three key-localities, *submitted to Journal of the Geological Society, London*]. For Mpl (middle *R. cushmani* to base *W. archaeocretacea* Zone), the biostratigraphy of *Luderer* [1999] was applied. This planktonic foraminiferal biostratigraphy was supplemented by calcareous nannofossil data [*Mutterlose, personal communication* January 2003].

A detailed cyclostratigraphic time model for late Cenomanian to early Turonian rhythmic sedimentation in the Tarfaya Basin recently supplemented by sub-division of the entire section into eight stages, using a combination of high-resolution density records as well as biostratigraphy and bulk carbon isotope profiles has been proposed (Fig. 2) [*Kuhnt et al.*, 1997, in press; *Luderer*, 1999]. Applying time-series analysis to density logs obtained from six sites (including S13 and S75), thirty-two sedimentary cycles were identified, each representing a couplet of one carbonate-rich and one OC-rich bank [*Kuhnt et al.*, 1997; *Luderer*, 1999]. The cycle containing the age-diagnostic last occurrence (LO) of *R. cushmani* (~93.9 Ma) was designated Cycle 0. The lateral consistency of sedimentary cycles allows basin-wide correlation of individual sites. We use these published results in combination with new biostratigraphy and carbon isotope chemostratigraphy to extend the correlation of the Tarfaya cycles over a distance of between 75 and 125 km, from the deepest part of the basin (S13) towards the paleocoastline (Mpl). At Mpl, bedding cycles were identified using detailed lithological descriptions obtained during fieldwork. The C/T boundary is placed in Cycle 3 using the first occurrence (FO) of the nannofossil *Quadrum gartneri* (the lowermost observation of this marker species in the Tarfaya Basin is just above a large coring gap at S57, resulting in the absence of Cycle 3; as such this event cannot be placed with more confidence).

7.5. Results and Discussion

7.5.1. Reconsideration of the stratigraphic extension of the OAE2 at Tarfaya: implications for time and depositional models

7.5.1.1. The OAE2 at Tarfaya

Although the OAE2 $\delta^{13}C$ excursion is characterized by several spikes and nudges in the various key sections reported from the Atlantic and Tethyan realms [*Gale et al.*, 1993; *Tsikos et al.,* Carbon-isotope stratigraphy recorded by the Cenomanian/Turonian Oceanic Anoxic Event: correlation and implications based on three key-localities, *submitted to Journal of the Geological Society, London*], it has been suggested that the excursion is most easily divided into three major phases [*Kuypers et al.*, 2002]: Phase A, a rapid increase in $\delta^{13}C$ values in the uppermost *R. cushmani* PFZ; Phase B, a plateau of maximum $\delta^{13}C$ values in the lower *W. archaeocretacea* PFZ; and Phase C, a gradual return to pre-excursion values, which ends in the *H. helvetica* PFZ. Phases A and B represent the isotopic expression, and thus the stratigraphic extension, of the OAE2.

The $\delta^{13}C_{org}$ record for S13 has been published by *Kuhnt et al.,* [1990], but is complemented in this study by additional samples and by previously unreported compound-specific $\delta^{13}C$ values for sulphur-bound phytane ($\delta^{13}C_{Ph}$) at lower resolution. Sulphur-bound phytane is a diagenetic product of algal cholorophyll [see Kuypers *et al.,* 2002 for a detailed discussion] and its isotopic composition reflects the isotopic composition of photoautotrophs at the time of deposition. $\delta^{13}C_{org}$ and $\delta^{13}C_{Ph}$ for S57 have been generated by *Tsikos et al.* [Carbon-isotope stratigraphy recorded by the Cenomanian/Turonian Oceanic Anoxic Event: correlation and implications based on three key-localities, *submitted to*

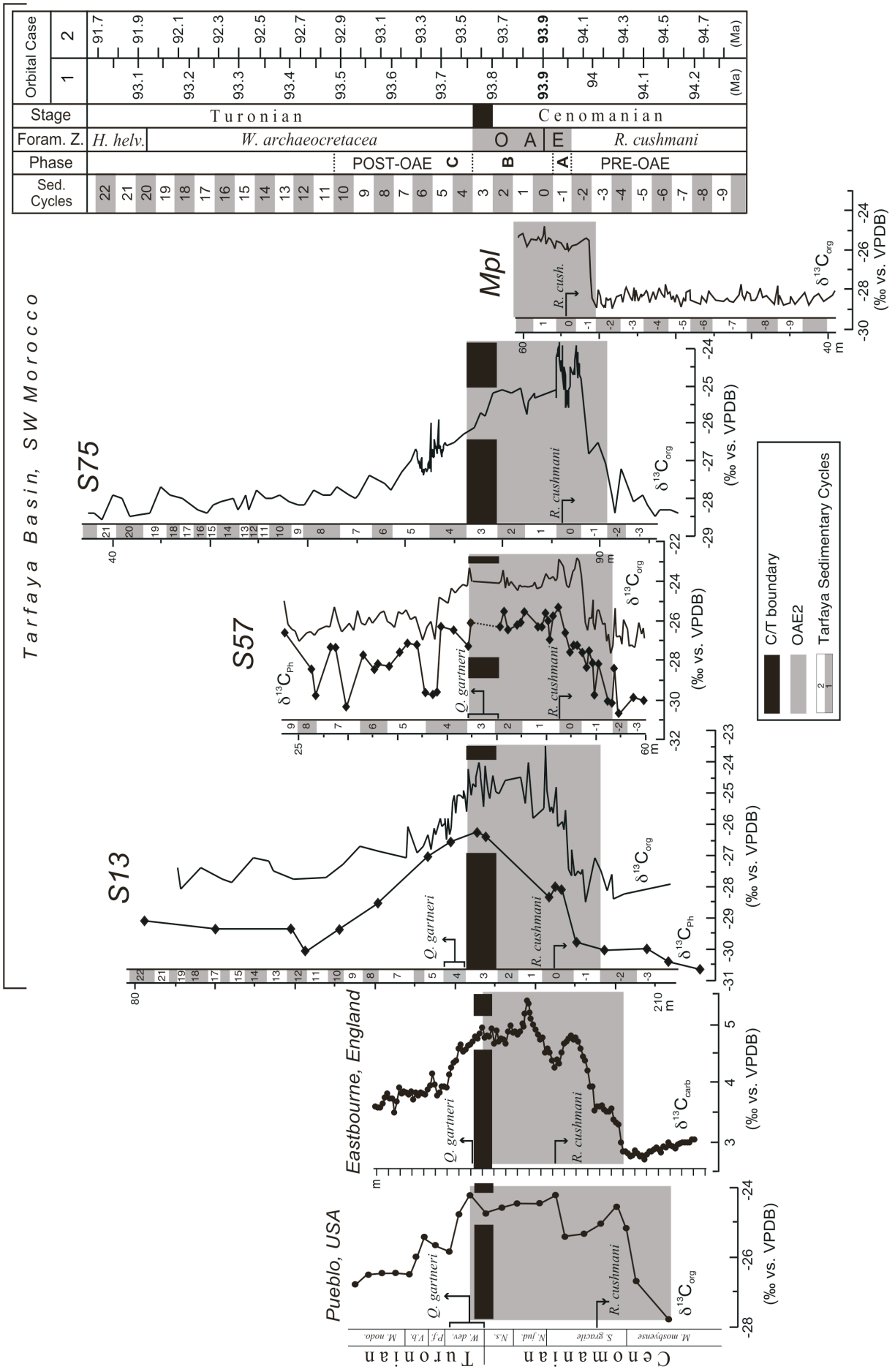
Orbital Case
Stage
Foram. Z.
Phase
Sed. Cycles
Turonian
Cenomanian
H. helv.
W. archaeocretacea
R. cushmani
OAE
POST-OAE
PRE-OAE
Tarfaya Basin, SW Morocco
S75
S57
S13
MpI
Eastbourne, England
Pueblo, USA
Q. gartneri
R. cushmani
R. cush.
C/T boundary
OAE2
Tarfaya Sedimentary Cycles
(‰ vs. VPDB)

Figure 2. Carbon isotope records (in ‰ vs. V-PDB) of bulk organic carbon and key bioevents from the investigated Tarfaya sites in comparison to the C/T reference sites at Pueblo (Colorado, USA) and Eastbourne (Sussex, UK). C/T boundary placed at Pueblo and Eastbourne using ammonites [*Kennedy et a*l., 2000; *Gale et al*., 1993], and at Tarfaya using the FO *Q. gartneri* (nannofossil). The $\delta^{13}C$ Phases of *Kuypers et al*. [2002] and the position of the OAE2 (Phases A and B) are shown, as are the ages assigned to the Tarfaya cycles based on Orbital Cases 1 and 2 (see text). Pueblo data (except FO *Q. gartneri*) from *Kennedy et al*. [2000] and references therein. Eastbourne $\delta^{13}C_{carb}$, S57 $\delta^{13}C_{org}$ and $\delta^{13}C_{Ph}$ from *Tsikos et al.* [submitted]; S75 $\delta^{13}C_{org}$ from *Kuhnt et al.* [2001, in press]. LO *R. cushmani* at Eastbourne and S57 from *Tsikos et al.* [submitted], at S13 and S75 from *Kuhnt et al*. [1997, in press], and at Mpl from *Luderer* [1999]. FO *Q. gartneri* at S13 from *Mutterlose* [personal communication January 2003].

Journal of the Geological Society, London], and $\delta^{13}C_{org}$ for S75 by *Kuhnt et al.* [2001, in press]; for Mpl a high-resolution $\delta^{13}C_{org}$ record has been generated (Fig. 2).

All $\delta^{13}C_{org}$ profiles from the Tarfaya sections clearly follow the threefold geometry identified by *Kuypers et al.* [2002], but also show higher frequency variations (Fig. 3). These high-frequency variations may to some extent be explained by variable contributions of terrestrial and marine OM, but more likely reflect differences in the composition of the marine OM itself. In principle, differences in bulk $\delta^{13}C_{org}$ may be related to different relative proportions of isotopically heavy and relatively light OM [*van Kaam-Peters et al.*, 1998]. It has been shown, for example, that variations in the contribution of sulphurized carbohydrates to the sedimentary OM may account for changes in the isotopic composition of OC of up to 6 ‰ in black shales of the Kimmeridge Clay [*van Kaam-Peters et al.*, 1998; *Sinninghe Damsté et al.,* 1998]. Large variations in the degree of OM sulphurization postulated for the Tarfaya black shales [*Kolonic et al.,* 2002] may well therefore account for the recorded high frequency variations in $\delta^{13}C_{org}$.

There is a good agreement between the isotopic and cyclostratigraphic records of sites S13, S57, S75 and Mpl (Fig. 2). In addition, the isotopic records provide a stratigraphic framework for the definition of the extent OAE2. Cycle -1 essentially corresponds to $\delta^{13}C$ Phase A, Cycles 0-3 to Phase B, and Cycles 4-10 to Phase C (Fig. 2). As such the OAE2 ($\delta^{13}C$ Phases A and B) is recorded by Cycles -1 to 3. The placement of the end of the OAE2 at the boundary of Cycles 3 and 4 contradicts previous work [*Kuhnt et al.*, 1997; *Kuypers et al.*, 2002] and is, therefore, addressed in more detail below. At Pueblo (Colorado, USA), the proposed Global Boundary Stratotype Section for the base of the Turonian [*Kennedy et al.,* 2000], the end of the OAE2 ($\delta^{13}C_{org}$ Phase B/C boundary) falls near the C/T boundary, as defined by the base of the *Watinoceras devonense* Ammonite Zone [*Kennedy et al.*, 2000] (Fig. 2). An associated bioevent is first occurrence (FO) *Q. gartneri* (nannofossil). These observations have been reproduced at Eastbourne (Sussex, England; Fig. 2), where a much more detailed OAE2 $\delta^{13}C_{carb}$ record is available [*Tsikos et al.,* Carbon-isotope stratigraphy recorded by the Cenomanian/Turonian Oceanic Anoxic Event: correlation and implications based on three key-localities, *submitted to Journal of the Geological Society, London*], together with ammonite [*Gale et al.*, 1993] and nannofossil biostratigraphy. At Tarfaya, the Phase B/C boundary falls at the top of Cycle 3. To ensure that our placement of the end of the OAE2 at Tarfaya is not compromised by the effect of heterotrophy, preservation and diagenesis on the carbon isotope signature of OC [*Kuypers et al.*, 2002], it is important to employ independent biostratigraphic evidence. Unfortunately, the *W. devonense* Ammonite Zone is not well constrained in the Tarfaya Basin [*Kuhnt et al.*, 1997]. However, the FO of *Q. gartneri* at S13 [*Mutterlose, personal communication January* 2003] and S57 supports the placement of the end of the OAE2 at the top of Cycle 3 (Fig. 2).

Using bulk ($\delta^{13}C_{org}$) data from S75 a much longer interval has been assigned to the OAE2 at Tarfaya [*Kuhnt et al.*, 1997; *Kuhnt et al.*, in press]. According to the more recent interpretation [*Kuhnt et al.*, in press], the OAE2 approximately corresponds to Cycles -2 to 8 (11 cycles) although the placement of the end of the OAE2 at the top of Cycle 8 is based on a problematic correlation of the FO *H. helvetica* (planktonic foraminifer) with the base of the *W. devonense* Ammonite Zone. Additionally, the FO *H. helvetica* is extremely late with regard to other bioevents and the $\delta^{13}C$ excursion at Tarfaya [*Kuhnt et al.,* in press]. *Kuypers et al.* [2002] followed this stratigraphic model and included an interval corresponding to Cycles -1 to 8 within the OAE2, based on compound-specific $\delta^{13}C$ values. This assignment, however, is not supported by either biostratigraphy or the $\delta^{13}C_{org}$ record, and may result from the relatively low resolution of their molecular isotope data. In fact

our new compound-specific $\delta^{13}C$ curves for sulphur-bound phytane ($\delta^{13}C_{Ph}$) for S13 and S57 are fully consistent with our new placement of the end of the OAE2 at the top of Cycle 3 (Fig. 2).

7.5.1.2. Duration of the OAE at Tarfaya

Differences in the definition of the OAE2 have resulted in a broad range of published estimates of its duration (estimates vary between 250 ka [*Arthur and Premoli Silva*, 1982; *Lamolda et al.,* 1994*; Paul et al.,* 1994] and 700 ka [*Arthur and Premoli Silva*, 1982]). Figures based on radiometric dating [*Obradovich*, 1993] are subject to large error, whilst those based on cyclostratigraphy [*Lamolda et al.*, 1994; *Paul et al.*, 1994; *Kuhnt et al.*, 1997; *Caron et al.*, 1999; *Prokoph et al.*, 2001] rely on correct identification of Milankovitch cycles and the absence of significant hiatuses. Arguably the most useful figure is still that of 500 ka, based on radiometric dating in the US Western Interior [*Obradovich*, 1993].

Kuhnt et al. [1997, in press] applied this estimate of 500 ka in identifying Tarfaya Cycles -2 to 8 as representing obliquity (39 ka periodicity), based on mean cycle duration calculated from their assignment of approximately eleven cycles to the OAE2. This is contradicted by our new chemo- and biostratigraphic assignment of only five cycles (Cycles -1 to 3) to the OAE2, which, following the same logic, suggests that cycle duration is more compatible with short eccentricity (100 ka). Whilst still subject to the error associated with radiometric ages, this new interpretation is consistent with results from the Bahloul Formation, Tunisia, where four 100 ka cycles have been reported from within the OAE2 interval [*Caron et al.*, 1999]. It is also more consistent with the order of Milankovitch cyclicity expected for a mid-Cretaceous low-latitude basin, when obliquity cycles were characteristic of higher latitudes. However, the obliquity interpretation of Kuhnt et al. [1997, in press] cannot be disregarded, as these authors not only advanced a paleoceanographic explanation for the obliquity record at Tarfaya but also supported it using spectral peak ratios.

In order to reconstruct controls on marine sedimentation during Tarfaya black shale formation, we present geochemical data as mass accumulation rates (*MARs*), applying both the earlier cyclostratigraphic model of Kuhnt et al. [1997, in press] (Orbital Case 1) and our new model (Orbital Case 2) for the periodicity of the cycles (Fig. 2):

Orbital Case 1: In this scenario, the Tarfaya cycles represent obliquity (39 ka). Although *Kuhnt et al*. [1997, in press] indicate that precession cycles may dominate above Cycle 8 in the more proximal parts of the basin (S75), we suggest that the coexistence of two modes of Milankovitch cyclicity in the same basin is unlikely, whilst obliquity is supported by their time-series analysis of the majority of sites. Based on the given stratigraphy, the investigated Tarfaya sections cover the time interval from 92.9 to 94.3 Ma (ages of individual samples are determined by linear interpolation between the assigned age control points for each individual cycle; the designated age fix-point in both orbital cases is LO *R. cushmani* at 93.9 Ma, in Cycle 0). The implied duration of the OAE2 (Cycles -1 to 3, as determined here) was ~200 ka; this appears somewhat brief even with regard to the shortest previous estimates (250 ka; *Arthur and Premoli Silva,* 1982; *Lamolda et al.,* 1994; *Paul et al.,* 1994).

Orbital Case 2: Following our new time model, the cycles represent short eccentricity (100 ka) and the studied interval represents the time span from 91.7 to 94.9 Ma. In this case the duration of the OAE2 (Cycles -1 to 3, as determined here) is ~500 ka (note that this is the radiometric estimate [Obradovich, 1993] 'transferred' to Tarfaya from the US Western Interior (see above), and used to estimate the duration of the cycles; as such this figure has not been independently established using the Tarfaya cycles).

7.5.2. Mechanisms of black shale deposition in the Tarfaya Basin

7.5.2.1. Variations in carbon, biomarker and trace metal contents

Despite the vicinity to the African continent, the Tarfaya Basin did not receive a significant terrestrial contribution during the C/T. This is clearly indicated by the extremely low abundance of metals of terrestrial origin like Zr (~0.004%), Al (~1%) and Ti (~0.07 %) throughout the depth-transect studied. Instead linear sedimentation rates (*SRs* in cm/ka) and mass accumulation rates (*MARs* in weight-unit/m^2·a) of the bulk sediments are primarily controlled by biogenic carbonate/silica

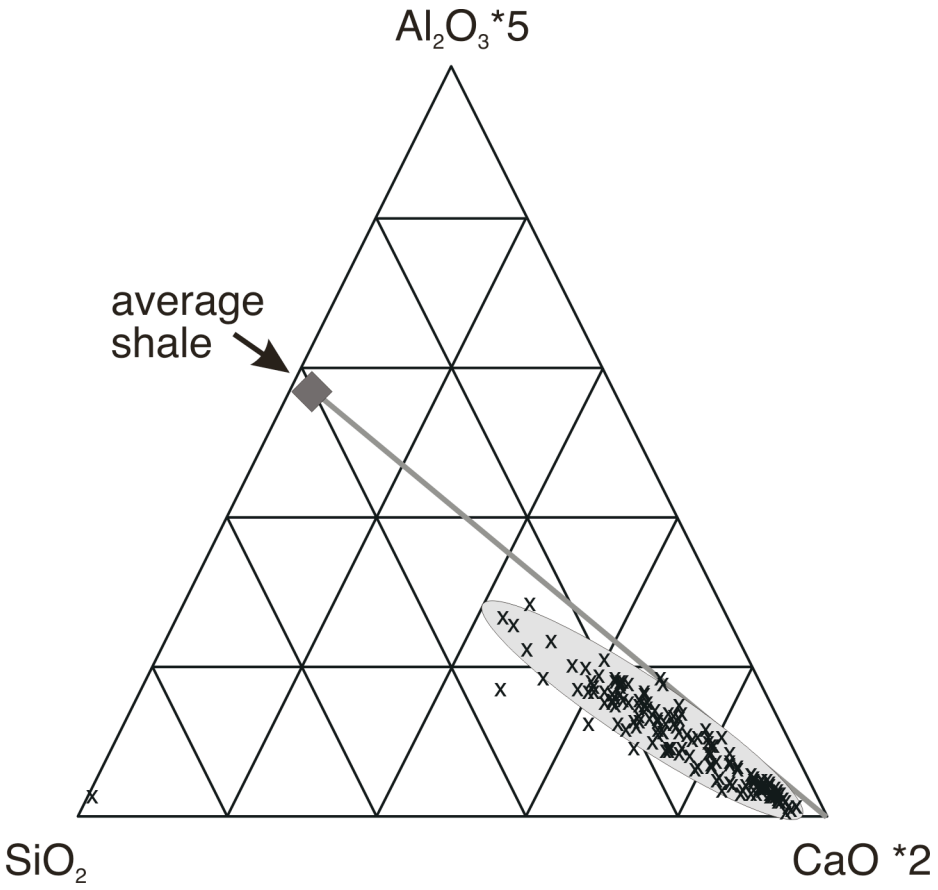

Figure 3. Triangle plot showing the major chemical components of the Tarfaya black shale (data from S13 and S57, as SiO_2 was not determined for S75 and Mpl). Arbitrary multipliers (Al_2O_3·5 and CaO_2·2) are introduced in order to centre the data on the graph. The chemical composition of the Tarfaya shales is very similar to a carbonate-diluted average shale [*Wedepohl*, 1971].

deposition. The significance of biogenic carbonate and silica as the most important components of the sediments is shown by the fact that the investigated samples plot slightly below the trend line connecting the carbonate and the average shale end members (Fig. 3) (we concede, however, that it is almost impossible to quantify biogenic silica using chemical methods, due to almost complete recrystallization into opal-CT). Hence the variations in OC, trace metal and biomarker abundances are expressed as MAR to obtain records that are independent of cyclic variations in carbonate/silica flux.

7.5.2.2. Linear sedimentation and mass accumulation rates

SRs and corresponding *MARs* of individual redox-and productivity-proxies are given for both orbital cases (***Orbital Case 2* in brackets**). On average, *SRs* are moderate to high, on the order of about 4 cm/ky *(1.6 cm/ky)* at Mpl, 6 cm/ky *(2.4 cm/ky)* at S57 and S75, and up to 12 cm/ky *(4.8 cm/ky)* at S13 (Fig. 4). They more than double over the stratigraphic interval and generally approach highest values at the transition from OAE2 Phase B to Phase C (Cycles 3 and 4), and decrease gradually within Phase C (Fig. 4). Also, SRs are often elevated in odd-numbered cycles. Small variations in this general pattern along the site transect are most likely attributable to local effects of topography, ocean currents, sediment grain size, and/or productivity. The general pattern, however, indicates the presence of a lower-frequency rhythm being superimposed on the well-developed bedding cycles. At S13, one such low-frequency cycle may cover between 8 and 11 high frequency bedding couplets (Fig. 4). The *MARs* are highest in Cycles -1 to 8 covering the OAE2 (Phases A and B) and the beginning of Phase C. Maximum *MARs* of up to 500 (200) g/m^2·a occur at the most distal Site S13. Averaged values of about 400 *(160)*, 150 *(60)*, 200 *(80)* and 100 *(40)* g/m^2•a for S13, S57, S75 and Mpl, respectively, indicate a distinct trend of decreasing MARs from the basin centre to the more proximal sites.

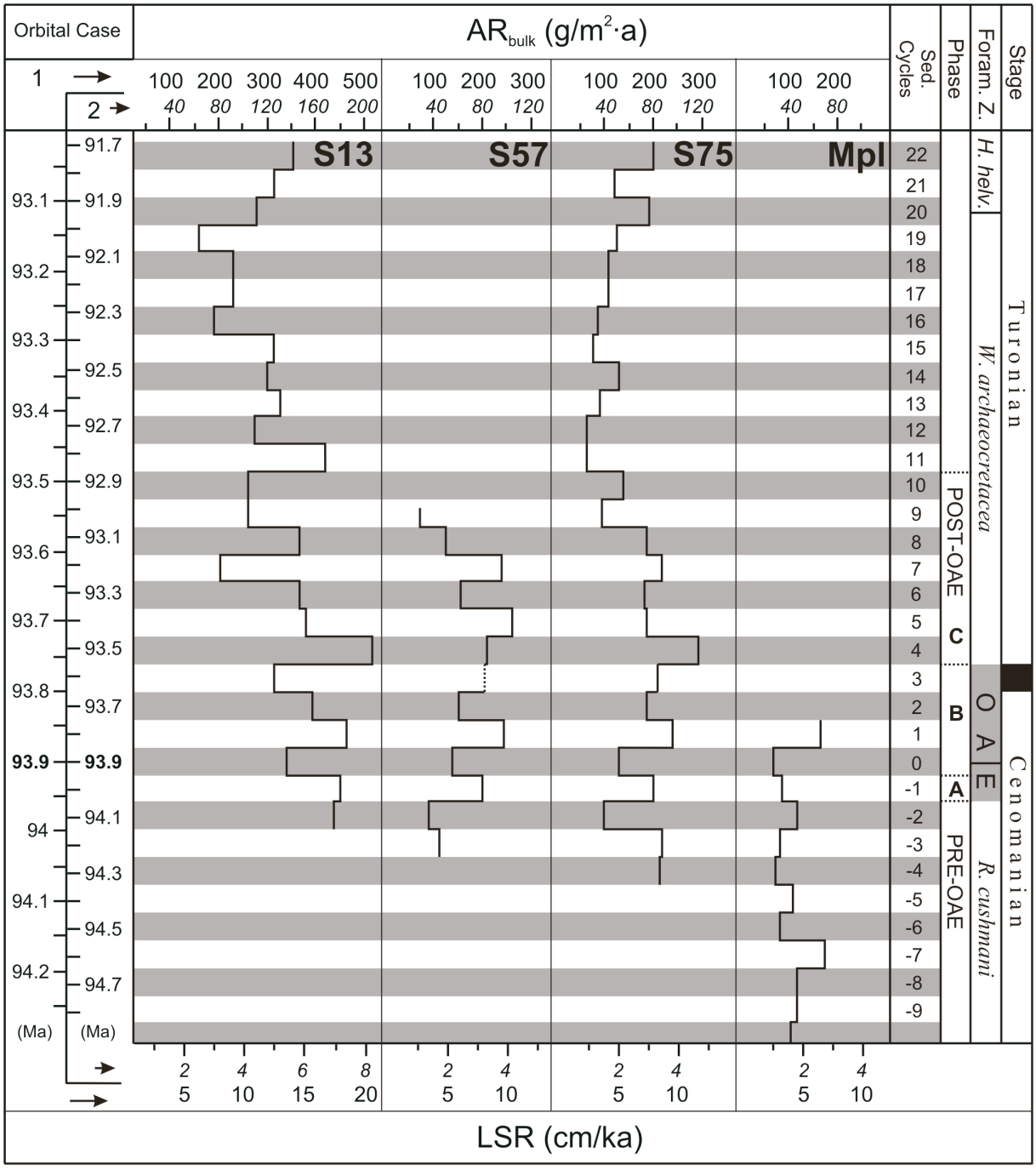

Figure 4. Linear sedimentation rates (cm/ka) and bulk accumulation rates (g/m^2·a) for the investigated Tarfaya sites given for both orbital cases.

7.5.2.3. Variations in organic carbon mass accumulation rates

Average OC accumulation rates (*OC MAR*) for the Tarfaya Basin (Fig. 5) increase from ~6 g/m^2·a before the OAE2 to ~16 *(6)* g/m^2·a during the OAE2 and remain high during post-OAE Phase C (~18 g/m^2·a). This general pattern is most pronounced in the basin centre at S13, where average *MAR OC* increases by a factor of six from ~4.5 *(2)* g/m^2·a prior to the OAE2 to ~31.1 *(12)* g/m^2·a during the OAE2. This distinct increase is followed by a moderate decrease during post-OAE Phase C down to ~25 *(10)* g/m^2·a. A similar, although less pronounced trend is observed for the transitional Sites S57 and S75 (for Mpl no data is available for Phase C). Average *OC MAR* at the transitional Sites S57 and S75 are two to four times lower than those at Site S13 in the basin centre (Fig. 5). At Site S75, the average trend differs from the other records by its relatively high *OC MAR* for the period pre-dating

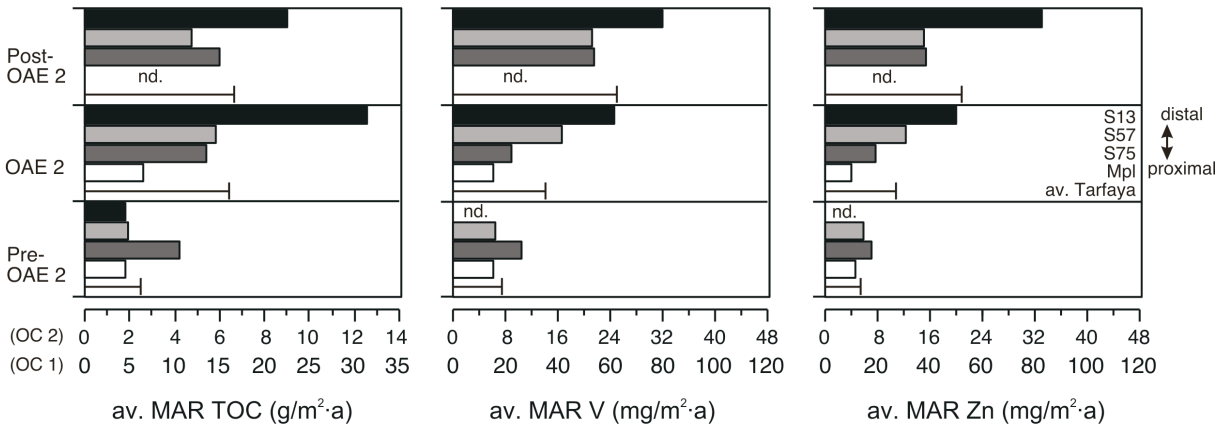

Figure 5. General trends of average accumulation rates of OC, V, and Zn (g/m^2·a) across the Tarfaya core transect and separated according to their stratigraphic position relative to the OAE2 (*S13*- Black bar; *S75* - dark grey bar; *S57* - light grey bar; *Mpl*- white bar; *Tarfaya Average* – bold line). *MARs* are given for *Orbital Case 1* (OC 1) and *Orbital Case 2* (OC 2). Pre-OAE2 essentially corresponds to the interval predating Cycle -1, 'OAE2' to Cycles -1 to 3 (Phases A and B), and 'post-OAE2' to Cycles 4-10 (Phase C) (see also Figure 2). Note that for the post-OAE2 estimated average Tarfaya values are based on three sites only because no data is available for Mpl. The same holds true for pre-OAE2 trace metal *MARs* where no data is available for S13. Since Mpl always has the lowest and S13 the highest values, it may not be appropriate to compare the pre-OAE2, OAE2 and post-OAE2 Tarfaya average values, since the latter are biased towards higher or lower values.

the OAE2. Opposite to the other sites, there is only a moderate increase in average *OC MAR* from ~10 *(4)* g/m^2·a during the pre-OAE2 to ~12.5 *(5)* g/m^2·a during OAE2 at Site S75. At Site Mpl, average *OC MAR* also exhibit a moderate increase from pre-OAE2 ~4.4 *(1.7)* g/m^2·a to OAE2 times ~6.2 *(2.5)* g/m^2·a.

Superimposed on the long-term trend are distinct higher frequency and high-amplitude fluctuations in *OC MAR* (Fig. 6). These amplitudes are generally higher in the central part of the basin (S13, S57 and S75) compared to the proximal Mpl, and often synchronous (e.g. in Cycles -1, 1, and 3/4). The extreme differences between baseline and maximum values approach 44 g/m^2·a (2-8 g/m^2·a baseline, 35-46 g/m^2·a maximum) at Sites S57 and S75. They even increase up to 70 g/m^2·a (2-8 g/m^2·a baseline, 73 g/m^2·a maximum) at S13 revealing widespread, drastic and short-term fluctuations in *OC MAR*. At the proximal Mpl, *OC MAR* is consistently lower, both in minimum and maximum values, ranging from baseline values below 1 g/m^2·a as high as 14 g/m^2·a (maximum amplitude 13 g/m^2·a, for comparison). Baseline, maximum, and average MARs clearly identify the basin centre as the primary site of OC burial. Given the different time resolution, stratigraphic range, and cyclostratigraphic uncertainty of the study sites, peak accumulation of OC was centred on Cycles -7 (pre-OAE) and 1 (Phase B) near the paleocoastline. In the deeper part of the basin, highest accumulation of OC was restricted to Cycles -1 (Phase A) through 8 (Phase C), approaching maximum values during cycles 1 (at all sites) and the upper part of cycle 3 (end of Phase B, S75) through the lower part of Cycle 5 (lower part of Phase C, S13 and S57) (Fig. 6). These periods of maximum OC accumulation are obviously structured by bundles of three to five individual peaks, best documented in Cycle 1 at S57 and in Cycle 8 at S13 (Fig. 6), but also recognizable at the other sites. These bundles cover about one sedimentary cycle, which, given their assigned duration of about 100 or 40 ka, most likely reflect precessional or millennial-scale (~5-7 ka) fluctuations in *OC MAR*. The identification of precessional- or higher-frequency forcing in the geological record, off course is restricted to a few sedimentary cycles where data resolution is sufficiently high. Sub-Milankovitch forcing with a wavelength of approximately 20-30 cm (corresponding to about 3-4 or 7.5-10 kyr, depending on whether Orbital Case 1 or 2 is applied) has been identified in the TOC profile of Cycle 0 at Site 75 [*Kuhnt et al*., 2001]. A similar frequency is recognized in mm-scale XRF scanning profiles of Sites S57 and S75 and power spectra obtained from high-resolution gray-scale data of the complete S75 section [*Kuhnt et al*., in press]. The presence and consistency of this high frequency variability in *OC MAR* strongly supports a close link to climate change.

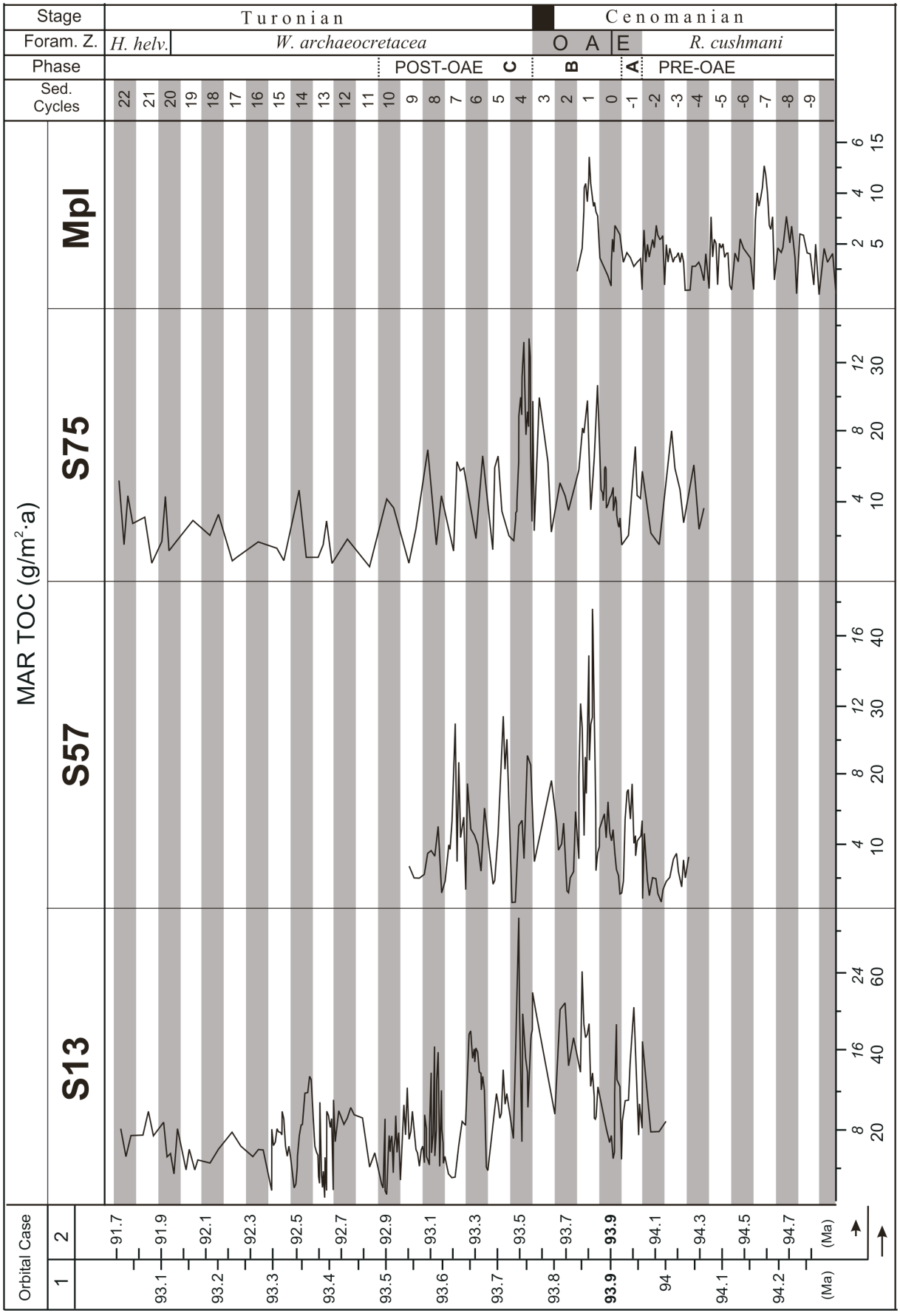

Figure 6. Organic carbon mass accumulation rates (g/m²·a) for the investigated Tarfaya sites and both orbital cases.

7.5.2.4. Bottom water anoxia

The repetitive deposition of laminated OC-rich sediments throughout the investigated sections and the very low abundances of benthic foraminifera especially in the interval representing OAE2 Phases A through C at S75 [*Kuhnt et al*., in press] already indicate predominantly suboxic to anoxic bottom water conditions in the Tarfaya Basin. However, the occurrence of thin (10-20 cm), bioturbated and carbonate-rich layers within the black shale beds suggests periodic occurrence of more oxic bottom waters. Additional information on bottom water redox conditions may be derived from chalcophilic elements (e.g. Mo and Zn) that precipitate as sulphides under euxinic conditions and certain redox sensitive elements (e.g. Mo and V) that are immobilised under reducing conditions [*Jones and Manning*, 1994; *Nijenhuis and De Lange,* 2000]. In accordance with the extraordinarily high enrichment of these metals in many C/T black shales from the deep proto-N Atlantic it has been proposed that the precipitation of trace metals derived from an expanded euxinic water column during the OAE2 [e.g., *Brumsack*, 1980, 1986; *Thurow et al.*, 1988; *Sinninghe Damsté and Köster,* 199*8; Kuypers et al.*, 2002]. The new high-resolution trace metals profiles from the Tarfaya Basin transect may thus provide key information as to whether the mid-Cretaceous NW African Shelf was coupled or decoupled from the euxinic N Atlantic deep- and intermediate waters, and to what extent the well-documented general (long-term) co-variation between black shale formation (peak OC burial) and trace metal accumulation [e.g. *Jones and Manning*, 1994] can also be confirmed on much shorter (millennial) time scales, i.e. on an individual sample-by-sample basis.

On average, Tarfaya black shales are significantly enriched in redox-sensitive and sulphide-forming trace metals relative to "average shale" [*Wedepohl*, 1991] with enrichment factors of ~140 for *Mo* and ~23 for *V* and *Zn* [see also *Lüning and Kolonic*, 2003]. These trace metal properties are comparable to those reported from deep-sea OAE2 black shales (e.g. *Brumsack*, 1980, 1986; *Thurow et al.*, 1988; *Arthur et al.*, 1990; *Kuypers et al.*, 2002). The highest enrichment in redox-sensitive and/or sulphide-forming trace metals at Tarfaya is observed during OAE2 Phases A through C (Fig. 5). Although not as pronounced as for *OC MAR*, there is a distinct spatial and temporal shift in *MARs* of trace metals, with highest values in the basin centre. Tarfaya average *MARs* for *V* and *Zn* almost double from pre-OAE2 values of ~17 *(~7)* mg/m^2·a and ~14 *(~6)* mg/m^2·a, respectively, to OAE2 values of ~33 *(~13)* mg/m^2·a and ~27 *(~11)* mg/m^2·a, respectively, and further increase by a factor of two to maximum values of ~61 (*~24)* mg/m^2·a and ~52 (*~21)* mg/m^2·a, respectively, for post-OAE2 Phase C (Fig. 5). On an average basis, trace metal accumulation was highest at S13 during Phases B and C with *MARs* for *V* and *Zn* up to twice as high as those calculated for the other sites (Fig. 5). Different to *OC MAR*, the average trace metal *MAR* record of S75 remains relatively constant from pre-OAE2 to OAE2 times (Fig. 5). Mpl exhibits lowest trace metal *MAR* values across the depth transect and, comparable to S75, does not reveal an increase from pre-OAE2 to OAE2 times (Fig. 5).

These long-term trends are modulated by higher-frequency and high-amplitude fluctuations in *MARs* of trace elements, often parallel and synchronous to *OC MAR* (Fig. 7). The amplitudes exhibit extreme differences between baseline and maximum values, revealing drastic and short-term fluctuations in trace element *MAR*. The highest amplitudes between baseline and maximum values are most pronounced at S57 within Phase B, where Zn exceeds 20 *(8)* mg/m^2·a, Mo approaches 160 *(64)* mg/m^2·a, and V is 120 *(48)* mg/m^2·a at the top of cycle 1 and the lowermost Phase C. At the adjacent Site S75, this general pattern remains comparable although highest amplitude variations are observed at the transition from Phase B to C (Cycles 3/4). At the proximal Mpl the amplitudes and extreme values, however, are lower, and approach levels below 7.5 *(3)* mg/m^2·a, 40*(16)* g/m^2·a, and 25 *(10)* g/m^2·a for Mo, V, and Zn, respectively (Fig. 7).

Despite scattering, there is an obvious positive correlation between *MARs of Mo*, *V*, and *Zn* and *OC MAR* on a sample-by-sample basis, at least for Sites S57 and Mpl (Fig. 7) where sample resolution is the highest and most regular over the whole profile and where geochemical analyses were carried out on exactly the same homogenized sample material. Furthermore, data from these two sites represent cm-scale sample intervals, whereas samples from S75 and S13 integrate over ~10 cm intervals (except for Cycles 0 and 4 at S75, where a high-resolution re-sampling had been performed [*Kuhnt et al*., 2001, in press]. Therefore, the integration of different sub-samples hampers direct comparison of the two datasets and, to some extent, probably also explains the few inconsistencies (non-correlation) between *OC MAR* and *MARs* in trace metals observed at S13 and S75 (e.g. Cycles 8, 11, and 15 at S13 and cycles -3, 1, 5 through 7 at S75; Fig. 7).

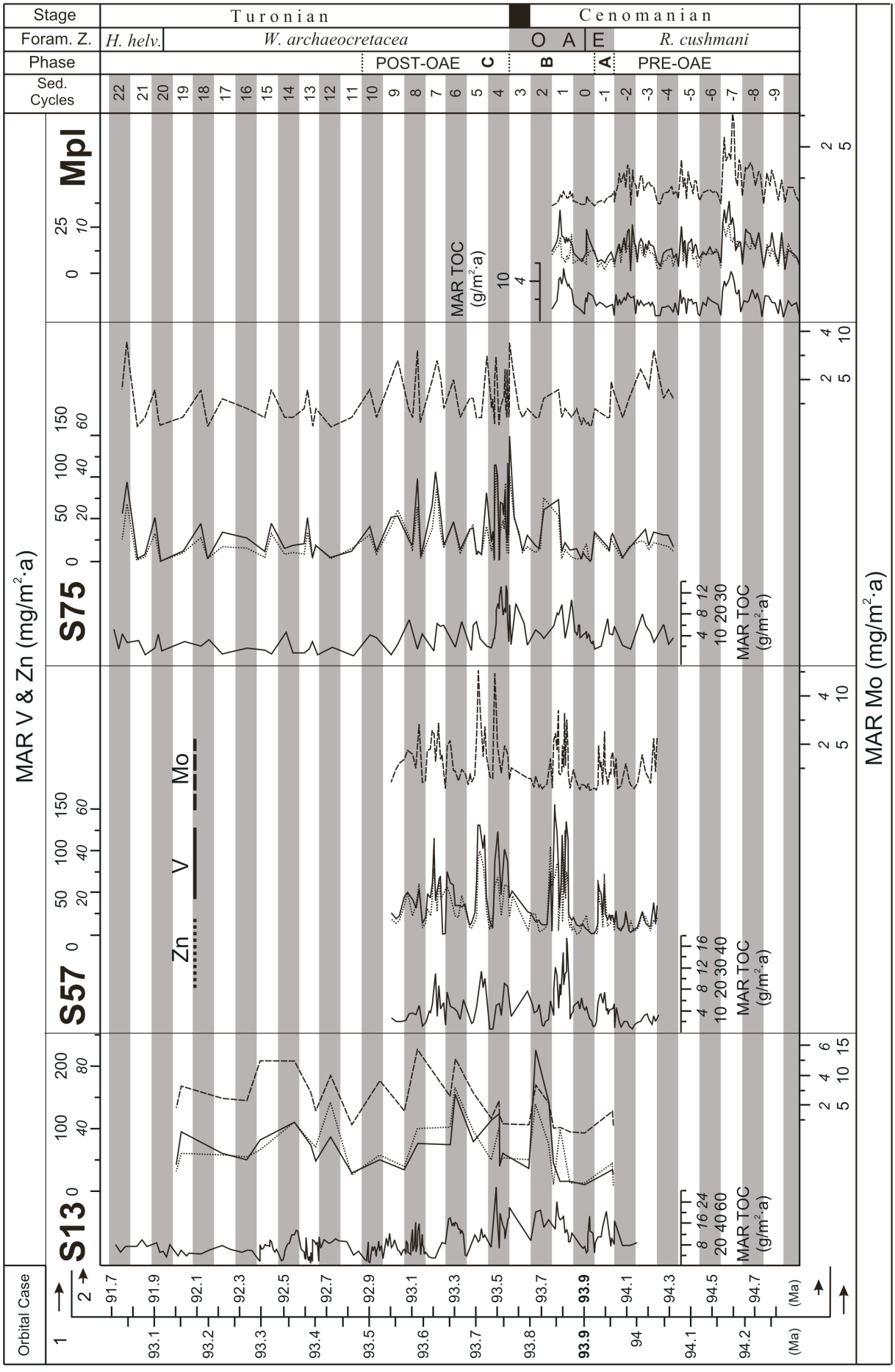
Stage
Turonian
Cenomanian
Foram. Z.
H. helv.
W. archaeocretacea
O A E
R. cushmani
Phase
POST-OAE
C
B
A
PRE-OAE
Sed. Cycles
22 21 20 19 18 17 16 15 14 13 12 11 10 9 8 7 6 5 4 3 2 1 0 -1 -2 -3 -4 -5 -6 -7 -8 -9
MAR V & Zn (mg/m²·a)
MAR Mo (mg/m²·a)
Orbital Case
1
2
MpI
S75
S57
S13
Zn
V
Mo
MAR TOC (g/m²·a)
(Ma)
91.7 91.9 92.1 92.3 92.5 92.7 92.9 93.1 93.3 93.5 93.7 93.8 93.9 94.1 94.3 94.5 94.7

Figure 7. Organic Carbon (g/m^2·a) and redox-sensitive/sulphide-forming trace metals V, Zn, Mo (in µg/m^2·a) mass accumulation rates for the investigated Tarfaya sites and both orbital cases. Note the close correlation between the *MAR's* for redox-sensitive trace metals and bulk OC MAR at S57 and Mpl.

The consistent relationship at S57 and Mpl, however, strongly supports the conclusion that variations in bottom water oxygenation were rapid and synchronous with OC burial at millennial time scales and thus should have had a distinct impact on the preservation of OM, with anoxic conditions leading to enhanced preservation of OM. Following that conclusion the new high-resolution data from the Tarfaya transect indicate drastic and short-term fluctuations in bottom water oxygen levels. Based on the extreme differences in *OC MAR* and *MARs* of trace metals in adjacent samples, the transition time between better-oxygenated and severely oxygen-depleted bottom water conditions can roughly be estimated. Despite limitations, the present data confirm repetitive fluctuations in the redox state of the bottom waters at Milankovitch and probably even shorter (seasonal to decadal) time scales. Both frequencies strongly propose a close link to climate forcing.

7.5.2.5. Photic zone euxina

To further investigate whether anoxic or euxinic redox conditions at least temporarily extended into the photic zone, a subset of samples was analysed for fossil derivatives of specific carotenoid pigments, isorenieratene and chlorobactene [*Koopmans et al.*, 1996]. Both carotenoids are exclusively biosynthesized by the brown and green coloured strain of green sulphur bacteria Chlorobiaceae, respectively [e.g., *Madigan et al.*, 2000]. As strict anaerobes, these bacteria require free hydrogen sulphide in the water column and light of a specific wavelength in order to photosynthesize. At present, these conditions are restricted to a few isolated marine basins, such as the Black Sea, where Chlorobiacea*e* thrive near the sulphide/oxygen interface (i.e. the chemocline) at light levels of less than 1% (or <0.5 µE) of surface irradiance [*van Gemerden and Mas*, 1995]. Chlorobiaceae from the green strain require higher light intensity and therefore thrive at shallower depths (~15 m water depth) than Chlorobiaceae from the brown strain (~30-150 m water depth). Assessing the presence and accumulation of these two biomarkers may thus be used to deduce the position of the chemocline and its variability within the photic zone. In addition, isorenieratane and chlorobactane are very labile organic compounds which rarely survive long-distance transport, and consequently are indicators of a local (autochthonous) marine source [*Sinninghe Damsté et al*., 2001] especially in case of the shallow (~400 m) Tarfaya Basin.

Isorenieratane and chlorobactane were detected at all sites and at all stratigraphic levels, although at different *MARs* and a high temporal variability (Fig. 8). For isorenieratane, highest *MAR*s of up to 3000 *(1200)* µg/m^2·a are observed in Cycles 8 (post-OAE Phase C) and 11 (above the OAE2) in the basin centre at S13. The corresponding *MARs* of isorenieratane strongly decrease towards the transitional sites S57 (below 350 *(140)* µg/m^2·a) and S75 (below 1500 *(600)* µg/m^2·a), and reach lowest values at the proximal Mpl (500 *(200)* µg/m^2·a). Maximum *MARs* of isorenieratane in the Tarfaya transect are similar to those reported from DSDP Site 367 (~2600 µg/m^2/a) but exceed those at DSDP Site 603 in the NE Atlantic [*Kuypers et al.*, 2002] by a factor of ~500 *(200)*. The gradual decline in *MARs* of isorenieratane towards the paleocoastline is not followed by *MARs* of chlorobactane (Fig. 8). Instead, *MARs* for chlorobactane remain in the same range across the transect with maximum values exceeding ~80 *(32)* µg/m^2·a between cycles -1 and 0 (the transition from OAE Phases A to B; S13 and Mpl), in the upper part of Cycle 1 (central part of OAE Phase B; S57, 75 and Mpl), and in the lowermost part of Cycle 3 (end of OAE Phase B; S57) (Fig. 8). The synchrony of maxima in *MARs* of chlorobactane and isorenieratane indicate intervals with an extremely shallow chemocline in the photic zone and thus most extreme redox conditions. Given the low time resolution of the biomarker records compared to the bulk geochemical records (with the exception of S57), basin-wide synchrony of photic zone euxinia can only be claimed for Cycles -1 and 1, although it appears reasonable to expect that other periods of basin-wide and synchronous peak OC accumulation represent comparable extreme redox conditions. Notably, the enrichment of biomarkers is not restricted to OAE2 Phases A and B, as would be expected from the global carbon isotopic excursion assuming that the shift in isotopic signatures is a direct record of maximum OC burial and anoxia/euxinia [*Kuypers et al*., 2002]. Instead, maximum *MARs* of isorenieratane and chlorobactane

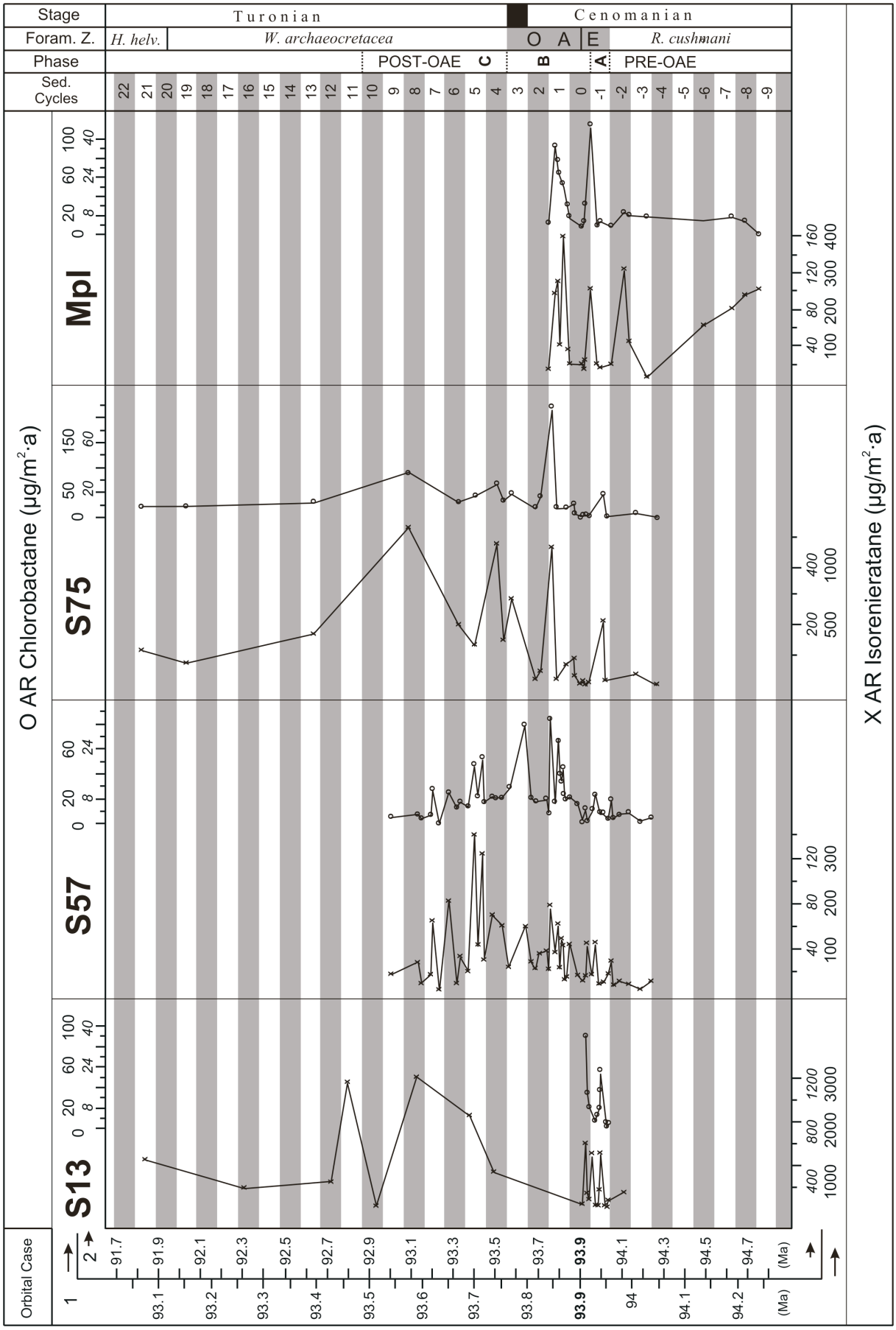

Figure 8. Isorenieratane and chlorobactane (µg/m^2·a) mass accumulation rates for the investigated Tarfaya sites and both orbital cases.

are not only recorded within, but also well after the OAE2 suggesting that the most extreme redox conditions prevailed well beyond the OAE2 Phase C at Tarfaya.

MARs of isorenieratane are about one order of magnitude lower at S57 than those from the adjacent S75 (Fig. 8). This distinct difference is difficult to reconcile with the consistent pattern of other geochemical data from these two sites, and therefore could relate to the different analytical procedures applied to isolate the biomarkers. At S57, quantification was performed on the polar sub-fraction of the total extract whereas total extracts were used at the other sites (see Methods for more detailed explanation). It may well be that this procedure resulted in the generally lower biomarker yields from the polar sub-fractions when compared to the total extract data from a similar setting. Despite the lower *MARs* there is a consistent and often parallel trend of the S57 biomarker data with those from the other profiles, e.g. at the transition from Cycles -1 to 0 (S57 to S13) or at the top of Cycle 1 (S57 to S75) (Fig. 8). We believe that this consistency allows confidence in the quality of the S57 biomarker record, which can thus be used as a reference profile for short-term variability of photic zone euxinia. This is of relevance since the time resolution of the S57 biomarker record to our knowledge is unique for OAE2 black shales, and thus bears an exceptional potential for assessing fluctuations in photic zone euxinia at orbital time-scales and discussing the linkage to bottom water anoxia and OC burial. Synchronous to *OC MAR* and *MARs* of trace metals, *MARs* of biomarkers reveal short-term and high amplitude fluctuations. Peak-to-peak correlation at S57, for example, shows that biomarker maxima exactly match maxima in OC except for a few samples where OC value are at transitional levels (e.g. in the central part of Cycle 7 and at the top of Cycle 6; Fig. 8). This positive correlation with OC burial strongly supports a direct and probably causal link between bottom water and photic zone redox conditions. The repetitive alternation of maxima and minima in *MARs* of all three parameters and their spatio-temporal pattern indicate a highly variable oxygen/sulphide boundary that was not uniformly developed over the entire shelf basin. The data instead propose a shallow chemocline well within the upper photic zone during peak OC burial that deepened (probably to the lower part of the photic zone) during reduced OC burial and migrated downwards to pore waters of the sedimentary column during deposition of limestone interlayers.

7.5.3. Depositional model

The investigated Tarfaya sites reveal extremely high *MARs* of OC, trace metals and photic zone euxinia biomarkers. It has been shown that high-amplitude and short-term variations generally occurred synchronously for all parameters on a sample-by-sample basis and across the core transect. The principle mechanisms responsible for these distinct patterns probably combine stratification-driven anoxia and marine productivity. Furthermore, OC burial and black shale formation must have been intimately linked to nutrient cycling processes. The strongly reduced and generally constant supply of minerals from continental sources excludes continental runoff as a primary mechanism controlling nutrient supply and thus black shale formation. This conclusion may not be expected from the geological context, considering the vicinity of the shelf basin to the African continent and the extremely warm global climate during the mid-Cretaceous, which should have stimulated an intensified hydrological cycle [*Huber and Norris*, 2002] with high precipitation and runoff from dense subtropical vegetation at low latitudes [e.g. *DeConto et al.*, 1999]. The reason for the depressed continental signature in the sedimentary record at Tarfaya remains enigmatic at present and requires further investigation. It may be speculated, however, that most of the continental matter, if it was supplied at all, either bypassed the study sites via small-scale channels in front of fossil river mouths or was trapped in lagoons or large-scale lakes near the river mouth or within the estuaries, comparable to the modern tropical African Comoe or Congo Rivers.

More probably, wind-induced continental upwelling of nutrient-rich and severely oxygen-depleted (or even euxinic) intermediate waters from the deep Atlantic was the primary mechanism that determined marine sedimentation on the mid-Cretaceous NW African shelf. Following that model, periods of enhanced (trade) wind intensity should have fostered the establishment of anoxia/euxinia and black shale formation along the NW African shelf through both enhanced marine productivity and inflow of oxygen-depleted intermediate waters. Weakening of the trade winds on the other hand should have resulted in reduced continental upwelling and thus partial re-oxidation of the water column. From a modern perspective such a situation would correspond to insolation-driven alternations of more arid and humid conditions on the African continent during the C/T with strong

trades at a southern position of the Inter-Tropical Convergence Zone (ITCZ) representing arid periods and weak trades at a northern position of the ITCZ during humid intervals. Modelling of global climate and precipitation across the C/T transition supports the presence of such insolation-driven fluctuations in aridity and humidity over low-latitude W Africa and S America [*Flögel*, 2001]. The consistency of conclusions deduced from the geological record with implications from modelling suggests that OC burial at Tarfaya was closely linked to atmospheric circulation dynamics, similar to its Quaternary analogue [e.g. *Tiedemann et al.,* 1994].

Since photic zone euxinia represents the most extreme and therefore most unstable oceanographic conditions during the C/T, it should have been vulnerable to wind-induced mixing of surface waters on the paleo-shelf. Short-term and repetitive admixture of oxygen to surface waters is a common feature of modern low-latitude marine sedimentation [e.g. *Ittekkott et al.,* 1992], the primary agent being seasonal changes in wind stress. Considering the higher-resolution biomarker records from S13 (Cycle -1) and S57, short-term (seasonal to decadal) fluctuations in surface-water mixing may be inferred. The repetitive and short-term breakdown of the chemocline, however, may have required the interaction of a variety of processes. Among others they may suggest wind-induced (seasonal?) depression of the mixed layer down to the sea floor (a process that is not considered likely, at least not for the basin centre given an estimated maximum water depth of about 400 m), periodic advance and retreat of severely oxygen-depleted intermediate waters from the adjacent Atlantic ocean combined with Eckmann pumping of these nutrient-rich and oxygen-depleted intermediate waters to the photic zone (a more reasonable scenario), or a mixture of both processes (the most probable scenario). The pacing and duration of such a mid-water advance and retreat and thus upward migration of nutrients and anoxia to the photic zone can hardly be assessed based on the present data. This process may have operated on a longer time scale (millenial to orbital?) compared to the build-up or break-down of photic zone euxinia which was likely to have been more of a seasonal or inter-annual oceanographic feature. Given the high-resolution biomarker patterns in Cycle -1 at S13 and in Cycle 1 at S57 (Fig. 8), break-down of the photic zone occurred at least four times within one sedimentary cycle, synchronous to OC and trace metal accumulation. This synchrony and pacing evidence a close interaction of photic zone and bottom water oxygenation and propose that the repetitive shoaling of the chemocline significantly fostered enhanced OM preservation in a highly dynamic depositional system.

To address the important and often contradictory issue of whether productivity or preservation was the primary control determining OC burial during black shale formation, we consider two principal variables, i.e. the preservation factor and export productivity. Assuming average properties for both variables from modern marine high-productive areas, i.e. ~300 gC/m^2•a for export productivity and a preservation factor of 1% [*Suess*, 1980], OC accumulation in the Tarfaya Basin should have been less than ~3 gC/m^2•a. The calculated maximum average *OC MAR* during the OAE2, instead, has been estimated to be between ~10 (*4*) gC/m^2•a and 33 (*13*) gC/m^2•a in the central part of the basin. If marine productivity was the only factor controlling OC burial on the Tarfaya shelf, an unrealistic export productivity in the order of 1000 to 3000 gC/m^2•a (*400 to 1200* gC/m^2•a for Orbital Case 2) or more has to be proposed for the mid-Cretaceous NW African continental margin. We therefore conclude that preservation of OM was considerably enhanced compared to modern marine upwelling systems. Consistent with this, very high hydrogen indices 550-850 mgHC/gTOC and the abundance of sulphur-bound compounds are indeed indicative for high preservation factors [*Kolonic et al.*, 2002]. Increasing the preservation factor to ~5%, an average value determined for the modern Black Sea [*Arthur et al.,* 1994; *Sinninghe Damsté and Köster,* 1998], results in an export productivity in the order of ~200 gC/m^2•a for the OAE2 in the Tarfaya Basin. However, given an estimated maximum water depth in the Tarfaya Basin centre of about 400 m, much of the OC flux can be related to rapid mass sinking, thus implying that preservation may have even been higher than the 5%. Apparently, if we assume a very high preservation factor of ~15% (as reported for the euxinic shallow water column of the Saanich Inlet; [*Sinninghe Damsté and Köster,* 1998]) to our data, an export productivity between 40 to 100 gC/m^2•a is required to account for the estimated OC accumulation at Tarfaya. Although the budget calculation herein is tentative, it strongly suggests that across the C/T transition essentially both, increased production as well as preservation played a crucial role in the deposition of these oil prone source rocks.

7.5.4. Global impact of OC burial on the NW African shelf during the OAE2

Globally enhanced OC burial associated with the OAE2 is considered a primary mechanism that caused drawdown of CO_2 from the atmosphere and consequently induced global cooling during the mid-Cretaceous [*Arthur et al.*, 1988; *Kuypers et al.*, 1999, 2002]. The widespread removal of reduced carbon during the OAE2 may also have strongly increased the oxygen concentration in the atmosphere, thus stimulating enhanced air pressure and temperature in the lower atmosphere [e.g. *Ohkouchi et al.,* 1999]. One major sink for reduced carbon across the C/T has been identified as the deep southern proto-N Atlantic [e.g. *Kuypers et al*., 2002]. In view of the exceptionally thick and OC-rich black shales in the Tarfaya area as part of the larger LaAaiun Basin (Fig. 1), the question arises as to what extent the NW African shelf was responsible for the global OC burial associated with the OAE2.

To provide a first-order approximation a simple budget calculation was applied that roughly estimates the magnitude of OC burial in the Tarfaya Basin during the C/T transition. In this budget calculation (I) an average Tarfaya *OC MAR* of 6 (*~2.5*) gC/m^2•a for the period predating the OAE2 and (II) 16 (*~6.5*) gC/m^2•a for the OAE2 (numbers representing the Tarfaya average values as displayed in Fig. 5), as well as (III) a gross total on- and offshore area of ~170,000 km^2 for the entire Tarfaya-LaAaiun Basin [*Leine*, 1986] is considered. The resulting overall excess OC burial in the Tarfaya-LaAaiun Basin is equivalent to $1 \cdot 10^{11}$ ($\sim 6 \cdot 10^{10}$) mols C per year, or, when extrapolated to the time period assumed for the OAE2 (i.e. ~500 ka), $\sim 7.1 \cdot 10^{16}$ ($\sim 2.8 \cdot 10^{16}$) mols C, respectively. The dimension of these numbers becomes apparent when they are compared to the overall global excess OC burial as proposed by *Arthur et al.* [1988] for the OAE2. *Arthur and co-workers* calculated a global excess OC burial above the C/T background in the order of $\sim 1.6 \cdot 10^{18}$ mols C for the OAE2 (implied duration ~500 ka), applying a carbon isotope mass-balance modelling approach. Comparing this global number with the estimate from the Tarfaya-LaAaiun Basin implies that approximately ~5% (*~2*%) of the overall global excess OC burial during the OAE2 was deposited in this small coastal basin. This number may appear small at first glance. However, it has to be taken into account that the Tarfaya-LaAaiun Basin barely represented ~0,05% of the total global C/T ocean floor (assuming the present day ocean floor size of $3.1 \cdot 10^8$ km^2 with an additional increase of 20% of continental areas due to the extremely high global sea level during the C/T). To give at least an order of magnitude on the enrichment of OC burial in the Tarfaya-LaAaiun Basin relative to the global C/T Ocean, we assume that OC burial over the vast area of the entire C/T Ocean was equally distributed per area unit (a gross simplification which nevertheless serves the purpose of this rough approximation). Following this simplified approach about $\sim 7.3 \cdot 10^{14}$ mols C are calculated for the area of the Tarfaya-LaAaiun Basin. Comparison of this number with the amount of excess OC actually stored based on the data presented above reveals an enrichment factor of OC burial in the order of ~130 (*~50*). Both enrichment factors (the first assuming obliquity, the second eccentricity) are conservative estimates; however, they clearly emphasize the importance of this small coastal basin with respect to global carbon burial during the OAE2.

These estimates may have considerable consequences for global OC budget calculations if we consider that thick OC-rich black shales of C/T age were not only deposited in the Tarfaya-LaAaiun Basin but all along the NW African margin (e.g. Sénégal, Agadir and various other smaller basins; Fig. 1) and beyond [see *Lüning et al.,* 2003 for review]. The exact area of OC-rich strata in these other basins (on and off-shore) and their average *OC MARs* are hardly constrained due to the lack of detailed and high-resolution records, prohibiting a reliable budget calculation for all NW African coastal basins. Despite these limitations we conclude that large-scale OC burial along the NW African shelf significantly contributed to global carbon burial associated with the OAE2. A reliable approximation of its proportion, however, requires additional detailed investigations, comparable to those for the Tarfaya Basin.

Acknowledgments

The authors are indebted to the management of Moroccan ONAREP and SHELL International (Dr. Kees Kommeren) for providing well material. We are grateful to Prof. Dr. El Hassane Chellai (University of Marrakech) for assistance during fieldwork in the Tarfaya-LaAaiun Basin. The manuscript benefited much from valuable discussions with Michael Böttcher, Elisabetta Erba, Hugh

Jenkyns and other members of the European Union-funded C/T-Net Research Training Network. Sabine Kasten, Sebastian Lüning and Verena Heuer (all University of Bremen) are thanked for fruitful discussions and comments. We acknowledge technical assistance provided by Marianne Baas (NIOZ), Renate Henning, and Helga Heilmann (University of Bremen). This project was supported by the Deutsche Forschungsgemeinschaft (DFG grants Wa1036/6 and Ku649/9), University of Bremen (FNK grant Sadat Kolonic) and the European Union's Improving Human Potential Programme under contract HPRN-CT-1999-00055, C/T-Net. The data presented in this study is available at http://www.pangaea.de/PangaVista2?query=kolonics

Part III

Conclusions and Perspectives

Conclusions and Perspectives

Cenomanian/Turonian (C/T) black shale successions from various N African basins and in particular from the Tarfaya-LaAyoune Basin (SW Morocco) have been studied in great detail using data from field geology (including gamma-ray resistivity logging), sedimentology and advanced geochemical trace metal, biomarker and stable isotope analyses. The research focused on the genetic analysis of oxygen-depleted sedimentary processes in the Tarfaya-LaAyoune Basin; the aim was to construct an integrated depositional model for black shale formation along the NW African continental margin during the C/T. Furthermore, this thesis offers a framework within which to interpret N African C/T black shale parameters and regional trends. The results of this study form a platform for future investigations of C/T black shale successions in regions lacking detailed geological/geochemical data. On the other hand, the results of this study have raised several questions, which warrant further study.

Main Conclusions:

Conclusions from this study of black shale sedimentation across the C/T transition in N Africa (and in particular in the Tarfaya-LaAyoune Basin) have a number of implications for current topics in marine geoscience and for hydrocarbon exploration strategies in the region. The main conclusions of this thesis are:

- C/T black shale deposition in N Africa was restricted to marine facies of a certain bathymetric zone which may represent the impingement of the oxygen minimum zone (OMZ) onto the continental shelf. Shallower facies, namely in the Moroccan Middle Atlas, NE Algeria and central Libya (Sirte Basin), were too oxygenated by the action of waves and other currents. Variations in eustatic sea level may have been one mechanism driving the expansion of the OMZ, which apparently did not reach to greater depths in NE African Tethyian realm as along the NE African Atlantic coast. The distribution of black shales in N Africa, therefore, closely follows the paleorelief that existed during the C/T. Contrasting with the NE African Tethys, the C/T NW African shelf was a site of highly dynamic marine sedimentation, where orbitally-forced climate variability determined oceanic processes resulting in distinct and expanded bedding cycles, well known from the Tarfaya-LaAyoune Basin. The resulting efficient burial of carbon in the Tarfaya-LaAyoune Basin (and thereby on the NW African shelf) significantly contributed to global OC burial associated with the OAE2. Between 2 and 5 % of the overall global excess organic carbon buried during the OAE2 was deposited in the relatively small Tarfaya-LaAyoune Basin.
- Detailed organic geochemical investigations performed on the Tarfaya Basin black shales provide a first order geochemical estimate of what can be expected from distal parts of the NW African continental margin. Hence, the results obtained from exploration wells in the Basin provide important information for future on-/offshore exploration and production plans.
- The successful application of field gamma-ray resistivity measurements in various outcrop sections qualifies this non-destructive technique as a powerful independent stratigraphic tool for basin-wide correlations in poorly exposed and tectonically highly dissected regions.
- A global chemostratigraphic framework for the OAE2 has been established in which Tarfaya is considered as one key reference section. Based on the given stratigraphy the duration of the OAE2 is estimated to be ~500ka.

Perspectives:

More data is clearly needed from areas such as Algeria, Libya and Egypt to understand more precisely the causes and consequences of the OAE2. In a joint effort between the petroleum industry and academia, more C/T data and study material of these regions should be analysed and subsequently be published to fill in these gaps. Major issues are the identification of synchronism of C/T source-

rock deposits, and a better understanding of their distribution in space and time. In particular, high resolution biostratigraphic, chemostratigraphic, and organic and inorganic geochemical data is needed to allow more precise correlations of the onset, peak and termination of the OAE2 across N Africa. Clearly, a better understanding of small- and large-scale processes gained from these N African black shale systems will help reconstructions of other organic-rich depositional systems.

In the case of the Tarfaya-LaAyoune Basin, the controlling parameters for the depositional processes discussed in the previous chapters is not equivalent for all sites and time-slices studied, which leaves the opportunity for much additional research. Alternatively, the relatively complete Coniacian/Santonian sedimentary record provides an opportunity to examine in great detail the mechanisms and processes of black shale deposition associated with OAE3. Results obtained from this time envelope could be compared to the OAE2, and perhaps provide a suitable platform for an integrated basin model. For this reason, additional field campaigns should be undertaken to investigate the central and southern area of the Tarfaya-LaAyoune Basin and should also be extended further to the Senegal Basin to the south. In particular the following studies are necessary:

- The strongly reduced and generally constant supply of minerals from continental sources excludes continental run-off as a primary mechanism controlling nutrient supply, and thus black shale formation, along the NW African shelf. The reason for the depressed continental signature in the sedimentary record observed at Tarfaya remains enigmatic at present and requires further investigation. It may be speculated, however, that most of the continental material, (if it was supplied at all) either bypassed the investigated sites via small-scale channels in front of palaeo-river mouths; or was trapped in lagoons or large-scale lakes or within estuaries, comparable to the modern tropical African Comoe and Congo Rivers. This scenario is, however, most unlikely to have lasted over time periods of a few million years during black shale sedimentation. Hence, the depressed continental signature in the sedimentary record at Tarfaya might indicate the absence of annual sustained rainfall, which is typical of the moderen Inter-Tropical Convergence Zone (ITCZ). This would be in sharp contrast to recent global climate modelling results of *Flögel* [2002], who proposes strong influence of the ITCZ and monsoon and trade wind systems on sedimentation processes at shallow water depths along the NW African shelf. A question which arises is: what if the NW African shelf was not under the influence of the ITCZ during the C/T because the equatorial humid belt was significantly reduced in width? Instead of the ITCZ, a broad zone of convective circulation could have been present along the NW African shelf (at ~15°N paleolatitude), which would result in a climate belt characterised by semi-arid to arid terrestrial environments. Such environments usually produce fine-grained sedimentary flux and are in agreement with the observed depressed continental signature in the sedimentary record of Tarfaya. Systematic grain-size studies are needed to further investigate this question.
- It is estimated, that during the OAE2, between 2 and 5 % of the overall global excess OC was buried in the Tarfaya-LaAyoune Basin. These estimates may have considerable consequences for global OC budget calculations, because thick OC-rich black shales of C/T age were deposited not only in the Tarfaya-LaAyoune Basin but also along the NW African and Mediterranean margins. The exact area of OC-rich strata in these other basins (on- and offshore) and their average OC accumulation rates are barely constrained due to a lack of detailed and high-resolution records, preventing a reliable budget to be calculated for the N African coastal basins. Its reliable approximation, however, will require future detailed investigations, comparable to those for the Tarfaya-LaAyoune Basin reported here.

Part IV

References

ABDALLAH, H. AND MEISTER, C., 1997. The Cenomanian–Turonian boundary in the Gafsa–Chott area (southern part of central Tunisia): biostratigraphy, palaeoenvironments. Cretac. Res. 18, pp. 197–236.

ABDALLAH, H., MEMMI, L., DAMOTTE, R., RAT, P. AND MAGNIEZ-JANNIN, F., 1995. Le Crétacé de la chaîne nord des Chotts (Tunisie du centre-sud): biostratigraphie et comparaison avec les régions voisines. Cretac. Res. 16 5, pp. 487–538.

ABDALLAH, H., SASSI, S., MEISTER, C. AND SOUISSI, R., 2000. Stratigraphie séquentielle et paléogéographie à la limite Cénomanien–Turonien dans la région de Gafsa–Chotts (Tunisie centrale). Cretac. Res. 21, pp. 35–106.

ACCARIE, H., EMMANUEL, L., ROBASZYNSKI, F., BAUDIN, F., AMÉDRO, F., CARON, M. AND DECONINCK, J.-F., 1996. La géochimie isotopique du carbone (13C) comme outil stratigraphique. Application à la limite Cénomanien/Turonien en Tunisie centrale. C. R. Acad. Sci., Paris 322 IIa, pp. 579–586.

AIZENSHTAT, Z., KREIN, E.B., VAIRAVAMURTHY, M.A. and GOLDSTEIN, T.P., 1995. Role of Sulfur in the Transformations of Sedimentary Organic Matter: A Mechanistic Overview. In: Vairavamurthy M.A. and Schoonen M.A.A., (Eds.), Geochemical Transformations of Sedimentary Sulfur. Amer. Chem. Soc., Symposium Series, 612. Washington DC, pp. 16-37.

AMARD, B., COLLIGNON, M. AND ROMAN, J., 1981. Ètude stratigraphique et paléontologique du Crétacé supérieur et Paléocene du Tinrhert-W et Tademaït-E (Sahara algérien). In: Mémoire Maurice Collignon (1981)—Notice, Bibliographie, Notes Posthumes Docum. Lab. Géol. Lyon, HS vol. 6 299 pp.

AMBLÉS, A., HALIM, M., JACQUESY, J.C., VITOROVIC, D. and ZIYAD, M., 1994. Characterization of kerogen from Timahdit shale (Y-layer) based on multistage alkaline permanganate degradation. Fuel, 73, 17-24.

AMÉDRO, F., BUSSON, G. AND CORNÉE, A., 1996. Révision des ammonites du Cénomanien supérieur et du Turonien inférieur du Tinrhert (Sahara algérien): implications biostratigraphiques. Bull. Mus. Natl. Hist. Nat., Paris, 4th Sér., 18, Section C 2–3, pp. 179–232.

ARIS, Y., COIFFAIT, P.E. AND GUIRAUD, M., 1998. Characterisation of Mesozoic–Cenozoic deformations and palaeostress fields in the central Constantinois, northeast Algeria. Tectonophysics 290, pp. 59–85.

ARTHUR, M.A., DEAN, A. W., NEFF, D.E., HAY, J.B., KING, J. AND JONES, G., 1994. Varve calibration records of carbonate and organic carbon accumulation over the last 2000 years in the Black Sea, Global Biochemical Cycles, 8, pp. 195-217.

ARTHUR, M.A. AND SAGEMAN, B.B., 1994. Marine black shales: a review of depositional mechanisms and environments of ancient deposits. Annu. Rev. Earth Planet. Sci. 22, pp. 499–552.

ARTHUR, M.A., AND PREMOLI SILVA, I., 1982, Development of widespread organic carbon-rich strata in the Mediterranean Tethys. In: Schlanger, S.O., and Cita, M.B., (Eds.), Nature and Origin of Cretaceous Carbon-Rich Facies. Academic Press, London, pp. 7-54.

ARTHUR M.A., SCHLANGER S.O. AND JENKYNS H.C., 1987. The Cenomanian-Turonian oceanic anoxic event, II. Palaeoceanographic controls on organic-matter production and preservation. In: Brooks, J. and Fleet J.A. (Eds.), Marine Petroleum Source Rocks. Geological Society Special Publication 26, pp. 401-420.

ARTHUR, M.A., DEAN, W.E. AND PRATT, L.M., 1988. Geochemical and climatic effects of increased marine organic carbon burial at the Cenomanian–Turonian boundary. Nature 335, pp. 714–717.

ARTHUR, M.A., DEAN, W.E. AND STOW, D.A.V., 1984. Models for the deposition of Mesozoic–Cenozoic fine-grained organic-carbon-rich sediment in the deep sea. In: Stow, D.A.V. and Piper, D.J.W., (Eds.), Deep-Water Processes and Facies. Geol. Soc., London, Special Publ. vol. 15, pp. 527–562.

ARTHUR, M.A., JENKYNS, H.C., BRUMSACK, H.J. AND SCHLANGER, S.O., 1990. Stratigraphy, geochemistry, and paleoceanography of organic-rich Cretaceous sequences. In: Ginsburg, R.N. and Beaudoin, B., (Eds.), Cretaceous Resources, Events and Rhythms: Background and Plans for Research. NATO ASI Series, Series C: Mathematical and Physical Sciences, Kluwer Academic, The Netherlands, pp. 75–119.

ARTHUR, M.A., SCHLANGER, S.O. AND JENKYNS, H.C., 1987. The Cenomanian–Turonian oceanic anoxia event: II. Paleoceanographic controls on organic matter production and preservation. In: Brooks, J. and Fleet, A.J., (Eds.), Marine and Petroleum Source Rocks. Geol. Soc., London, Special Publ. vol. 26, pp. 401–420.

ASKRI, H., BELMECHERI, A., BENRABAH, B., BOUDJEMA, A., BOUMENDJEL, K., DAOUDI, M., DRID, M., GHALEM, T., DOCCA, A.M., GHANDRICHE, H., GHOMARI, A., GUELLATI, N., KHENNOUS, M., LOUNICI, R., NAILI, H., TAKHERIST, D. AND TERKMANI, M., 1995. Geology of Algeria. In: Schlumberger, (Eds.), Well Evaluation Conference Algeria 1995, pp. 1–93.

BAAIR, M.Y., RABTI, I. AND SWIRE, P.H., 2001. Hydrocarbon source rock quality, distribution and migration in the northwest Sirt Basin, Libya (abstr.). North Africa Research Workshop, Oxford Brookes, Abstract volume, 2001.

BARAKAT, H., 1982. Geochemical criteria for source rock, Gulf of Suez. In: 6th Petrol. Explor. Seminar, EGPC, Cairo, Egypt 13 pp.

BARAKAT, M.G., DARWISH, M. AND ABDEL-HAMID, M.L., 1987. Hydrocarbon source-rock evaluation of Upper Cretaceous (Abu Roash Formation), east Abu-Gharadig area, north Western Desert, Egypt. M.E.R.C. Ain Shams Univ. Cairo, Earth Sci. Ser. 1, pp. 120–150.

BARBIERI, R., 1996. Micropalaeontology of the Rakb Group (Cenomanian to Early Maastrichtian) in the Hameimat Basin, northern Libya. In: Salem, M.J., Mouzughi, A.J. and Hammuda, O.S., (Eds.), The Geology of Sirt Basin vol. 1, Elsevier, Amsterdam, pp. 185–194.

BARIC, G., SPANIC, D. AND MARICIC, M., 1996. Geochemical characteization of source rocks in NC-157 Block (Zlatan Platform), Sirt Basin. In: Salem, M.J., Mouzughi, A.J. and Hammuda, O.S., (Eds.), The Geology of Sirt Basin vol. 2, Elsevier, Amsterdam, pp. 541–553.

BARR, F.T. AND HAMMUDA, O.S., 1971. Biostratigraphy and planktonic zonation of the Upper Cretaceous Atrun Limestone and Hilal Shale, northeastern Libya. In: Farinacci, A., (Eds.), Proc. 2nd Int. Conf. Plankt. Microfossils (Rome 1970), pp. 27–38.

BARR, F.T. AND WEEGAR, A.A., 1972. Stratigraphic nomenclature of the Sirte Basin, Libya. Petrol. Explor. Soc. Libya (179 pp.).

BARR, F.T., 1972. Cretaceous biostratigraphy and planktonic foraminifera of Libya. Micropaleontology 18, pp. 1–46.

BARRETT, P., 1998. A comparative organic geochemical and stable isotope study of the Cenomanian–Turonian organic-rich sediments from Tunisia, Germany and the UK. PhD thesis, University of Newcastle. 250 pp.

BARRON, E.J., 1983. A warm equable cretaceous: the nature of the problem. Earth-Sci. Rev. 19, pp. 305-338.

BATT, R.J., 1996. Faunal and lithologic evidence for small-scale cyclicity in the Wanakah shale (Middle Devonian) of western New York. Palaios 11, pp. 230–243.

BAUDIN, F., 1995. Depositional controls on Mesozoic source rocks in the Tethys. In: Huc, A.-Y., (Eds.), Paleogeography, Paleoclimate, and Source Rocks. AAPG Studies in Geology vol. 40, pp. 191–211.

BAUER, J., KUSS, J., STEUBER, T., in press. Sequence architecture and carbonate platform configuration (Late Cenomanian–Santonian), Sinai, Egypt. Sedimentology.

BAUER, J., MARZOUK, A.M., STEUBER, T. AND KUSS, J., 2001. Lithostratigraphy and biostratigraphy of the Cenomanian–Santonian strata of Sinai, Egypt. Cretac. Res. 22, pp. 497–526.

BAYOUMI, T., 1996. The influence of interaction of depositional environment and synsedimentary tectonics on the development of some Late Cretaceous source rocks, Abu Gharadig Basin, Western Desert, Egypt. Proc. EGPC 13th Petrol. Expl. Prod. Conf., Cairo II, pp. 475–495.

BECHTEL, A., PEVAZ, M. AND PÜTTMANN, W., 1998. Role of organic matter and sulphate-reducing bacteria for metal sulphide precipitation in the Bahloul Formation at the Bou Grine Zn/Pb deposit (Tunisia). Chem. Geol. 144, pp. 1–21.

BECKMANN, B., HOFMANN, P. AND WAGNER, T., in press. Linking Coniacian-Santonian (OAE3) black shale formation to African climate variability: a reference section from the eastern tropical Atlantic at orbital time scales (ODP Site 959, off Ivory Coast/Ghana). In: Pradier, B. and N. Harris (Eds.), Source Rock Development: Bioproductivity, Organic Preservation or Sedimentation Rate? SEPM Special Publication.

BÉDIR, M., BOUKADI, N., TLIG, S., TIMZAL, F.B., ZITOUNI, L., ALOUANI, R., SLIMANE, F., BOBIER, C. AND ZARGOUNI, F., 2001. Subsurface Mesozoic basins in the central Atlas of Tunisia: tectonics, sequence deposit distribution, and hydrocarbon potential. AAPG Bull. 85 5, pp. 885–907.

BEHRENS, M., KRUMSIEK, K., MEYER, D.E., SCHÄFER, A., SIEHL, A., STETS, J., THEIN, J. AND WURSTER, P., 1978. Sedimentationsabläufe im Atlas-Golf (Kreide Küstenbecken Marokko). Geol. Rundsch. 67, pp. 424–453.

BEIN, A. AND SOFER, Z., 1987. Origin of oils in Helez region, Israel-implications for exploration in the eastern Mediterranean. AAPG Bull. 71, pp. 65–75.

BEIN, A., ALMOGI-LABIN, A. AND SASS, E., 1990. Sulfur sinks and organic carbon relationships in Cretaceous organic-rich carbonates: implications for evaluation of oxygen- poor depositional environments. American Journal of Science 290(8), 882-911.

BELHADJ, F., 1996. Palaeozoic and Mesozoic stratigraphy of eastern Ghadamis and western Sirt basins. In: Salem, M.J., Mouzughi, A.J. and Hammuda, O.S., (Eds.), The Geology of Sirt Basin vol. 1, Elsevier, pp. 57–96.

BELHADJ, Z., NAILI, H., NACERBEY, R., 1998. Stratigraphie et sedimentologie des reservoirs carbonates du Cenomano–Turonien dans le permis Negrine. Internal report, Sonatrach (unpublished).

BELL, K.G., GOODMAN, C. and W.L. WHITEHEAD, 1940. Radioactivity of sedimentary rocks and associated petroleum. AAPG Bull. 24, 1529-1547.

BEN FERJANI, A., BUROLLET, P.F. AND MEJRI, F., 1990. Petroleum Geology of Tunisia. Entreprise Tunisienne d'Activités Pétrolières, Tunis.

BENKHEROUF, F., 1987. Microbiostratigraphie et paléoenvironnement des marnes Cénomaniennes du Dj, Dyr (Tebessa, Algérie). Rev. Micropaléontol. 30, pp. 69–78.

BERNER, R.A., 1983. Atmospheric carbon dioxide over Phanerozoic time. Science 249, pp. 1382–1386.

BERNER, R.A., 1984. Sedimentary pyrite formation: an update. Geochim. Cosmochim. Acta, 48, pp. 605-615.

BERNER, R.A., 1991. A model for atmospheric CO2 over Phanerozoic time. American Journal of Science, 291, pp.339-376.

BERNER, R.A., 1993. Weathering and its effect on atmospheric CO2 over Phanerozoic time. Chem. Geol. 107, pp. 373–374.

BERNER, R.A., 1994. GEOCARB II: a revised model of atmospheric CO2 over Phanerozoic time. Am. J. Sci. 294, pp. 56–91.

BESSEREAU G., GUILLOCHEAU F., AND HUC A.Y., 1995. Source rock occurrence in a sequence stratigraphic framework: the example of the Lias of the Paris Basin. AAPG Studies in Geology, 40, 273-301.

BICE, K.L., AND NORRIS, P.R., 2002. Possible atmospheric CO2 extremes of the Middle Cretaceous (late Albian-Turonian), Paleoceanography, 17(4).

BISHOP, W.F., 1975. Geology of Tunisia and adjacent parts of Algeria and Libya. AAPG Bull. 59, pp. 413–450.

BISHOP, W.F., 1988. Petroleum geology of east–central Tunisia. AAPG Bull. 72 9, pp. 1033–1054.

BLAYAC, J., 1912. Esquisse géologique du bassin de la Seybouse et quelques regions voisines. Bull. Serv. Géol. Algérie, Algiers, 2ème sér., 6 (490 pp.).

BOOTE, D.R.D., CLARK-LOWES, D.D., AND TRAUT, M.W., 1998. Palaeozoic petroleum systems of North Africa. In: Macgregor, D. S., Moody, R. T. J., Clark-Lowes, D. D. (Eds.), Petroleum Geology of North Africa. Geol. Soc. London Sp. Publ., 132, 7-68.

BÖTTCHER, M.E., SMOCK, A. and CYPIONKA, H., 1998. Sulfur isotope fractionation during experimental precipitation of iron(II) and manganese(II) sulfide at room temperatures. Chem. Geol., 146, 127-134.

BÖTTCHER, M.E., THAMDRUP, B. and VENNEMANN, T.W., 2001. Oxygen and sulfur isotope fractionation during anaerobic bacterial disproportionation of elemental sulfur. Geochim. Cosmochim. Acta, 10, 1601-1609

BÖTTCHER, M.E. and SCHNETGER, B., 2002. Direct measurement of the concentration and isotopic composition of sulfur in black shales by means of combustion-isotope-ratio-monitoring mass spectrometry (C-irmMS). In: de Groot, P. (Eds.), Handbook of Stable Isotope Analytical Techniques, Elsevier, in press.

BOUSSAFIR, M. and LALLIER-VERGES, E., 1997. Accumulation of organic matter in the Kimmeridge Clay Formation (KCF): an update fossilisation model for marine petroleum source-rocks. Marine and Petroleum Geology, 14, 75-83,

BOUSSAFIR, M., LALLIER-VERGES, E., BERTRAND, P. and BADAUT-TRAUTH, D., 1995a. SEM and TEM studies on isolated organic matter and rock microfacies from a short-term organic cycle of the Kimmeridge Clay Formation (Yorkshire, GB). In: Lallier-Vergès, E. et al., (Eds.), Organic matter accumulation. Lecture Notes in Earth Sciences, Springer, Heidelberg, 57, 15-30.

BOUSSAFIR, M., GELIN, F., LALLIER-VERGES, E., DERENNE, S., BERTRAND, P. AND LARGEAU, C., 1995b. Electron microscopy and pyrolysis of kerogens from the Kimmeridge Clay Formation, UK: source organisms, preservation processes and origin of microcycles. Geochim. Cosmochim. Acta, 59, 3731-3747.

BOWN, P.R., YOUNG, J.R., 1998. Techniques. In: Bown, P.R. (Eds.), Calcareous Nannofossil Biostratigraphy. Chapman and Hall, London, pp. 16-28.

BRALOWER, T.J. AND THIERSTEIN, H.R., 1984. Low productivity and slow deep-water circulation in Mid-Cretaceous oceans. Geology 12, pp. 614–618.

BRALOWER, T.J. AND THIERSTEIN, H.R., 1987. Organic carbon and metal accumulation rates in Holocene and Mid-Cretaceous sediments: palaeoceanographic significance. In: Brooks, J. and Fleet, A.J., (Eds.), Marine Petroleum Source Rocks. Geol. Soc., Special Publ. vol. 26, pp. 345–369.

BRALOWER, T.J., LECKIE, R.M., SLITER, W.V., THIERSTEIN, H.R., 1995. An integrated Cretaceous microfossil biostratigraphy. In: Bergren, W.A., Kent, D.V., Aubry, M.P., and Hardenbol, J., (Eds.), Geochronology, Time Scales and Global Stratigraphic Correlation. Society of Economic Paleontologists and Mineralogists Special Publication vol. 54, pp. 65-79.

BRASS, G.W., SOUTHAM, J.R. AND PETERSON, W.H., 1982. Warm saline bottom water in the ancient ocean. Nature 296, pp. 620–623.

BRASSELL, S.C., WARDROPER, A.M.K., THOMSON, I.D., MAXWELL, J.R. and EGLINTON, G., 1981. Specific acyclic isoprenoids as biological markers of methanogenic bacteria in marine sediments. Nature, 290, pp. 693-696.

BROECKER, W.S., AND PENG, T.-H, 1982. Tracers in the sea. Palisades, New York, Lamont-Doherty Geological Observatory, Columbia Univ., 690 p.

BRUMSACK, H.-J., 1980. Geochemistry of Cretaceous black shales from the Atlantic ocean (DSDP Legs 11, 12, 36, and 41), Chemical Geology, 31, 1-25.

BRUMSACK, H.-J. AND LEW, M., 1982. Inorganic geochemistry of Atlantic Ocean sediments with special reference to Cretaceous black shales. In: von Rad, U. et al., (Eds.), Geology of the Northwest African Continental Margin, Springer-Verlag, Berlin, pp. 661–685.

BRUMSACK, H.-J. AND THUROW, J., 1986. The geochemical facies of black shales from the Cenomanian/Turonian Boundary Event (CTBE). In: Degens, E.T., Meyers, P.A. and Brassell, S.C., (Eds.), Biogeochemistry of Black Shales. SCOPE/UNEP Sonderband, Mitt. Geol.-Paläont. Inst. Univ. Hamburg vol. 60, pp. 247–265.

BRUMSACK, H.-J., 1986. The inorganic geochemistry of Cretaceous black shales (DSDP Leg 41) in comparison to modern upwelling sediments from the Gulf of California. In: Summerhayes, C.P. and Shackleton, J.N. (Eds.), North Atlantic Palaeoceanography. Geological Society, Special Publications, London, pp. 447-462.

BUCHBINDER, B., BENJAMINI, C. AND LIPSON-BENITAH, S., 2000. Sequence development of Late Cenomanian–Turonian carbonate ramps, platforms and basins in Israel. Cretac. Res. 21, pp. 813–843.

BUGGISCH, W., 1972. Zur Geologie und Geochemie der Kellwasserkalke und ihrer begleitenden Sedimente (Unteres Oberdevon). Abh. hess. L.-Amt Bodenforsch. 62, 1-68.

BUGGISCH, W., 1991. The global Frasnian Famennian " Kellwasser Event". Geol. Rundschau, 80, 49-72.

BUROLLET, P.F., 1956. Contribution à l'etude stratigraphique de la Tunisie Centrale. Ann. Mines Geol. (Tunis) 18 (345 pp.).

BUROLLET, P.F., 1991. Structures and tectonics of Tunisia. Tectonophysics 195, pp. 359–369.

BUROLLET, P.F., DUMSTRE, A., KEPPEL, D. AND SALVADOR, A., 1954. Unites stratigraphiques en Tunisie centrale. 19e Congress geologie internationale. Algiers 21, pp. 243–254.

BURWOOD, R., REDFERN, J., COPE, M.J., in press. Geochemical evaluation of East Sirte Basin (Libya) petroleum systems and oil provnance. Geol. Soc., London, Special Publ.

BUSH, A.B.G. AND PHILANDER, S.G.H., 1997. The Late Cretaceous: simulation with a coupled atmosphere–ocean GCM. Paleoceanography 21, pp. 475–516.

BUSSON, G. AND CORNÉE, A., 1991. The Sahara from the Middle Jurassic to the Middle Cretaceous: data on environments and climates based on outcrops in the Algerian Sahara. J. Afr. Earth Sci. 12, pp. 105–285.

BUSSON, G. AND CORNÉE, A., 1996. L'événement océanique anoxique du Cénomanien supérieur-terminal. Soc. Géol. Nord. Publ. 23 (143 pp.) .

BUSSON, G., 1984. Relations entre la sédimentation du Crétacé moyen et supérieur de la plate-forme du Nord-Ouest africain et les dépôts contemporains de l'Atlantique centre et nord. Eclogae Geol. Helv. 77, pp. 221–235.

BUSSON, G., 1998. Sedimentary dynamics of the epicontinental platform: Middle Cretaceous of the Algero–Tunisian Sahara. Dynamics and Methods of Study of Sedimentary Basins. Oxford and IBH Publishing and Editions Technip, Paris, pp. 111–128.

BUSSON, G., AMÉDRO, F., NÉRAUDEAU, D. AND CORNÉE, A., 1996. Comparaison entre la Série riche en matière organique du Cénomanien supérieur–Turonien basal du Maghreb oriental (Membre Bahloul) et la Série contemporaine calcaire cratonique du Tinrhert (Sahara Central, Algérie). Strata, Sér. 1, 8, pp. 51–53.

BUSSON, G., DHONDT, A., AMEDRO, F., NERAUDEAU, D. AND CORNEE, A., 1999. La grande transgression du Cénomanien supérieur–Turonien inférieur sur la Hamada de Tinrhert (Sahara algérien): datations biostratigraphiques, environments de dépot et comparaison d'un témoin épicratonique avec les séries contemporaines à matière organique du Maghreb. Cretac. Res. 20, pp. 29–46.

CAIRE, A., 1957. Etude géologique de la région des Biban (Algérie). Pub. Serv. Carte géol. Algérie, Algiers 16 2 tomes (793 pp.).

CALDEIRA, K. AND RAMPINO, M.R., 1991. The Mid-Cretaceous super plume, carbon dioxide, and global warming. Geophys. Res. Lett. 18, pp. 987–990.

CAMOIN, G., 1989. Les plates-formes carbonatées du Turonien et du Sénonien de Méditerranée centrale, Tunisie, Algérie, Sicile. Thesis, Univ. Marseille. 899 pp.

CAMOIN, G.F., 1991. Sedimentologic and paleotectonic evolution of carbonate platforms on a segmented continental margin: example of the African Tethyan margin during Turonian and Early Senonian times. Palaeogeogr. Palaeoclimatol. Palaeoecol. 87, pp. 29–52.

CARON, M., ROBASZYNSKI, F., AMÉDRO, F., BAUDIN, F., DECONINCK, J.-F., HOCHULI, P., VON SALIS-PERCH NIELSEN, K. AND TRIBOVILLARD, N., 1999. Estimation de la durée de l'événement anoxique global au passage Cénomanien/Turonien. Approche cyclostratigraphique dans la Formation Bahloul en Tunisie centrale. Bull. Soc. Géol. Fr. 170 2, pp. 145–160.

CHAMBERS, L.A. and TRUDINGER, P.A., 1979. Microbial fractionation of stable sulfur isotopes: A review and critique. Geomicrobiol. Journ., 1, 249-293.

CHARRIÈRE, A., 1996. Contexte paléogéographique et paléotectonique de la formation des bassins crétacés du Moyen Atlas (Maroc) à la lumière des données stratigraphiques récentes. Bull. Soc. Géol. Fr. 167 5, pp. 617–626.

CHARRIÈRE, A., ANDREU, B., CISZAK, R., KENNEDY, W.J., ROSSI, A. AND VILA, J.-M., 1998. La transgression du Cénomanien supérieur dans la Haute Moulouya et le Moyen Atlas Méridional. Maroc. Geobios 31 5, pp. 551–569.

CHERIF, O.H., AL-RIFAIY, I.A., AL AFIFI, F.I. AND ORABI, O.H., 1989. Foraminiferal biostratigraphy and paleoecology of some Cenomanian–Turonian exposures in west–central Sinai (Egypt). Rev. Micropaleontol. 31, pp. 243–262.

CHOUBERT, G., FAURE-MURET, A. and HOTTINGER, L., 1966. Aperçu géologique du Basin Côtier de Tarfaya. Notes et Mém. Serv. Geól. Maroc, 175 (I), 7-106, Rabat.

CHOUBERT, G., FAURE-MURET, A. and HOTTINGER, L., 1972. La série stratigraphique de Tarfaya Maroc sud occidental, et le problème de la naissance de l´Atlantique. Notes et Mém. Serv. Géol. Maroc, 31, 29-40.

CLIFFORD, H.J., ROGERS, G. AND MUSRATI, H., 1980. Geology of a stratigraphic giant: messla Oil Field, Libya. In: Halbouty, M., (Eds.), Giant Oil Fields of the Decade 1968–1978. AAPG Mem. vol. 30, pp. 507–524.

COCCIONI, R., AND GALEOTTI, S., 2003, The Mid-Cenomanian Event: prelude to OAE 2. Palaeogeography, Palaeoclimatology, Palaeoecology 2978, pp. 1-14.

COLLIGNON, M. AND LEFRANC, J.P., 1974. Mise en evidence de la communication saharienne entre Tethys et Atlantique Sud d'après les fossiles cenomaniens et turoniens du Tademait (Sahara Algerien). C. R. Acad. Sci. Paris 278 D, pp. 2257–2261.

CREANEY, S. AND PASSEY, Q.R., 1993. Recurring patterns of total organic carbon and source rock quality within a sequence stratigraphic framework. AAPG Bull. 77, 386-401.

CYPIONKA H., SMOCK A.M. and BÖTTCHER M.E., 1998. A combined pathway of sulfur compound disproportionation in Desulfovibrio desulfuricans. FEMS Microbiol. Letters, 166, 181-186.

DA GAMA, R., RAVILIOUS, K., BROWN, P.R. AND STREET, C., 2000. Calcareous nannoplankton palaeoecology from the Cenomanian–Turonian of Tarfaya, Morocco (abstr.). Intern. Workshop on North African Micropalaeontology for Petroleum Exploration, Univ. College London, 21-25 Aug 2000, Abstracts., p. 18.

DARWISH, M., ABU KHADRA, A.M., ABDEL HAMID, M.L. AND HAMED, A., 1994. Sedimentology, environmental conditions and hydrocarbon habitat of the Bahariya Formation, Central Abu Gharadig basin, Western Desert, Egypt. Proc. EGPC 12th Petrol. Expl. Prod. Conf., Cairo I, pp. 429–449.

DEAN, W.E., ARTHUR, A.M. AND STOW, V.A.D., 1984. Origin and geochemistry of Cretaceous deep-sea black shales and multicolored claystones, with emphasis on Deep Sea Drilling Project Site 530, southern Angola Basin. In: Hay, W.W., et al. (Eds.), Initial Reports of the Deep Sea Drilling Project, 75, pp. 819-844.

DE GRACIANSKY, P.C., DEROO, G., HERBIN, J.P., JACQUIN, T., MAGNI, F., MONTADERT, L. AND MÜLLER, C., 1986. Ocean-wide stagnation episodes in the Late Cretaceous. Geol. Rundsch. 75, pp. 17–41.

DE GRACIANSKY, P. C., DEROO, G., HERBIN, J.P., MONTADERT, L., MÜLLER, C., SCHAAF, A. AND SIGAL, J., 1984. Ocean -wide stagnation episode in the late Cretaceous, Nature, 308, pp. 346-349.

DE LEEUW, J.W., van BERGEN, P.F., van AARSSEN, B.G.K., GATELLIER, J.L.A., SINNINGHE DAMSTÉ, J.S. and COLLINSON, M.E., 1991. Resistant biomacromolecules as major contributors to kerogen. Phill. Trans. R. Soc. London, 333, 329-337.

DE WEVER, P., DUÉE, G. AND EL KADIRI, K., 1985. Les séries stratigraphiques des klippes de Chrafate (Rif septentrional, Maroc) témoins d'une marge continentale subsidente au cours du Jurassique–Crétacé. Bull. Soc. Géol. Fr. (8), t. I 3, pp. 363–379.

DECONTO, R.M., HAY, W.W., THOMPSON, L.S. AND BERGENGREN, J., 1999. Late Cretaceous climate and vegetation interactions: The cold continental interior paradox. In: Barrera, E. and Johnson, C. (Eds.), The Evolution of Cretaceous Ocean/Climate Systems. Geological Society of America Special Publication, 332, pp. 391-406.

DELSOL, D., 1995. Well Evaluation Conference 1995-Algerie 1995, Schlumberger.

DEMAISON, G.J., AND MOORE, T.G., 1980. Anoxic environments and oil source bed genesis. Organic Geochemistry 2, pp. 9-31.

DERENNE, S., LARGEAU, C., BERKALOFF, C., ROUSSEAU, B., WILHELM, C. and HATCHER, P.G., 1992. Non-hydrolysable macromolecular constituents from outer walls of Chlorella fusca and Nanochlorum eucaryotumm. Phytochemistry, 31, 1923-1929.

DIDYK, B.M., SIMONEIT, R.T. and BRASSELL, S.C., 1978. Geochemical indicators of paleoenvironmental conditions of sedimentation. Nature, 272, 216-222.

DOKKA, A.M., GUELLATI, N. AND HAMEL, A., 1990. Cenomanian–Turonian carbonate reservoirs of Guerguett-El-Kihal, a new discovery in the Southeast Constantine Basin, Algeria [abstr.]. AAPG Bull. 74, p. 643.

DOSTAL, J. AND CAPEDRI, S., 1978. Uranium in metamorphic rocks. Contrib. Mineral. Petrol.-Beitr. Mineral. Petrol., 66, 409-414.

DURONIO, P., DAKSHE, A. AND BELLINI, E., 1991. Stratigraphy of the offshore Cyrenaica (Libya). In: Salem, M.J., Hammuda, O.S. and Eliagoubi, B.A., (Eds.), The Geology of Libya vol. 4, Elsevier, Amsterdam, pp. 1589–1620.

DYPVIK, H. AND ERIKSEN, D.Ø., 1983. Natural radioactivity of clastic sediments and the contributions of U, Th and K. Journ. Petrol. Geol., 5, 409-416.

EGLINTON, T.I., IRVINE, J.E., VAIRAVAMURTHY, A., ZHOU, W., and MANOWITZ, B., 1994. Formation and diagenesis of macromolecular organic sulfur in Peru Margin sediments. Org. Geochem., 22, 781-799.

EINSELE, G. AND WIEDMANN, J., 1982. Turonian black shales in the Moroccan coastal basins: first upwelling in the Atlantic Ocean?. In: von Rad, U., Hinz, K., Sarntheim, M. and Seibold, E., (Eds.), Geology of the Northwest African Continental Margin, Springer, Berlin, pp. 396–414.

EL ALBANI, A., CARON, M., DECONINCK, J.-F., ROBASZYNSKI, F., AMÉDRO, F., DAOUDI, L., EZAIDI, A., TERRAB, S. AND THUROW, J., 1997. Origines et signification sédimentologique de la nodulisation dans les dépots anoxiques du Turonien inférieur du bassin de Tarfaya (Maroc). C. R. Acad. Sci. Paris 324 Iia, pp. 9–16.

EL ALBANI, A., KUHNT, W., LUDERER, F., HERBIN, J.P. AND CARON, M., 1999a. Palaeoenvironmental evolution of the Late Cretaceous sequence in the Tarfaya Basin (southwest of Morocco). In: Cameron, N.R., Bate, R.H. and Clure, V.S., Editors, 1999. The Oil and Gas Habitats of the South Atlantic. Geol. Soc., London, Special Publ. vol. 153, pp. 223–240.

EL ALBANI, A., VACHARD, D., KUHNT, W. AND CHELLAI, H., 1999b. Signature of hydrodynamic activity caused by rapid sea level changes in pelagic organic-rich sediments, Tarfaya Basin (southern Morocco). C. R. Acad. Sci. Paris, Sci. Terre Planètes 329, pp. 397–404.

EL-ALAMI, M., RAHOUMA, S. AND BUTT, A.A., 1989. Hydrocarbon habitat in the Sirte Basin Northern Libya. Pet. Res. J. (Tripoli, PRC) 1, pp. 19–30.

EL-ALAMI, M.A., 1996. Habitat of oil in Abu Attiffel area, Sirt Basin, Libya. In: Salem, M.J., El-Hawat, A.S. and Sbeta, A.M., (Eds.), The Geology of Sirt Basin vol. 2, Elsevier, Amsterdam, pp. 337–348.

EL-BAKAI, M.T., 1997. Petrography and palaeoenvironment of the Sidi as Sid Formation in Northwest Libya. Pet. Res. J. (Tripoli, PRC) 9, pp. 9–26.

ELLOUZ, N., 1984. Etude de la subsidence de la Tunisie Atlasique, orientale et de la Mer Pelagienne. PhD thesis. Paris. 134 pp.

EMBERGER, J., 1960. Esquisse géologique de la partie orientale des monts de Ouled Nails. Bull. du Service de la Carte Géologique de l'Algérie Sér. 27, pp. 1–398.

EMEIS, K.-C., SAKAMOTO, T., WEHAUSEN, R. AND BRUMSACK, H.J., 2000. The sapropel record of the eastern Mediterranean Sea—Results of Ocean Drilling Program Leg 160. Palaeogeography, Palaeoclimatology, Palaeoecology 158, pp. 371–395.

ENSSLIN, R., 1992. Cretaceous synsedimentary tectonics in the Atlas system of central Morocco. Geol. Rundsch. 81, pp. 91–104.

ERBACHER, J., THUROW, J. AND LITTKE, R., 1996. Evolution patterns of radiolaria and organic matter variations, a new approach to identify sea-level changes in mid-Cretaceous pelagic environments. Geology 24, 499-502.

ERBACHER, J., HUBER, B.T., NORRIS, R.D. AND MARKEY, M., 2001. Increased thermohaline stratification as a possible cause for an ocean anoxic event in the Cretaceous period. Nature, 409, pp. 325-327.

ESPITALIE, J., LAPORTE, J.L., MADEC, J., MARQUIS, F., LEPLAT, P., PAULET, J. and BOUTEFEAU, A., 1977. Méthode rapide de caracterisation des roches mers de leur potential pétrolier et de leur degré d`évolution. Rév. Inst. Français du Pétrole, 33, 23-42.

FARRIMOND, P., EGLINTON, G., BRASSELL, S.C. AND JENKYNS, H.C., 1990. The Cenomanian/Turonian anoxic event in Europe: an organic geochemical study. Mar. Pet. Geol. 7, pp. 75–89.

FENET, B., 1975. Recherches Sur L'alpinisation de la Bordure Septentrionale du Bouclier Africain à Partir de L'étude D'un Élément de L'orogène Nord-Maghrébin: Les Monts du Djebel Tessala et les Massifs du Littoral Oranais., Thèse Sciences, Nice.

FERTL, W.H. AND CHILINGARIAN, G.V., 1990. Hydrocarbon resource evaluation in the Woodford shale using well logs. Journ. Petrol. Science and Engineering, 4, 347-357.

FERTL, W.H. AND RIEKE, H.H. III, 1980. Gamma ray spectral evaluation techniques identify fractured shale reservoirs and source-rock characteristics. Journ. Petroleum Technology, November 1980, 2053-2062.

FISHER, Q.J. AND WIGNALL, P.B., 2001. Palaeoenvironmental controls on the uranium distribution in an Upper Carboniferous black shale (Gastrioceras listeri Marine Band) and associated strata; England. Chemical Geology, 175, 605-621.

FLEXER, A., ROSENFELD, A., LIPSON-BENITAH, S. AND HONIGSTEIN, A., 1986. Relative sea level changes during the Cretaceous in Israel. AAPG Bull. 70, pp. 1685–1699.

FLÖGEL, S., 2002. On the influence of precessional Milankovitch cycles on the Late Cretaceous climate system: comparison of GCM results, geochemical, and sedimentary proxies for the Western Interior Seaway of North America. PhD thesis. Kiel University, Kiel, Germany, pp. 1–236.

FOSSING, H. and JØRGENSEN, B.B., 1989. Measurement of bacterial sulfate reduction in sediments: Evaluation of a single-step chromium reduction method. Biogeochem 8, 205 222.

GAAYA, A. AND GHENIMA, R., 1998. Major and potential petroleum systems in Tunisia. Prospectivity and expectations. In: Proc. 6th Tunis. Petroleum Expl. and Prod. Conf., Tunis 5–9 May 1998. ETAP Memoir vol. 12, pp. 169–177.

GALE, A.S., JENKYNS, H.C., KENNEDY, W.J. AND CORFIELD, R.M., 1993. Chemostratigraphy versus biostratigraphy: data from around the Cenomanian–Turonian boundary. J. Geol. Soc. (Lond.) 150, pp. 29–32.

GALE, A.S., SMITH, A.B., MONKS, N.E.A., YOUNG, J.R., HOWARD, A., WRAY, D.S., AND HUGGETT, J.M., 2000. Marine biodiversity through the late Cenomanian-early Turonian: palaeoceanographic controls and sequence stratigraphic biases. J. Geol. Soc. (Lond.) 157, pp. 745-757.

GALE, A.S., HARDENBOL, J., HATHWAY, B., KENNEDY, W.J., YOUNG, J.R. AND PHANSALKAR, V., 2002. Global correlation of Cenomanian (Upper Cretaceous) sequences: evidence for Milankovitch control on sea level. Geology 30, pp. 291–294.

GEALEY, W.K., 1988. Plate tectonic evolution of the Mediterranean–Middle East region. Tectonophysics 155, pp. 285–306.

GÉLARD, J.P., 1979. Géologie du Nord-Est de la Grande Kabylie. Mém. géol. Univ. Dijon 5 (335 pp.) .

GELIN, F., BOOGERS, I., NOORDELOOS, A.A.M., SINNINGHE DAMSTÉ, J.S., HATCHER, P.G. and DE LEEUW, J.W., 1996. Novel, resistant microalgal polyethers: An important sink of organic carbon in the marine environment? Geochim. Cosmochim. Acta 60, 1275-1280.

GHORI, K.A.R., 1999. Silurian-Devonian petroleum source-rock potential and thermal history, Carnarvon Basin, Western Australia. Geol. Surv. Western Australia, Report 72, Perth, 88 p.

GLATZMALER, G.A., COE, R.S., HONGRE, L. AND ROBERTS, P.H., 1999. The role of the Earth's mantle in controlling the frequency of geomagnetic reversals. Nature 401, pp. 885-890.

GLANCY, T.J.J., ARTHUR, M.A., BARRON, E.J. AND KAUFFMAN, E.G., 1993. A paleoclimate model for the North American Cretaceous (Cenomanian–Turonian) epicontinental sea. In: Caldwell, W.G.E. and Kaufman, E.G., Editors, 1993. Evolution of the Western Interior Basin. Geol. Assoc. of Canada, Spec. Pap. vol. 39, pp. 219–241.

GLLENNIE, K.W., (Ed.), 1998. Petroleum Geology of the North Sea. Blackwell Science, 4th Edition.

GOOSSENS, H., DE LEEUW, J.W., SCHENCK, P.A. and BRASSEL, S.C., 1984. Tocopherols as likely precursors of pristane in ancient sediments and crude oils. Nature, 312, 440-442.

GOUDIE, A.S. AND MIDDLETON, N.J., 2001. Saharan dust storms: nature and consequences. Earth-Sci. Rev. 56, pp. 179–204.

GRADSTEIN, F.M., AGTERBERG, P.F., OGG, G.J., HARDENBOL, J., VAN VEEN, P., THIERRY, J. AND HUANG, Z., 1995. A Triassic, Jurassic and Cretaceous time scale. In: e.a. W.A. Berggren (Eds.), Geochronology, Time Scales and Global Stratigraphic Correlation. Spec. Soc. Econ. Paleontol. Mineral., pp. 95-126.

GRAS, R. AND THUSU, B., 1998. Trap architecture of the Early Cretaceous Sarir Sandstone in the eastern Sirt Basin, Libya. In: MacGregor, D.S., Moody, R.T.J. and Clark-Lowes, D.D., (Eds.), Petroleum Geology of North Africa. Geological Society, Special Publication vol. 132, pp. 317–334.

GRASSO, M., TORELLI, L. AND MAZZOLDI, G., 1999. Cretaceous–Palaeogene sedimentation patterns and structural evolution of the Tunisian shelf, offshore the Pelagian islands (central Mediterranean). Tectonophysics 315, pp. 235–250.

GREINER, A.CH., SPYCKERELLE, C. and ALBRECHT, P., 1976. Aromatic hydrocarbons from geological sources. Part I: New natural occurring phenanthrene and chrysene derivatives. Tetrahedron, 32, 257-260.

GREINER, A.CH., SPYCKERELLE, C., ALBRECHT, P. and OURISSON, G., 1977. Aromatic hydrocarbons from geological sources. Part V: Mono- and Di-aromatic hopane derivatives. Journ. Chem. Res. (S), 334.

GRICE, K., KLEIN-BRETELER, W.C.M., SCHOUTEN, S., GROSSI, V., DE LEEUW, J.W. and SINNINGHE DAMSTÉ, J.S., 1998. The effects of zooplankton herbivory on biomarker proxy records. Palaeoceanography, 13, 686-693.

GRÖCKE, D.R., 1997. Carbon-isotope stratigraphy of terrestrial plant fragments in the Early Cretaceous from south-eastern Australia. In: Wolberg, D.L., Stump, E. and Rosenberg, G. (Eds.), DinoFest International. Proceedings of a symposium held at Arizona State University, Academy of Natural Sciences, Philadelphia. pp. 457-461.

GUILLEMOT, J., 1952. La bordure sud-tellienne dans le Titteri. 19e Congr. Géol. Intern. Alger. Monograph Rég. 1re sér., Algérie.

GUIRAUD, R. AND BOSWORTH, W., 1999. Phanerozoic geodynamic evolution of northeastern Africa and the northwestern Arabian platform. Tectonophysics 315, pp. 73–108.

GUIRAUD, R. AND MAURIN, J.C., 1991. Le rifting en Afrique au Crétacé inférieur: synthèse structurale, mise en évidence de deux étapes dans la genèse des bassins, relations avec les ouvertures océaniques péri-africaines. Bull. Soc. Géol. Fr. 162, pp. 811–823.

GUIRAUD, R., 1990. Evolution post-triasique de l'avant-pays de la chaine alpine en Algérie. Office National de la Géologie, Mem. 3 (266 pp.) .

GUIRAUD, R., BELLION, Y., BENKHELIL, J. AND MOREAU, C., 1987. Post-Hercynian tectonics in northern and western Africa. Geol. J. 22, pp. 433–466.

HALIM, M., JOFFRE, J. AND AMBLÈS, A., 1997. Characterization and classification of Tarfaya kerogen (South Morocco) based on its oxidation products. Chem. Geol. 141, pp. 225–234.

HALLETT, D., 2002. Petroleum Geology of Libya. Elsevier, Amsterdam 503 pp.

HAMMAD, M., GHANEM, M. AND EL-NADY, M., 1992. Organogeochemical evaluation of potential source beds and oil generation in Abu Gharadig Basin, north Wesern Desert, Egypt. In: Proc. RGPC 11th Petrol. Expl. Prod. Conf., Cairo, pp. 199–218.

HAMMUDA, O.S., SBETA, A.M., MOUZUGHI, A.J. AND ELIAGOUBI, B.A., 1985. Stratigraphical nomenclature of northwestern offshore Libya. Earth Sci. Soc. Libya (169 pp.).

HAMMUDA, O.S., SBETA, A.M. AND WORSLEY, D., 2000. Field guide to the Mesozoic succession of Jabal Nefusah, NW Libya. Fielguide Post-Conference Fieldtrip 9-12 Nov. 2000, Sedimentary Basins of Libya. Second Symposium. Geology of Northwest Libya. 50 pp.

HANDOH, I.C., BIGG, G.R., JONES, E.J.W. AND INOUE, M., 1999. An ocean modeling study of the Cenomanian Atlantic: equatorial paleo-upwelling, organic-rich sediments and the consequences for a connection between the proto-North and South Atlantic. Geophys. Res. Lett. 26, pp. 223–226.

HAQ, B.U., HARDENBOL, J. and VAIL, P.R., 1987. Chronology of fluctuating sea-levels since the Triassic. Science, 235, 1156-1167.

HARDENBOL, J., CARON, M., AMEDRO, F., DUPUIS, C. AND ROBASZYNSKI, F., 1993. The Cenomanian–Turonian boundary in central Tunisia in the context of a sequence-stratigraphic interpretation. Cretac. Res. 14, pp. 449–454.

HARDENBOL, J., THIERRY, J., FARLEY, M.B., JACQUIN, T., DE GRACIANSKY, P.-C. AND VAIL, P.R., 1998. Cretaceous sequence chronostratigraphy. In: De Graciansky, P.-C., Hardenbol, J., Jacquin, T. and Vail, P.R., (Eds.), Mesozoic and Cenozoic Sequence Stratigraphy of European Basins. Soc. Econ. Paleontol. Mineral. Spec. Publ. vol. 60 Chart 4; Tulsa .

HART, M.B. AND LEARY, P.N., 1989. The stratigraphic and paleogeographic setting of the Late Cenomanian `anoxic event'. J. Geol. Soc. (Lond.) 146, pp. 305–310.

HARTGERS, W.A., LOPEZ, J.F., SINNINGHE DAMSTÉ, J.S., REISS, C., MAXWELL, J.R. and GRIMALT, J.O., 1997. Sulphur-binding in recent environments. Part I: Speciation of sulfur and iron and implications for the occurrence of organo-sulphur compounds. Geochim. Cosmochim. Acta, 61, 4769-4788.

HARTMANN, M. and NIELSEN, H., 1969. $\delta^{34}S$-Werte in rezenten Meeressedimenten und ihre Deutung am Beispiel einiger Sedimentprofile aus der westlichen Ostsee. Geologische Rundschau, 58, 621-655

HASEGAWA, T., 1997. Cenomanian–Turonian carbon isotope events recorded in terrestrial organic matter from northern Japan. Palaeogeogr. Palaeoclimatol. Palaeoecol. 130, pp. 251–273.

HAUGLUSTAINE, D., EMMONS, L., NEWCHURCH, M., BRASSEUR, G., TAKAO, T., MATSUBARA, K., JOHNSON, J., RIDLEY, B., STITH, J. AND DYE, J., 2001. On the role of lightning NOx in the formation of tropospehric ozone plumes: a global model perspective. Journal of Atmospheric Chemistry 38, pp. 277-294.

HAY, W.W., 1988. Paleoceanography: a review for the GSA Centennial. Geol. Soc. of Am. Bulletin 100, pp. 1934-1956.

HAY, W.W. AND DECONTO, M.R., 1999. A comparison of modern and Late Cretaceous meridional energy transport and oceanology. In: Barrera, E. and Johnson, C., (Eds.), The Evolution of Cretaceous Ocean/Climate Systems. Geological Society of America Special Publication, 332, pp. 283-300.

HAY, W.W., DECONTO, R., WOLD, C.N., WILSON, K.M., VOIGT, S., SCHULZ, M., WOLD-ROSSBY, A., DULLO, W.C., RONOV, A.B., BALUKHOVSKY, A.N., AND SOEDING, E., 1999. Alternative global Cretaceous paleogeography. In: Barrera, E. and Johnson, C., (Eds.), The Evolution of Cretaceous Ocean/Climate Systems. Geological Society of America Special Paper 332, pp. 1-47.

HAYS J.D. AND PITMAN W.C., 1973. Lithospheric plate motion, sea level changes and ecological consequences. Nature 246, pp. 18-22.

HEINRICHS, H., BRUMSACK, H.-J., LOFTFIELD, N. AND KÖNIG, N., 1986. Verbessertes Druckaufschlußsystem für biologische und anorganische Materialien, Zur Pflanzenernährung und Bodenkunde, 149, pp. 350-353.

HERBIN, J.P., MONTADET, L., MÜLLER, C., GOMEZ, R., THUROW, J. AND WIEDMANN, J., 1986. Organic-rich sedimentation at the Cenomanian–Turonian boundary in oceanic and coastal basins in the North Atlantic and Tethys. In: Summerhayes, C.P. and Shackleton, N.J., (Eds.), North American Palaeoceanography Geol. Soc., London, Special Publ. vol. 21, pp. 389–422.

HERKAT, M. AND DELFAUD, J., 2000. Genèse des séquences du Crétacé supérieur des Aurès (Algérie). Rôle de l'eustasime, de la tectonique, de la subsidence: une mise au point. C. R. Acad. Sci., Sér. IIa 330, pp. 785–792.

HERKAT, M., 2001. Eustatic and palaeogeographic control on the Aures Basin Upper Cretaceous sedimentation (Algeria) [abstr.]. 21st Int. Assoc. Sedimentol. Meeting, 3-5 Sep. 2001, Davos.

HERRLE, J.O., 2003. Reconstructing nutricline dynamics of mid-Cretaceous oceans: evidence from calcareous nannofossils from the Niveau Paquier black shale (SE France), Marine Micropaleontology, 47, 307-321.

HERRON, S.L., 1991. In situ evaluation of potential source rocks by wireline logs. In: Merrill, K., (Eds.), Source and migration processes and evaluation techniques: AAPG Treatise of Petroleum Geology, Handbook of Petroleum Geology, 127-134.

HERRON, S.L., LE TENDRE, L., 1990. Wireline source-rock evaluation in the Paris Basin. In: Huc, A.Y., (Eds.), Deposition of organic facies. AAPG Studies in Geology, 30, 57-71.

HESELDEN, R.G.W., CUBITT, J.M., BORMAN, P. AND MADI, F.M., 1996. Lithofacies study of the Lidam and Maragh formations (Late Cretaceous) of the Masrab Field and adjacent areas, Sirt basin, Libya. In: Salem, M.J., El-Hawat, A.S. and Sbeta, A.M., (Eds.), The Geology of the Sirt Basin vol. II, Elsevier, Amsterdam, pp. 197–210.

HEYMAN, M.A.W., 1990. Tectonic and depositional history of the Moroccan continental margin. In: Tankard, A.J. and Balkwill, H.R., (Eds.), Extensional Tectonics and Stratigraphy of the North Atlantic Margins. AAPG Memoir vol. 46, pp. 323–340.

HILBRECHT, H., ARTHUR, M.A. AND SCHLANGER, S.O., 1986. The Cenomanian–Turonian boundary event: sedimentary, faunal and geochemical criteria developed from stratigraphic studies in Germany. In: Walliser, O., (Eds.), Global Bio-Events, Lecture Notes in Earth Science, Springer, Heidelberg, pp. 345–351.

HIRSCH, F., FLEXER, A., ROSENFELD, A. AND YELLIN-DROR, A., 1995. Palinspastic and crustal setting of the eastern Mediterranean. J. Pet. Geol. 18, pp. 149–170.

HOFMANN, P., BECKMANN, B. AND WAGNER, T., 2003. A millennial to centennial-scale record of African climate variability and organic carbon accumulation in the Coniacian-Santonian eastern tropical Atlantic (ODP Site 959, off Ivory Coast/Ghana), Geology, 31, pp. 135-138.

HOLBOURN, A., KUHNT, W., EL ALBANI, A., LY, A., GOMEZ, R. AND HERBIN, J.P., 1999a. Palaeoenvironments and palaeobiogeography of the Late Cretaceous Casamance transect (Senegal, NW Africa): distribution patterns of benthic foraminifera, organic carbon and terrigenous flux. Neues Jahrb. Geol. Paläontol. Abh. 212, pp. 335–377.

HOLBOURN, A., KUHNT, W., EL ALBANI, A., PLETSCH, T., LUDERER, F. AND WAGNER, T., 1999b. Upper Cretaceous palaeoenvironments and benthonic foraminiferal assemblages of potential source rocks from the western African margin, central Atlantic. In: Cameron, N.R., Bate, R.H. and Clure, V.S., (Eds.), The Oil and Gas Habitats of the South Atlantic, Geol. Soc., London, Special Publ. vol. 153, pp. 195–222.

HONIGSTEIN, A., LIPSON-BENITAH, S., CONWAY, B., FLEXER, A. AND ROSENFELD, A., 1989. Mid-Turonian anoxic event in Israel—a multidisciplinary approach. Palaeogeogr. Palaeoclimatol. Palaeoecol. 69, pp. 103–112.

HUBER, B.T., LECKIE, R.M., NORRIS, R.D., BRALOWER, T.J. COBABE, E., 1998. Foraminiferal assemblage and stable isotopic change across the Cenomanian-Turonian boundary in the subtropical North Atlantic. Journal of Foraminiferal Research, 29(4), 392-417.

HUBER, B.T., NORRIS, R.D. AND NACLEOD, K.D., 2002. Deep-sea paleotemperature record of extreme warmth during the Cretaceous. Geology, 30, pp. 123-126.

HUGHES, W.B. AND REED, J.D., 1995. Oil and source geochemistry and exploration implications in northern Tunisia. In: Proc. Seminar on Source Rocks and Hydrocarbon Habitat in Tunisia, Tunis, 15–18 Nov. 1995, ETAP Mem. vol. 9, pp. 49–67.

HUTTON, A.C., 1987. Petrographic classification of oil shales. Int. Journ. Coal Geology, 8, 203-231.

HUNT, M.J., 1996. Petroleum Geochemistry and Geology. Freeman and Company, New York, USA, p. 743.

IBOUH, H. AND ZARGOUNI, F., 1998. Nouvelles donnees sur la tectonique synsedimentaire du Cretace inferieur et le debut du Cretace superieur au niveau de la jonction des Jebels Orbata et Bouhedma (Tunisie meridionale). Afr. Geosci. Rev. 5, pp. 207–215.

IBRAHIM, M.W., 1991. Petroleum geology of the Sirt Group Sandstone, eastern Sirt Basin. In: Salem, M.J. et al., (Eds.), The Geology of Libya vol. VII, Elsevier, Amsterdam, pp. 2757–2779.

INGRAM, B.L., COCCIONI, R. MONTANARI, A. AND RICHTER F.M., 1994. Strontium isotopic composition of mid-Cretaceous seawater. Science 264, pp. 546-550.

ITTEKKOT, V., HAAKE, B., BARTSCH, M., NAIR, R.R. AND RAMASWAMY, V., 1992. Organic carbon removal in the sea: the continental connection. In: Summerhayes, C.P., Prell, W.L. and Emeis, K.C. (Eds.), Upwelling Systems: Evolution Since the Early Miocene. Geological Society Special Publication, pp. 167-176.

JACOBS, D.K. AND SAHAGIAN, D.L., 1993. Climate-induced fluctuations in sea level during non-glacial times. Nature 361, pp. 710–712.

JARVIS, I., CARSON, G.A., COOPER, M.K.E., HART, M.B., LEARY, P.N., TOCHER, B.A., HORNE, D. AND ROSENFELD, A., 1988. Microfossil assemblages and the Cenomanian–Turonian (Late Cretaceous) oceanic anoxic event. Cretac. Res. 9, pp. 3–103.

JARVIS, J., PHILIP, F. AND GARWOOD, T., 1999. Morocco's Tarfaya deepwater prospects encouraging. Oil Gas J. 16, pp. 90–94.

JENKYNS, H.C., 1980, Cretaceous anoxic events: from continents to oceans. J. Geol. Soc. (Lond.) 137, pp. 171-188.
JENKYNS, H.C., 1985. The Early Toarcian and Cenomanian–Turonian anoxic events in Europe: comparisons and contrasts. Geol. Rundsch. 74, pp. 505–518.
JENKYNS, H.C., 1997. Mesozoic anoxic events and palaeoclimate, Zbl. Geol. Paläont., 1, 943-949.
JENKYNS, H.C., Gale, A.S. and Corfield, R.M., 1994. Carbon- and oxygen-isotope stratigraphy of the English Chalk and Italian Scaglia and its paleoclimatic significance. Geol. Mag. 131, pp. 1–34.
JIA-ZHONG, Z. AND MILLERO, J.F., 1993. The chemistry of the anoxic waters in the Cariaco Trench. Deep Sea Research Part I: Oceanographic Research Papers, 40(5), pp. 1023-1041
JONES C.E., JENKYNS H.C., COE A.L. AND HESSELBO S.P., 1994. Strontium isotopic variations in Jurassic and Cretaceous sewater. Geochim. Cosmochim. Acta, 58, pp. 3061-3074.
JONES, B., AND MANNING, C.A.D., 1994. Comparison of geochemical indices used for the interpretation of palaeoredox conditions in ancient mudstones. Chemical Geology, 111, pp. 111-129.
JONES, C.E., AND JENKYNS, H.C., 2001. Seawater strontium isotopes, Oceanic Anoxic Events, and seafloor hydrothermal activity in the Jurassic and Cretaceous. American Journal of Science, 301, pp. 112-149.
JONGSMA, D., VAN HINTE, J.E. AND WOODSIDE, J.M., 1985. Geologic structure and neotectonics of the North African continental margin south of Sicily. Mar. Pet. Geol. 2, pp. 156–179.
JØRGENSEN, B.B., 1988. Ecology of the sulfur cycle: oxidative pathways in sediment. In: Cole J. A. and Ferguson S. J. (Eds.), Soc. Gen. Microbiol. Symposium, 42, pp. 31-63.
JUIGNET, P. AND BRETON, G., 1992. Mid-Cretaceous sequence stratigraphy and sedimentary cyclicity in the western Paris Basin. Palaeogeogr. Palaeoclimatol. Palaeoecol. 91, pp. 192–218.
JUNGHANS, W.D., RÖHL, H.-J., SCHMID-RÖHL, A. AND AIGNER, T., in press. Spektrale Gamma-Ray Messungen - ein Schlüssel für Sequenzstratigraphie in Schwarzschiefern: Beispiel Posidonienschiefer (Lias , SW-Deutschland). N. Jb. Geol. Paläont. Mh.
KALKREUTH, W. and MACAULEY, G., 1984. Organic Petrology of selected oil shale samples from the Lower Carboniferous Alberta Formation, New Brunswick, Canada. Bull. Canad. Petrol. Geol., 32, 38-51.
KATZ, B.J. AND PHEIFER, R.N., 1986. Organic geochemical characteristics of Atlantic Ocean Cretaceous and Jurassic black shales. Mar. Geol. 70, pp. 43–66.
KAZI-TANI, N., 1986. Evolution geodynamique de la bordure nord africaine: le domaine intraplaque nord algerien, approche sequentielle. These sd. Univ. Pau, 2 vol., 871 pp.
KEELEY, M.L. AND MASSOUD, M.S., 1998. Tectonic controls on the petroleum geology of NE Africa. In: Macgregor, D.S., Moody, R.T.J. and Clark-Lowes, D.D., (Eds.), Petroleum Geology of North Africa. Geol. Soc., London, Special Publ. vol. 132, pp. 265–281.
KENT, D.V. AND OLSEN, P.E. 2000. Magnetic polarity stratigraphy and paleolatitude of the Triassic-Jurassic Blomidon Formation in the Fundy Basin (Canada): implications for early Mesozoic tropical climate gradients. Earth and Planetary Science Letters 170, pp. 311-324.
KELLER, G., HAN, Q., ADATTE, T. AND BURNS, S.J., 2001. Palaeoenvironment of the Cenomanian–Turonian transition at Eastbourne, England. Cretaceous Research 22, pp. 391–422.
KENNEDY, W.J., WALASZCZYK, I., AND COBBAN, W.A., 2000, Pueblo, Colorado, USA, candidate Global Boundary Stratotype Section and point for the base of the Turonian stage of the Cretaceous, and for the base of the middle Turonian substage, with a revision of the Inoceramidae (Bivalvia). Acta Geologica Polonica, 50, pp. 295-334.
KHALED, K.A., 1999. Cretaceous source rocks at the Abu Gharadig oil-and gasfield, northern Western Desert, Egypt. J. Petroleum Geol. 22 4, pp. 377–395.
KIEKEN, M., 1962. Les traits essentials de la Géologie Algérienne. In: Livre à la Mémoir du Professeur Paul Fallot. Soc. Géol. de France, 1, 545–614.
KLEMME, H.D. AND ULMISHEK, G.F., 1991. Effective petroleum source rocks of the world: stratigraphic distribution and controlling depositional factors. AAPG Bull. 75, pp. 1809–1851.
KLEN, L., 1974. Geological Map of Libya, 1:250.000, Sheet NI 34-14 Benghazi, and Explanatory Booklet. Industrial Research Center, Tripoli 56 pp.
KLETT, T.R., 2001. Total petroleum systems of the Pelagian Province, Tunisia, Libya, Italy, and Malta–The Bou Dabbous–Tertiary and Jurassic–Cretaceous composite. US Geol. Survey Bull. 2202-D 79 pp. .
KLINKHAMMER, G. P. AND PALMER, M. R., 1991. Uranium in the oceans: Where it goes and why. Geochim. Cosmochim. Acta, 55, 1799-1806.
KOHNEN, M.E.L., SCHOUTEN, S., SINNINGHE DAMSTÉ, J.S., DE LEEUW, J.W., MERRITT, D.A., AND HAYES, J.M., 1992. Recognition of paleobiochemicals by a combined molecular sulfur and isotope geochemical approach. Science, 256, pp. 358-362.
KOK, M.D., SCHOUTEN, S. and SINNINGHE DAMSTÉ, J.S., 2000. Formation of insoluble, nonhydrolyzable, sulfur-rich macromolecules via incorporation of inorganic sulfur species into algal carbohydrates. Geochim. Cosmochim. Acta, 64, 2689-2699.
KOLONIC, S., WAGNER, T., SINNINGHE-DAMSTE, J., KUHNT, W., WAND, U., WEHNER, H., 2001. A combined geochemical approach to reconstruct the depositional environment of Cenomanian/Turonian

hydrocarbon source rocks in the Tarfaya–Layoune Basin (southern Morocco). North Africa Research Workshop, Oxford Brookes, Abstract volume, 2001.

KOLONIC, S., SINNINGHE-DAMSTÉ, J., BÖTTCHER, M.E., KUYPERS, M.M.M., KUHNT, W., BECKMANN, B., SCHEEDER, G. AND WAGNER, T., 2002. Geochemical characterization of Cenomanian/Turonian black shales from the Tarfaya Basin (SW Morocco). J. Pet. Geol. 25, pp. 325–350.

KOMINZ, M.A., 1984. Oceanic ridge volumes and sea-level change: an error analysis. AAPG Mem. 36, pp. 109–127.

KOOPMANS, P.M., DE LEEUW, J.W., LEWAN, M.D. and SINNINGHE DAMSTÉ, J.S., 1996a. Impact of dia- and catagenesis on sulphur and oxygen sequestration of biomarkers as revealed by artificial maturation of an immature sedimentary rock. Org. Geochem., 25, 391-426.

KOOPMANS, P.M., KÖSTER, J., VAN KAAM-PETERS, H.M.E., KENIG, F., SCHOUTEN, S., HARTGERS, W.A., DE LEEUW, J.W. AND SINNINGHÉ DAMSTÉ, J.S., 1996b. Diagenetic and catagenetic products of isorenieratane: molecular indicators for photic zone anoxia. Geochim. Cosmochim. Acta 60, pp. 4467–4496.

KÖSTER, J., VAN KAAM-PETERS, H.M.E., KOOPMANS, M.P., DE LEEUW, J.W. and SINNINGHE DAMSTÉ, J.S., 1997. Natural sulphurisation of homohopanoids: Effects on carbon number distribution, speciation and 22S/22R epimer ratios. Geochim. Cosmochim. Acta, 61, 2431-2452.

KOUTSOUKOS, E.A.M., MELLO, M.R. AND DE AZAMBUJA FILHO, N.C., 1991. Micropalaeontological and geochemical evidence of Mid-Cretaceous dysoxic–anoxic palaeoenvironments in the Sergipe Basin, northeastern Brazil. In: Tyson, R.V. and Pearson, T.H., (Eds.), Modern and Ancient Continental Shelf Anoxia. Geol. Soc., London, Special Publ. vol. 58, pp. 427–447.

KRUIJS, E. AND BARRON, E., 1990. Climate model prediction of paleoproductivity and potential source-rock distribution. In: Huc, A.Y., (Eds.), Deposition of Organic Facies. AAPG Studies in Geology vol. 30, pp. 195–216.

KUHNT, W., HERBIN, J.P., THUROW, J. AND WIEDMANN, J., 1990. Distribution of Cenomanian–Turonian organic facies in the western Mediterranean and along the adjacent Atlantic margin. In: Huc, A.Y., (Eds.), Deposition of Organic Facies. AAPG Studies in Geology vol. 30, pp. 133–160.

KUHNT, W. AND WIEDMANN, J., 1995. Cenomanian–Turonian source rocks: paleobiogeographic and paleoenvironmental aspects. In: Huc, A.-Y., (Eds.), Paleogeography, Paleoclimate, and Source Rocks AAPG Studies in Geology vol. 40, pp. 213–231.

KUHNT, W., NEDERBRAGT, A. AND LEINE, L., 1997. Cyclicity of Cenomanian–Turonian organic-carbon-rich sediments in the Tarfaya Atlantic coastal basin (Morocco). Cretac. Res. 18, pp. 587–601.

KUHNT, W., WIEDMANN, J., HERBIN, J.P., MOULLADE, M. AND THUROW, J., 2000. Paleogeographic distribution patterns of Cenomanian/Turonian source rocks: a North African perspective (abstract). Intern. Workshop on North African Micropalaeontology for Petroleum Exploration, Univ. College London, 21-25 Aug 2000, Abstracts., pp. 39–40.

KUHNT, W., EL CHELLAI, H., HOLBOURN, A., LUDERER, F., THUROW, J., WAGNER, T., EL ALBANI, A., BECKMANN, B., HERBIN, J.-P., KAWAMURA, H., KOLONIC, S., NEDERBRAGT, S., STREET, C., RAVILIOUS, K., 2001. Morocco basin's sedimentary record may provide correlations for Cretaceous paleoceanographic events worldwide. EOS 82 (33), 361, 364.

KUHNT, W., LUDERER, F., NEDERBRAGT, S., THUROW, J. AND WAGNER, T., in press. Orbital-scale Record of the Late Cenomanian-Turonian Oceanic Anoxic event (OAE2) in the Tarfaya Basin (Morocco), Geologische Rundschau.

KUSS, J. AND BACHMANN, M., 1996. Cretaceous paleogeography of the Sinai Peninsula and neighbouring areas. C. R. Acad. Sci., Ser. II, Sci. Terre Planetes 322, pp. 915–933.

KUYPERS, M.M.M., PANCOST, R.D. AND SINNINGHE DAMSTÉ, J.S., 1999. A large and abrupt fall in atmospheric CO2 concentrations during Cretaceous times. Nature 399, pp. 342–345.

KUYPERS, M.M.M., BLOKKER, P., HOPMANS, E.C., KINKEL, H., PANCOST, R.D., SCHOUTEN, S., AND SINNINGHE DAMSTÉ, J.S., 2002. Archaeal remains dominate marine organic matter from the early Albian oceanic anoxic event 1b. Palaeogeography, Palaeoclimatology, Palaeoecology, 185, pp. 211-234.

KUYPERS, M.M.M., PANCOST, R.D., NIJENHUIS, I.A. AND SINNINGHE DAMSTÉ, J.S., 2002. Enhanced productivity led to increased organic carbon burial in the euxinic North Atlantic basin during the Late Cenomanian oceanic anoxic event. Paleoceanography 17 (4).

LALLIER-VERGES, E., HAYES, J.M., BOUSSAFIR, M., ZABACK, D.A., TRIBOVILLARD, N.P., CONNAN, J AND BERTRAND, P. 1997. Productivity-induced sulphur enrichment of hydrocarbon-rich sediments from the Kimmeridge Clay Formation. Chem. Geol., 134, 277-288.

LAMOLDA, M.A., GOROSTIDI, A. AND PAUL, C.R.C., 1994. Quantitative estimates of calcareous nannofossil changes across the Plenus Marls (latest Cenomanian), Dover, England: implications for the generation of the Cenomanian–Turonian boundary event. Cretac. Res. 15, pp. 143–164.

LANDAIS, P., 1996. Organic geochemistry of sedimentary uranium ore deposits. Ore Geology Reviews, 11, 33-51.

LANGFORD, F.F. and BLANC-VALLERON, M.M., 1990. Interpreting Rock-Eval pyrolysis data using graphs of pyrolizable hydrocarbons vs. total organic carbon. AAPG. Bull., 76, 1491-1506.

LARGEAU, C. and DERENNE, S., 1993. Relative efficiency of the selective preservation and degradation recondesation pathways in kerogen formation. Source and environment influence on their contributions to type I and II kerogens. Org. Geochem., 20, 611-616.

LARSON, R.L., 1991a. Geological consequences of superplumes. Geology 19, pp. 963–966.

LARSON, R.L., 1991b. Latest pulse of earth: evidence for a Mid-Cretaceous superplume. Geology 19, pp. 547–550.

LARSON, R.L. AND OLSON, P., 1991. Mantle plumes control magnetic reversal frequency. Earth and Planetary Science Letters 107, pp. 437-447.

LARSON, R.L. AND ERBA, E., 1999. Onset of the mid-Cretaceous greenhouse in the Barremian-Aptian: igneous events and biological, sedimentary, and geochemical responses, Paleoceanography, 14, pp. 663-678.

LAVILLE, E., 1985. Evolution sedimentaire, tectonique et magmatique du bassin jurassique du haut Atlas (Maroc): modele en relai multiple de decrochement. These Sci. Univ. de Montpellier. 166 pp.

LECKIE, R.M., BRALOWER, J.T. AND CASHMAN, R., 2002. Oceanic anoxic events and plankton evolution: biotic response to tectonic forcing during the mid-Cretaceous, Paleoceanography, 17.

LEINE, L., 1986. Geology of the Tarfaya oil shale deposit, Morocco. Geol. Mijnb. 65, pp. 57–74.

LENES, J.M., DARROW, B.P., CATTRALL, C., HEIL, C.A., CALLAHAN, M., VARGO, G.A., BYRNE, R.H., PROSPERO, J.M., BATES, D.E., FANNING, K.A. AND WALSH, J.J., 2001. Iron fertilization and the Trichodesmium response on the West Florida shelf. Limnol. Oceanogr. 46 6, pp. 1261–1277.

LEV, S. M., MCLENNAN, S. M., HANSON, G. N., 2000. Late diagenetic redistribution of uranium and disturbance of the U-Pb whole rock isotope system in a black shale. Journ. Sedim. Res., 70, 1234-1245.

LEWAN, M., 1998. Sulfur-radical control on petroleum formation rates. Nature, 391, 164-165.

LEWY, Z., 1989. Correlation of lithostratigraphic units in the upper Judea Group (Late Cenomanian–Late Coniacian) in Israel. Israel J. Earth Sci. 38, pp. 37–43.

LIPSON-BENITAH, S., FLEXER, A., ROSENFELD, A., CONWAY, B. AND ERIS, H., 1990. DYSOXIC SEDIMENTATION IN THE CENOMANIAN–TURONIAN DALIYYA FORMATION, ISRAEL. In: Huc, A.Y., (Eds.), Deposition of Organic Facies. AAPG Studies in Geology vol. 30, pp. 27–39.

LITTKE, R. and SACHSENHOFER, R.F., 1994. Organic petrology of deep sea sediments: a compilation of results from the Ocean Drilling Program and the Deep Sea Drilling Project. Energy and Fuels, 8, 1498-1512.

LÜCKGE, A., BOUSSAFIR, M., LALLIER-VERGES, E., and LITTKE, R., 1996. Comparative study of organic matter preservation in immature sediments along the continental margins of Peru and Oman. Part I: Results of petrographical and bulk geochemical data. Org. Geochem., 24, 437-451.

LUDERER, F., AND KUHNT, W., 1997. A high resolution record of the Rotalipora extinction in laminated organic-carbon rich limestones of the Tarfaya Atlantic coastal basin (Morocco). Annales de la Société Géologique du Nord, 5, pp. 199-205.

LUDERER, F., 1999. Das Cenoman/Turon Grenzereignis im Tarfaya-Becken (SW Marokko). Unpublished PhD thesis, Univ. Kiel, Germany. 114 pp.

LÜNING, S., MARZOUK, A.M. AND KUSS, J., 1998a. The Paleocene of central East Sinai, Egypt: `sequence stratigraphy' in monotonous hemipelagites. J. Foraminiferal Res. 28, pp. 19–39.

LÜNING, S., KUSS, J., BACHMANN, M., MARZOUK, A.M. AND MORSI, A.M., 1998b. Sedimentary response to basin inversion: Mid-Cretaceous–Early Tertiary pre- to syndeformational deposition at the Areif El Naqa anticline (northern Sinai, Egypt). Facies 38, pp. 103–136.

LÜNING, S., CRAIG, J., LOYDELL, D.K., TORCH, P. AND FITCHES, B., 2000. Lower Silurian `Hot Shales' in North Africa and Arabia: regional distribution and depositional model. Earth-Sci. Rev. 49, pp. 121–200.

LÜNING, S., KOLONIC, S., BELHADJ, M.E., BELHADJ, Z., COTA, L., BARIC, G. AND WAGNER, T., 2003. Integrated depositional model for the Cenomanian–Turonian organic-rich strata in North Africa, Earth-Sci. Rev., in press.

LÜNING, S. AND KOLONIC, S., 2003. Uranium spectral gamma-ray response as a proxy for organic richness in black shales: applicability and limitations. Journal of Petroleum Geology, 26, pp. 153-174.

LÜNING, S., ARCHER, R., CRAIG, J. AND LOYDELL, D.K., in press a. The single and double Silurian hot shales in North Africa and Arabia. In: Geology of NW Libya.

LÜNING, S., ADAMSON, K. AND CRAIG, J., in press b. Frasnian organic-rich shales in North Africa: regional distribution and depositional model. In: Arthur, T. J., Macgregor, D. S. and Cameron, N. R. (Eds), Petroleum Geology of Africa: New Themes and Developing Technologies. Geol. Soc. (London) Sp. Publ. 207.

LÜNING, S., KOLONIC, S., LOYDELL, D.K. and CRAIG, J., in press c. Reconstruction of the original richness in weathered Silurian shale outcrops (S Libya). GeoArabia.

MAAMOURI, A.L., ZAGHBIB-TURKI, D., MATMATI, M.F., CHIKHAOUI, M. AND SALAJ, J., 1994. La Formation Bahloul en Tunisie centro-septrentionale: variations latérales, nouvelle datation et nouvelle interprétation en terme de stratigraphie séquentielle. J. Afr. Earth Sci. 18 1, pp. 37–50.

MACKENZIE, A.S., BRASSELL, S.C., EGLINGTON, G.J. and MAXWELL, J.R., 1982. Chemical fossils: The geological fate of steroids. Science, 217, 491-504.

MADIGAN, T.M., MARTINKO, M.J. and PARKER, J., 2000. Biology of Microorganisms. Brock Prentice Hall International, Inc. pp. 991.

MAJORAN, S., 1987. Notes on mid-Cretaceous biostratigraphy of Algeria. J. Afr. Earth Sci. 6, pp. 781–786.

MALLA, M.S. AND BACI, S., 1995. Organic geochemistry and well logging. In: Schlumberger (ed), Well Evaluation Conference Algeria 1995, II-4/1-14.

MANGINI, A. AND DOMINIK, J., 1979. Late Quaternary sapropel on the Mediterranean Ridge: U-budget and evidence for low sedimentation rates. Sedimentary Geology, 23, 113-125.

MANGINI, A., JUNG, M. AND LAUKEMANN, S., 2001. What do we learn from peaks of uranium and of manganese in deep sea sediments? Marine Geology, 177, 63-78.

MANN, U., LEYTHAEUSER, D. AND MÜLLER, P.J., 1986. Relation between source rock properties and wireline log parameters. An example from Lower Jurassic Posidonia Shale, NW-Germany. In: Leythaeuser, D. and Rullkötter, J., (Eds.), Advances in Organic Geochemistry, Pergamon Press, Oxford, pp. 1105-1112.

MARTINIS, B. and VISINTIN, V., 1966. Données géologiques sur le bassin sédimentaires côtier de Tarfaya (Maroc méridional). In: Reyre, D., (Eds.), Bassins Sédimentaires du Littoral African. Assoc. Serv. Géol. Afr. Paris, 1, pp. 13-26,

MASCLE, J., LOHMAN, G.P. AND MOULLARD, M., 1996. Proceedings of the Ocean Drilling Program, Scientific Results, 159. College Station, TX (Ocean Drilling Program), 557-574.

MATTAUER, M., 1958. Etude géologique de l'Ouarsensis oriental (Algérie). Bull. Serv. Carte Géol. Algér. (Nouvelle Séries) 17, pp. 1–534.

MAURIN, J.-C. AND GUIRAUD, R., 1993. Basement control in the development of the Early Cretaceous west and central African Rift System. Tectonophysics 228, pp. 81–95.

MAYNARD, J.R., WIGNALL, P.B. AND VARKER, W.J., 1991. A 'hot' new shale facies from the Upper Carboniferous of northern England. Journ. Geol. Soc., London, 148, 805-808.

MCGHEE, G.R., 1996. The Late Devonian Mass Extinction. Critical Moments in Palaeobiology and Earth History Series, Columbia University Press, New York, 303 p.

MEGERISI, M. AND MAMGAIN, V.D., 1980. The Upper Cretaceous–Tertiary formations of northern Libya. In: Salem, M.J. and Busrewil, M.T., (Eds.), The Geology of Sirt Basin vol. 1, Elsevier, Amsterdam, pp. 67–72.

MEKIRECHE, K., SABAOU, N. AND ZAZOUN, R.-S., 1998. Critical factors in the exploration of an Atlas intramontane basin; the western Hodna Basin of northern Algeria. In: MacGregor, D.S., Moody, R.T.J. and Clark-Lowes, D.D., (Eds.), 1998, Petroleum Geology of North Africa.. Geol. Soc. London, Special Publ. vol. 132, pp. 423–432.

MENDELSSON, J.D. AND TOKSÖZ, M.N., 1985. Source rock characterization using multivariate analysis of log data. SPWLA 26th Ann. Logging Symp., June 17-20 1985, pp. 1-21.

MESHREF, W., 1996. Cretaceous tectonics and its impact on oil exploration in northern Egypt. Geol. Soc. Egypt, Spec. Publ. 2, pp. 199–241.

MEYER, B.L. AND NEDERLOF, M.H., 1984. Identification of source rocks on wireline logs by density/resistivity and sonic transit time/resistivity crossplots. Am. Assoc. Pet. Geol. Bull. 68 2, pp. 121–129.

MIALL, A.D., 1991. Stratigraphic sequences and their chronostratigraphic correlation. J. Sediment. Petrol. 61, pp. 497–505.

MIALL, A.D., 1992. Exxon global cycle chart: an event for every occasion?. Geology 20, pp. 787–790.

MONGENOT, T., DERENNE, S., LARGEAU, C., TRIBOVILLARS, N.P., LALLIER-VERGES, E., DESSORT, D. and CONNAN, J. 1999. Spectroscopic, kinetic and pyrolytic studies of kerogen from the dark parallel laminae facies of sulphur-rich Orbagnoux deposit (Upper Kimmeridgian, Jura). Org. Geochem. 30, 39-56.

MONTACER, M., DISNAR, J.R. AND ORGEVAL, J.J., 1986. Etude préliminaire de la matière organique de la formation Bahloul dans l'environment sédimentaire du gisement Zn–Pb de Bou Grine (Tunisie). BRGM Principal Sci. Tech. Results 1987, p. 121.

MONTACER, M., DISNAR, J.R., ORGEVAL, J.J. AND TRICHET, J., 1988. Relationship between Zn–Pb ore and oil accumulation process: example of the Bou Grine deposit (Tunisia). Org. Geochem. 13 1–3, pp. 423–431.

MONTACER, M., 1995. Comparative organic geochemistry of two Tunisian oil source rocks (Bahloul and Bou Dabbous) as an approach of oil exploration in the northern part of Tunisia. In: Proc. Seminar on Source Rocks and Hydrocarbon Habitat in Tunisia, Tunis, 15–18 Nov. 1995ETAP Mem. vol. 9, pp. 45–48.

MOSTAFA, A.R. AND GANZ, H., 1990. Source rock evaluation of a well in Abu Rudeis area, Gulf of Suez. Berl. Geowiss. Abh., A, Berlin 120 2, pp. 1027–1040.
MOSTAFA, A.R., 1992. Organic Geochemistry of Source Rocks and related Crude Oils in the Gulf of Suez, Egypt. Berl. Geowiss. Abh., A, Berlin, 147, 168 p.
MOSTAFA, A.R., 1993. Organic Geochemistry of source rocks and related oils in the Gulf of Suez Area (Egypt). PhD Thesis. Berl. Geowiss. Abh., A, Berlin 147, 163 pp.
MOSTAFA, A.R., 1999. Organic geochemistry of the Cenomanian–Turonian sequence in the Bakr area, Gulf of Suez, Egypt. Pet. Geosci. 5, pp. 43–50.
MOUSTAFA, A.R. AND KHALIL, M.H., 1990. Structural characteristics and tectonic evolution of north Sinai fold belts. In: Said, R., Editor, , 1990. The Geology of Egypt, Balkema, Rotterdam, pp. 381–389.
MYERS, K.J. AND WIGNALL, P.B., 1987. Understanding Jurassic organic-rich mudrocks - New concepts using gamma ray spectrometry and palaeoecology: Examples from the Kimmeridge Clay of Dorset and the Jet Rock of Yorkshire. In: J.K. Leggett, and Zuffa, G.G., (Eds), Marine clastic sedimentology. Graham and Trotman, pp. 172-189.
NACER BEY, R., BERGHEUL, M. AND GUELLAL, S., 1995. Etude et characterisation des roches mères Crétacées du Bassin S.E. Constantinois. In: Proc. Seminar on Source Rocks and Hydrocarbon Habitat in Tunisia, Tunis, 15–18 Nov. 1995ETAP Mem. vol. 9, pp. 29–43.
NAILI, H., BELHADJ, Z., ROBASZYNSKI, F., CARON, M. AND DUPUIS, C., 1994. Présence de roche-mère "Bahloul" au passage Cénomano–Turonien dans la région de Tébessa (Algérie). In: , pp. 167–168.
NEDERBRAGT, A.J. AND FIORENTINO, A., 1999. Stratigraphy and palaeoeoceanography of the Cenomanian–Turonian Boundary Event in Oued Mellegue, north–western Tunisia. Cretac. Res. 20, pp. 47–62.
NEGRA, M.H., M'RABET, A., TROUDI, H., EL ASMI, K. AND SAIDI, F., 1996. Lithofacies and paleogeographic evolution of the Upper Cretaceous reservoir rocks in central Tunisia. In: Proc. 5th Tunisian Petrol. Explor. Conference, Tunis, 15–18 Oct. 1996. ETAP Mem. vol. 10, pp. 173–194.
NERETIN, L., VOLKOV, I.I., BÖTTCHER, M.E. and GRINENKO, V.A., 2001. A sulfur budget for the Black Sea anoxic zone. Deep-Sea Res. I, 48, 1569-1593.
NIJENHUIS, I.A., AND DE LANGE, J.G., 2000. Geochemical constraints on Pliocene sapropel formation in the eastern Mediterranean. Marine Geology, 163, pp. 41-63.
OBERT, D., 1981. Etude géologique des Babors orientaux (domaine tellien, Algérie). PhD thesis, Univ. P. et M. Curie, Paris, 635 pp.
OBRADOVICH, J.D., 1993. A Cretaceous time scale, in Evolution of the Western Interior Basin. In: Caldwell, W.G.E. and Kauffman, E.G. (Eds.), Geological Association of Canada Special Paper 39, pp. 379-396.
OHKOUCHI, N., KAWAMURA, K., KAJIWARA, Y., WADA, E., OKADA, M., KANAMATSU, T. AND TAIRA, A., 1999. Sulfur isotope records around Livello Bonarelli (northern Apennines, Italy) black shale at the Cenomanian-Turonian boundary. Geology, 27, pp. 535-538.
OHMOTO, H., KAISER, C.J., and GEER, K.A., 1990. Systematics of sulphur isotopes in recent marine sediments and ancient sediment-hosted base metal deposits. In: Herbert, H.K. (Eds.), Stable isotopes and fluid processes in mineralization. 23, pp. 70-120.
ORGEVAL, J.J., 1994. Peridiapiric metal concentration: example of the Bou Grine deposit (Tunisian Atlas). In: Fontboté/Boni (Ed.), Sediment-Hosted Zn–Pb OresSpec. Publ. 10, Soc. Geol. Applied to Mineral Deposits, Springer, Berlin, pp. 354–389.
OYARZUN, R., DOBLAS, M., LÓPEZ-RUIZ, J. AND CEBRIÁ, J.M., 1997. Opening of the central Atlantic and asymmetric mantle upwelling phenomena: implications for long-lived magmatism in western North Africa and Europe. Geology 25, pp. 727–730.
PARRISH, J.T. AND CURTIS, R.L., 1982. Atmospheric circulation, upwelling, and organic-rich rocks in the Mesozoic and Cenozoic. Palaeogeography, Palaeoclimatology, Palaeoecology 40, pp. 31–66.
PARRISH, J.T., 1995. Paleogeography of Corg-rich rocks and the preservation versus production controversy. In: Huc, A.-Y. (Ed.), Paleogeography, Paleoclimate, and Source RocksAAPG Studies in Geology vol. 40, pp. 1–20.
PARSONS, M.G., ZAGAAR, A.M. AND CURRAY, J.J., 1980. Hydrocarbon occurrences in the Sirte Basin, Libya. In: Miall, D.A., (Ed.), Facts and Principles of World Petroleum Occurrence. Mem. Can. Soc. Petrol. Geol. vol. 6, pp. 723–732.
PASSEY, Q.R., CREANEY, S., KULLA, J.B., MORETTI, F.J. AND STROUD, J.D. 1990. A practical model for organic richness from porosity and resistivity logs. American Association of Petroleum Geologists Bulletin, 74, 1777-1794.
PASSIER, H.F., BOSCH, H.-J., NIJENHUIS, I.A., LOURENS, L.J., BÖTTCHER, M.E., LEENDERS, A., DAMSTÉ, J.S.S., DE LANGE, G.J. AND DE, LEEUW J.W., 1999a. Sulfidic Mediterranean surface waters during Pliocene sapropel formation. Nature, 397, 146-149.
PASSIER H.F., MIDDELBURG J.J., DE LANGE G.J. and BÖTTCHER M.E., 1999b. Modes of sapropel formation in the eastern Mediterranean: some constraints based on pyrite properties. Mar. Geol., 153, 199-219.

PAUL, C.R.C., MITCHELL, S.F., LAMOLDA, M.A. AND GOROSTIDI, A., 1994. The Cenomanian-Turonian Boundary Event in northern Spain. Geological Magazine, 131, pp. 810-817.

PAUL, C.R.C., LAMOLDA, M.A., MITCHELL, S.F., VAZIRI, M.R., GOROSTIDI, A. AND MARSHALL, J.D., 1999. The Cenomanian–Turonian boundary at Eastbourne (Sussex, UK): a proposed European reference section. Palaeogeogr. Palaeoclimatol. Palaeoecol. 150, pp. 83–121.

PEDERSEN T.F. AND CALVERT, S.E., 1990. Anoxia vs. productivity: what controls the formation of organic carbon-rich sediments and sedimentary rocks? Bull. Am. Assoc. Petrol Geol., 74, pp. 454-466.

PERCH-NIELSEN, K., 1979. Calcareous nannofossils from the Cretaceous between the North Sea and the Mediterranean. Aspekte Kreide Europas, IUGS Ser. A 6, pp. 335–350.

PERCH-NIELSEN, K., 1983. Recognition of Cretaceous stage boundaries by means of calcareous nannofossils. In: Birkelund, T. et al., (Eds.), Symposium on Cretaceous Stage boundaries, Copenhagen, Abstract, pp. 152–156.

PERCH-NIELSEN, K., 1985. Mesozoic calcareous nannofossils. In: Bolli, H.M., Saunders, J.B. and Perch-Nielsen, K., (Eds.), Plankton Stratigraphy, Cambridge Univ. Press, Cambridge, pp. 329–426.

PERTHUISOT, V., 1981. Diapirism in northern Tunisia. J. Struct. Geol. 3, pp. 231–235.

PETERS, E.K. AND MOLDOWAN, J.M., 1993. In: The Biomarker Guide: Interpreting Molecular Fossils in Petroleum and Ancient Sediment, Prentice Hall, Englewood Cliffs, NJ, p. 347.

PETIT, G.R. and VAN TAMELEN, E.E., 1962. Raney Nickel desulphurization. In: Organic Reactions, John Wiley and Sons, 12, pp. 356-380.

PEYPOUQUET, J.-P., GROUSSET, F. AND MOURQUIART, P., 1986. Paleooceanography of the Mesogean Sea based on ostracods of the northern Tunisian continental shelf between the Late Cretaceous and Early Paleogene. Geol. Rundsch. 75, pp. 159–174.

PHILIP, J. et al., 1993. Late Cenomanian (94–92 Ma). In: Dercourt, J. et al., (Eds.), Atlas Tethys, Palaeoenvironmental Maps, Explanatory Notes, Gauthier-Villars, Paris, pp. 153–178.

PHILIP, J. et al., 2000. Late Cenomanian. In: Dercourt, J. et al., (Eds.), Atlas Peri-Tethys, Paleogeographical maps. CCGM/CGMW, Paris, map 13.

PICKERING, K.E., WANG, Y., TAO, W.K., PRICE, C. AND MÜLLER, J.F., 1998. Vertical distributions of lightning NOx for use in regional and global chemical transport models. Journal of Geophysical Research 103 (D), 31,203-31,216.

PLETSCH, T., ERBACHER, J., HOLBOURN, A., KUHNT, W., MOULLADE, M., OBOH-IKUENOBE, E.F., SÖDING, E. AND WAGNER, T., 2001. Cretaceous opening history of the Equatorial Atlantic Gateway: The view from the West African continental margin (ODP Leg 159). Journal of South American Earth Sciences 14, pp. 147-174.

POLVÊCHE, J., 1960. Contribution à l'étude géologique de l'Ouarsenis oranais. Pub. Serv. carte géol. Algérie, n. sér.,24, 2 volumes, 577 pp.

POSTMA, G. AND TEN VEEN, J.H., 1999. Astronomically and tectonically linked variations in gamma-ray intensity in Late Miocene hemipelagic successions of the Eastern Mediterranean Basin. Sedimentary Geology, 128, 1-12.

POULSEN, C.J., SEIDOV, D., BARRON, J.E. AND PETERSON, H.W., 1998. The impact of paleogeographic evolution on the surface oceanic circulation and the marine environment within the mid-Cretaceous Tethys. Paleoceanography, 13, pp. 546-559.

PRATT, L.M. AND THREKELD, C.N., 1984. Stratigraphic significance of 13C/12C ratios in Mid-Cretaceous rocks of the Western Interior, U.S.A. In: Stott, D.F. and Glass, D.J., (Eds.), The Mesozoic North America. Canadian Soc. of Petroleum Geol., Memoir vol. 9, pp. 305–312.

PRATT, L.M., ARTHUR, M.A., DEAN, W.E., AND SCHOLLE, P.A., 1993. Paleoceanographic cycles and events during the Late Cretaceous in the Western Interior Seaway of North America. In: Caldwell, W.G.E., and Kauffman, E.G., (Eds.), Cretaceous evolution of the Western Interior Basin of North America. Geological Association of Canada, Special Paper 39, pp. 333-353.

PROKOPH, A., VILLENEUVE, M., AGTERBERG, F.P. AND RACHOLD, V., 2001. Geochronology and calibration of global Milankovitch cyclicity at the Cenomanian–Turonian boundary. Geology 29, pp. 523–526.

QUESNE, D. AND FERRY, S., 1995. Detailed relationships between platform and pelagic carbonates (Barremian, SE France). In: House, M.R. and Gale, A.S., (Eds.), Orbital Forcing Timescales and Cyclostratigraphy. Geol. Soc., Special Publ. vol. 85, pp. 165–176.

RAISWELL, R., BUCKLEY, F., BERNER, R.A. and ANDERSON, T.F., 1988. Degree of pyritisation as a palaeoenvironmental indicator of bottom-water oxygenation. Journ. Sedim. Petrol. 58, 812-819.

RANKE, U., RAD, U.V. AND WISSMANN, G., 1982. Stratigraphy, facies and tectonic development of the On- and Offshore Aaiun-Tarfaya Basin- A review. In: Rad, U.V., Hinz, K., Sarntheim, M. and Seibold, E., (Eds.), Geology of the Northwest African Continental Margin, Springer, Heidelberg, pp. 86–107.

RAZGALLAH, S., PHILIP, J., THOMEL, G., ZAGHBIB-TURKI, D., CHAABANI, F., BEN HAJ ALI, N. AND M'RABET, A., 1994. La limite Cénomanien–Turonien en Tunisie centrale et méridionale: biostratigraphie et paléoenvironnements. Cretac. Res. 15 5, pp. 507–533.

REYMENT, R.A., 1980. Biogeography of the Saharan Cretaceous and Paleocene epicontinental transgressions. Cretac. Res. 1, pp. 299–327.
REYMENT, R.A. AND DINGLE, R.V., 1987. Palaeogeography of Africa during the Cretaceous period. Palaeogeogr. Palaeoclimatol. Palaeoecol. 59, pp. 93–116.
RHORBACK, B.G., 1983. Crude oil geochemistry of the Gulf of Suez. In: Bjørøy, M. et al., (Eds.), Advances in Organic Geochemistry, 1981, Wiley, Chichester, pp. 39–48.
RIBOULLEAU, A., DERENNE, S., SARRET, G., LARGEAU, C., BAUDIN, F., and CONNAN, J., 2000. Pyrolytic and spectroscopic study of a sulphur-rich kerogen from the Kashpir oil shales (Upper Jurassic, Russian platform). Org. Geochem., 31, 1641-1661.
RICOU, L.E., 1995. The plate tectonic history of the past Tethys Ocean. In: Nairn, A.E.M., Ricou, L.-E., Vrielynck, B. and Dercourt, J., (Eds.), The Ocean Basins and Margins. The Tethys Ocean, Plenum, New York, pp. 3–70.
ROBASZYNSKI, F., CARON, M., DUPUIS, C., AMEDRO, F., GONZALEZ DONOSO, J.-M., LINARES, D., HARDENBOL, J., GARTNER, S., CALANDRA, F. AND DELOFFRE, R., 1990. A tentative integrated stratigraphy in the Turonian of central Tunisia: formations, zones and sequential stratigraphy in the Kalaat Senan area. Bull. Cent. Rech. Explor. Prod. Elf-Aquitaine 14 1, pp. 213–384.
ROBASZYNSKI, F., HARDENBOL, J., CARON, M., AMÉDRO, F., DUPUIS, C., GONZALEZ DONOSO, J.-M., LINARES, D. AND GARTNER, S., 1993. Sequence stratigraphy in a distal environment: the Cenomanian of the Kalaat Senan region (central Tunisia). Bull. Cent. Rech. Explor. Prod. Elf Aquitaine 17 2, pp. 395–433.
ROBASZYNSKI, F., AMÉDRO, F. AND CARON, M., 1993. La limite Cénomanien–Turonien et la Formation Bahloul dans quelques localités de Tunisie Centrale. Cretac. Res. 14, pp. 477–486.
ROBERTSON RESEARCH INTERNATIONAL, 1979. The petroleum geochemistry of oils and source rocks in the southeastern Sirt Basin, Libya. Tech. Rept., Arabian Gulf Oil.
ROBERTSON, A.H.F., 1998. Lithofacies evidence for the Cretaceous–Paleogene sedimentary history of Eratosthenes Seamount, eastern Mediterranean, in its regional tectonic context (sites 966 and 967). In: Robertson, A.H.F., Emeis, K.-C., Richter, C. and Camerlenghi, A., Editors, 1998. Proceedings of the Ocean Drilling ProgramScientific Results vol. 160, pp. 403–417.
ROBISON, V.D., 1995. Source rock characterization of the Late Cretaceous Brown Limestone of Egypt. In: Katz, B., (Ed.), Petroleum Source Rocks, Springer Verlag, Berlin, pp. 256–281.
RÖHLICH, P., 1974. Geological map of Libya, 1:250.000. Sheet Al Bayda (NI 34-15). Explanatory booklet. Industrial Research Center, Tripoli 70 pp.
ROHMER, M., BISSERET, P. and NEUNLIST, S., 1992. The hopanoids, prokaryotic triterpenoids and precursors of ubiquitous molecular fossils. In : Moldowan, J.M. et al, (Eds.), Biological markers in sediment and petroleum. Prentice Hall, pp. 1-17.
ROSELL-MELÉ, A., MASLIN, A.M., MAXWELL, R.J. AND SCHAEFFER, P., 1997. Biomarker evidence for "Heinrich" events. Geochim. Cosmochim. Acta, 61, pp. 1671-1678.
ROTH, P.H., 1978. Cretaceous nannoplankton biostratigraphy and oceanography of the northwestern Atlantic Ocean. Initial Reports of the Deep Sea Drilling Project, 44, pp. 731-760.
ROTH, P.H. AND KRUMBACH, K.R., 1986. Middle Cretaceous calcareous nannofossil biogeography and preservation in the Atlantic and Indian Oceans: implications for paleoceanography. Mar. Micropaleontol. 10, pp. 235–266.
RUSK, D.C., 2001. Libya: petroleum potential of the underexplored basin centers—a twenty-first-century challenge. In: Downey, M.W., Threet, J.C. and Morgan, W.A., (Eds.), Petroluem Provinces of the Twenty-First Century. AAPG Mem. vol. 74, pp. 429–452.
RUSSEL, W.L., 1945. Relation of radioactivity, organic content, and sedimentation. AAPG Bull., 29, 1470-1494.
SAIDI, F., BEN ISMAIL, M.H. AND M'RABET, A., 1997. Le Turonien de Tunisie centro-occidentale: faciès, paléogéographie et stratigraphie séquentielle d'une plate-forme carbonatée ennoyée. Cretac. Res. 18, pp. 63–85.
SAIZ-JIMENEZ, C. AND DE LEEUW, J.W., 1984. Pyrolysis–gas chromatography–mass spectrometry of isolated, synthetic and degraded lignins. In: Schenck, P.A. et al. (Eds.), Advances in Organic Geochemistry (1983), Org. Geochem. vol. 6, pp. 417–422.
SAIZ-JIMENEZ, C. AND DE LEEUW, J.W., 1986. Lignin pyrolysis products: their structures and their significance as biomarkers. In: Leythaeuser, D. and Rullkötter, J. (Eds.), Advances in Organic Geochemistry (1985), Org. Geochem. vol. 10, pp. 869–876.
SALAJ, J., 1978. The geology of the Pelagian Block: the eastern Tunisian platform. In: Nairn, A.E.M., Kanes, W.H. and Stehli, F.G. (Eds.), The Ocean Basins and Margins, vol. 4B: The Western Mediterranean, pp. 361–416.
SAVORNIN, J., 1920. Etude géologique de la région du Hodna et du Plateau Sétifien. Bull. Serv. Géol. Algérie, Algiers, 2ème sér., 7 (499 pp.).

SCHAAF, M. AND THUROW, J., 1997. Tracing short cycles in long records: the study of inter-annual to inter-centennial climate change from long sediment, examples from the Santa Barbara Basin. J.Geol.Soc. 154, pp. 613-622.

SCHAEFFER, P., REISS, C., TRENDEL, J.M., ADAM, P. and ALBRECHT, P., 1995. A novel series of hopanoid sulphides; Evidence for ring A/B functionalised precursors. In Grimalt J.O. et al. (Eds.), Organic Geochemistry: Developments and applications to energy, climate, environment and human history. A.I.G.O.A., Donostia-San Sebastián, pp. 1053-1054.

SCHINDLER, E., 1990. Die Kellwasser-Krise (hohe Frasne-Stufe, Ober-Devon). Göttinger Arb. Geol. Paläont. 46, 115 p., Göttingen.

SCHLANGER, S.O. AND JENKYNS, H.C., 1976. Cretaceous oceanic anoxia events: causes and consequences. Geol. Mijnb. 55, pp. 179–184.

SCHLANGER, S.O., JENKYNS, H.C. AND PREMOLI SILVA, I., 1981. Volcanism and vertical tectonics in the Pacific Basin related to global Cretaceous transgressions. Earth Planet Sci. Lett., 52, pp. 435-449.

SCHLANGER, S.O., ARTHUR, M.A., JENKYNS, H.C. AND SCHOLLE, P.A., 1987. The Cenomanian–Turonian oceanic anoxic event: I. Stratigraphy and distribution of organic-rich beds and the marine 13C excursion. In: Brooks, J. and Fleet, A.J. (Eds.), Marine and Petroleum Source Rocks. Geol. Soc., London, Special Publ. vol. 26, pp. 371–399.

SCHLUMBERGER, 1995. Well Evaluation Conference, Egypt 1995 Schlumberger, Dubai 87 pp.

SCHMOKER, J.W., 1980. Organic content of Devonian shale in Western Appalachian Basin. AAPG Bulletin, 64, 2156-2165.

SCHMOKER, J.W., 1981. Determination of organic-matter content of Appalachian Devonian shales from gamma-ray logs. AAPG Bulletin, 65, 1285-1298.

SCHOLLE, P.A., AND ARTHUR, M.A., 1980. Carbon-isotope fluctuations in Cretaceous pelagic limestones: potential stratigraphic and petroleum exploration tool. AAPG Bulletin, 64, pp. 67-87.

SCHOUTEN, S., EGLINTON, T.E., SINNINGHE DAMSTÉ, J.S. and DE LEEUW, J.W., 1995a. Influence of sulphur-crosslinking on the molecular size distribution of sulphur-rich macromolecules in bitumen. In: Vairavamurthy M.A. and Schoonen M.A.A (Eds.), Geochemical Transformations of Sedimentary Sulfur. ACS Symp. Series, 612, pp. 80-92.

SCHOUTEN, S., SINNINGHE DAMSTÉ, J.S. and DE LEEUW, J.W., 1995b. Occurrence and distribution of low-molecular-weight sulphoxides in polar fractions of sediment extracts and petroleum. Org. Geochem., 23, 129-138.

SCHOUTEN, S., DE LOUREIRO, M.R.B., SINNINGHÉ DAMSTÉ, J.S. and DE LEEUW, J.W., 1998a. Molecular biogeochemistry of Monterey sediments (Naples Beach, USA). Part I: Distributions of hydrocarbons and organic sulphur compounds. In Isaacs C. and Rullkötter J. (Eds.), The Monterey Formation: From Rock to Molecule. Columbia Univ. Pres, New York.

SCHOUTEN, S., SCHOELL, M., SUMMONS, R.E., SINNINGHÉ DAMSTÉ, J.S. and DE LEEUW, J.W., 1998b. Molecular biogeochemistry of Monterey sediments (Naples Beach, USA). Part II: Distributions of hydrocarbons and organic sulphur compounds. In Isaacs C. and Rullkötter J. (Eds.), The Monterey Formation: From Rock to Molecule. Columbia Univ. Press, New York.

SCHULZE, F. AND KUSS, J., 2000. Biostratigraphy and cyclicities of the Late Albian to Turonian carbonate platform in central Jordan [abstr.]. 6th Int. Cretaceous Symp., 27 Aug-4 Sep 2000, Vienna, Austria, Abstracts, p. 133.

SELLEY, R.C., 1997. The Sirte Basin of Libya. In: Selley, R.C. (Ed.), African Basins. Sedimentary Basins of the World vol. 3, Elsevier, Amsterdam, pp. 27–37.

SENGÖR, A.M.C., 1985. Die Alpiden und die Kimmeriden: die verdoppelte Geschichte der Tethys. Geol. Rundsch. 74, pp. 181–213.

SHAHIN, A.N., SHARAF, L. M. AND EL LEBOUDY, M. M., 1999. Recognition of Thebes and Lower Sudr formations as petroleum source rocks in the central Gulf of Suez, using wire-line logs. M.E.R.C. Ain Shams University (Cairo), Earth Sci. Ser., 13, 82-91.

SHAHIN, A.N. AND SHEHAB, M.M., 1984. Petroleum generation, migration and occurrence in Gulf of Suez off-shore of south Sinai. In: Proceedings 7th Petroleum Exploration Seminar, EGPC, Cairo, pp. 126–151.

SHAHIN, A.N., 1988. Oil window in the Gulf of Suez Basin, Egypt. AAPG Bull. 72, pp. 1024–1025.

SHAHIN, A.N., SHEHAB, M.M. AND MANSOUR, H.F., 1986. Quantitative evaluation and timing of petroleum generation in the Abu Gharadig Basin, Western Desert, Egypt. In: Proc. EGPC 8th Petrol. Expl. Prod. Conf., Cairo.

SHAHIN, A.N., 1991. Cenomanian–Turonian ostracods from Gebel Nezzazat, southwestern Sinai, Egypt, with observations on 13C values and the Cenomanian/Turonian boundary. J. Micropalaeontol. 10 (2), pp. 133–150.

SHIMY, FARAMAWY, S., EL-SABAG, S.M. AND HAMMAD, M.M., 1991. Crude oil classification and maturation of Abu Gharadig basin, Western Desert, Egypt. Bull. Fac. Sci. Zagazig Univ. 1 13, pp. 56–75.

SINNINGHE DAMSTÉ, J.S., TEN HAVEN, H.L., DE LEEUW, J.W. and SCHENCK, P.A., 1986. The organic geochemistry of a Messinian evaporitic basin, Northern Apennines (Italy). Part II. Isoprenoid and n-alkyl

thiophenes and thiolanes. In: Leythaeuser, D. and Rullkötter, J. (Eds.), Advances in Organic Geochemistry 1985, Org. Geochem., 10, 791-805.

SINNINGHE DAMSTÉ, J.S., KOCK-VAN DALEN, A.C., DE LEEUW, J.W., SCHENCK, P.A., GUOYING, S. and BRASSELL, S.C., 1987. The identification of mono-, di and trimethyl 2-methyl-2-(4,8,12-trimethyltridecyl)chromans and their occurrence in the geosphere. Geochim. Cosmochim. Acta, 51, 2393-2400.

SINNINGHE DAMSTÉ, J.S., EGLINTON, T.I., DE LEEUW, J.W. and SCHENCK, P.A., 1989a. Organic sulphur in macromolecular sedimentary organic matter. Part I. Structure and origin of sulphur-containing moieties in kerogen, asphaltene and coal as revealed by flash pyrolysis. Geochim. Cosmochim. Acta, 53, 873-889.

SINNINGHE DAMSTÉ, J.S., RIJPSTRA, W.I.C., KOCK-VAN DALEN, A.C., DE LEEUW J.W. and SCHENCK, P.A., 1989b. Quenching of labile functionalised lipids by inorganic sulphur species: Evidence for the formation of sedimentary organic sulphur compounds at the early stages of diagenesis. Geochim. Cosmochim. Acta, 53, 1343-1355.

SINNINGHE DAMSTÉ, J.S. and DE LEEUW, J.W., 1990. Analysis, structure and geochemical significance of organically-bound sulphur in the geosphere: State of the art and future research. In: B. Durand and F. Behar (Eds.), Advances in Organic Geochemistry 1989. Org. Geochem. 16, 1077-1101.

SINNINGHE DAMSTÉ, J.S., KEELY, B., BETTS, S., BAAS, M., MAXWELL, J.R. and DE LEEUW, J.W., 1993. Variations in abundances and distributions of isoprenoid chromans and long-chain alkylbenzenes in sediments of the Mulhouse Basin: A molecular sedimentary record of palaeosalinity. Org. Geochem., 20, 1201-1215.

SINNINGHE DAMSTÉ, J.S., RIJPSTRA, C.I.W., DE LEEUW, J.W. AND LIJMBACH, M.W.G., 1994. Molecular characterization of organically bound sulphur in crude oils. A feasibility study for the application of Raney Nickel desulphurization as a new method to characterize crude oils. Journ. High Res. Chromatogr. 17, pp. 489-500.

SINNINGHE DAMSTÉ, J.S. AND KÖSTER, J., 1998. A euxinic southern North Atlantic Ocean during the Cenomanian/Turonian oceanic anoxic event. Earth Planet. Sci. Lett. 158, pp. 165–173.

SINNINGHE DAMSTÉ, J.S., KOK, J.S., KÖSTER, M.D. and SCHOUTEN, S., 1998 Sulfurized carbohydrates: an important sink for organic carbon? Earth and Planetary Science Letters, 164, 219-234.

SINNINGHE DAMSTÉ, J.S., SCHOUTEN, S. AND VAN DUIN, T.C.A., 2001. Isorenieratane derivates in sediments: possible controls on their distribution. Geochimica et Cosmochimica Acta, 65, pp. 1557-1571.

SISSINGH, W., 1977. Biostratigraphy of Cretaceous calcareous nannoplankton. Geol. Mijnb. 56, pp. 37–65.

SISSINGH, W., 1978. Microfossil biostratigraphy and stage-stratotypes of the Cretaceous. Geol. Mijnb. 57, pp. 433–440.

SMITH, D.N. AND KARKI, M., 1996. Basin development of the offshore Sirt Basin to the west of Binghazi, Libya. In: Salem, M.J., Mouzughi, A.J. and Hammuda, O.S., (Eds.), The Geology of Sirt Basin vol. 1, Elsevier, Amsterdam, pp. 129–137.

SOYER, C. AND TRICART, P., 1989. Tectonique d'inversion en Tunisie centrale: le chainon atlasique Segdale-Boudinar. Bol. Soc. Geol. Fr. 5, pp. 829–836.

SPIRAKIS, C.S., 1996. The roles of organic matter in the formation of uranium deposits in sedimentary rocks. Ore Geology Reviews,11, 53-69.

STAMM, R. AND THEIN, J., 1982. Sedimentation in the Atlas-Gulf. III: Turonian carbonates. In: von Rad, U., Hinz, K., Sarntheim, M. and Seibold, E., (Eds.), Geology of the Northwest African Continental Margin, Springer, Berlin, pp. 459–474.

STAMM, R., 1981. Die dolomitische Fazies des Turon im Hohen Atlas zwischen Atlantik und Sahara (Marokko). PhD thesis, Univ. Bonn. 182 pp.

STAMPFLI, G.M., BOREL, G., CAVAZZA, W., MOSAR, J. AND ZIEGLER, P.A., 2001. The Paleotectonic Atlas of the Peritethyan Domain. Eur. Geophys. Soc. (CD-ROM realized by <e-public>—Electronic Publishing & Consulting, Berlin).

STANKIEWICZ, A.B., KRUGE, A.M., MASTALERZ, M. and SALOMON, L.G., 1996. Geochemistry of the alginite and amorphous organic matter from Type II-S kerogens. Org. Geochem., 24, 495-509.

STASIUK, L.D., 1994. Oil-prone alginite macerals from organic rich Mesozoic and Palaeozoic strata, Saskatchewan, Canada. Canad. Mar. Petrol. Geol., 11, 208-218.

STEIN, R., RULLKÖTTER, J., LITTKE, R., SCHAEFER, R.G. AND WELTE, D., 1988. Organofacies reconstruction and lipid geochemistry of sediments from the Galicia Margin, northeast Atlantic (ODP Leg 103). In: Boillot, G., Winterer, E.L. et al. (Eds.), Proc. of the ODP Scientific Results vol. 103, pp. 567–585.

STEIN, R., 1991. Accumulation of Organic Carbon in Marine Sediments. Lecture Notes in Earth Sciences 34, pp. 1-216.

STETS, J. AND WURSTER, P., 1982. Atlas and Atlantic—structural relations. In: von Rad, U., Hinz, K., Sarntheim, M. and Seibold, E. (Eds.), Geology of the Northwest African Continental Margin, Springer, Berlin, pp. 69–85.

STOCKS, A.E. AND LAWRENCE, S.R., 1990. Identification of source rocks from wireline logs. In: Hurst, A., Lovell, M.A. and Morton, A.C. (Eds), Geological applications of wireline logs. Geol. Soc. Sp. Publ., 48, 241-252.

STOLL, H.M., AND SCHRAG, D.P., 2000. High resolution stable isotope records from the Upper Cretaceous rocks of Italy and Spain: glacial episodes in a greenhouse planet? Geological Society of America Bulletin, 112, pp 308-319.

STRASSER, A., 1994. Milankovitch cyclicity and high-resolution sequence stratigraphy in lagoonal-peritidal carbonates (Upper Tithonian–Lower Berriasian, French Jura Mountains). In: de Boer, P.L. and Smith, D.G. (Eds.), Orbital Forcing and Cyclic Sequences. Spec. Publs. Int. Ass. Sediment vol. 19, pp. 285–301.

STRAUSS, H., 1999. Geological evolution from isotope proxy signals – sulfur. Chem. Geol., 161, 89-101.

SUESS, E., 1980. Particulate organic carbon flux in the oceans - surface productivity and oxigen utilization. Nature 288, pp. 260-263.

SUMMERHAYES, C.P., 1981. Organic facies of Middle Cretaceous black shales in the deep North Atlantic. AAPG Bull. 65, pp. 2364–2380.

SUMMONS, R.E., VOLKMANN, J.K. and BOREHAM, C.J., 1987. Dinosterane and other steroidal hydrocarbons of dinoflagellate origin in sediments and petroleum. Geochim. Cosmochim. Acta, 51, 3075-3082.

SUMMONS, R.E., JAHNKE, L.L., HOPE, J.M. AND LOGAN, G.A., 1999. 2-Methylhopanoids as biomarkers for cyanobacterial oxygenic photosynthesis. Nature, 400, 554-557.

SUPERNAW, I.R., ARNOLD, D.M. AND LINK, A.J., 1978. Method for in situ evaluation of the source rock potential of earth formations: U.S. Patent 4,071,755.

SWANSON, V.E., 1960. Oil yield and uranium content of black shales. US Geol. Surv. Prof. Paper 356-A, 44 p.

TAWADROS, E.E., 2001. Geology of Egypt and Libya. Balkema, Rotterdam 480 pp.

TAYLOR, G.H., TEICHMÜLLER, M., DAVIS, A., DISSEL, C.F.K., LITTKE, R. and ROBERT, P., 1998. Organic Petrology. Borntraeger, Berlin, Stuttgart. pp. 1-685.

TAYLOR, S.R., 1965. The application of trace element data to problems in petrology. In: Ahrens, L.A., Press, F., Runcorn, S.K. and Urey, C. (Eds), Physics and Chemistry of the Earth. Pergamon Press, Oxford, pp. 133-214.

TEICHMÜLLER, M. and OTTENJANN, K., 1977. Art und Diagenese von Liptiniten und lipoiden Stoffen in einem Erdölmuttergestein auf Grund fluoreszenzmikroskopischer Untersuchungen. Erdöl und Kohle, 30, 387-398.

TEN HAVEN, H.L., DE LEEUW, J.W., RULLKÖTTER, J. and SINNINGHE DAMSTÉ, J.S., 1987. Restricted utility of the pristane/phytane ratio as a palaeoenvironmental indicator? Nature, 330, 641-643.

TEN HAVEN, H.L., DE LEEUW, J.W., RULLKÖTTER, J. and SINNINGHE DAMSTÉ, J.S., 1988. Pristane/phytane ratio as environmental indicator. Nature, 333, 604.

TEN VEEN, J.H. AND POSTMA, G., 1996. Astronomical variation in gamma-ray intensity: Late Miocene hemipelagic successions in the eastern Mediterranean basin as a test case. Geology, 24, 15-18.

THEIN, J., 1988. Turonian Paleogeography of the High Atlas Mountains (Morocco) and the North Atlantic. Z. Deutsch. Geol. Ges. 139, pp. 261–287.

THOMSON, J., HIGGS, N.C., WILSON, T.R.S., CROUDACE, I.W., DE LANGE, G.J. AND VAN SANTVOORT, P.J.M., 1995. Redistribution and geochemical behaviour of redox-sensitive elements around S1, the most recent eastern Mediterranean sapropel. Geochimica et Cosmochimica Acta, 59, 3487-3501.

THUBURN, J. AND CRAIG, G.C., 1997. GCM tests of theories for the height of the tropopause. Journal of the Atmospheric Sciences 54, pp. 869-882.

THUROW, J. AND KUHNT, W., 1986. Mid-Cretaceous of the Gibraltar Arch area. In: Summerhayes, C.P. and Shackleton, N.J. (Eds.), North American Palaeoceanography Geol. Soc., London, Special Publ. vol. 21, pp. 423–445.

THUROW, J., MOULLADE, M., BRUMSACK, H.-J., MASURE, E., TAUGOURDEAU-LANTZ, J. AND DUNHAM, K., 1988. The Cenomanian/Turonian boundary event (CTBE) at Hole 641A, ODP Leg 103 (compared with the CTBE interval at Site 398). In: Boillot, G., Winterer, E.L. et al. (Eds.), Proc. of the ODP Scientific Results vol. 103, pp. 587–634.

THUROW, J., 1988. Creataceous radiolarians of the North Atlantic Ocean: ODP Leg 103 (sites 638, 640 and 641) and DSDP Legs 93 (site 603) and 47B (site 398). In: Boillot, G. and Winterer, E.L. (Eds.), Proc. of the ODP Scientific Results vol. 103, pp. 379–397.

THUROW, J., BRUMSACK, H.-J., RULLKÖTTER, J., LITTKE, R. AND MEYERS, P., 1992. The Cenomanian/Turonian boundary event in the Indian Ocean—a key to understand the global picture. In: Duncan, R.A., Rea, D.K., Kidd, R.B., Rad, U.V. and Weissel, J.K. (Eds.), Synthesis of Results from Scientific Drilling in the Indian OceanAmeric. Geophysical Union, Geophysical Monograph vol. 70, pp. 253–273.

TIE, X., ZHANG, R., BRASSEUR, G., EMMONS, L. AND LEI, W., 2001. Effects of lightning on reactive nitrogen and nitrogen reservoir species in the troposphere. Journal of Geophysical Research 106 (D), pp. 3167-3178.

TIEDEMANN, R., SARNTHEIN, M. AND SHACKLETON, J.N., 1994. Astronomic timescale for the Pliocene Atlantic $\delta^{18}O$ and dust flux records of Ocean Drilling Program Site 659. Paleoceanography 9, pp. 619-638.

TIRATSOO, N.E., 1986. Oilfields of the World.Third Edition, Gulf Publishing Co., Houston, Texas, USA, p. 392.

TISSOT, B.P. and WELTE, D.H., 1984. Petroleum formation and occurrence. Springer Verlag, Berlin, Heidelberg, New York, pp. 1-669.

TOUATI, M.A., DEMBICKI JR., H. AND TEN HAVE, L.E., 1995. Northeast Tunisia foreland basin: source rock characterization and petroleum habitat. In: Proceedings of the Seminar on Source Rocks and Hydrocarbon Habitat in Tunisia, Tunis, 15–18 Nov. 1995 ETAP Memoir vol. 9, pp. 69–70.

TRUEMPY, D.M. AND REEVE, S.C., 2001. The hydrocarbon habitat of the Agadir Basin offshore Morocco [abstr.]. 21st Annual GCSSEPM (Gulf Coast Section of SEPM) Foundation Bob F. Perkins Research Conference, Dec 2-5, Houston, Texas.

TSIKOS, H., JENKYNS, C.H., WALSWORTH-BELL, B., PETRIZZO, R.M., ERBA, E., PREMOLI-SILVA, I., FORSTER, A., KOLONIC, S., BAAS, M., WAGNER, T. AND SINNINGHE DAMSTÉ, S.J., submitted. Carbon-isotope stratigraphy recorded by the Cenomanian/Turonian Oceanic Anoxic Event: correlation and implications based on three key-localities, Journal of the Geological Society of London.

TUCHOLKE, B.E. AND VOGT, P.R., 1979. Western North Atlantic: sedimentary evolution and aspects of tectonic history. In: Tucholke, B.E., Vogt, P.R. et al. (Eds.), Init. Repts. of the SDP vol. 43, US Government Printing Office, Washington, pp. 791–825.

TYSON, R.V., 1995. Sedimentary Organic Matter: Organic Facies and Palynofacies. Chapman and Hall, London 615 pp.

ULMISHEK, G.F. AND KLEMME, H.D., 1990. Depositional controls, distribution, and effectiveness of world's petroleum source rocks. US Geol. Surv. Bull. 1931 (59 pp.).

VAN BUCHEM, F.S.P., MELNYK, D. H. AND MCCAVE, I. N., 1992. Chemical cyclicity and correlation of Lower Lias mudstones using gamma-ray logs, Yorkshire, UK. Journ. Geol. Soc., London, 149, 991-1002.

VAN BUCHEM, F.S.P., DE BOER, P.L., MCCAVE, I.N. AND HERBIN, J.-P., 1995. The organic carbon distribution in marine sediments and the influence of orbital climatic cycles. In: Huc, A.Y. and Schneidermann, N. (Eds.), Palaeogeography, Paleoclimate and Source Rocks. AAPG Spec. Publ. 303-335.

VAN BUCHEM, F.S.P., CHAIX, M., EBERLI, G.P., WHALEN, M.T., MASSE, P., AND MOUNTJOY, E.W., 2000. Outcrop to subsurface correlation of the Upper Devonian (Frasnian) in the Alberta Basin (W. Canada) based on the comparison of Miette and Redwater Carbonate Buildup Margins: In: Homewood, P.W., and Eberli, G.P. (Eds), Genetic stratigraphy on the exploration and production scales - Case studies from the Pennsylvanian of the Paradox Basin and the Upper Devonian of Alberta: Bulletin, Centre Recherche Elf Exploration-Production, Mémoire, 24, 225-267.

VAN BUCHEM, F.S.P., RAZIN, P., HOMEWOOD, P. W., OTERDOOM, W. H. AND PHILIP, J., 2002. Stratigraphic organization of carbonate ramps and organic-rich intrashelf basins: Natih Formation (middle Cretaceous) of northern Oman. AAPG Bull., 86, 21-53.

VAN DER WEIJDEN, C.H., MIDDELBURG, J.J., DE LANGE, G.J., VAN DER SLOOT, H.A., HOEDE, D. AND WOITTIEZ, J.R.W., 1993. Profiles of the redox-sensitive trace elements As, Sb, V, Mo and U in the Tyro and Bannock Basins (eastern Mediterranean). Mar. Chem. 31, 171-186

VAN DER WEIJDEN, C.H., REICHART, J.G. AND VISSER, J.H., 1999. Enhanced preservation of organic matter in sediments deposited within the oxygen minimum zone in the northeastern Arabian Sea, Deep Sea Research 1, pp. 807-830.

VAN DER MEER M.T.J., SCHOUTEN, S. AND SINNINGHE DAMSTÉ, J.S., 1998. The effect of the reversed tricarboxylic acid cycle on the 13C contents of bacterial lipids. Org. Geochem. 28, pp. 527-533.

VAN GEMERDEN, H. and MASS, J., 1995. Ecology of phototrophic sulfur bacteria. In: Blankenship R.E. et al. (Eds.), Anoxygenic photosynthetic bacteria. Kluwer Academic Publishers, Dodrecht, pp. 49-85.

VAN KAAM-PETERS, H.M.E., RIJPSTRA, W.I.C., DE LEEUW, J.W. and SINNINGHE DAMSTÉ, J.S., 1998. A high resolution biomarker study of different lithofacies of organic sulfur-rich carbonate rocks of a Kimmeridgian lagoon (French southern Jura). Org. Geochem., 28, 151-177.

VILA, J.M., 1980. La chaîne alpine d'Algérie orientale et des confins algéro-tunisiens. Thèse Univ. P. et M. Curie, Paris, 3 vol. 665 pp.

VIOTTI, C., 1965. Microfaunes et microfaciés du sondage Puerto Cansado I (Maroc méridional-province de Tarfaya). Mém. BRGM, 32, Colloque intern. Micropaléontol., Dakar, 6-11 mai 1963 (1), pp. 29-40, Paris.

VIOTTI, C., 1966. Résultats stratigraphiques du sondage Puerto Cansado I du Bassin Côtier de Tarfaya. Notes et Mém. Serv, Géol. Maroc, 175 (I), pp. 223-253, Rabat.

VONHOF, H.B., 1998. Synchronous strontium and carbon isotope excursions across the Cenomanian-Turonian Oceanic Anoxic Event. Ph.D. Thesis Vrije Universiteit Amsterdam.

VON DAMM, K.L. EDMUND, J.M. GRANT, B., MEASURES, C.I., WALDEN, B. AND WEISS, R.F., 1985. Chemistry of submarine hydrothermal solutions at 21°N, East Pacific Rise. Geochim. Cosmochim. Acta 49, pp. 2197-2220.

VON RAD, U. and ARTHUR, M.A., 1979. Geodynamic, sedimentary and vulcanic evolution of the Cap Bojador contnental margin (NW Africa). In: Talwani M., (Eds.), Deep drilling results in the Atlantic Ocean: continental margin and palaeoenvironment. Amer. Geophys. Union, 3, pp. 187-203.

VON RAD, U. and EINSELE, G., 1980. Mesozoic-Cenozoic subsidence history and palaeobathymetry of the northwest African continental margin (Aaiun Basin to DSDP 397). The evolution of passive continental margins. Phil. Trans. Royal Soc. London Ser. A, 294, 37-50.

WAGNER, T. AND PLETSCH, T., 1999. Tectono-sedimentary controls on black shale deposition along the opening Equatorial Atlantic Gateway (ODP Leg 159). In: Camron, N. (Ed.), Oil and Gas Habitats of the South Atlantic. Geological Society of London, Special Publication, London vol. 153, pp. 241–265.

WALLMANN, K., 2001. Controls on the Cretaceous and Cenozoic evolution of seawater, atmospheric CO2 and climate. Geochim. Cosmochim. Acta, 65, pp. 3005-3025.

WALSWORTH-BELL, B., WATKINS, D.K., ERBA, E., TSIKOS, H., AND JENKYNS, H.C., Reassessing the calcareous nannofossil biostratigraphy of the Cenomanian/Turonian boundary interval (in prep.)

WATKINS, D.K. 1985. Biostratigraphy and paleoecology of calcareous nannofossils in the Greenhorn marine cycle. Society of Economic Paleontologists and Mineralogists Field Trip Guidebook 4, pp. 151-156.

WALKER, J.C.G., 1986. Global biogeochemical cycles of carbon, sulfur and oxygen. Mar. Geol. 70, pp. 159-174.

WEDEPOHL, K.H., 1971. Enviro nmental influences on the chemical composition of shales and clays. In: Ahrens, L.H., Press, F., Runcorn, S.K. and Urey, H.C. (Eds.), Physics and Chemistry of the Earth. Pergamon, Oxford, UK, pp. 307-331.

WEDEPOHL, K.H., 1991. The composition of the upper Earth´s crust and the natural cycles of selected metals. Metals in natural raw materials. Natural resources. In: Merian, E., (Ed.), Metals and their Compounds in the Environment. VCH, Weinheim, pp. 3-17.

WELTE, D.H., 1974. Recent advances in organic geochemistry of humic substances and kerogen. In: Tissot B.P. and Bienner F. (Eds.), Advances in Organic Geochemistry (1973), Technip, Paris, pp. 3-4.

WENNEKERS, J.H.N., WALLACE, F.K. AND WALLACE, Y.I., 1996. The geology and hydrocarbons of the Sirt Basin: a synopsis. In: Salem, M.J., Mouzughi, A.J. and Hammuda, O.S. (Eds.), The Geology of Sirt Basin vol. 1, Elsevier, Amsterdam, pp. 3–56.

WERNE, J.P., HOLLANDER, D.J., BEHRENS, A., SCHAEFFER, P., ALBRECHT, P. and SINNINGHE DAMSTÉ J.S., 2000. Timing of early diagenetic sulfurization of organic matter: A precursor-product relationship in Holocene sediments of the anoxic Cariaco Basin, Venezuela. Geochim. Cosmochim. Acta, 64, 1741-1751.

WIEDMANN, J., BUTT, A. AND EINSELE, G., 1978. Vergleich von marokkanischen Kreide-Küstenaufschlüssen und Tiefseebohrungen (DSDP): Stratigraphie, Paläoenvironment und Subsidenz an einem passiven Kontinentalrand. Geol. Rundsch. 67, pp. 454–508.

WIEDMANN, J., BUTT, A. AND EINSELE, G., 1982. Cretaceous stratigraphy, environment, and subsidence history at the Moroccan continental margin. In: von Rad, U., Hinz, K., Sarntheim, M. and Seibold, E., Editors, 1982. Geology of the Northwest African Continental Margin, Springer, Berlin, pp. 366–395.

WIGNALL, P.B. AND MYERS, K.J., 1988. Interpreting benthic oxygen levels in mudrocks: a new approach. Geology, 16, 452-455.

WIGNALL, P.B., 1991. Model for transgressive black shales?. Geology 19, pp. 167–170.

WIGNALL, P.B., 1994. Black shales. Clarendon Press, Oxford, 127 p.

WIGNALL, P.B., 2001. Large igneous provinces and mass extinctions. Earth Science Reviews 53, pp. 1-33.

WILDI, W., 1983. La chaine tello-rifaine (Algérie, Maroc, Tunisie): structure, stratigraphique et évolution du Trias au Miocène. Rev. Geol. Dyn. Géogr. Phys. 24, pp. 201–297.

WILSON, P.A. AND NORRIS, R.D., 2001. Warm tropical ocean surface and global anoxia during the mid-Cretaceous period. Nature 412, pp. 425-429.

WONIK, T., (in press). Erste Ergebnisse der geophysikalischen Messungen in der Forschungsbohrung Messel 2001. Courier, Frankfurt/M.

WURSTER, P. AND STETS, J., 1982. Sedimentation in the Atlas Gulf. II: Mid-Cretaceous events. In: von Rad, U., Hinz, K., Sarntheim, M. and Seibold, E. (Eds.), Geology of the Northwest African Continental Margin, Springer, Berlin, pp. 439–458.

ZABACK, D.A. and PRATT L.M., 1992. Isotopic composition and speciation of sulfur in the Miocene Monterey Formation: Reevaluation of sulfur reactions during early diagenesis in marine environments. Geochim. Cosmochim. Acta, 56, 763-774.

ZEEBE, R.E., 2001. Seawater pH and isotopic paleotemperatures of Cretaceous oceans. Palaeogeography, Palaeoclimatology, Palaeoecology, 170, pp. 49-57.

ZEIN EL-DIN, M.Y., 1983. Subsurface geochemical study in the central part of the northern Western Desert, Egypt. Qatar Univ. Sci. Bull. 3, pp. 207–215.

ZELT, F.B., 1985. Natural gamma-ray spectrometry, lithofacies, and depositional environments of selected Upper Cretaceous marine mudrocks, western United States, including Tropic Shale and Tununk Member of Mancos Shale. Ph.D. thesis, Princeton University, 284 p.

ZIEGLER, P.A. AND ROURE, F., 1999. Petroleum systems of Alpine–Mediterranean foldbelts and basins. In: Durand, B., Jolivet, L., Horvath, F. and Seranne, M., Editors, 1999. The Mediterranean Basins: Tertiary Extension within the Alpine OrogenGeol. Soc., London, Special Publ. vol. 156, pp. 517–540.

ZIEGLER, W.H., 1978. Regional geology of the western offshore of Libya. Esso Standard Libya Inc., Weybridge, England 17 pp. (unpublished report).

ZIMMERLE, W., 1995. Petroleum Sedimentology. Kluwer, Dordrecht, 413 p.

ZIMMERMANN, H.B., BOERSMA, A. AND MCCOY, W.F., 1987. Carbonaceous sediments and palaeoenvironment of the Cretaceous South Atlantic Ocean. In: Fleet, J.B.A (Ed.), Marine Petroleum Source Rocks. Geological Society Special Publication London, pp. 271-286.

Publications of this series:

No. 1 **Wefer, G., E. Suess and cruise participants**
Bericht über die POLARSTERN-Fahrt ANT IV/2, Rio de Janeiro - Punta Arenas, 6.11. - 1.12.1985.
60 pages, Bremen, 1986.

No. 2 **Hoffmann, G.**
Holozänstratigraphie und Küstenlinienverlagerung an der andalusischen Mittelmeerküste.
173 pages, Bremen, 1988. (out of print)

No. 3 **Wefer, G. and cruise participants**
Bericht über die METEOR-Fahrt M 6/6, Libreville - Las Palmas, 18.2. - 23.3.1988.
97 pages, Bremen, 1988.

No. 4 **Wefer, G., G.F. Lutze, T.J. Müller, O. Pfannkuche, W. Schenke, G. Siedler, W. Zenk**
Kurzbericht über die METEOR-Expedition No. 6, Hamburg - Hamburg, 28.10.1987 - 19.5.1988.
29 pages, Bremen, 1988. (out of print)

No. 5 **Fischer, G.**
Stabile Kohlenstoff-Isotope in partikulärer organischer Substanz aus dem Südpolarmeer (Atlantischer Sektor). 161 pages, Bremen, 1989.

No. 6 **Berger, W.H. and G. Wefer**
Partikelfluß und Kohlenstoffkreislauf im Ozean.
Bericht und Kurzfassungen über den Workshop vom 3.-4. Juli 1989 in Bremen.
57 pages, Bremen, 1989.

No. 7 **Wefer, G. and cruise participants**
Bericht über die METEOR - Fahrt M 9/4, Dakar - Santa Cruz, 19.2. - 16.3.1989.
103 pages, Bremen, 1989.

No. 8 **Kölling, M.**
Modellierung geochemischer Prozesse im Sickerwasser und Grundwasser.
135 pages, Bremen, 1990.

No. 9 **Heinze, P.-M.**
Das Auftriebsgeschehen vor Peru im Spätquartär. 204 pages, Bremen, 1990. (out of print)

No. 10 **Willems, H., G. Wefer, M. Rinski, B. Donner, H.-J. Bellmann, L. Eißmann, A. Müller, B.W. Flemming, H.-C. Höfle, J. Merkt, H. Streif, G. Hertweck, H. Kuntze, J. Schwaar, W. Schäfer, M.-G. Schulz, F. Grube, B. Menke**
Beiträge zur Geologie und Paläontologie Norddeutschlands: Exkursionsführer.
202 pages, Bremen, 1990.

No. 11 **Wefer, G. and cruise participants**
Bericht über die METEOR-Fahrt M 12/1, Kapstadt - Funchal, 13.3.1990 - 14.4.1990.
66 pages, Bremen, 1990.

No. 12 **Dahmke, A., H.D. Schulz, A. Kölling, F. Kracht, A. Lücke**
Schwermetallspuren und geochemische Gleichgewichte zwischen Porenlösung und Sediment im Wesermündungsgebiet. BMFT-Projekt MFU 0562, Abschlußbericht. 121 pages, Bremen, 1991.

No. 13 **Rostek, F.**
Physikalische Strukturen von Tiefseesedimenten des Südatlantiks und ihre Erfassung in Echolotregistrierungen. 209 pages, Bremen, 1991.

No. 14 **Baumann, M.**
Die Ablagerung von Tschernobyl-Radiocäsium in der Norwegischen See und in der Nordsee.
133 pages, Bremen, 1991. (out of print)

No. 15 **Kölling, A.**
Frühdiagenetische Prozesse und Stoff-Flüsse in marinen und ästuarinen Sedimenten.
140 pages, Bremen, 1991.

No. 16 **SFB 261 (ed.)**
1. Kolloquium des Sonderforschungsbereichs 261 der Universität Bremen (14.Juni 1991):
Der Südatlantik im Spätquartär: Rekonstruktion von Stoffhaushalt und Stromsystemen.
Kurzfassungen der Vorträge und Poster. 66 pages, Bremen, 1991.

No. 17 **Pätzold, J. and cruise participants**
Bericht und erste Ergebnisse über die METEOR-Fahrt M 15/2, Rio de Janeiro - Vitoria,
18.1. - 7.2.1991. 46 pages, Bremen, 1993.

No. 18 **Wefer, G. and cruise participants**
Bericht und erste Ergebnisse über die METEOR-Fahrt M 16/1, Pointe Noire - Recife,
27.3. - 25.4.1991. 120 pages, Bremen, 1991.

No. 19 **Schulz, H.D. and cruise participants**
Bericht und erste Ergebnisse über die METEOR-Fahrt M 16/2, Recife - Belem, 28.4. - 20.5.1991.
149 pages, Bremen, 1991.

No. 20 **Berner, H.**
Mechanismen der Sedimentbildung in der Fram-Straße, im Arktischen Ozean und in der Norwegischen See. 167 pages, Bremen, 1991.

No. 21 **Schneider, R.**
Spätquartäre Produktivitätsänderungen im östlichen Angola-Becken: Reaktion auf Variationen im Passat-Monsun-Windsystem und in der Advektion des Benguela-Küstenstroms.
198 pages, Bremen, 1991. (out of print)

No. 22 **Hebbeln, D.**
Spätquartäre Stratigraphie und Paläozeanographie in der Fram-Straße. 174 pages, Bremen, 1991.

No. 23 **Lücke, A.**
Umsetzungsprozesse organischer Substanz während der Frühdiagenese in ästuarinen Sedimenten.
137 pages, Bremen, 1991.

No. 24 **Wefer, G. and cruise participants**
Bericht und erste Ergebnisse der METEOR-Fahrt M 20/1, Bremen - Abidjan, 18.11.- 22.12.1991.
74 pages, Bremen, 1992.

No. 25 **Schulz, H.D. and cruise participants**
Bericht und erste Ergebnisse der METEOR-Fahrt M 20/2, Abidjan - Dakar, 27.12.1991 - 3.2.1992.
173 pages, Bremen, 1992.

No. 26 **Gingele, F.**
Zur klimaabhängigen Bildung biogener und terrigener Sedimente und ihrer Veränderung durch die Frühdiagenese im zentralen und östlichen Südatlantik. 202 pages, Bremen, 1992.

No. 27 **Bickert, T.**
Rekonstruktion der spätquartären Bodenwasserzirkulation im östlichen Südatlantik über stabile Isotope benthischer Foraminiferen. 205 pages, Bremen, 1992. (out of print)

No. 28 **Schmidt, H.**
Der Benguela-Strom im Bereich des Walfisch-Rückens im Spätquartär. 172 pages, Bremen, 1992.

No. 29 **Meinecke, G.**
Spätquartäre Oberflächenwassertemperaturen im östlichen äquatorialen Atlantik.
181 pages, Bremen, 1992.

No. 30 **Bathmann, U., U. Bleil, A. Dahmke, P. Müller, A. Nehrkorn, E.-M. Nöthig, M. Olesch, J. Pätzold, H.D. Schulz, V. Smetacek, V. Spieß, G. Wefer, H. Willems**
Bericht des Graduierten Kollegs. Stoff-Flüsse in marinen Geosystemen.
Berichtszeitraum Oktober 1990 - Dezember 1992. 396 pages, Bremen, 1992.

No. 31 **Damm, E.**
Frühdiagenetische Verteilung von Schwermetallen in Schlicksedimenten der westlichen Ostsee.
115 pages, Bremen, 1992.

No. 32 **Antia, E.E.**
Sedimentology, Morphodynamics and Facies Association of a mesotidal Barrier Island Shoreface (Spiekeroog, Southern North Sea). 370 pages, Bremen, 1993.

No. 33 **Duinker, J. and G. Wefer (ed.)**
Bericht über den 1. JGOFS-Workshop. 1./2. Dezember 1992 in Bremen. 83 pages, Bremen, 1993.

No. 34 **Kasten, S.**
Die Verteilung von Schwermetallen in den Sedimenten eines stadtbremischen Hafenbeckens.
103 pages, Bremen, 1993.

No. 35 **Spieß, V.**
Digitale Sedimentographie. Neue Wege zu einer hochauflösenden Akustostratigraphie.
199 pages, Bremen, 1993.

No. 36 **Schinzel, U.**
Laborversuche zu frühdiagenetischen Reaktionen von Eisen (III) - Oxidhydraten in marinen Sedimenten.189 pages, Bremen, 1993.

No. 37 **Sieger, R.**
CoTAM - ein Modell zur Modellierung des Schwermetalltransports in Grundwasserleitern.
56 pages, Bremen, 1993. (out of print)

No. 38 **Willems, H. (ed.)**
Geoscientific Investigations in the Tethyan Himalayas. 183 pages, Bremen, 1993.

No. 39 **Hamer, K.**
Entwicklung von Laborversuchen als Grundlage für die Modellierung des Transportverhaltens von Arsenat, Blei, Cadmium und Kupfer in wassergesättigten Säulen. 147 pages, Bremen, 1993.

No. 40 **Sieger, R.**
Modellierung des Stofftransports in porösen Medien unter Ankopplung kinetisch gesteuerter Sorptions- und Redoxprozesse sowie thermischer Gleichgewichte. 158 pages, Bremen, 1993.

No. 41 **Thießen, W.**
Magnetische Eigenschaften von Sedimenten des östlichen Südatlantiks und ihre paläozeanographische Relevanz. 170 pages, Bremen, 1993.

No. 42 **Spieß, V. and cruise participants**
Report and preliminary results of METEOR-Cruise M 23/1, Kapstadt - Rio de Janeiro, 4.-25.2.1993. 139 pages, Bremen, 1994.

No. 43 **Bleil, U. and cruise participants**
Report and preliminary results of METEOR-Cruise M 23/2, Rio de Janeiro - Recife, 27.2.-19.3.1993 133 pages, Bremen, 1994.

No. 44 **Wefer, G. and cruise participants**
Report and preliminary results of METEOR-Cruise M 23/3, Recife - Las Palmas, 21.3. - 12.4.1993 71 pages, Bremen, 1994.

No. 45 **Giese, M. and G. Wefer (ed.)**
Bericht über den 2. JGOFS-Workshop. 18../19. November 1993 in Bremen. 93 pages, Bremen, 1994.

No. 46 **Balzer, W. and cruise participants**
Report and preliminary results of METEOR-Cruise M 22/1, Hamburg - Recife, 22.9. - 21.10.1992. 24 pages, Bremen, 1994.

No. 47 **Stax, R.**
Zyklische Sedimentation von organischem Kohlenstoff in der Japan See: Anzeiger für Änderungen von Paläoozeanographie und Paläoklima im Spätkänozoikum. 150 pages, Bremen, 1994.

No. 48 **Skowronek, F.**
Frühdiagenetische Stoff-Flüsse gelöster Schwermetalle an der Oberfläche von Sedimenten des Weser Ästuares. 107 pages, Bremen, 1994.

No. 49 **Dersch-Hansmann, M.**
Zur Klimaentwicklung in Ostasien während der letzten 5 Millionen Jahre: Terrigener Sedimenteintrag in die Japan See (ODP Ausfahrt 128). 149 pages, Bremen, 1994.

No. 50 **Zabel, M.**
Frühdiagenetische Stoff-Flüsse in Oberflächen-Sedimenten des äquatorialen und östlichen Südatlantik. 129 pages, Bremen, 1994.

No. 51 **Bleil, U. and cruise participants**
Report and preliminary results of SONNE-Cruise SO 86, Buenos Aires - Capetown, 22.4. - 31.5.93 116 pages, Bremen, 1994.

No. 52 **Symposium: The South Atlantic: Present and Past Circulation.**
Bremen, Germany, 15 - 19 August 1994. Abstracts. 167 pages, Bremen, 1994.

No. 53 **Kretzmann, U.B.**
^{57}Fe-Mössbauer-Spektroskopie an Sedimenten - Möglichkeiten und Grenzen. 183 pages, Bremen, 1994.

No. 54 **Bachmann, M.**
Die Karbonatrampe von Organyà im oberen Oberapt und unteren Unteralb (NE-Spanien, Prov. Lerida): Fazies, Zyklo- und Sequenzstratigraphie. 147 pages, Bremen, 1994. (out of print)

No. 55 **Kemle-von Mücke, S.**
Oberflächenwasserstruktur und -zirkulation des Südostatlantiks im Spätquartär. 151 pages, Bremen, 1994.

No. 56 **Petermann, H.**
Magnetotaktische Bakterien und ihre Magnetosome in Oberflächensedimenten des Südatlantiks. 134 pages, Bremen, 1994.

No. 57 **Mulitza, S.**
Spätquartäre Variationen der oberflächennahen Hydrographie im westlichen äquatorialen Atlantik. 97 pages, Bremen, 1994.

No. 58 **Segl, M. and cruise participants**
Report and preliminary results of METEOR-Cruise M 29/1, Buenos-Aires - Montevideo, 17.6. - 13.7.1994
94 pages, Bremen, 1994.

No. 59 **Bleil, U. and cruise participants**
Report and preliminary results of METEOR-Cruise M 29/2, Montevideo - Rio de Janiero 15.7. - 8.8.1994. 153 pages, Bremen, 1994.

No. 60 **Henrich, R. and cruise participants**
Report and preliminary results of METEOR-Cruise M 29/3, Rio de Janeiro - Las Palmas 11.8. - 5.9.1994. Bremen, 1994. (out of print)

No. 61 **Sagemann, J.**
Saisonale Variationen von Porenwasserprofilen, Nährstoff-Flüssen und Reaktionen in intertidalen Sedimenten des Weser-Ästuars. 110 pages, Bremen, 1994. (out of print)

No. 62 **Giese, M. and G. Wefer**
Bericht über den 3. JGOFS-Workshop. 5./6. Dezember 1994 in Bremen.
84 pages, Bremen, 1995.

No. 63 **Mann, U.**
Genese kretazischer Schwarzschiefer in Kolumbien: Globale vs. regionale/lokale Prozesse.
153 pages, Bremen, 1995. (out of print)

No. 64 **Willems, H., Wan X., Yin J., Dongdui L., Liu G., S. Dürr, K.-U. Gräfe**
The Mesozoic development of the N-Indian passive margin and of the Xigaze Forearc Basin in southern Tibet, China. – Excursion Guide to IGCP 362 Working-Group Meeting "Integrated Stratigraphy". 113 pages, Bremen, 1995. (out of print)

No. 65 **Hünken, U.**
Liefergebiets - Charakterisierung proterozoischer Goldseifen in Ghana anhand von Fluideinschluß - Untersuchungen. 270 pages, Bremen, 1995.

No. 66 **Nyandwi, N.**
The Nature of the Sediment Distribution Patterns in ther Spiekeroog Backbarrier Area, the East Frisian Islands. 162 pages, Bremen, 1995.

No. 67 **Isenbeck-Schröter, M.**
Transportverhalten von Schwermetallkationen und Oxoanionen in wassergesättigten Sanden. - Laborversuche in Säulen und ihre Modellierung -. 182 pages, Bremen, 1995.

No. 68 **Hebbeln, D. and cruise participants**
Report and preliminary results of SONNE-Cruise SO 102, Valparaiso - Valparaiso, 95.
134 pages, Bremen, 1995.

No. 69 **Willems, H. (Sprecher), U.Bathmann, U. Bleil, T. v. Dobeneck, K. Herterich, B.B. Jorgensen, E.-M. Nöthig, M. Olesch, J. Pätzold, H.D. Schulz, V. Smetacek, V. Speiß. G. Wefer**
Bericht des Graduierten-Kollegs Stoff-Flüsse in marine Geosystemen.
Berichtszeitraum Januar 1993 - Dezember 1995.
45 & 468 pages, Bremen, 1995.

No. 70 **Giese, M. and G. Wefer**
Bericht über den 4. JGOFS-Workshop. 20./21. November 1995 in Bremen. 60 pages, Bremen, 1996. (out of print)

No. 71 **Meggers, H.**
Pliozän-quartäre Karbonatsedimentation und Paläozeanographie des Nordatlantiks und des Europäischen Nordmeeres - Hinweise aus planktischen Foraminiferengemeinschaften.
143 pages, Bremen, 1996. (out of print)

No. 72 **Teske, A.**
Phylogenetische und ökologische Untersuchungen an Bakterien des oxidativen und reduktiven marinen Schwefelkreislaufs mittels ribosomaler RNA. 220 pages, Bremen, 1996. (out of print)

No. 73 **Andersen, N.**
Biogeochemische Charakterisierung von Sinkstoffen und Sedimenten aus ostatlantischen Produktions-Systemen mit Hilfe von Biomarkern. 215 pages, Bremen, 1996.

No. 74 **Treppke, U.**
Saisonalität im Diatomeen- und Silikoflagellatenfluß im östlichen tropischen und subtropischen Atlantik. 200 pages, Bremen, 1996.

No. 75 **Schüring, J.**
Die Verwendung von Steinkohlebergematerialien im Deponiebau im Hinblick auf die Pyritverwitterung und die Eignung als geochemische Barriere. 110 pages, Bremen, 1996.

No. 76 **Pätzold, J. and cruise participants**
Report and preliminary results of VICTOR HENSEN cruise JOPS II, Leg 6, Fortaleza - Recife, 10.3. - 26.3. 1995 and Leg 8, Vítoria - Vítoria, 10.4. - 23.4.1995.
87 pages, Bremen, 1996.

No. 77 **Bleil, U. and cruise participants**
Report and preliminary results of METEOR-Cruise M 34/1, Cape Town - Walvis Bay, 3.-26.1.1996.
129 pages, Bremen, 1996.

No. 78 **Schulz, H.D. and cruise participants**
Report and preliminary results of METEOR-Cruise M 34/2, Walvis Bay - Walvis Bay, 29.1.-18.2.96
133 pages, Bremen, 1996.

No. 79 **Wefer, G. and cruise participants**
Report and preliminary results of METEOR-Cruise M 34/3, Walvis Bay - Recife, 21.2.-17.3.1996.
168 pages, Bremen, 1996.

No. 80 **Fischer, G. and cruise participants**
Report and preliminary results of METEOR-Cruise M 34/4, Recife - Bridgetown, 19.3.-15.4.1996.
105 pages, Bremen, 1996.

No. 81 **Kulbrok, F.**
Biostratigraphie, Fazies und Sequenzstratigraphie einer Karbonatrampe in den Schichten der Oberkreide und des Alttertiärs Nordost-Ägyptens (Eastern Desert, N'Golf von Suez, Sinai).
153 pages, Bremen, 1996.

No. 82 **Kasten, S.**
Early Diagenetic Metal Enrichments in Marine Sediments as Documents of Nonsteady-State Depositional Conditions. Bremen, 1996.

No. 83 **Holmes, M.E.**
Reconstruction of Surface Ocean Nitrate Utilization in the Southeast Atlantic Ocean Based on Stable Nitrogen Isotopes. 113 pages, Bremen, 1996.

No. 84 **Rühlemann, C.**
Akkumulation von Carbonat und organischem Kohlenstoff im tropischen Atlantik: Spätquartäre Produktivitäts-Variationen und ihre Steuerungsmechanismen.
139 pages, Bremen, 1996.

No. 85 **Ratmeyer, V.**
Untersuchungen zum Eintrag und Transport lithogener und organischer partikulärer Substanz im östlichen subtropischen Nordatlantik. 154 pages, Bremen, 1996.

No. 86 **Cepek, M.**
Zeitliche und räumliche Variationen von Coccolithophoriden-Gemeinschaften im subtropischen Ost-Atlantik: Untersuchungen an Plankton, Sinkstoffen und Sedimenten.
156 pages, Bremen, 1996.

No. 87 **Otto, S.**
Die Bedeutung von gelöstem organischen Kohlenstoff (DOC) für den Kohlenstoffffluß im Ozean.
150 pages, Bremen, 1996.

No. 88 **Hensen, C.**
Frühdiagenetische Prozesse und Quantifizierung benthischer Stoff-Flüsse in Oberflächensedimenten des Südatlantiks.
132 pages, Bremen, 1996.

No. 89 **Giese, M. and G. Wefer**
Bericht über den 5. JGOFS-Workshop. 27./28. November 1996 in Bremen. 73 pages, Bremen, 1997.

No. 90 **Wefer, G. and cruise participants**
Report and preliminary results of METEOR-Cruise M 37/1, Lisbon - Las Palmas, 4.-23.12.1996.
79 pages, Bremen, 1997.

No. 91 **Isenbeck-Schröter, M., E. Bedbur, M. Kofod, B. König, T. Schramm & G. Mattheß**
Occurrence of Pesticide Residues in Water - Assessment of the Current Situation in Selected EU Countries. 65 pages, Bremen 1997.

No. 92 **Kühn, M.**
Geochemische Folgereaktionen bei der hydrogeothermalen Energiegewinnung.
129 pages, Bremen 1997.

No. 93 **Determann, S. & K. Herterich**
JGOFS-A6 "Daten und Modelle": Sammlung JGOFS-relevanter Modelle in Deutschland.
26 pages, Bremen, 1997.

No. 94 **Fischer, G. and cruise participants**
Report and preliminary results of METEOR-Cruise M 38/1, Las Palmas - Recife, 25.1.-1.3.1997, with Appendix: Core Descriptions from METEOR Cruise M 37/1. Bremen, 1997.

No. 95 **Bleil, U. and cruise participants**
Report and preliminary results of METEOR-Cruise M 38/2, Recife - Las Palmas, 4.3.-14.4.1997.
126 pages, Bremen, 1997.

No. 96 **Neuer, S. and cruise participants**
Report and preliminary results of VICTOR HENSEN-Cruise 96/1. Bremen, 1997.

No. 97 **Villinger, H. and cruise participants**
Fahrtbericht SO 111, 20.8. - 16.9.1996. 115 pages, Bremen, 1997.

No. 98 **Lüning, S.**
Late Cretaceous - Early Tertiary sequence stratigraphy, paleoecology and geodynamics of Eastern Sinai, Egypt. 218 pages, Bremen, 1997.

No. 99 **Haese, R.R.**
Beschreibung und Quantifizierung frühdiagenetischer Reaktionen des Eisens in Sedimenten des Südatlantiks. 118 pages, Bremen, 1997.

No. 100 **Lührte, R. von**
Verwertung von Bremer Baggergut als Material zur Oberflächenabdichtung von Deponien - Geochemisches Langzeitverhalten und Schwermetall-Mobilität (Cd, Cu, Ni, Pb, Zn). Bremen, 1997.

No. 101 **Ebert, M.**
Der Einfluß des Redoxmilieus auf die Mobilität von Chrom im durchströmten Aquifer. 135 pages, Bremen, 1997.

No. 102 **Krögel, F.**
Einfluß von Viskosität und Dichte des Seewassers auf Transport und Ablagerung von Wattsedimenten (Langeooger Rückseitenwatt, südliche Nordsee). 168 pages, Bremen, 1997.

No. 103 **Kerntopf, B.**
Dinoflagellate Distribution Patterns and Preservation in the Equatorial Atlantic and Offshore North-West Africa. 137 pages, Bremen, 1997.

No. 104 **Breitzke, M.**
Elastische Wellenausbreitung in marinen Sedimenten - Neue Entwicklungen der Ultraschall Sedimentphysik und Sedimentechographie. 298 pages, Bremen, 1997.

No. 105 **Marchant, M.**
Rezente und spätquartäre Sedimentation planktischer Foraminiferen im Peru-Chile Strom. 115 pages, Bremen, 1997.

No. 106 **Habicht, K.S.**
Sulfur isotope fractionation in marine sediments and bacterial cultures. 125 pages, Bremen, 1997.

No. 107 **Hamer, K., R.v. Lührte, G. Becker, T. Felis, S. Keffel, B. Strotmann, C. Waschkowitz, M. Kölling, M. Isenbeck-Schröter, H.D. Schulz**
Endbericht zum Forschungsvorhaben 060 des Landes Bremen: Baggergut der Hafengruppe Bremen-Stadt: Modelluntersuchungen zur Schwermetallmobilität und Möglichkeiten der Verwertung von Hafenschlick aus Bremischen Häfen. 98 pages, Bremen, 1997.

No. 108 **Greeff, O.W.**
Entwicklung und Erprobung eines benthischen Landersystemes zur *in situ*-Bestimmung von Sulfatreduktionsraten mariner Sedimente. 121 pages, Bremen, 1997.

No. 109 **Pätzold, M. und G. Wefer**
Bericht über den 6. JGOFS-Workshop am 4./5.12.1997 in Bremen. Im Anhang: Publikationen zum deutschen Beitrag zur Joint Global Ocean Flux Study (JGOFS), Stand 1/1998. 122 pages, Bremen, 1998.

No. 110 **Landenberger, H.**
CoTReM, ein Multi-Komponenten Transport- und Reaktions-Modell. 142 pages, Bremen, 1998.

No. 111 **Villinger, H. und Fahrtteilnehmer**
Fahrtbericht SO 124, 4.10. - 16.10.199. 90 pages, Bremen, 1997.

No. 112 **Gietl, R.**
Biostratigraphie und Sedimentationsmuster einer nordostägyptischen Karbonatrampe unter Berücksichtigung der Alveolinen-Faunen. 142 pages, Bremen, 1998.

No. 113 **Ziebis, W.**
The Impact of the Thalassinidean Shrimp *Callianassa truncata* on the Geochemistry of permeable, coastal Sediments. 158 pages, Bremen 1998.

No. 114 **Schulz, H.D. and cruise participants**
Report and preliminary results of METEOR-Cruise M 41/1, Málaga - Libreville, 13.2.-15.3.1998. Bremen, 1998.

No. 115 **Völker, D.J.**
Untersuchungen an strömungsbeeinflußten Sedimentationsmustern im Südozean. Interpretation sedimentechographischer Daten und numerische Modellierung. 152 pages, Bremen, 1998.

No. 116 **Schlünz, B.**
Riverine Organic Carbon Input into the Ocean in Relation to Late Quaternary Climate Change. 136 pages, Bremen, 1998.

No. 117 **Kuhnert, H.**
Aufzeichnug des Klimas vor Westaustralien in stabilen Isotopen in Korallenskeletten. 109 pages, Bremen, 1998.

No. 118 **Kirst, G.**
Rekonstruktion von Oberflächenwassertemperaturen im östlichen Südatlantik anhand von Alkenonen. 130 pages, Bremen, 1998.

No. 119 **Dürkoop, A.**
Der Brasil-Strom im Spätquartär: Rekonstruktion der oberflächennahen Hydrographie während der letzten 400 000 Jahre. 121 pages, Bremen, 1998.

No. 120 **Lamy, F.**
Spätquartäre Variationen des terrigenen Sedimenteintrags entlang des chilenischen Kontinentalhangs als Abbild von Klimavariabilität im Milanković- und Sub-Milanković-Zeitbereich. 141 pages, Bremen, 1998.

No. 121 **Neuer, S. and cruise participants**
Report and preliminary results of POSEIDON-Cruise Pos 237/2, Vigo – Las Palmas, 18.3.-31.3.1998. 39 pages, Bremen, 1998

No. 122 **Romero, O.E.**
Marine planktonic diatoms from the tropical and equatorial Atlantic: temporal flux patterns and the sediment record. 205 pages, Bremen, 1998.

No. 123 **Spiess, V. und Fahrtteilnehmer**
Report and preliminary results of RV SONNE Cruise 125, Cochin – Chittagong, 17.10.-17.11.1997. 128 pages, Bremen, 1998.

No. 124 **Arz, H.W.**
Dokumentation von kurzfristigen Klimaschwankungen des Spätquartärs in Sedimenten des westlichen äquatorialen Atlantiks. 96 pages, Bremen, 1998.

No. 125 **Wolff, T.**
Mixed layer characteristics in the equatorial Atlantic during the late Quaternary as deduced from planktonic foraminifera. 132 pages, Bremen, 1998.

No. 126 **Dittert, N.**
Late Quaternary Planktic Foraminifera Assemblages in the South Atlantic Ocean: Quantitative Determination and Preservational Aspects. 165 pages, Bremen, 1998.

No. 127 **Höll, C.**
Kalkige und organisch-wandige Dinoflagellaten-Zysten in Spätquartären Sedimenten des tropischen Atlantiks und ihre palökologische Auswertbarkeit. 121 pages, Bremen, 1998.

No. 128 **Hencke, J.**
Redoxreaktionen im Grundwasser: Etablierung und Verlagerung von Reaktionsfronten und ihre Bedeutung für die Spurenelement-Mobilität. 122 pages, Bremen 1998.

No. 129 **Pätzold, J. and cruise participants**
Report and preliminary results of METEOR-Cruise M 41/3, Vítoria, Brasil – Salvador de Bahia, Brasil, 18.4. - 15.5.1998. Bremen, 1999.

No. 130 **Fischer, G. and cruise participants**
Report and preliminary results of METEOR-Cruise M 41/4, Salvador de Bahia, Brasil – Las Palmas, Spain, 18.5. – 13.6.1998. Bremen, 1999.

No. 131 **Schlünz, B. und G. Wefer**
Bericht über den 7. JGOFS-Workshop am 3. und 4.12.1998 in Bremen. Im Anhang: Publikationen zum deutschen Beitrag zur Joint Global Ocean Flux Study (JGOFS), Stand 1/ 1999. 100 pages, Bremen, 1999.

No. 132 **Wefer, G. and cruise participants**
Report and preliminary results of METEOR-Cruise M 42/4, Las Palmas - Las Palmas - Viena do Castelo; 26.09.1998 - 26.10.1998. 104 pages, Bremen, 1999.

No. 133 **Felis, T.**
Climate and ocean variability reconstructed from stable isotope records of modern subtropical corals (Northern Red Sea). 111 pages, Bremen, 1999.

No. 134 **Draschba , S.**
North Atlantic climate variability recorded in reef corals from Bermuda. 108 pages, Bremen, 1999.

No. 135 **Schmieder, F.**
Magnetic Cyclostratigraphy of South Atlantic Sediments. 82 pages, Bremen, 1999.

No. 136 **Rieß, W.**
In situ measurements of respiration and mineralisation processes – Interaction between fauna and geochemical fluxes at active interfaces. 68 pages, Bremen, 1999.

No. 137 **Devey, C.W. and cruise participants**
Report and shipboard results from METEOR-cruise M 41/2, Libreville – Vitoria, 18.3. – 15.4.98. 59 pages, Bremen, 1999.

No. 138 **Wenzhöfer, F.**
Biogeochemical processes at the sediment water interface and quantification of metabolically driven calcite dissolution in deep sea sediments. 103 pages, Bremen, 1999.

No. 139 **Klump, J.**
Biogenic barite as a proxy of paleoproductivity variations in the Southern Peru-Chile Current. 107 pages, Bremen, 1999.

No. 140 **Huber, R.**
Carbonate sedimentation in the northern Northatlantic since the late pliocene. 103 pages, Bremen, 1999.

No. 141 **Schulz, H.**
Nitrate-storing sulfur bacteria in sediments of coastal upwelling. 94 pages, Bremen, 1999.

No. 142 **Mai, S.**
Die Sedimentverteilung im Wattenmeer: ein Simulationsmodell. 114 pages, Bremen, 1999.

No. 143 **Neuer, S. and cruise participants**
Report and preliminary results of Poseidon Cruise 248, Las Palmas - Las Palmas, 15.2.-26.2.1999.
45 pages, Bremen, 1999.

No. 144 **Weber, A.**
Schwefelkreislauf in marinen Sedimenten und Messung von *in situ* Sulfatreduktionsraten.
122 pages, Bremen, 1999.

No. 145 **Hadeler, A.**
Sorptionsreaktionen im Grundwasser: Unterschiedliche Aspekte bei der Modellierung des Transportverhaltens von Zink. 122 pages, 1999.

No. 146 **Dierßen, H.**
Zum Kreislauf ausgewählter Spurenmetalle im Südatlantik: Vertikaltransport und Wechselwirkung zwischen Partikeln und Lösung. 167 pages, Bremen, 1999.

No. 147 **Zühlsdorff, L.**
High resolution multi-frequency seismic surveys at the Eastern Juan de Fuca Ridge Flank and the Cascadia Margin – Evidence for thermally and tectonically driven fluid upflow in marine sediments. 118 pages, Bremen 1999.

No. 148 **Kinkel, H.**
Living and late Quaternary Coccolithophores in the equatorial Atlantic Ocean: response of distribution and productivity patterns to changing surface water circulation. 183 pages, Bremen, 2000.

No. 149 **Pätzold, J. and cruise participants**
Report and preliminary results of METEOR Cruise M 44/3, Aqaba (Jordan) - Safaga (Egypt) – Dubá (Saudi Arabia) – Suez (Egypt) - Haifa (Israel), 12.3.-26.3.-2.4.-4.4.1999. 135 pages, Bremen, 2000.

No. 150 **Schlünz, B. and G. Wefer**
Bericht über den 8. JGOFS-Workshop am 2. und 3.12.1999 in Bremen. Im Anhang:
Publikationen zum deutschen Beitrag zur Joint Global Ocean Flux Study (JGOFS), Stand 1/ 2000.
95 pages, Bremen, 2000.

No. 151 **Schnack, K.**
Biostratigraphie und fazielle Entwicklung in der Oberkreide und im Alttertiär im Bereich der Kharga Schwelle, Westliche Wüste, SW-Ägypten. 142 pages, Bremen, 2000.

No. 152 **Karwath, B.**
Ecological studies on living and fossil calcareous dinoflagellates of the equatorial and tropical Atlantic Ocean. 175 pages, Bremen, 2000.

No. 153 **Moustafa, Y.**
Paleoclimatic reconstructions of the Northern Red Sea during the Holocene inferred from stable isotope records of modern and fossil corals and molluscs. 102 pages, Bremen, 2000.

No. 154 **Villinger, H. and cruise participants**
Report and preliminary results of SONNE-cruise 145-1 Balboa – Talcahuana, 21.12.1999 – 28.01.2000.
147 pages, Bremen, 2000.

No. 155 **Rusch, A.**
Dynamik der Feinfraktion im Oberflächenhorizont permeabler Schelfsedimente. 102 pages, Bremen, 2000.

No. 156 **Moos, C.**
Reconstruction of upwelling intensity and paleo-nutrient gradients in the northwest Arabian Sea derived from stable carbon and oxygen isotopes of planktic foraminifera. 103 pages, Bremen, 2000.

No. 157 **Xu, W.**
Mass physical sediment properties and trends in a Wadden Sea tidal basin. 127 pages, Bremen, 2000.

No. 158 **Meinecke, G. and cruise participants**
Report and preliminary results of METEOR Cruise M 45/1, Malaga (Spain) - Lissabon (Portugal),
19.05. - 08.06.1999. 39 pages, Bremen, 2000.

No. 159 **Vink, A.**
Reconstruction of recent and late Quaternary surface water masses of the western subtropical Atlantic Ocean based on calcareous and organic-walled dinoflagellate cysts. 160 pages, Bremen, 2000.

No. 160 **Willems, H. (Sprecher), U. Bleil, R. Henrich, K. Herterich, B.B. Jørgensen, H.-J. Kuß, M. Olesch, H.D. Schulz,V. Spieß, G. Wefer**
Abschlußbericht des Graduierten-Kollegs Stoff-Flüsse in marine Geosystemen.
Zusammenfassung und Berichtszeitraum Januar 1996 - Dezember 2000. 340 pages, Bremen, 2000.

No. 161 **Sprengel, C.**
Untersuchungen zur Sedimentation und Ökologie von Coccolithophoriden im Bereich der Kanarischen Inseln: Saisonale Flussmuster und Karbonatexport. 165 pages, Bremen, 2000.

No. 162 **Donner, B. and G. Wefer**
Bericht über den JGOFS-Workshop am 18.-21.9.2000 in Bremen:
Biogeochemical Cycles: German Contributions to the International Joint Global Ocean Flux Study.
87 pages, Bremen, 2000.

No. 163 **Neuer, S. and cruise participants**
Report and preliminary results of Meteor Cruise M 45/5, Bremen – Las Palmas, October 1 – November 3, 1999. 93 pages, Bremen, 2000.

No. 164 **Devey, C. and cruise participants**
Report and preliminary results of Sonne Cruise SO 145/2, Talcahuano (Chile) - Arica (Chile), February 4 – February 29, 2000. 63 pages, Bremen, 2000.

No. 165 **Freudenthal, T.**
Reconstruction of productivity gradients in the Canary Islands region off Morocco by means of sinking particles and sediments. 147 pages, Bremen, 2000.

No. 166 **Adler, M.**
Modeling of one-dimensional transport in porous media with respect to simultaneous geochemical reactions in CoTReM. 147 pages, Bremen, 2000.

No. 167 **Santamarina Cuneo, P.**
Fluxes of suspended particulate matter through a tidal inlet of the East Frisian Wadden Sea (southern North Sea). 91 pages, Bremen, 2000.

No. 168 **Benthien, A.**
Effects of CO_2 and nutrient concentration on the stable carbon isotope composition of C37:2 alkenones in sediments of the South Atlantic Ocean. 104 pages, Bremen, 2001.

No. 169 **Lavik, G.**
Nitrogen isotopes of sinking matter and sediments in the South Atlantic. 140 pages, Bremen, 2001.

No. 170 **Budziak, D.**
Late Quaternary monsoonal climate and related variations in paleoproductivity and alkenone-derived sea-surface temperatures in the western Arabian Sea. 114 pages, Bremen, 2001.

No. 171 **Gerhardt, S.**
Late Quaternary water mass variability derived from the pteropod preservation state in sediments of the western South Atlantic Ocean and the Caribbean Sea. 109 pages, Bremen, 2001.

No. 172 **Bleil, U. and cruise participants**
Report and preliminary results of Meteor Cruise M 46/3, Montevideo (Uruguay) – Mar del Plata (Argentina), January 4 – February 7, 2000. Bremen, 2001.

No. 173 **Wefer, G. and cruise participants**
Report and preliminary results of Meteor Cruise M 46/4, Mar del Plata (Argentina) – Salvador da Bahia (Brazil), February 10 – March 13, 2000. With partial results of METEOR cruise M 46/2. 136 pages, Bremen, 2001.

No. 174 **Schulz, H.D. and cruise participants**
Report and preliminary results of Meteor Cruise M 46/2, Recife (Brazil) – Montevideo (Uruguay), December 2 – December 29, 1999. 107 pages, Bremen, 2001.

No. 175 **Schmidt, A.**
Magnetic mineral fluxes in the Quaternary South Atlantic: Implications for the paleoenvironment.
97 pages, Bremen, 2001.

No. 176 **Bruhns, P.**
Crystal chemical characterization of heavy metal incorporation in brick burning processes.
93 pages, Bremen, 2001.

No. 177 **Karius, V.**
Baggergut der Hafengruppe Bremen-Stadt in der Ziegelherstellung. 131 pages, Bremen, 2001.

No. 178 **Adegbie, A. T.**
Reconstruction of paleoenvironmental conditions in Equatorial Atlantic and the Gulf of Guinea Basins for the last 245,000 years. 113 pages, Bremen, 2001.

No. 179 **Spieß, V. and cruise participants**
Report and preliminary results of R/V Sonne Cruise SO 149, Victoria - Victoria, 16.8. - 16.9.2000.
100 pages, Bremen, 2001.

No. 180 **Kim, J.-H.**
Reconstruction of past sea-surface temperatures in the eastern South Atlantic and the eastern South Pacific across Termination I based on the Alkenone Method. 114 pages, Bremen, 2001.

No. 181 **von Lom-Keil, H.**
Sedimentary waves on the Namibian continental margin and in the Argentine Basin – Bottom flow reconstructions based on high resolution echosounder data. 126 pages, Bremen, 2001.

No. 182 **Hebbeln, D. and cruise participants**
PUCK: Report and preliminary results of R/V Sonne Cruise SO 156, Valparaiso (Chile) - Talcahuano (Chile), March 29 - May 14, 2001. 195 pages, Bremen, 2001.

No. 183 **Wendler, J.**
Reconstruction of astronomically-forced cyclic and abrupt paleoecological changes in the Upper Cretaceous Boreal Realm based on calcareous dinoflagellate cysts. 149 pages, Bremen, 2001.

No. 184 **Volbers, A.**
Planktic foraminifera as paleoceanographic indicators: production, preservation, and reconstruction of upwelling intensity. Implications from late Quaternary South Atlantic sediments. 122 pages, Bremen, 2001.

No. 185 **Bleil, U. and cruise participants**
Report and preliminary results of R/V METEOR Cruise M 49/3, Montevideo (Uruguay) - Salvador (Brasil), March 9 - April 1, 2001. 99 pages, Bremen, 2001.

No. 186 **Scheibner, C.**
Architecture of a carbonate platform-to-basin transition on a structural high (Campanian-early Eocene, Eastern Desert, Egypt) – classical and modelling approaches combined. 173 pages, Bremen, 2001.

No. 187 **Schneider, S.**
Quartäre Schwankungen in Strömungsintensität und Produktivität als Abbild der Wassermassen-Variabilität im äquatorialen Atlantik (ODP Sites 959 und 663): Ergebnisse aus Siltkorn-Analysen. 134 pages, Bremen, 2001.

No. 188 **Uliana, E.**
Late Quaternary biogenic opal sedimentation in diatom assemblages in Kongo Fan sediments. 96 pages, Bremen, 2002.

No. 189 **Esper, O.**
Reconstruction of Recent and Late Quaternary oceanographic conditions in the eastern South Atlantic Ocean based on calcareous- and organic-walled dinoflagellate cysts. 130 pages, Bremen, 2001.

No. 190 **Wendler, I.**
Production and preservation of calcareous dinoflagellate cysts in the modern Arabian Sea. 117 pages, Bremen, 2002.

No. 191 **Bauer, J.**
Late Cenomanian – Santonian carbonate platform evolution of Sinai (Egypt): stratigraphy, facies, and sequence architecture. 178 pages, Bremen, 2002.

No. 192 **Hildebrand-Habel, T.**
Die Entwicklung kalkiger Dinoflagellaten im Südatlantik seit der höheren Oberkreide. 152 pages, Bremen, 2002.

No. 193 **Hecht, H.**
Sauerstoff-Optopoden zur Quantifizierung von Pyritverwitterungsprozessen im Labor- und Langzeit-in-situ-Einsatz. Entwicklung - Anwendung – Modellierung. 130 pages, Bremen, 2002.

No. 194 **Fischer, G. and cruise participants**
Report and Preliminary Results of RV METEOR-Cruise M49/4, Salvador da Bahia – Halifax, 4.4.-5.5.2001. 84 pages, Bremen, 2002.

No. 195 **Gröger, M.**
Deep-water circulation in the western equatorial Atlantic: inferences from carbonate preservation studies and silt grain-size analysis. 95 pages, Bremen, 2002.

No. 196 **Meinecke,G. and cruise participants**
Report of RV POSEIDON Cruise POS 271, Las Palmas - Las Palmas, 19.3.-29.3.2001. 19 pages, Bremen, 2002.

No. 197 **Meggers, H. and cruise participants**
Report of RV POSEIDON Cruise POS 272, Las Palmas - Las Palmas, 1.4.-14.4.2001. 19 pages, Bremen, 2002.

No. 198 **Gräfe, K.-U.**
Stratigraphische Korrelation und Steuerungsfaktoren Sedimentärer Zyklen in ausgewählten Borealen und Tethyalen Becken des Cenoman/Turon (Oberkreide) Europas und Nordwestafrikas. 197 pages, Bremen, 2002.

No. 199 **Jahn, B.**
Mid to Late Pleistocene Variations of Marine Productivity in and Terrigenous Input to the Southeast Atlantic. 97 pages, Bremen, 2002.

No. 200 **Al-Rousan, S.**
Ocean and climate history recorded in stable isotopes of coral and foraminifers from the northern Gulf of Aqaba. 116 pages, Bremen, 2002.

No. 201 **Azouzi, B.**
Regionalisierung hydraulischer und hydrogeochemischer Daten mit geostatistischen Methoden. 108 pages, Bremen, 2002.

No. 202 **Spieß, V. and cruise participants**
Report and preliminary results of METEOR Cruise M 47/3, Libreville (Gabun) - Walvis Bay (Namibia), 01.06 - 03.07.2000. 70 pages, Bremen 2002.

No. 203 **Spieß, V. and cruise participants**
Report and preliminary results of METEOR Cruise M 49/2, Montevideo (Uruguay) - Montevideo, 13.02 - 07.03.2001. 84 pages, Bremen 2002.

No. 204 **Mollenhauer, G.**
Organic carbon accumulation in the South Atlantic Ocean: Sedimentary processes and glacial/interglacial Budgets. 139 pages, Bremen 2002.

No. 205 **Spieß, V. and cruise participants**
Report and preliminary results of METEOR Cruise M49/1, Cape Town (South Africa) - Montevideo (Uruguay), 04.01.2000 - 10.02.2000. 57 pages, Bremen, 2003.

No. 206 **Meier, K.J.S.**
Calcareous dinoflagellates from the Mediterranean Sea: taxonomy, ecology and palaeoenvironmental application. 126 pages, Bremen, 2003.

No. 207 **Rakic, S.**
Untersuchungen zur Polymorphie und Kristallchemie von Silikaten der Zusammensetzung $Me_2Si_2O_5$ (Me:Na, K). 139 pages, Bremen, 2003.

No. 208 **Pfeifer, K.**
Auswirkungen frühdiagenetischer Prozesse auf Calcit- und Barytgehalte in marinen Oberflächen-sedimenten. 110 pages, Bremen, 2003.

No. 209 **Heuer, V.**
Spurenelemente in Sedimenten des Südatlantik. Primärer Eintrag und frühdiagenetische Überprägung. 136 pages, Bremen, 2003.

No. 210 **Streng, M.**
Phylogenetic Aspects and Taxonomy of Calcareous Dinoflagellates. 157 pages, Bremen 2003.

No. 211 **Boeckel, B.**
Present and past coccolith assemblages in the South Atlantic: implications for species ecology, carbonate contribution and palaeoceanographic applicability. 157 pages, Bremen, 2003.

No. 212 **Precht, E.**
Advective interfacial exchange in permeable sediments driven by surface gravity waves and its ecological consequences. 131 pages, Bremen, 2003.

No. 213 **Frenz, M.**
Grain-size composition of Quaternary South Atlantic sediments and its paleoceanographic significance. 123 pages, Bremen, 2003.

No. 214 **Meggers, H. and cruise participants**
Report and preliminary results of METEOR Cruise M 53/1, Limassol - Las Palmas – Mindelo, 30.03.2002 - 03.05.2002. 81 pages, Bremen, 2003.

No. 215 **Schulz, H.D. and cruise participants**
Report and preliminary results of METEOR Cruise M 58/1, Dakar – Las Palmas, 15.04..2003 - 12.05.2003. Bremen, 2003.

No. 216 **Schneider, R. and cruise participants**
Report and preliminary results of METEOR Cruise M 57/1, Cape Town – Walvis Bay, 20.01. – 08.02.2003. 123 pages, Bremen, 2003.

No. 217 **Kallmeyer, J.**
Sulfate reduction in the deep Biosphere. 157 pages, Bremen, 2003.

No. 218 **Røy, H.**
Dynamic Structure and Function of the Diffusive Boundary Layer at the Seafloor. 149 pages, Bremen, 2003.

No. 219 **Pätzold, J., C. Hübscher and cruise participants**
Report and preliminary results of METEOR Cruise M 52/2&3, Istanbul – Limassol – Limassol, 04.02. – 27.03.2002, Bremen, 2003.

No. 220 **Zabel, M. and cruise participants**
Report and preliminary results of METEOR Cruise M 57/2, Walvis Bay – Walvis Bay, 11.02. – 12.03.2003, 136 pages, Bremen 2003.

No. 221 **Salem, M.**
Geophysical investigations of submarine prolongations of alluvial fans on the western side of the Gulf of Aqaba-Red Sea. 100 pages, Bremen, 2003.

No. 222 **Tilch, E.**
Oszillation von Wattflächen und deren fossiles Erhaltungspotential (Spiekerooger Rückseitenwatt, südliche Nordsee). 137 pages, Bremen, 2003.

No. 223 **Frisch, U. and F. Kockel**
Der Bremen-Knoten im Strukturnetz Nordwest-Deutschlands. Stratigraphie, Paläogeographie, Strukturgeologie. 379 pages, Bremen, 2004.

No. 224 **Kolonic, S.**
Mechanisms and biogeochemical implications of Cenomanian/Turonian black shale formation in North Africa: An integrated geochemical, millennial-scale study from the Tarfaya-LaAyoune Basin in SW Morocco. 174 pages, Bremen, 2004.

No. 225 **Panteleit, B.**
Geochemische Prozesse in der Salz- Süßwasser Übergangszone. 106 pages, Bremen, 2004.